The University of Nottingham

UNITED KINGDOM · CHINA · MALAYSIA

Investigating genotype and sex susceptibility to a systemic infection in APPswe/PS1ΔE9 mouse model of Alzheimer's disease, at an early stage of amyloid plaque deposition.

Alessandra Agostini (BSc, MSc, MRes)

Thesis submitted to the University of Nottingham for the degree of Doctor of Philosophy

February 2020

Abstract

Systemic bacterial infection can worsen Alzheimer's disease (AD) progression by compromising the central microglia and astrocytes immune response implicated in the clearance of amyloid-β (Aβ) plaques, one of the AD hallmarks. In the present thesis, I investigated whether systemic infection with lipopolysaccharide (LPS) enhanced glial activation, increased amyloid plaque load and infiltration of peripheral macrophages into the brain and whether tolerance occurred following repeated LPS injections. The incidence of AD is higher in women than in men, thus sex-differences in the immune response were also investigated.

Method. 4.5 months old females and males, APPswe/PS1ΔE9 and wild-type littermates were used. LPS (100 µg/kg, i.v) or vehicle (PBS) were systemically administered. Behavioural changes were investigated both at baseline and post-injection assessing spontaneous alternation, food burrowing and open field, to measure spatial working memory daily living and locomotor activity respectively. Peritoneal machrophages and brain cell were collected and the expression of pro- and anti-inflammatory markers were analysed by flow cytometry.

In the first experiment (n=5-6/ group) (chapter 3) brain tissue and blood were collected from the mice 4 hours after the challenge to study the acute effects of LPS. In the second experiment (n=8/group) (chapter 4) brain tissue, blood and peritoneal macrophages were collected 7 days after the treatment to examine the long term effect of an acute immune challenge on amyloid plaque load and glial response. In the third study (chapter 5), mice (n=8/group) received an LPS or PBS injection at 4.5months of age, and a second LPS or PBS challenge 2 weeks later, yielding to 3 experimental groups: PBS-PBS-treated (control), PBS-LPS- treated and LPS-LPS-treated mice. The long term effects of an acute challenge was analysed on

slightly older animals (5 months old) than the previous study (PBS-LPS-treated group). The effect of repeated exposure to LPS (LPS-LPS-treated group) was also determined. Quantification of amyloid plaque load, microglia and astrocytes density in cortex and hippocampus was assessed by immunostaining of Aβ, Iba-1 and GFAP, respectively. Microglia and astrocytes clusters were also measured to analyse the glial response to the presence of plaques. Identification of the possible infiltration of peripheral macrophages into the brain was performed by flow cytometry staining for the surface receptors CD11b and CD45, to distinguish between infiltrated macrophages ($CD11b^{+}$ $CD45^{+Hi}$) and resident microglia ($CD11b^{+}$ $CD45^{+Low}$). Characterization of the immune phenotype was assessed by flow cytometry: the expression of the chemotactic receptor CCR2, the pro-inflammatory marker CD80, and anti-inflammatory marker CD206, as well as the presence of intracellular Aβ in resident microglia and macrophages were analysed.

Results. LPS induced an increase in the pro-inflammatory cytokines IL-6 and TNF-α, and an increase in the anti-inflammatory cytokine IL-10, after 4 hours. A single systemic LPS challenge induced an increase in the number of microglial cells in APPswe/PS1ΔE9 males and females challenged at 4.5 months of age, after 7 days (LPS-treated group). A single systemic LPS challenge, given at 5 months of age (PBS-LPS-treated group), induced an increase in the number of microglial cells, a reduction in the size of small amyloid plaques and a reduction in the levels of IFN-γ in the plasma, in APPswe/PS1ΔE9 female mice after 7 days.

Two challenges of LPS within 3 weeks did not affect amyloid plaque load but induced a reduction in IFN-γ plasma levels in APPswe/PS1ΔE9 females, 7 days after the last injection. This reduction was associated with increased microglia density in the brain. LPS-LPS-treated females developed tolerance to LPS after the second injection, compared to the first challenge. Improvement in spatial working memory

was seen in LPS-LPS-treated APPswe/PS1ΔE9 females, 7 days after the second challenge. Unexpectedly, LPS did not affect the migration of peripheral macrophages into the brain and the expression of the immune phenotypic markers in any of the studies.

In conclusion the present thisis showed that LPS was able to activate the immune system at the dose of 100µg/kg, modulating microglia activation and amyloid plaque deposition as well at 7 days and 3 weeks time points. The initial hypothesis was supported by the data shown revealing also macophages infiltration into the brain. However, further investigation is needed to evaluate genotype susceptibility to the immune challenge and the impact of the systemic LPS infection on the age-dependent amyloid plaque accumulation, in order to clarify the effect of the central inflammatory response on disease progression.

Declaration

All of the experiments and analysis detailed within this thesis were carried out by myself unless otherwise stated.

Acknowledgments

Thanks to my supervisors Marie-Christine Pardon and for Fran Ebling for all the guidance and support throughout my PhD. In particular, thanks to Marie- Christine Pardon for giving me the opportunity to study and research here.

The research was supported by Vice-Chancellor's PhD Scholarship for Research Excellence.

I would like to thank Yuchun Ding for his collaboration in writing the MatLab code used in this thesis, and most of all for his availability to help me whenever I had

problem with the software. His help was invaluable. Thanks to his patience I have also learned the basis of MatLab.

I am grateful to David Onion for his guidance during my new adventure with flow cytometry. I would also like to thank the staff working at the SLIM facility (Medical School) for teaching me all the secrets to have impeccable brain slices for my experiments, and for all the pleasant conversations that I had with them during the time spent at the microtome.

I would like to deeply thank Clare Spicer and David Watson for their technical help with the animal work when I was overwhelmed by experiments.

Within the lab I thank Matthew Young and Sasha-Marhys Antoine for their support and optimism. A special thank goes to my super colleague and friend Matthew Barron that supported me during this journey and celebrated with me each success achieved at work and outside work. I would also like to thank Philippine Geiszler that taught me the behavioral experiments used in this thesis and, in particular, how important research and ethical integrity is when working with animals. I loved my lab group and I considered myself fortunate to have worked with them.

Most of all I thank my partner Andrea Bertoneri. He has been so supportive and encouraging throughout all this journey, for believing in me and inspiring me to give the best I could. I thank him also for all the time that he came to pick me up at the QMC in the middle of the night after a long day of experiments or a long day in the library.

I would love to thank my family that thought me to work with passion, being curious and ambitious. Within my family, I would love to dedicate this thesis to my mother,

Elisabetta Agostino, the strongest and most altruistic person I ever known. Her support and her energy was invaluable.

Abbreviations

AchE	Acetylcholinesterase
AD	Alzheimer's disease
ANOVA	Analysis of variance
APOE	Apolipoprotein E
APP	Amyloid precursor protein
Arg-1	Arginase-1
Aβ	Amyloid-beta
BBB	Blood-Brain-Barrier
BDNF	Brain Derived Neurotrophic Factor
CA	Cornu Ammonis
CAA	Cerebral Amyloid Angiopathy
CCL2	C-C Chemokine ligand 2
CCR2	C-C Chemokine receptor 2
CNS	Central nervous system
CRP	C-reactive protein
CSF	Cerebrospinal fluid
CSF1R	Colony Stimulating Factor 1 Receptor
DAB	3,3'-Diaminobenzidine
DAMPs	Damage-associated molecular patterns
DG	Dentate gyrus
E2	Estradiol
ECE	Endothelin converting enzyme
EOAD	Early-onset Alzheimer's disease
ER	Estrogen receptor
ERT	Estrogen-replacing therapy
FAD	Familiar form of Alzheimer's disease
GFAP	Glial fibrillary acidic protein
GWAS	Genome-wide association study
HLA	Human leukocyte antigen
Iba-1	Ionized calcium binding adaptor molecule 1
IDE	Insulin-degrading enzyme

IFN	Interferon
IL	Interleukin
ISF	Interstitial fluid
LOAD	Late-onset Alzheimer's disease
LPS	Lipopolysaccharide
LRP1	Lipoprotein receptor–related protein-1
MARCO	Macrophage receptor with collagenous structure
MCP-1	Monocyte chemotactic protein-1
MHC	Major histocompatibility complex
NEP	Neprilysin
NF-kB	Nuclear factor-κB
NLRP3	NOD-like receptor family, pyrin domain containing 3
NTFs	Neurofibrillary tangles
PAMP	Pathogen-associated molecular patterns
PBS	Phosphate-buffered saline
PET	Positron emission tomography
PFA	Paraformaldehyde
PGE2	Prostaglandin E2
PSEN	Presenilin
RAGE	Receptor for Advanced Glycation Endproducts
SAD	Sporadic Alzheimer's disease
SCAR	Scavenger receptor
SEM	Standard Error of Mean
TGF-β	Transforming growth factor-β
TLRs	Toll-like receptors
TNF	Tumor necrosis factor
TREM2	Triggering receptor expressed on myeloid cells 2
VEGF	Vascular endothelial growth factor
AD	Alzheimer's disease
ANOVA	Analysis of variance
APOE	Apolipoprotein E
APP	Amyloid precursor protein
Arg-1	Arginase-1

Table of contents

CHAPTER 1

General introduction

1.1 Alzheimer's disease (AD)

Alzheimer's disease (AD) is a progressive and irreversible neurodegenerative disease. It leads to cognitive dysfunction and memory loss, affecting daily living activities, language, mood and behaviour. AD patients develop short-term memory impairment at the early stage and gradually lose their ability to think critically, make judgments, and communicate properly. In later stage they become aggressive, lose attention and spatial orientation with long-term memory impairment (Prasansuklab and Tencomnao, 2013).

Almost 50 million people suffer from dementia worldwide (World Alzheimer Report 2018), with an estimated new case diagnosed every 3.2 seconds (Bronzuoli et al., 2016a). Neurological hallmarks and clinical symptoms were described for the first time by Alois Alzheimer in 1906 who reported a case of a 55 year old woman with progressive dementia. Although at the time it was considered a rare disease, nowadays it is the most common form of dementia among elderly, highly debilitative and deadly.

The major risk factor for AD is age and the risk increases after 65 years of age (Qui et al., 2009). Also sex influences the risk to develop the disease as it has been affirmed that the occurrence of AD is higher in women than in men, particularly in the most elderly (Mazure and Swendsen, 2016b), but chromosomal, hormonal and cultural differences are likely to play an important role in the development and the progression of the disease itself. Genetic factors, family history, Down Syndrome, head trauma and environmental factors represent an additional risk for AD

(Panpalli Ates et al., 2016). Epidemiologic studies have demonstrated that vascular diseases and stroke are also connected to cognitive impairment, and represent a risk for developing AD, aggravating the severity of clinical symptoms (Breteler, 2000).

Based on the age onset, AD can be also divided into two subtypes: early-onset AD (EOAD) or late-onset AD (LOAD). EOAD accounts for 1-6% of all cases with an onset from 40-60 years old, while LOAD is defined with an age onset from 60-65 years old onwards. The possibility to develop the disease increases with age, in particular the prevalence double every 5 years after aged 65, reaching the peak at 85 years of age (Qui et al., 2009). Prevalence may decline slightly afterwards according to the latest research conducted by Farfel et al, that showed that AD pathology level off in the 10^{th} decade (Farfel et al, 2019).

Generally, the disease is divided into two forms, the familial and sporadic case (Drummond and Wisniewski, 2017). The familial AD (FAD) form is rare, with 5-10% of the cases and it is due to mutations in three major genes: amyloid precursor protein (APP) gene, presenilin1 (PSEN1) gene, and presenilin 2 (PSEN2) gene. Mutations in these genes increase the risk of developing the disease and it is inheritable (Guerreiro et al., 2012). The sporadic AD (SAD) form is the most common form of the disease and comprises 90-95% of the cases with both genetic and environmental factors that contribute to the etiopathology of the disease (Lista et al., 2015). Potential risk genes for SAD have been identified with the use of advanced genomic methods giving a big contribution to the understanding of the genetic complexity of the pathology. The genome-wide association studies (GWASs) identified more than 20 genetic loci associated with increased risk of

developing AD (Piaceri et al., 2013). The allelic variation in the Apolipoprotein E (APOE) gene has been identified as an important risk factor for SAD, especially in late-onset AD, and individuals that carry two copies of the allele *ε*4 (APOE4) have higher risk of developing AD than the age-matched controls (Armstrong, 2014).

1.1.1 Neuropathological Hallmarks of AD

Brains from AD patients are characterized by hippocampal atrophy, considered the best established feature to stage the progression of AD pathology (Drummond and Wisniewski, 2017), as well as cerebral cortex shrinkage and ventricle enlargement. Post-mortem analysis of brain slices reveal the neuropathological hallmarks of the disease, characterized by the accumulation of extracellular deposits of amyloid-β (Aβ) peptide in senile plaques, and by the aggregation of intracellular neurofibrillary tangles (NFTs) caused by hyperphosphorylation of the microtubule building protein tau. Healthy and AD brains are compared in Figure 1.

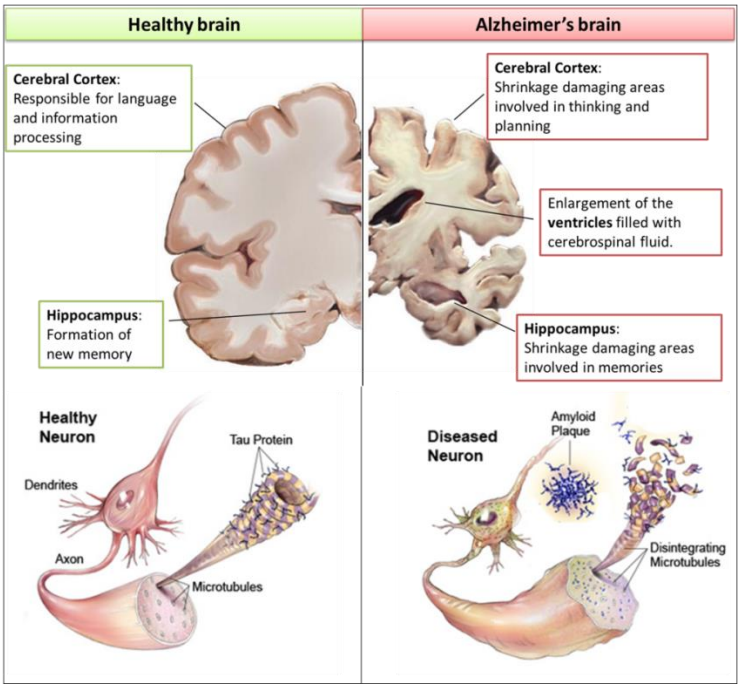

Figure 1**. Healthy and a pathological brain section affected by AD.** A normal healthy brain section (on the left) and an Alzheimer's brain section (on the right) are compared. The hallmarks of the disease are evident in the AD brain section (bottom right) (Modified illustration from Bob Morreale, American Health Assistance Foundation).

Senile plaques are aggregates of Aβ proteins and they are considered the central pathological process in AD due to an abnormal processing of the amyloid precursor protein (APP) (Serrano-Pozo et al., 2011). APP is a transmembrane protein that is constitutively cleaved into peptides during cells metabolism. It is processed by two different pathways (O'Brien and Wong, 2011): the amyloidogenic pathway involves β- and γ- secretase cleavage, generating the Aβ peptide. In the non-amyloidogenic pathway APP is cleaved by α and γ-secretase to generate soluble and neuroprotective fragments. Aβ peptide is quickly removed from the brain in normal conditions, but in case of overproduction or impaired clearance, it aggregates into extracellular oligomers, fibrils and plaques (Pearson and Peers, 2006). The generated Aβ peptide can be of different length: $A\beta_{40}$ and $A\beta_{42}$, based on the

number of amino acids that constitute the peptide. $A\beta_{42}$ is considered the most pathogenic as it has more hydrophobic amino acids which tend to form aggregates in aqueous solutions that in AD brains contributes to plaques formation (Yan & Wang 2006). Many genetic studies demonstrated how mutations in the APP, in the internal region close to the Aβ sequence, enhance the self-aggregation of Aβ into amyloid plaques and the production of the toxic form of $A\beta_{42}$ (O'Brien and Wong, 2011, Bernstein et al., 2005). Aβ peptides are toxic to neurons and induce neuronal and synaptic damage when assembled into amyloid fibrils.

NFTs are insoluble aggregates of helical tau filaments in the neuron cell bodies due a hyperphosphorylation of the tau protein (Serrano-Pozo et al., 2011). Tau is an intracellular microtubule-associated protein that is essential for the microtubule integrity that maintains neuron structure and axonal transport. All these functions are modulated by site-specific phosphorylation. An unregulated phosphorylation of tau results in tau dysfunction and loss of microtubule binding, leading to a compromised microtubule-mediated transport, and formation of aggregated tau fibrils called NFTs (Johnson and Stoothoff, 2004). In adult human brain, there are six major isoforms of tau generated by alternative mRNA splicing, and either 3 or 4 microtubule-binding domains (Vanleuven, 2011). Both the splicing and the phosphorylation of tau are highly regulated in normal conditions, but compromised in AD.

Amyloid plaques and neurofibrillary tangles spread through the brain as the disease progresses (see Figure 2): amyloid plaque origin in the frontal and temporal lobes,

hippocampus and limbic system, and NFTs spread from the medial temporal lobes and hippocampus to neocortical areas (Masters et al., 2015).

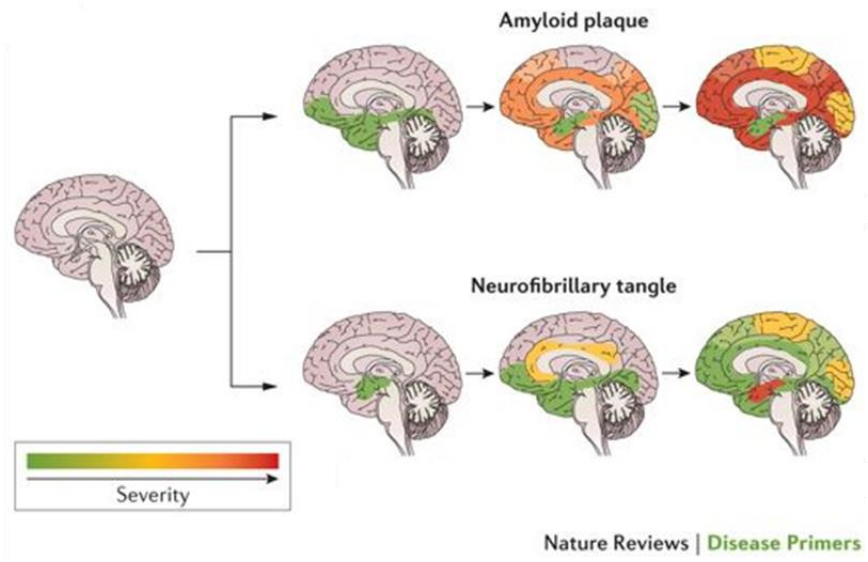

Figure 2. **Illustration of the spread of amyloid plaques and NFTs in the AD brain, as the disease progresses.** Image adapted from (Masters et al., 2015).

1.1.2 Biomarkers for AD

The post-mortem identification of the pathological hallmarks of the disease is the only definitive diagnosis of AD. Significant progresses in neuroimaging techniques have been made in order to provide the structure and physiology of AD brains and identify possible markers (Anoop et al., 2010). Guidelines to assess the clinical diagnosis of the cognitive or behavioral (neuropsychiatric) symptoms of AD are established, but they are not highly accurate and, mostly, the disease is identified only after the manifestation of clinical symptoms (Jack et al., 2011). However, the preclinical stage of AD takes 10-20 years before the onset of cognitive decline, thus the need for additional biomarkers to increase the accuracy of the diagnostic criteria is essential.

Many studies in the past 25 years have been trying to validate biomarkers for the development of effective diagnosis and treatment for AD (Anoop et al., 2010, Rosen et al., 2013). The main cerebrospinal fluid (CSF) biomarkers identified are $A\beta_{42}$, total tau and phosphorylated tau (Lista et al., 2015). Alzheimer's disease is associated with lower CSF levels of $A\beta_{42}$, due to cortical amyloid deposition, higher CSF levels of total and phosphorylated tau, due to cortical neuronal loss and NFTs formation. These three biomarkers revealed 85–90% specificity and sensitivity to diagnosed patients with AD or mild cognitive impairment (MCI), a symptomatic pre-dementia phase of AD. However, more recently emerging biomarkers have been studied as promising diagnostic tools in CSF and blood reflecting APP metabolism, neurodegeneration and glial cell activation (Olsson et al., 2016). A meta-analysis study has revealed novel biomarkers that have been reported to be increased in the CSF of AD patients: neurofilament light protein (NFL) neuron-specific enolase (NSE), visinin-like protein-1 (VLP-1), heart fatty acid binding protein (HFABP) and glial activation marker (YKL-40) (Olsson et al., 2016). More work needs to be done before blood biomarkers can give reliable results and can be considered useful for AD diagnosis and prognosis.

1.1.3 Etiopathology and risk genes factors

AD is a disease with significant genetic roots. The key genes involved in the disease are associated to an increased risk of developing the pathology. The familial form of the disease has been linked to mutations in APP, PSEN1 and PSEN2 genes that affect Aβ production. APP encodes the amyloid precursor protein, located on chromosome 21; presenilin-1 and 2 (PSEN1, PSEN2), encode subunits of the γ-secretase proteolytic enzyme that cleaves APP into amyloid-β and other fragments

(Tanzi, 2012). Since APP gene is located on chromosome 21, individuals affected by Down syndrome have an extra copy of the gene and a greater risk of developing the pathology at early age (Quintanilla et al., 2012). Genetic evidences suggested that APP has a central role as an early event that precedes cognitive decline in AD (Rovelet-Lecrux et al., 2006). APP mutations, which involve the amino acids located in the cleavage site of the APP, as well as the PSEN1-2 mutations, lead to an overproduction and secretion of the most pathological form of Aβ, $A\beta_{42}$ (Hardy and Selkoe, 2002). So far, 178 mutations in PSEN1 and 14 mutations in PSEN2 have been identified, all in the catalytic site of the enzyme, causing an increment in the ratio between $A\beta_{42}$ and $A\beta_{40}$ (Galimberti and Scarpini, 2010). Most of these mutations result in a single amino acid substitutions, but the most severe one is the splice mutation that causes a two amino acid substitution and an in-frame deletion of exon 9 (PS1ΔE9). Identifying new genetic variations to optimize an early diagnosis of the common sporadic form of AD is essential to determine which variant increases the susceptibility of the disease.

The major risk gene associated with the sporadic form is the apolipoprotein E (APOE) (Spinney, 2014). APOE is a regulator of lipoprotein metabolism and plays an important role in cholesterol transport and inflammation. APOE binds Aβ peptides influencing its clearance or accumulation (Martins, 2006). The gene is located on chromosome 19 and has three different alleles named APOε2, APOε3 and APOε4. Mutation on the ε4 allele of APOE (APOE4) is the major risk factor associated with the late-onset of the disease, reported for the first time in 1993 (Saunders et al., 1993), and more recently confirmed by several longitudinal studies where APOε4 carriers presented two-fold increase in developing AD (Gatz et al., 2006). In particular, two *APO*ε4 alleles was correlated to higher risk of developing AD than

the one *APOE*ε4 allele (Karch and Goate, 2015). Until recently, possession of an APOE 4 allele was the only reliably reproducible genetic risk factor for SAD.

With the beginning of the GWAS studies, more gene variations have been linked to the risk of developing AD (Ertekin-Taner, 2010), contributing to further understand the underlying etiology of the disease. Newly identified genes point at pathways implicated in Aβ accumulation. A study conducted principally by Lambert et al. and Harold et al. selected three other genetic variations implicated in late-onset AD susceptibility: CLU (clusterin), PICALM (phosphatidylinositol binding clathrin assembly protein), CR1 (complement receptor 1). CLU is an apolipoprotein present in amyloid plaques that are involved in the aggregation of Aβ in insoluble plaques (Harold et al., 2009). PICALM mediates endocytosis of proteins, lipids, growth factors and neurotransmitters important in the intracellular trafficking (Harold et al., 2009). CR1 is a component receptor 1 and is correlated with the disease prevalence only in Harold's research (Lambert et al., 2009). Additionally, Bridging integrator 1 (BIN1), was also identified as a genetic variation correlated to the risk to develop AD. BIN1 is a widely expressed adaptor protein and mediates endocytosis, actin dynamics and membrane trafficking (Chapuis et al., 2013). A table that summarize the main genes, which variants have been associated to the risk of developing AD, influencing also the innate immune system, can be seen in Table 1. The discovery that the innate immunity genes as risk factors for AD further strengthens the link between immune activation and AD pathogenesis.

Table 1. **Genes associated with risk of developing AD**. Adapted from (Zuroff et al., 2017).

Gene	AD form	Variant	Risk	Effects on Aβ	Effect on Neuroinflammation	References
APP	FAD	Mutations Trisomy 21	High	↑ Aβ production ↑ $Aβ_{42/40}$ ratio	–	(McNaughton et al., 2012)
PSEN1	FAD	Mutations	High	↑ Aβ production ↑ $Aβ_{42/40}$ ratio	–	(Guerreiro et al., 2012)
PSEN2	FAD	Mutations	High	↑ Aβ production ↑ $Aβ_{42/40}$ ratio	–	(Guerreiro et al., 2012)
APOE4	LOAD	Q170H R181G	Moderate-High	↓ Aβ clearance ↑Aβ aggregation	↑ Inflammation	(Verghese et al., 2013) (Martins, 2006) (Finneran et al., 2019)
BIN1	LOAD	ε4 Allele rs6733839	Low-moderate	↑ Aβ production ↓ Aβ clearance	–	(Miyagawa et al., 2016) (Chapuis et al., 2013) (Lambert et al., 2013)
CD33	LOAD	rs744373, rs7561528 rs3865444	Low-moderate	↓ Aβ clearance	↓ Anti-fiammatory, and anti-phagocitic function	(Bradshaw et al., 2013)
CLU	LOAD	rs3865444g, rs3826656	Low-moderate	↓ Aβ clearance	↓ Immune response	(Lambert et al., 2013) (Lambert et al., 2009)
CR1	LOAD	rs9331896 rs6656401	Low-moderate	↓ Aβ clearance	↓ Immune response	(Lambert et al., 2009)
PICALM	LOAD	rs3818361 rs6701713 rs6656401	Low-moderate	↑ Aβ production ↓ Aβ clearance by decreasing trafficking of Aβ across the BBB	–	(Harold et al., 2009, Zhao et al., 2015)
TREM2	LOAD	rs3851179g, rs541458g rs9381040	Moderate	↓ Aβ clearance by decreasing phagocytosis	↓ Anti-fiammatory, and pro-phagocitic function – Microglia distophy	(Jonsson et al., 2013) (Lambert et al., 2013)
HLA-cluster		rs2516049 rs9271192	Moderate	↓ Aβ clearance	↑Immune activation	(Yokoyama et al., 2016) (Verheijen et al., 2018)

1.1.4 Inflammatory role in AD

The pathogenic mechanisms that lead to the development of AD, particularly the sporadic form of AD, are not fully understood. Compelling evidence indicates that the immune system is intrinsically involved in the progression of AD. Autoantibodies, produced in order to recognize esogenoous antigents, have been detected against a variety of molecules in patients with AD. Autoantibodies, produced under physiological or pathophysiological conditions, identify self-antigens to facilitate the recognition and clearance of dead and dying cells, inhibiting the inflammatory pathways (Wu and Li., 2016). Autoantibodies can also affect the central nervous system (CNS) to react with neurons in neurological diseases, including AD. However, the roles of these autoantibodies in AD are not clear: some may contribute to the pathogenesis of AD, and others may play a protective role (D'Andrea, 2005). Gaskin et al. observed in 1993 the presence of secreted Aβ-specific antibodies in B cells derived from a patient with AD (Gaskin et al., 1993). This discovery raised the the interest in searching for autoantibodies against Aβ in the circulation with the hope of using these autoantibodies as a potential biomarker for AD. The presence of immunoglobulins (Ig), high affinity autoantibodies that are promoted by inflammations and infections, have been detected in serum and CSF of AD patients, with higher levels of Aβ-IgG in AD patients compared to control subjects (Maftei et al., 2013). In particular, presence of Ig has been detected in neurons that showed degenerative, apoptotic features, expressing activated caspase-3, contained these vascular-derived antibodies (D'Andrea, 2003; Wu and Li., 2016).

Subsequent studies detected the presence of complement components in the Ig-positive neurons: C1q and C5b-9, part of the classical complement pathway

(D'Andrea, 2005). Thus, it is possible that the presence of anti-neuronal autoantibodies in the serum, may be without pathological consequence until there is a BBB dysfunction to allow the deleterious effects of these autoantibodies access on their targets. Hence, these observations suggest autoimmunity-induced cell death in AD (D'Andrea, 2005).

1.1.5 Gender differences in AD

Brain structure, function and neurochemistry differs between men and women (Cosgrove et al., 2007). These gender differences in the brain are initiated through sex-determining genes and hormonal levels (Mazure and Swendsen, 2016b). Few studies have examined the biological relationships between gender and AD prevalence (Mielke et al., 2014a, Mazure and Swendsen, 2016a). A recent cross-cohort study with clinically normal male and female individuals, showed that the cognitive decline was greater in females with Aβ levels comparables to males, suggesting a modulating role of sex in AD-related cognitive impairment (Buckley et al., 2018). In terms of brain structure, women with AD showed a faster progression of hippocampal atrophy than men (Ardekani et al., 2016). A clinical study on both genders diagnosed with MCI, reported that cerebrovascular diseases represent a higher risk factor for AD in men, while women showed higher incidence of depressive symptoms before AD (Kim et al., 2015). Difference in clinical presentations was also reported from this study: men develop a more aggressive behaviour, more comorbidities and higher mortality than women that develop disabilities but live longer (Kim et al., 2015).

Genetic studies also reported that women who carry the ε4 allele of APOE4 have greater risk of developing AD than are men with this allele (Ungar et al., 2014).

Elevated levels of APOE are correlated to impaired hippocampal function and memory performance that are worse in women than in men (Fleisher et al. 2005). A polymorphism associated with an increased risk factor for AD has been reported on one allele of the brain derived neurotrophic factor (BDNF) gene (Fukumoto et al. 2010). A mutation in this allele reduces the transport of BDNF in the brain, compromising neuronal functions (Fukumoto et al. 2010). Lower levels of BDNF in the blood stream or cerebral fluid have been correlated with the prognosis of AD (Chan and Ye, 2017) and higher susceptibility of this mutation was reported in women (Fukumoto et al. 2010). Low levels of estrogens, the female hormone, has been considered a risk factor for AD (Pike, 2017). Estrogens are important in the maintenance of normal brain function, influencing gene expression and protein function. Indeed, women are much more likely to develop AD after the menopause, when the levels of estrogen decreases (Tang et al. 1996). In a recent clinical observation it was revealed that subjects that underwent surgical menopause by oophorectomy or hysterectomy, showed an increase in developing AD (Pike, 2017). Moreover, it was found that women who took estrogens during the menopause had lower rates of AD, or developed AD later in life (Jamshed et al. 2014). Therefore, estrogen-replacing therapy (ERT) is supported as a potential treatment for AD. From epidemiological studies it was observed that ERT in women with AD enhanced cognitive functions, while ERT in healthy women has the potentiality to reduce the risk to develop AD (Zec & Trivedi 2002). Thus, all these evidences suggest that differences in neuropathologies between men and women might and certainly necessitate different management strategies to serve men and women with dementia.

1.1.6 Overview of the current treatments for AD

Current treatments available for AD patients include acetylcholinesterase (AchE) inhibitors: donepezil, rivastigmine, and galantamine, for patients with any stage of dementia (Weller and Budson, 2018). Indeed, cholinesterase inhibitors aim to block the enzyme responsible for metabolizing acetylcholine (ACh), one of the excitatory neurotransmitters in the brain, increasing the availability of ACh in the synaptic cleft. Indeed, cholinergic dysfunction has been associated with cognitive decline in AD (Parsons et al., 2013). These compounds prevent the loss of cholinergic neurons that are responsible for the decline of cognitive functions. In addition, another licenced treatment is memantine, a N-methyl-D-aspartate (NMDA) receptor antagonist that prevents the effects mediated by glutamate excessive transmission, seen in AD (Weller and Budson, 2018).

However, these drugs available on the market are only treating the symptoms of the disease, improving the quality of life, but do not stop the progress of the disease. Recently, two humanized monoclonal antibodies that target Aβ have been developed aiming to promote Aβ removal from the brain: solanezumab (Doody et al., 2014) and bapineuzumab (Salloway et al., 2014). Both these drugs, employing passive Aβ immunotherapy, are in phase III of clinical trials for the treatment of mild-to-moderate AD but failed to show any cognitive benefits so far in AD patients. Solanezumab was promising in preclinical trial showing Aβ clearance from the brain in a dose-dependent manner, and increased levels of Aβ in plasma and CSF (Doody et al., 2014). Also preclinical studies on bapineuzumab showed an effective removal of Aβ in the brain, associated with memory improvement in transgenic mice overproducing Aβ (Salloway et al., 2014). These results were not replicated in

clinical trials. It has been suggested that therapies targeting Aβ could be effective at early stage of the disease, before the clinical symptoms appear.

Recently, Aducanumab, a human antibody that selectively targets aggregated forms of Aβ, soluble and insolubles, showed to reduce Aβ plaques load and the clinical decline in patients with mild AD, (Budd et al., 2017). However, the development of the drug has been discontinued in phase III of the clinical trial as it failed to meet show effective results in slowing down the disease progression (Cline et al., 2018).

Moreover also crenezumab (Cummings et al., 2018), a monoclonal IgG Aβ antibody able to bind different forms of Aβ, inhibiting its aggregation, and gantenerumab (Ostrowitzki et al., 2017), a human IgG Aβ antibody that strongly binds to the aggregated Aβ, promoting Aβ clearance from the brain, showed promising results in the initial phases of clinical trials but failed to significantly improve symptoms in mild or moderate AD patients.

Multiple clinical trials are ongoing to test higher doses of these drugs and their potential treatment benefits in reducing the cerebral Aβ in mild AD patients (Dong et al., 2019).

1.2 Amyloid plaques

Amyloid plaques, are aggregates of Aβ peptides and represent one of the hallmarks of AD as discussed above. Aβ is derived by the sequential cleavage of the transmembrane protein APP (see Figure 3 for the schematic processing of APP). APP can be processed by two different pathways: the non-amyloidogenic pathways

and the amyloidogenic pathways. In the non-amyloidogenic pathway APP is cleaved by α-secretase, that yields the release of the extracellular αAPP and the membrane-bound C83 fragment, which is further processed by γ-secretase to produce p3 peptides. Alternatively, in the amyloidogenic pathway APP is cleaved by β-secretase that yield to the generation of the extracellular βAPP and the membrane-bound fragment C99, which is cleaved by γ-secretase to form Aβ (Figure 3).

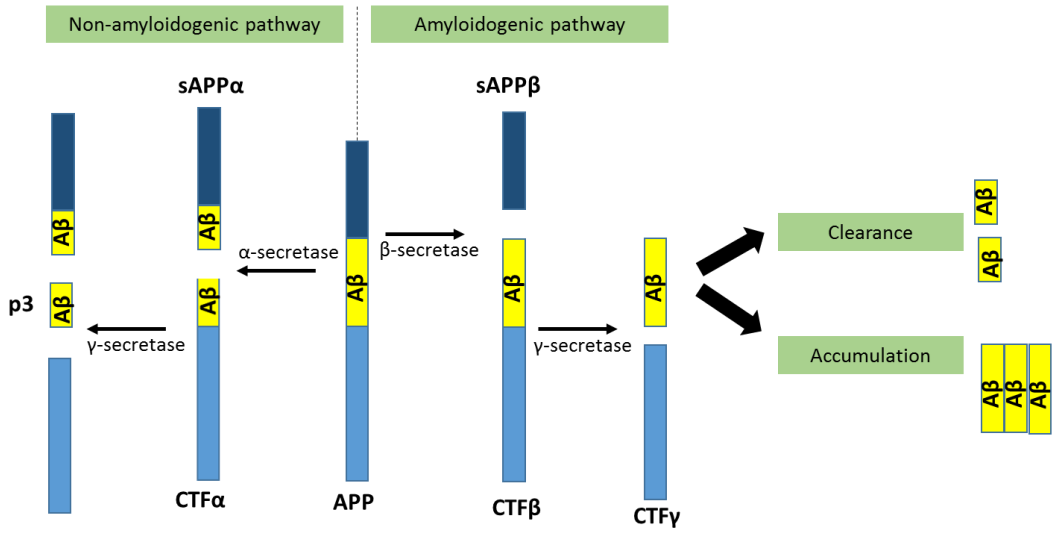

Figure 3. **Schematic processing of APP and generation of Aβ peptide**. Figure drawn by the author.

Aβ can vary in length: the 40-amino acid form of Aβ ($Aβ_{40}$) accounts for 90% of all Aβ normally released from cells, while the 42-amino acid form of Aβ ($Aβ_{42}$) makes up only 10% of the total Aβ (Gu and Guo, 2013, Citron et al., 1996). $Aβ_{42}$ is the most predominant isoform found in amyloid plaques of the brain parenchyma, as, due to is enhanced hydrophobicity, tends to spontaneously aggregate in oligomers, fibrils and insoluble plaques (Nyarko et al., 2018). $Aβ_{40}$ is less toxic and it is the prevalent

isoform found in the brain vessels as cerebral amyloid angiopathy (CAA) (Rovelet-Lecrux et al., 2006).

Amyloid plaques are formed in multiple stages: from the generation of the peptide to formation of beta-sheet monomers, oligomers, and ultimately in larger protofibrils, fibrils and amyloid plaques (Drolle et al., 2014). Based on their morphology, amyloid plaques can be classified as dense-cored, or diffuse plaques (see Figure 4). Dense-core plaques contain Aβ fibrils arranged radially into a central core and are typically surrounded by reactive astrocytes and activated microglial cells (Hohsfield and Humpel, 2015). Diffuse plaques are amorphous amyloid deposits that lack β-sheet structure (Rak et al., 2007).

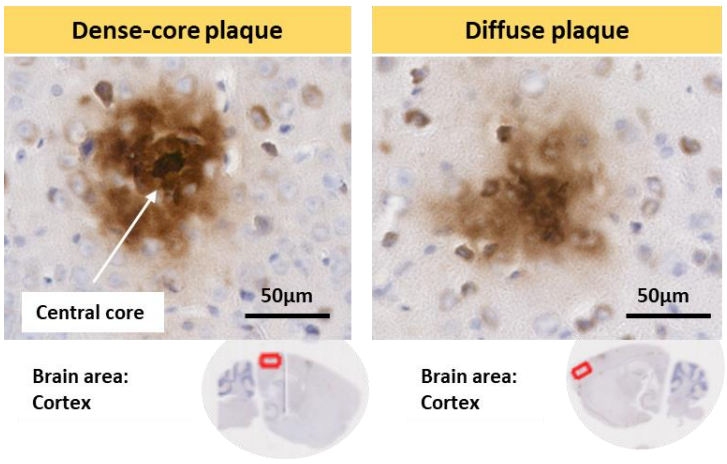

Figure 4.**Illustration of the different plaque morphology.** Images taken from the author from the cortexof APPswe/PS1 immunostained brain slices used in this study. Scale bar 50µm.

1.2.1 Amyloid cascade hypothesis

The Aβ cascade hypothesis is considered the dominant hypothesis for the cause of AD originally proposed by Selko in 1991. This hypothesis considers Aβ overproduction or failure in Aβ clearance the initial trigger for AD

neurodegeneration (Selkoe, 1991, Hardy and Selkoe, 2002). Indeed, accumulation of Aβ has been proposed to initiate a cascade of events that influence the formation of NFTs, synapse loss, neuronal death and widespread neuroinflammation, ultimately leading to neurodegeneration (see Figure 5 for the schematic representation of the Aβ hypothesis) (Morris et al., 2014).

The strongest data supporting this hypothesis come from genetic studies that have linked the familial form of AD to mutations in three genes, APP, PSEN1, and PSEN2, which are all integrally involved in Aβ production (Bettens et al., 2013). Moreover, patients with Down syndrome, who have three copies of the chromosome 21, where the APP locus is located, have high risk to develop AD, due to increase production of Aβ (Lott and Head, 2001). The hypothesis is also supported by APP variants that were seen associated to a decreased in Aβ production, protecting against AD pathogenesis and increasing longevity (Jonsson et al., 2012).

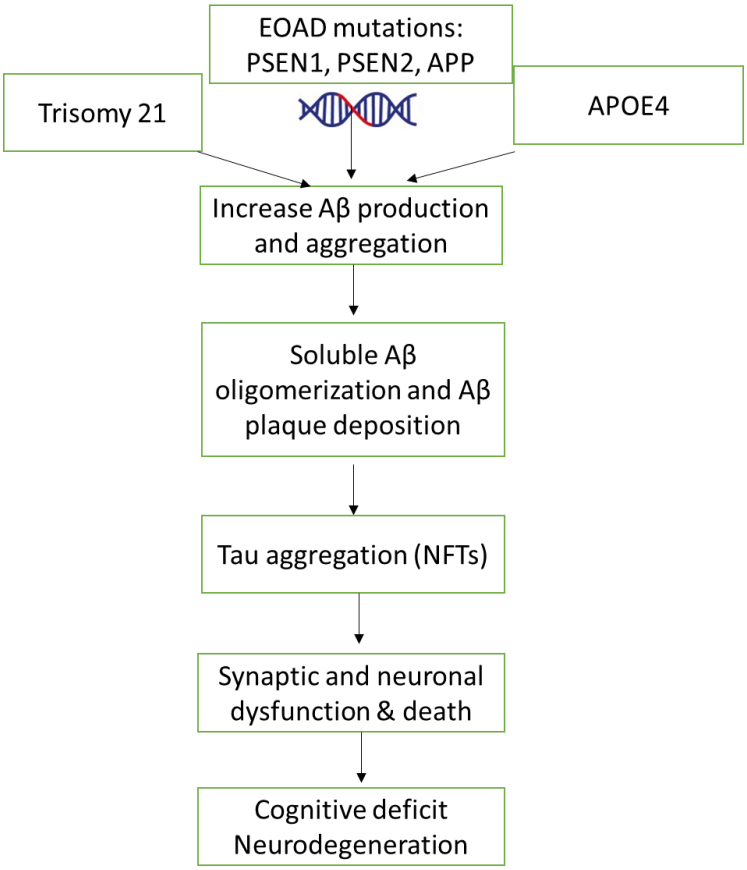

Figure 5. **Amyloid cascade hypothesis**. Excess accumulation of Aβ is the causative agent of the pathology that leads to extracellular accumulation of plaques, intracellular formation of NFTs, synaptic and neuronal loss and ultimately cognitive deficit and neurodegeneration. Figure drawn by the author.

According to this hypothesis, Aβ plaque formation proceed NFTs. However, the pathways that underline the relationship between amyloid plaques and NFTs, in the development of the disease is still a matter of debate. There is evidence to support tau-dependent Aβ toxicity (Reitz et al., 2009, Bejanin et al., 2017), tau pathology occuring downstream of Aβ deposition (Bloom, 2014). An *in-vivo* study showed that injecting synthetic $A\beta_{42}$ fibrils into brains of P301L tau transgenic mouse model, characterized by overexpression of human tau, increases the number of tangles near the site of injection (Gotz et al., 2001). Further evidence comes from another

in-vivo study that created a mouse model crossing JNPL3 transgenic mice, which develop tangles, with Tg2576 mice, characterized by overexpression of Aβ in the brain (Lewis et al., 2001). Accelerated tangle formation was observed in the hybrid mouse model compared to the parental JNPL3 strain but plaque formation was similar to the parental Tg2576 strain (Lewis et al., 2001). The same conclusion has been made from a more recent *in-vivo* experiments that revealed accelerated NFTs formation with the presence of Aβ, but not vice-versa, where the presence of NFTs did not accelerate formation of amyloid plaques (Hurtado et al., 2010).

A possible influence of Aβ on activation of the tau kinases has been also observed. In particular, Aβ is thought to induce GSK3β activation, one of the tau kinases responsible for the phosphorylation of tau. GSK3β have been seen activated at the early stage of the amyloid pathology resulting in an increased tyrosine phosphorylation of tau (Terwel et al., 2008). Indeed, tau hyperphosphorylation was attributed to the increased activity of kinases (Park and Ferreira, 2005). GSK3 kinase, in particular, has been identified as the link in the signalling pathway for amyloid to tau pathology (Terwel et al., 2008, Muyllaert et al., 2006).

Beside these supporting evidences, clinical trials have failed to find a cure based on this hypothesis: from Aβ42 immunotherapies (Bayer et al., 2005), to BACE (Panza et al., 2018) and γ-secretase inhibitors (Doody et al., 2013) have raised doubts, dispate genetics, neuropathology, and clinical biomarker evidences (Tolar et al., 2019).

However, it has been observed that Aβ is produced normally by the intramembranous proteolysis of APP, protein found to circulate in extracellular fluids, CSF and plasma. This observation, lead to several evidences that linked the disease pathogenesis not to the plaques, but mainly to soluble Aβ oligomers (Gibbs

et al., 2019 and Cline et al., 2018), considered to be the drivers of neurodegeneration and pathological symptoms (Tolar et al., 2019, Cline et al., 2018, and Haass & Selkoe, 2007). Soluble Aβ can diffuse into sinaptic clefts more easily than plaques, exposing higher Aβ surface area to neuronal membranes leading to neuronal and synaptic dysfunction (Haass & Selkoe, 2007).

1.2.2 Mechanism of Aβ clearance

In FAD, amyloid plaque formation is associated with increased production of Aβ. In the sporadic form of AD, Aβ accumulates due to an imbalance between production and clearance (Mawuenyega et al., 2010, Selkoe and Hardy, 2016). Therapeutic strategies that have tried to inhibit Aβ synthesis, blocking the activity of the enzymes responsible for its generation, have failed so far (Folch et al., 2016). Thus, the attention has been drifted to manipulating the mechanism involved in Aβ clearance and degradation. There is increasing evidence that deficient clearance, rather than increased production of Aβ contributes to its accumulation in late-onset AD (Weller et al., 2000, Bateman et al., 2006).

Clearance of Aβ from the brain is mediated by several non-enzymatic and enzymatic mechanisms (Figure 6). The non-enzymatic pathways include 1) transport across the BBB (Storck et al., 2016) 2) uptake by microglial or astrocytic phagocytosis (Mandrekar-Colucci and Landreth, 2010) and 3) bulk flow of the interstitial fluid (ISF) into the CSF (Weller et al., 2008). The enzymatic pathways mostly studied include insulin-degrading enzyme (IDE) (Qiu and Folstein, 2006) and neprilysin (NEP) (Iwata et al., 2001).

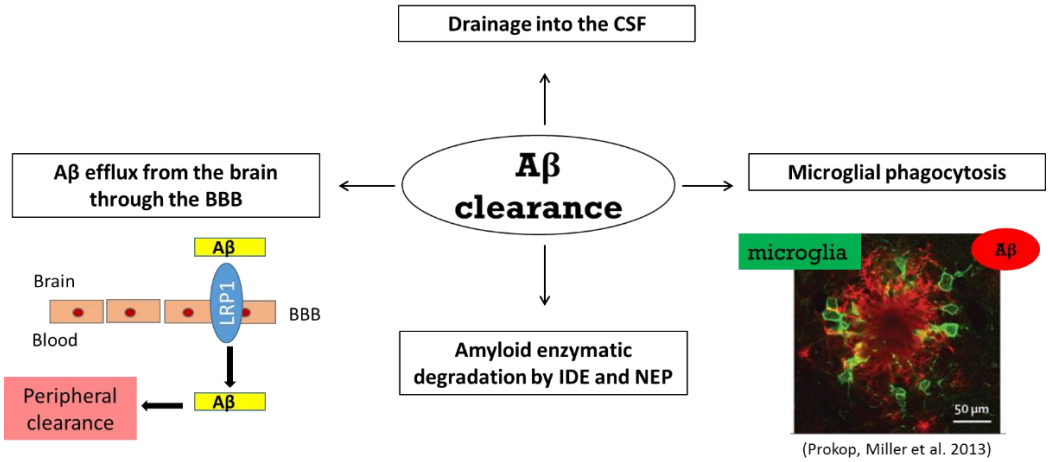

Figure 6. **Mechanism of Aβ clearance.** Figure drawn by the author.

1) Aβ peptides can be transported across the blood vessel walls into the circulation to be cleared from the brain. Low-density lipoprotein receptor–related protein-1 (LRP1) is the main transporter for Aβ. LRP1 is a multifunctional scavenger receptor expressed in the brain capillary endothelium mediates the transport across the BBB from the brain to the periphery (Storck et al., 2016). LRP1 is also expressed on astrocytes and regulates brain Aβ levels through endocytic uptake of Aβ (Shibata et al., 2000). $A\beta_{40}$ is cleared rapidly across the BBB via LRP1 while $A\beta_{42}$ is removed across the BBB at a slower rate (~50%) than $A\beta_{40}$ (Deane et al., 2009).
2) Aβ can also be cleared by microglia phagocytosis. Microglia are the main immune cells of the CNS that can recognise Aβ as toxic peptides and mediate the clearance through phagocytosis (Mandrekar-Colucci and Landreth, 2010). Microglia express receptors that are able to identify and bind Aβ oligomers and fibrils, mediating the phagocytosis: the scavenger receptors SCARA1 and SCARA2, which have a high affinity for soluble and fibrillar Aβ (Frenkel et al.,

2013), the macrophage receptor with collagenous structure (MARCO) (Rogers et al., 2002), CD36, and RAGE (Jarosz-Griffiths et al., 2016). Binding to TLR4 and TREM2 expressed on microglia can also mediate phagocytosis (Hohsfield and Humpel, 2015).

3) The ISF drainage pathway takes Aβ in the CSF, followed by drainage through perivascular basement membranes. Accumulation of Aβ on the wall of capillaries and arteries forms CAA deposits. Several lines of evidence suggested that Aβ deposit in the wall reflects a failure of the elimination of Aβ along the perivascular ISF drainage pathways of the brain (Weller et al., 2000). As the wall of arteries become stiff with age, the drainage of Aβ is reduced and the accumulation of CAA is increased (Weller et al., 2008).
4) IDE, a zinc-endopeptidase and NEP, a membrane-bound zinc endopeptidase, participate in Aβ catabolism. Reduction in NEP was seen in AD patients post-mortem analysis (Wang et al., 2010). Reduction of the IDE mRNA and protein levels was also reported in the brain of AD patients, especially in the hippocampus (Cook et al., 2003).

1.3 Systemic infection as a risk factor in AD

Despite many years of research and many clinical trials designed to understand the complex molecular mechanisms underlying AD etiopathology and progression, there is not an efficient treatment that has been found so far. The majority of the studies assume that the molecular mechanism that characterizes the familial form

of AD is similar also in the sporadic AD. The familiar form of AD is linked to the mutation of three genes involved in APP processing, as explained before. However risk factors for the sporadic form identified so far may vary: from genetic susceptibility to environmental factors or to pathogenic causes such as vascular disease, systemic atherosclerosis, high blood pressure, high cholesterol levels and head trauma (Wan et al., 2008). A central role for systemic inflammation as a risk factor of the disease has been claimed from different studies (Monastero et al., 2014, Lim et al., 2015, Perry et al., 2007). These studies reported an increase in circulating inflammatory mediators associated with brain inflammation. Infective agents may prime and drive activation of microglia and may be responsible for the induction of brain inflammation and decline of cognitive performances (Cunningham et al., 2009), aspects that characterize AD.

A more recent clinical study, that compared AD patients to healthy controls and examined the association between infectious burden and AD, provided evidence that cumulative infections, mediated by both viruses (HSV-1 and cytomegalovirus) and bacteria (Borrelia burgdorferi, Chlamydophila pneumoniae and Helicobacter pylori) are associated with AD (Bu et al., 2015). This study also reported a strong association between increasing infections and increase levels of serum Aβ and pro-inflammatory cytokines (IFN-γ, TNF-α, IL-1β and IL-6). A case cohort study showed that plasma levels of inflammatory proteins, such as IL-6 and C-reactive protein (CRP) were elevated in AD patients, even before the clinical onset of dementia (Engelhart et al., 2004). Markers for systemic inflammation, like pro-inflammatory cytokines and CRP, have also been associated with cognitive decline (Holmes et al., 2009). Other evidence showed that peripheral inflammation is present at early stage of AD (Brosseron et al., 2014b), and long-time exposure to infectious agents

predispose to develop AD at a later age (Lim et al., 2015). Systemic inflammation and infections also caused alteration in inflammatory response seen in patients with MCI (Monastero et al., 2009) and are correlated with AD progression (Qian and Ge, 2018). A clinical study showed that delirium accelerated cognitive decline in AD patients (Fong et al., 2009). Delirium is often caused by infections that induce changes in cognition and attention. Delirium has been reported in up to 66%–89% of patients with AD during hospitalization (Fong et al., 2009) and has been associated with increased incidence of development of dementia in elderly patients (Rahkonen et al., 2000).

An immune response to infections can trigger acute or chronic inflammation (Lucas et al., 2006). An acute infection mediates a transient response that stimulates the resolution of the infection and restores the homeostasis. A chronic infection is, instead, a prolonged stimulation of the immune system that results in an exaggerated pro-inflammatory response. Viruses, in particular, have the potential to remain latent in the body after a first infection and reactivate when the immune system is altered (Honjo et al., 2009).

1.3.1 Bacterial and viral infections in AD

Studies have shown that early-life or life-long systemic inflammation, whether it is acute or chronic, triggers long-lasting modulation of CNS immune responses leading to AD development later in life (Krstic and Knuesel, 2013, Licastro et al., 2014). Positive association between viral infection and AD has been firstly demonstrated decades ago when the presence of herpes simplex virus type 1 (HSV-1) was observed in the AD brain (Jamieson et al., 1992). The link between infectious agent

and AD was reported more recently with observations of *Helicobacter pylori (Roubaud Baudron et al., 2016), C. pneumoniae* (Gerard et al., 2006, Paradowski et al., 2007) *,* and *Borrelia burgdorferi* (Bu et al., 2015) as risk factors for neurodegeneration.

HSV1 has been widely studied in correlation to AD since the first observation. Subsequent studies confirmed HSV1 to be a strong risk factor for AD, especially when its presence is detected in the brains of patients that carry the APOEε4 allele (Itzhaki, 2014). Wozniak et al., suggested that HSV1 could induce an increase in Aβ production in the brain, showing a dramatic increase in the intracellular levels of $A\beta_{40}$ and $A\beta_{42}$ in a cultured neuronal and glial cells infected with HSV1 (Wozniak et al., 2007). Moreover, genes regulating the immune defense against herpes viruses have been associated with age-related cognitive deterioration and AD (Licastro et al., 2014, Porcellini et al., 2010).

C. pneumoniae and spirochetes have also been detected in the brains of AD patients, often alongside amyloid plaques and NFTs (Honjo et al., 2009). *C. pneumoniae,* a gram-negative intracellular bacteria, usually cause respiratory infections. It has been associated with LOAD: post-mortem analyses of AD brain tissue showed that astrocytes, microglia, and neurons served as host cells for *C. pneumoniae*, that was found metabolically active and in close proximity to both amyloid plaques and NFTs (Gerard et al., 2006). A higher presence of *C. pneumoniae* was also observed in APOE ε4 carriers AD patients (Gerard et al., 2005). These studies demonstrated further the influence that a systemic infection has on the brain and AD pathology.

1.4 Neuroinflammation

Multiple risk factors play a critical pathogenic role in AD, such as aging, stress, environmental and life style factors (Hersi et al., 2017). However, mounting evidence continues to support the involvement of neuroinflammation in the development of AD (Akiyama et al., 2000, Heppner et al., 2015, Hong et al., 2018). Neuroinflammation is an inflammatory reaction that originated in the CNS, characterized by increased microglia and astrocyte activation, release of pro-inflammatory mediators, BBB permeability, and leukocyte infiltration into the brain (Xanthos and Sandkühler 2014). The role of neuroinflammation in AD etiopathology and progression is still poorly understood, but it is generally considered that persistent stimuli that trigger neuroinflammation have detrimental effect on disease progression (Hong et al., 2018). Elevated levels of pro-inflammatory cytokines have been observed in the brain of human patients (Morimoto et al., 2011) and animal models of AD (Patel et al., 2005), in association with the disease. Kristic and Knuesel used the term “inflammation hypothesis of AD” in their review that showed evidence correlating the inflammatory processes to AD onset and progression (Krstic and Knuesel, 2013). In particular they concluded that chronic inflammation may be the cause of impaired clearance of Aβ misfolded peptides in the aging brain (Krstic and Knuesel, 2013).

1.4.1 Regulators of the neuroinflammatory response

Microglia and astrocyte reactivity plays a central tole in regulating the immune response to inflammation and the levels of cytokines in the brain. Astrocytes maintain the structure and regulate the homeostasis of the brain, interacting with

neurons and other immune cells of the CNS, while microglia scan the environment to provide the first line of defence against injuries or infections. Astrocytes and microglia need to acquire a reactive phenotype in order to rapidly act in response of an insult. Such an activation is mainly protective, aiming to remove the traumatic or toxic stimuli. However, when the activation is uncontrolled and prolonged, such as under pathological conditions and neurodegeneration, the inflammatory response may cause detrimental effects, overriding the beneficial effects, with a consequence increased production of pro-inflammatory mediators (Zhang and Jiang, 2015). This altered activation is believed to drive chronic neuroinflammatory response in neurodegenerative diseases, including AD (Fakhoury, 2018).

Astrocytes

Astrocytes are the most abundant cells in the brain characterized by elaborate radial ramifications that give them a star shape. There are three types of astrocytes: fibrous (in the white matter), protoplasmic (located mainly in the grey matter) and radial (in the ventricles). Astrocytes are important for ensuring a normal neuronal activity by regulating synaptogenesis and synaptic transmission and by maintaining extracellular ion homeostasis as well as glutamate levels (Ben Haim and Rowitch, 2017). Astrocytes are essential for neuronal survival, growth and excitability and maintaining the brain homeostasis (Sofroniew & Vinters 2010). In addition, astrocytes end-feet are essential support for the BBB, controlling the flow of oxygen and nutrients through the BBB (Alvarez et al., 2013). These cells become reactive in response to signals released from injured neurons or cytokines released from activated microglia (Medeiros and LaFerla, 2013). During an infection or an injury, astrocytes proliferate and migrate over the site of injury, surrounding the

area (Liddelow and Barres, 2017). Activated astrocytes show morphological changes becoming hypertrophic, increasing cell body size with thicker and longer processes in order to create a wall around the area of infection (Chun and Lee, 2018). Phenotypically, reactive astrocytes upregulate the expression of GFAP (glial fibrillary acidic protein), and intermediate filament proteins, like vimentin and nestin (Chun and Lee, 2018).Immunohistological analysis of AD brains patients showed upregulation of GFAP also around amyloid plaques (Kamphuis et al., 2014), but astrocytes proliferation has not been documented (Serrano-Pozo et al., 2013). Altered astrocyte function leads to chronic inflammation that affect the neuron-glial crosstalk and BBB integrity by releasing pro-inflammatory cytokines, reactive oxygen species (ROS), nitric oxide (NO), proteolytic enzymes and complement factors (Liu et al., 2012). *In vitro* data suggest that astrocyte production of pro-inflammatory cytokines, such as TNFα, play a key role in facilitating leukocyte extravasation from the bloodstream across the BBB into the CNS parenchyma and this may amplify the inflammatory response in chronic disease (Sofroniew and Vinters 2010).

There are two two different types of reactive astrocytes, named A1 and A2 (Miller 2018 and Liddelow et al., 2018): A1 astrocytes are neurotoxic and can exacerbate disease pathogenesis inducing the trascription of neuroinflammatory genes (e.g., complement cascade genes). In contrast, A2 astrocytes are neuroprotective, upregulating genes that promote neuronal survival (as S100 and Stat3). The activation of either A1 or A2 is triggered by the cross-talk with activated microglia (Miller 2018 and Liddelow et al., 2018).

Microglia

In addition to astrocytes functions, microglia provide the initial response against injuries that occur within the brain. Microglia are the main resident immune cells of the CNS and represent 10-15% of the total glia cells (Meraz-Ríos et al. 2013). Microglia have important functions in both physiological and pathological conditions (Subramaniam and Federoff, 2017). The main role of microglia is to survey the environment through continuous remodelling of cellular processes and morphology, gaining different levels of activation. In normal conditions these cells are in an inactive or resting state, characterized by small cell body and thin, long, ramified and dynamic processes that constantly move, scanning the environment for damaged tissue or infections. Microglia functions are mediated by receptors-ligand interaction with neurons (like CD200R, CX_3CR_1, TREM2) that inhibit the activation of these cells, keeping them in a resting state (Kierdorf and Prinz, 2013). However, when an insult is recognised, these cells go through morphological changes increasing the size of the cell body and retracting the ramifications. At this morphological state microglial proliferate and multiply around the site of insult adopting a primed activated state. This process, referred as “priming” (Perry and Holmes, 2014) render microglia more susceptible to inflammatory stimuli which can exaggerate the inflammatory response. Fully active microglia have bigger soma, amoeboid morphology and very short processes ready to phagocyte debris or damaged cells. Persistently active microglia lead to neurodegeneration (Li et al., 2018). Figure 7 illustrates the morphological changes and related function of microglia.

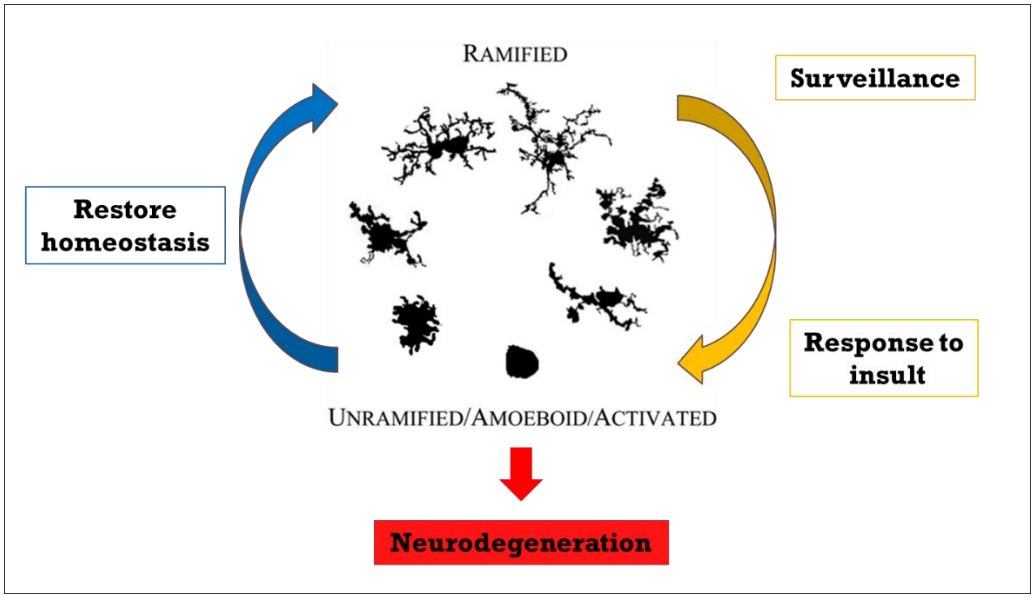

Figure 7. **Microglia morphological changes and related functions.** Modified figure from (Karperien et al., 2013).

Microglia phenotype changes

The transition from resting to activated microglia lead to upregulation or downregulation of certain receptors that change the cell phenotype. Microglia, similar to macrophages, drive the immune response via the recognition of pathogen-associated molecular patterns (PAMPs) or damage-associated molecular patterns (DAMPs) that initiate the cellular defence mechanisms (Meraz-Ríos et al. 2013). PAMPs are molecules such as bacterial endotoxin, lipoproteins, bacterial DNA or viral RNA, while DAMPs are endogenous molecules, such as misfolded or unfolded proteins (Hong et al., 2018). DAMPs are recognised by pattern recognition receptors (PRRs) such as TLRs, RAGE, scavenger receptors and chemokine receptors (Land, 2015).

Activated microglia can acquire a pro-inflammatory phenotype (also called "classic") or an anti-inflammatory phenotype (also called "alternative") (Saijo and Glass, 2011) (Figure 8). Different cell phenotypes can be distinguished based on the

type of cytokine released and on the stimuli that activate microglia. Classical activation (M1) leads to cytotoxicity and tissue injury and can be activated via TLRs ligands such as lipopolysaccharide (LPS), IFN-γ or TNF-α, inducing expression of ROS, NO, and pro-inflammatory mediators (such as TNFα, IL-6, IFN-γ and IL-1β). The alternative activation (M2) can be activated by IL-4, IL-13, Il-10 or the anti-inflammatory receptor TREM2, inducing expression of anti-inflammatory cytokines (such as TGFβ, IL-10), vascular endothelial growth factor (VEGF) and arginase-1 (Arg-1), to help immune suppression and tissue repair (Ransohoff, 2016, Saijo and Glass, 2011).

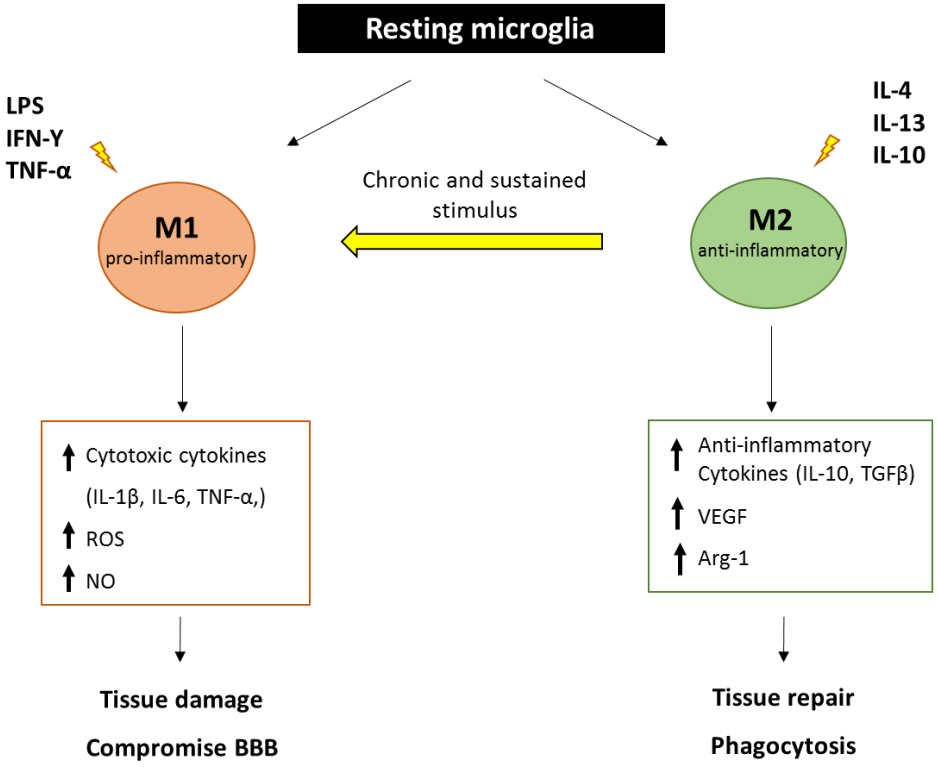

Figure 8. Illustration of the two immune phenotypes of microglia.

In particular, the M2 phenotype can be further subdivided in M2a, M2b and M2c: M2a, promote tissue repair and regeneration, M2b, an immune-regulatory phenotype that promote phagocytosis and M2c which is an acquired-deactivating phenotype (Walker and Lue, 2015, Martinez and Gordon, 2014). During neurodegenerative diseases, where neuroinflammation is a prominent feature and potential contributor to disease, the M2 activated microglia would be beneficial in resolving pathology. Thus, the transition from the M1 to M2 phenotype restores the homeostasis promoting phagocytosis of debris, as well as tissue repair and angiogenesis (Varin and Gordon 2009). However, in pathological cases the pro-inflammatory response persists, and the prolonged activation of M1 leads to neuronal cell death and further tissue damage (Cherry, Olschowka, and O'Banion 2014).

This simplistic distinction of microglia phenotypes in M1/M2 has been used to investigate the inflammatory profile of microglia in neurodegenerative diseases (Tang and Le, 2016), but this concept has been challenged by Ransohoff that suggested that microglia have mixed phenotype instead (Ransohoff, 2016). Both pro-and anti-inflammatory stimuli play a role in the inflammatory response, leading to a beneficial or detrimental activation of the cells (Boissonneault et al. 2009). Because of this dual nature, the role played by microglia in regulating the homeostasis of the brain is still controversial.

Cytokines

Cytokines are molecules that modulated the immune system and are secreted by peripheral immune cells, microglia and astrocytes in the CNS (Galic et al., 2012). Cytokines are released in response to infections or other cytokines signalling

pathways and exert their function both peripherally and centrally. They regulate the intensity and duration of the immune response (Kronfol and Remick, 2000). There are many classes of cytokines including numerous interleukins (IL), chemokines, hematopoietins, interferons (IFN), transforming growth factor (TGF) and tumor necrosis factor (TNF) families (Galic et al., 2012). Cytokines are classified also as pro-inflammatory and anti-inflammatory based on the response mediated to inflammation. The anti-inflammatory cytokines (such as IL-10, IL-4) function as immunoregulators to control the potentially detrimental pro-inflammatory response (Opal and DePalo, 2000). Pro-inflammatory cytokines (such as IL-1, TNF) promote and enhance the inflammation (Dinarello, 2000). IFN-γ is also considered a pro-inflammatory cytokine enhancing TNF-mediated effects and inducing expression of NO (Dinarello, 2000).

Cytokines signalling from the periphery to the CNS

Peripheral or central inflammation induces upregulation of cytokines and their receptors in the brain. Peripheral cytokines transduce the systemic inflammation into the brain via neural and humoral routes (illustrated in Figure 9): 1) through afferent vagal and trigeminal nerves (Skelly et al., 2013) 2) through the active transport by soluble receptor on the endothelial cells of the BBB or by direct diffusion across the BBB (Skelly et al., 2013) 3) through leakage of the BBB in the circumventricular organs (small areas of the brain where the BBB is absent or not intact) (Eskandari et al., 2003). In neurodegenerative disease, like AD, the BBB could be altered facilitating cytokine signalling between the periphery and the brain (Eskandari et al., 2003). Indeed, a clinical study in early AD patients showed

increased BBB leakage that was associated to increased cognitive decline (van de Haar et al., 2016).

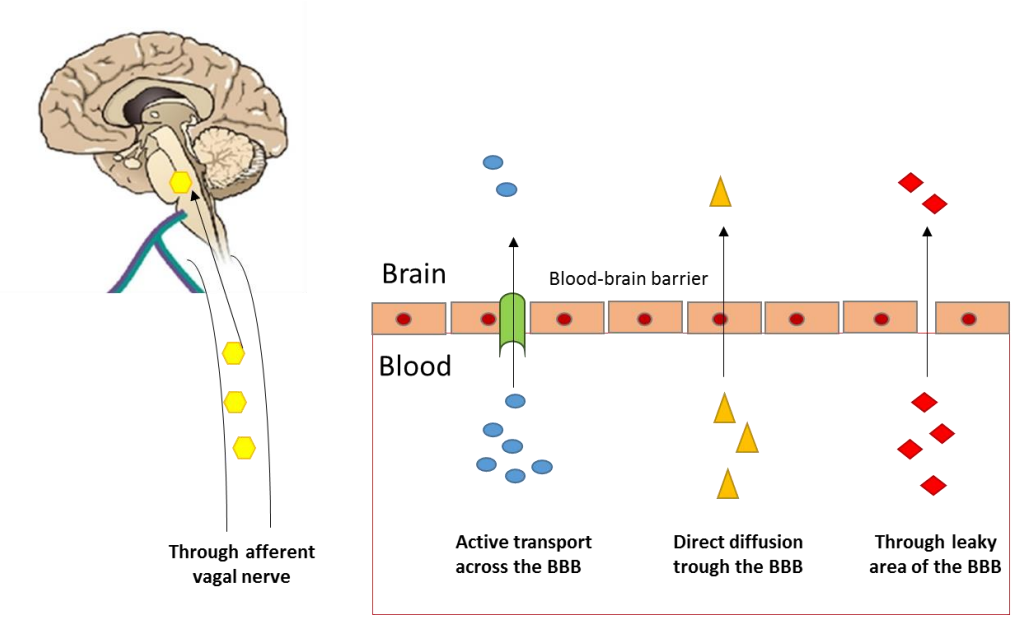

Figure 9. Illustration of the peripheral cytokines transduce signalling to the brain. Figure drawn by the author.

The pro-inflammatory cytokines TNFα, IL-1β, and IL-6 have been implicated in mediating signaling through direct diffusion or active transport across the BBB, contrary to IL-10 that does not cross the BBB (Kastin et al., 2003).

Chemokines

Chemokines are important mediators during homeostasis, controlling the migration of cells in normal processes involved in tissue maintenance. During a pro-inflammatory response, chemokines as release from immune cells to regulate migration of cells towards the site of infection or injury that triggered the inflammatory response (Liu et al., 2014). Chemokines are subdivided into 3 main

groups according to highly conserved cysteine residues: CXC, CC, and CX3C (Miller and Mayo, 2017). Chemokine receptors are expressed on neurons (CXCR2, CXCR3 and CXCR4), microglia (CCR2, CCR5 and CX3CR1), and astrocytes (CXCR2, CXCR4, CCR1, CCR2, CCR3, CCR5, CCR10, CCR11 and CX3CR1) (Liu et al., 2014). Particular attention has been given to study the CCR2 and CCL2 role in mediating infiltration of peripheral monocytes in the brain in response to damaged brain areas or presence of toxic amyloid deposit (Simard and Rivest, 2004, Simard et al., 2006b, Dzenko et al., 2001, Hohsfield and Humpel, 2015). In translational research CCR2 and CCL2 have been considered as a candidate biomarker to monitor the progression of AD (Olsson et al., 2016). More recently plasma CCL2 have been reported in correlation with cognitive deficit in AD patients as patients with greater severity of the disease with faster cognitive decline showed higher plasma level of this chemokine (Lee et al., 2018).

1.5 Neuroinflammation in AD

Neuroinflammation in AD is often viewed as a double-edged sword where immune cells both have beneficial effects, by promoting Aβ phagocytosis, and adverse effects, by producing cytotoxic molecules that contribute to disease progression (Bronzuoli et al., 2016b). The implication of a mechanistic role of neuroinflammation in AD was firstly suggested when activated immune cells and inflammatory proteins were found surrounding the amyloid plaques (Mcgeer & Mcgeer 1999). Subsequent *in vivo* studies have correlated the expression of pro-inflammatory cytokines to increase neuronal loss (Cunningham et al. 2005), synaptic loss (Rao et al., 2012), increased amyloid plaques (Wu et al., 2015, Patel et al., 2005) and increased tau-phosphorylation in AD (Liu et al., 2016). Secretion of pro-inflammatory cytokines can be toxic to neurons and potentially promote further Aβ formation and plaque accumulation, leading to neurodegeneration (Akiyama 2000).

Post-mortem analysis of AD brains have reported the presence of pro- and anti-inflammatory cytokines around the amyloid plaques in the brain of AD patients (Zheng et al., 2016). Changes in the levels of cytokines in the brain have also been correlated with amyloid burden (Zheng et al., 2016). Studies that have aimed to assess levels of cytokines in the CSF or serum of patients with MCI and AD have reported contradictory or inconclusive results (Zheng et al., 2016, Wang et al., 2015). A detailed review from Brosseron et al., on cytokine levels in the CSF and plasma of AD patients revealed higher upregulation of these mediators in MCI cases, while lower upregulations in advanced AD case (Brosseron et al., 2014a).

However, most studies agreed on the importance of cytokines to drive disease progression.

The involvement of microglia and astrocytes in the onset of the disease, as well as their association with the disease hallmarks, has also been increasingly recognized in driving disease progression (Mrak, 2009, Agostinho et al., 2010). However, evidence also suggests that activation of the innate immune response could be neuroprotective, leading to Aβ clearance (Farfara et al., 2008). To date, the timing and role of neuroinflammation in AD, whether neuroinflammation is an underlying cause or a consequence of the disease, is still a matter of debated (Heppner et al., 2015).

1.5.1 Inflammatory genes related to AD

More convincing evidence for the role of neuroinflammation in AD pathophysiology has been recently brought by genome-wide association studies (GWAS). The GWAS studies identified a number of risk variants implicated in inflammatory response linked to LOAD. In particular variant of the CRP, CD33, TREM2 have been associated with increase risk of developing AD.

Yasojima et al. showed the importance of CRP, as an acute phase inflammatory molecules, in association with amyloid plaques reporting CRP upregulation in amyloid affected areas of AD brains (Yasojima et al., 2000). CRP gene polymorphism is associated with high levels of this mediator (Kok et al., 2011). Griciuc et al. showed that variant of the CD33, a transmembrane protein, are associated with increased Aβ accumulation (Griciuc et al., 2013). CD33 has also been shown to inhibit microglial uptake of $A\beta_{42}$ peptides (Malik et al. 2013).

TREM2, a membrane receptor expressed mainly on microglia, is important for the recognition of amyloid fibrils. A TREM2 variant has been linked to 3-fold increase in the risk of developing AD (Guerreiro and Hardy, 2013). Mutations in TREM2 genes have been linked to microglia dysfunction and increased risk for AD (Jonsson et al., 2013). A mutation in TREM2 reduces phagocytosis of amyloid plaques (Lue et al. 2014). Genetic ablation of *TREM2 gene* resulted in less severe plaque pathology at early stages of plaque deposition but in more severe plaque pathology at later stages (Carmona et al., 2018). AD patients that carry a TREM2 genetic variants have showed a faster development of the disease, supporting the central role of TREM2 in AD pathogenesis (Slattery et al., 2014).

While none of these genes exerts as great a risk as possessing an APOE 4 allele, improved understanding of factors leading to the development of AD may provide insights into disease pathogenesis and allow for identification of novel therapeutic targets.

1.5.2 Microglia in AD

Microglia activation in AD can be beneficial, promoting Aβ clearance, or detrimental producing cytotoxic molecules that exacerbate the inflammatory response in the brain and contribute to disease progression (Prokop et al., 2013). Many of the cytokines and chemokines secreted by activated microglia (such as IL-1β, IL-6, TNF-α, MCP-1) have been found to have altered expression in AD patients (Solito and Sastre, 2012). The extent of microglial activation is directly dependent on the amyloid load, as Aβ is known to activate microglia by inducing the activation of the NFκB-dependent pathway that mediate cytokine expression (Solito and Sastre, 2012).

Microglia can mediate clearance of Aβ in early plaque development by phagocytosis and by producing the proteolytic enzymes (such as IDE) that degrade Aβ (Zhang and Jiang, 2015). A recent study pointed toward early inflammatory changes in microglial cells even before the accumulation of Aβ (Boza-Serrano et al., 2018). Indeed, activated microglia cells can be detected in MCI patients (Okello et al., 2009), suggesting the important role of microglia response since the beginning of the pathology (Cagnin et al., 2001). However, in neurodegenerative diseases, such as AD, the immune response is uncontrolled leading to an increased release of pro-inflammatory mediators and amplification of the inflammation (Hoeijmakers et al., 2016). Consequences of exaggerated inflammatory responses by microglia include the development of cognitive deficits, impaired synaptic plasticity and accelerated neurodegeneration (Norden et al., 2015b). Microglial activation *in vivo* can be detected with positron emission tomography (PET) and could be predictive of the disease processes at an early stage (Zhang 2015). Microglial activation has been first assessed *in vivo* using the 18-kDa translocator protein (TSPO) radioligands, a protein that is dramatically upregulated in AD conditions (Tronel et al., 2017).

Microglia response to amyloid plaques

It is well-documented that reactive microglia co-localize around Aβ plaques in both humans and animal models of AD (Zhao et al., 2017b) Miller, and Heppner 2013). *In vivo* observation showed ramification of microglia cells infiltrating the core of the amyloid plaque (Simard et al., 2006b). *In vivo* imaging studies have also shown that microglia surrounding plaques correlated with the decrease of plaque size, providing evidence of microglia uptake of Aβ (Bolmont et al., 2008). This study supports the important role of microglia to prevent plaque growth and mediate Aβ

clearance. On the other hand, another *in vivo* study reported that elimination of microglia, by inhibition of their colony-stimulating factor 1 receptor (CSF1R) in a 10-month old mouse model of AD, did not alter amyloid plaque load (Spangenberg et al., 2016). These contradictory findings can indicate that, even if microglia can uptake Aβ, additional factors are necessary to modulate an effective phagocytic activity. Microglia surrounding plaques express activation markers such as MHC-II and promote the release of pro-inflammatory mediators such as TNF-α, IL-1β, and IL-6 and MCP-1, (Akiyama et al., 2000). MHC-II receptor is increased specifically on microglia of aged brains (Henry et al., 2009). Indeed, the capacity of microglia to phagocytose Aβ efficiently is compromised in aging and AD (Floden and Combs, 2011).

Microglia can recognise amyloid plaques through their surface receptors. Microglia ability to phagocyte amyloid plaques had been linked to the activation of the surface receptor TREM2. TREM 2 mediates its role via its interaction with the activating adaptor protein DAP12 (Guerreiro and Hardy, 2013). Activation of TREM2 promote microglial chemotaxis, phagocytosis, survival, and proliferation (Hansen et al., 2017). High expression of TREM2 have been observed in microglia surrounding amyloid plaques (Lue et al. 2014; Tahara et al. 2006). However, TREM2 signaling pathway has been reported down-regulated with the progression of the disease (Melchior et al., 2010). Indeed, phagocytosis is reduced in AD, with a consequent decrease of amyloid beta clearance and increase plaques deposition (Takahashi et al., 2005). An in-vivo study showed that TREM2 deficiency prevents microglia clustering around Aβ plaques and induce neuronal loss (Wang et al., 2016). Also a recent *in vivo* study showed increase in the number of plaques and dystrophic neurites on TREM2-deficiency 5XFAD mice (Udeochu et al., 2018).

Udeochu et al., also reported that enhanced expression of TREM2 in these mice was sufficient to restore Aβ clearance and reduce the area of the plaque (Udeochu et al., 2018), suggesting that modulation of microglia function could be beneficial to reduce amyloid plaques. Indeed, TREM2 activation attenuates the expression of pro-inflammatory cytokines (Neumann and Takahashi, 2007) preventing the propagation of the inflammatory response. TREM2 was found highly regulated in unstimulated microglia while down-regulated after pro-inflammatory stimulus (Schmid et al. 2009). Down-regulation of TREM2, not only reduces clearance, but also enhances the inflammatory reaction. The receptor's anti-inflammatory property was demonstrated also in TREM2 KO mice that showed impaired clearance of apoptotic neurons and increased gene transcription of TNF-α and NO synthase-2 (Takahashi et al., 2005).

All the studies so far have tried to make progress in understanding the role of microglia in AD, but it is still debated whether Aβ accumulation proceed microglia activation or whether microglia dysregulation induces Aβ deposition (Rodriguez et al., 2010, Jung et al., 2015). Microglial accumulation appears to increase with the progression of the disease (Mott and Hulette, 2005), however, microglial phagocytic function may be compromised, with decreased ability to effectively phagocyte Aβ (Hohsfield and Humpel, 2015). The cause of this loss of activity is not well understood. Recent evidence has demonstrated that infiltrating blood/bone-marrow macrophages have an important role in mediating phagocytosis of Aβ and preventing plaque accumulation (Hohsfield and Humpel, 2015, Hickman and El Khoury, 2010).

1.5.3 Peripheral macrophages infiltration in response to amyloid plaques

In chronic conditions microglia lose their capacity to recognize and phagocytose Aβ (Simard et al., 2006b). It has been demonstrated that, the central immune response induces infiltration of peripheral monocytes in the brain (Eikelenboom et al., 2010) and that peripheral cells are attracted by damaged areas of the brain (Prinz and Priller, 2010). Recruited macrophages from the periphery have been reported having higher Aβ phagocytic activity than resident microglia (Simard et al., 2006b). Indeed, circulating monocytes that infiltrate the CNS are able to differentiate into parenchymal microglia and acquire the same functions (Simard and Rivest, 2004). Evidence came from an *in vivo* study that created chimeric mice by transplanting GFP-expressing bone-marrow cells into APPswe/PS1Δ9 mice, an animal model that overexpresses amyloid plaques (Simard et al., 2006b). This study showed that bone-marrow cells, and not microglia, were surrounding the amyloid deposits, suggesting an effective response of the peripheral immune cells to the accumulation of the plaques. In particular, Simard et al showed that the most toxic form of Aβ has the ability to attract blood-derived cells into the brain (Simard et al., 2006a), suggesting a specific migration of these cells in response to $A\beta_{42}$. This migration was associated to the expression of the chemokine MCP-1 (also names CCL2), induced by Aβ.

A mechanism has been proposed by Hohsfield & Humpel for macrophage recruitment in the AD brain (illustration in Figure 10): the recruitment of monocytes into the brain is triggered by Aβ-induced activation of astrocytes, microglia and endothelial cells. Subsequently, activated astrocytes secrete the CCL2 which recruit CCR2+ immune effector cells from the blood (Hohsfield and Humpel, 2015). El

Khoury et al, reported an impaired trafficking of peripheral macrophages and resident microglia to Aβ plaques in a CCR2 deficient mice crossed with AD mouse model (El Khoury et al., 2007a). CCR2 deficiency was also associated with higher Aβ levels in the brain, specifically around blood vessels (Hickman and El Khoury, 2010).

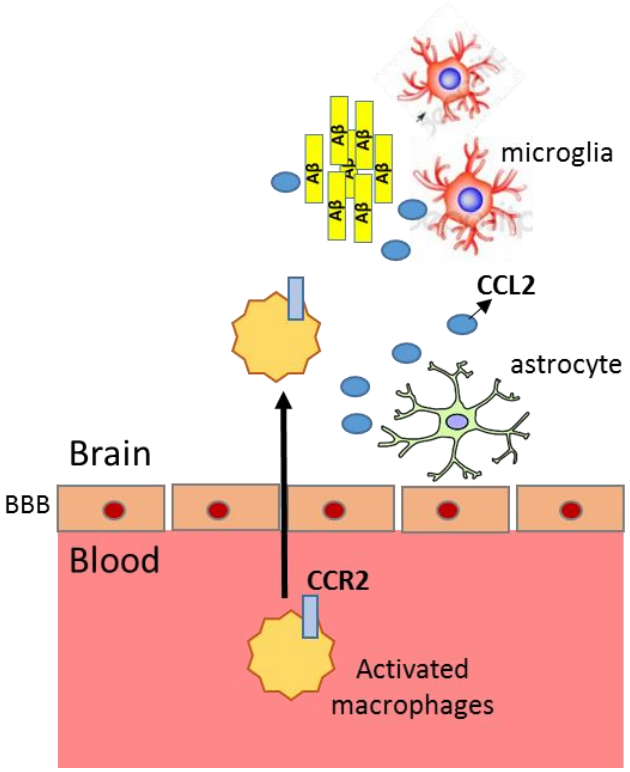

Figure 10**. Illustration of macrophages recruitment in response to plaque accumulation**. Figure drawn by the author.

These findings suggested that monocyte recruitment is dependent on CCR2/CCL2 signaling and accumulation at sites of Aβ deposition with initial attempt to clear these deposits. In translational research CCR2 and its ligand CCL2 have been considered a potential biomarker used to monitor the progression of AD (Olsson et al., 2016). In particular a recent publication showed that plasma MCP-1 levels increase with the progression of the disease, reporting higher levels of this marker in moderate and severe AD patients compared with MCI patients and controls (Lee

et al., 2018). Changes in chemokines levels and in the levels of their receptors have been reported in serum, CSF and brain tissue in patients with AD (Olsson et al., 2016).

1.5.4 Anti-inflammatory treatment for AD

Numerous therapeutic studies to prevent or stop AD have targeted Aβ with the aim to remove Aβ, inhibiting its generation or aggregation (Hellwig et al., 2015). However, these studies have failed at various phases of research. The mechanisms of Aβ plaque formation and maintenance is, indeed, still poorly understood. Accordingly to the database of clinical trials in 2018 there are 1979 studies around the world that are trying to find an efficient treatment to cure AD. Some have explored the possibility of using anti-inflammatory drugs (NSAIDs) to prevent AD. The best-characterized action of NSAIDs is the inhibition of cyclooxygenase (COX). COX enzymes mediate the synthesis of prostaglandins that can suppress synthesis of several cytokines involved in inflammatory processes and implicated in the pathogenesis of AD (Szekely et al. 2007).

The neuroprotective effects of the NSAIDs was first hypothesise by McGreer Rogers *et al* who noticed that patients suffering from arthritis, and under NSAIDs for a chronic period, had a lower risk of developing AD compared to the rest of the patients (McGeer et al. 1990). Their later epidemiological study showed a reduction of the risk by 80% in cases where the use of anti-inflammatory drugs were protracted for at least 2 years (McGeer et al. 1996). Unfortunately recent clinical trials for ibuprofen didn't show any effective benefits in preventing the development of AD and slowing cognitive decline (Pasqualetti et al. 2009). In

addition, other clinical studies evaluating the efficacy of naproxen and celecoxib for the primary prevention of AD in healthy volunteers, 70-years-old in average, with family history of AD, showed no clear benefit of these drugs (Lichtenstein et al., 2010). However, after 4 years of follow-up, naproxen showed a protection in patients that were taking the drug 4 years before the development of clinical signs (Lichtenstein et al., 2010), suggesting a role of NSAID effective only in preclinical stages. Indeed, data from a systematic review on nine clinical studies with adults aged more than 55 years, confirmed that the protective effects of NSAIDs were dependent on the duration of NSAIDs use: decreased risk on developing AD was reported in individuals that used the anti-inflammatory treatment for at least one year before any clinical symptoms (Etminan et al., 2003). Previous studies showed reduced risk of AD after NSAID treatment also in subject carrying the APOε4 allele (Szekely et al., 2008).

Several mechanism of actions have been proposed for NSAIDs in AD pathology: 1) inhibition of COX-2-mediated prostaglandin E2 (PGE2) response suppressing synthesis of pro-inflammatory cytokines (Kotilinek et al., 2008), 2) inhibition of the activity of the nuclear factor-κB (NF-kB) involved in the expression of pro-inflammatory genes (Sung et al., 2004), and 3) influencing APP processing, Aβ production and Aβ aggregation (Imbimbo et al., 2010). Some NSAIDs, ibuprofen and indomethacin, were shown to alter the activity of γ-secretase *in vitro*, lowering levels of $A\beta_{42}$. These effects were also reported in APP-transgenic mouse models of AD (Weggen et al., 2001). The inhibition of $A\beta_{42}$ production was shwn to be independent from COX activity and with no significant benefit in clinical trials (Imbimbo et al., 2010).

Targeting the immune system has resulted in contradictory findings that might depend on the period of use and the initial time of use before the clinical symptoms of dementia appear.

1.6 Immune challenges targeting microglial receptors

Numerous evidence demonstrated that peripheral inflammation influence the central immune response, activating the first line of defence, microglia (Perry et al., 2010, Zhang and Jiang, 2015), which can induce neuroinflammation in chronic diseases (Li et al., 2018). The inflammatory response induced by a systemic immune challenge can elicit behavioural impairments and cognitive deficits altering the brain's inflammatory status (Skelly et al., 2013). These changes could be exaggerated during ageing and under chronic conditions, such AD (Hoeijmakers et al., 2016). Indeed, systemic inflammation has emerged as an important factor for the occurrence or progression of neuroinflammation. Systemic infections can be mediated by endogenous or exogenous immune stimulators. As endogenous stimulators, pro-inflammatory cytokines IL-1β and TNFα have been used for their ability to cross the BBB and directly trigger inflammation both in the periphery and the CNS (Skelly et al., 2013, Hennessy et al., 2017). However, administration of one cytokine doesn't mimic the vast inflammatory response in the brain triggered by a systemic infection. To direct targeting microglia receptors, exogenous stimulators have been used. Among these, systemic inflammation induced by TLRs ligand have been extensively studied: Polyinosinic:polycytidylic acid (polyI:C), a TLR3 ligand (Field et al. 2010) and lipopolysaccharide (LPS), a TLR4 agonist (Cunningham et al. 2005). Both LPS and polyI:C induce a wider spectrum of behavioural changes than would any single cytokine (Skelly et al., 2013). PolyI:C is a synthetic double-stranded RNA, agonist of TLR3, expressed on microglia, that has been used to mimic the acute phase of a viral infection (De Miranda et al., 2010). Stimulation of TLR3 leads to a potent immune response characterized by the production of inflammatory

cytokines such as IL-1β, IL-6, TNFα as well as type I interferons (Matsumoto and Seya, 2008). Acute poly I:C induces IFN-α and IFN-β that mediate a wide spectrum of behavioural changes, such a repression of locomotor activity and engagement in a species-typical behaviour, burrowing (Cunningham et al., 2007). PolyI:C has been mostly used as a prenatal immune challenge to investigate the role of inflammatory processes in brain development as well as the long-term effect on the development of AD (Krstic et al., 2012). Stimulation with high doses of poly I:C (3 mg/kg) has also been used as a model of chronic fatigue syndrome *in vivo* (Katafuchi et al., 2003). Although, poly I:C is a synthetic peptide and is not naturally found in the body. LPS, instead, is an endotoxin of endotoxin of the wall of gram-negative bacteria which may better mimic an infection. Systemic poly I:C has been reported to disrupt the BBB (Field et al., 2010), while only minimal penetration of systemic LPS (0.025% of the dose injected) has been found to cross the BBB (Banks and Robinson, 2010)

Systemic administered LPS is mainly used to mimic a systemic infection in both acute and chronic inflammatory conditions. Moreover, LPS modulates TLR4 signaling pathway involved in AD pathogenesis (Go et al., 2016b) Indeed, an *in-vivo* study suggested that alterations in microglial TLR4 signaling pathway is mediated by chronic exposure of microglia to Aβ deposits, contributing to AD pathogenesis in APP/PS1 mice (Go et al., 2016b). Reduced microglial activation was reported in TLR4 knockout mouse model of AD, together with an increased Aβ deposition, and reduced cognitive function (Song et al., 2011). Increased TLR4 expression have been revealed in brains of a mouse model of AD and brains of AD patients, in particular in microglia surrounding amyloid plaques (Walter et al., 2007). TLR4 activation can induce an inflammatory response activating two different signaling pathways:

MyD88-dependent pathway, which leads to the induction of pro-inflammatory cytokines and COX2 or MyD88-independent pathway that induce expression of interferon inducible genes (Fiebich et al., 2018, Glass et al., 2010).

1.6.1 LPS-induced neuroinflammation

LPS binds CD14 on microglia membranes and the complex LPS-CD14 binds TLR4 on peripheral macrophages and central microglia (Lehnardt et al., 2003). LPS activates these cells inducing signal transduction cascades leading to rapid transcription and release of pro-inflammatory cytokines (IL-1, IL-6, IL-12 and TNF-α), anti-inflammatory cytokines like IL-10 and TGF-β, chemokines (CCL2, CCL5, and CXCL8) and the complement system proteins (Nazem et al., 2015, Lehnardt et al., 2003).

Systemic injection of LPS can induce exaggerated inflammation and sickness behaviour response in chronic neurodegenerative disease, due to a pronounced pro-inflammatory cytokines production. Sickness syndrome mediated by LPS includes lethargy, decreased locomotor activity and appetite, anhedonia. LPS-induced neuroinflammation was also reported in association with cognitive impairment related to spatial learning tasks (Nazem et al., 2015), and spatial working memory impairment (Zhu et al., 2014). LPS-induced acute response is a dose and time dependent mechanism. A sub-pyrogenic dose of LPS (1 μg/kg), is sufficient to induce a significant reduction in daily living activity even in a mild inflammation condition (Sparkman et al. 2006). Likewise, an injection of 0.06–0.2 ng/kg leads to a marked increase of TNFα and IL-6 levels in serum that reaches a pick after 3h (Krabbe et al. 2005). On the other hand an injection of high dose of LPS (500 μg/kg) induces severe systemic inflammation and fever typical of a septic

shock that are not reflected in normal infection in humans and animals (Kondo et al. 2011).

Few studies have used LPS to modulate the immune response in amyloid pathology to investigate the impact of systemic infection on the production of Aβ. However, contradictory results have been reported. *In-vivo* studies using APP mice models of AD showed that systemic LPS induced increase in Aβ production through enhanced β-secretase activity (Wu et al., 2015), or through down regulation of α-secretase activity (Zhan et al., 2018). Another *in-vivo* study showed that peritoneal injection of LPS, given once a week for 12 weeks, showed increase in microglia activation and proliferation, enhancing brain levels of APP and $A\beta_{40}$ and $A\beta_{42}$ (Catorce and Gevorkian, 2016). However, DiCarlo et al., reported that intrahippocampal LPS administration induced reduction of Aβ plaques, stimulating Aβ clearance (DiCarlo et al., 2001).

LPS also act on the BBB, impairing LRP1 activity and leading to a reduction in Aβ efflux from brain (Banks et al., 2015). Distribution of the BBB was also documented after systemic LPS (Varatharaj and Galea, 2017), suggesting the role of LPS in enhancing inflammation of the BBB and facilitating the cross talk between the periphery and the CNS.

The immune response to LPS is also age-dependent. A previous *in vivo* study also correlated the impact of LPS infection with age, suggesting that age influences the response to infections (Bardou et al., 2014). This study administered LPS in the brain of rats of different ages (3, 9 and 23 months of age) for either 3 or 8 weeks, showing an increase in the expression and the protein levels of pro-inflammatory cytokines as well as microglia activation (Bardou et al., 2014).

1.6.2 LPS- tolerance

Repeated exposure of LPS show reduced responses of macrophages or microglia to secondary stimuli with LPS. This response is known as LPS tolerance. LPS tolerance occurs through alteration of the intracellular signaling pathways mediated by LPS. LPS tolerance induces a transient period of hyporesponsiveness characterized by a reduced release and production of pro-inflammatory cytokines and increased production of anti-inflammatory mediators (Cavaillon et al., 2003).

Evidences of tolerance were found in patients with gram-negative sepsis that did not develop endotoxin shock due to reduced response to subsequent infections (Medvedev et al., 2006). Furthermore, an *in-vivo* study provided evidence that endotoxin tolerance could also limit the effect of a lethal dose of infection in mice, suggesting a protective role of endotoxin tolerance against the excessive inflammatory response induced during an infection (Biswas and Lopez-Collazo, 2009). LPS-tolerance was not associated with a decreased expression of CD14 (Medvedev et al., 2000). However the TLR4-MyD88-dependent signaling cascade was reported to be compromised in LPS-tolerance (Nomura et al., 2000).

1.6.3 Sex differences in immune response

Numerous studies have reported sex differences in immune responsiveness (García-Gómez et al., 2013, Roved et al., 2017). Indeed, sex hormones can suppress or enhance the immune response.

The neuromodulatory and neuroprotective effects of estrogens result in a suppression of inflammation. It mainly inhibits microglia activation and expression of pro-inflammatory cytokines (as IL1β and TNFα), while enhancing the expression

of anti-inflammatory cytokines (Cholerton et al. 2002). The estrogen anti-inflammatory effects are mediated by two nuclear estrogen receptors ERα and ERβ that regulate immune cell function in the central nervous system. The two receptors are both expressed mainly in the brain. Estradiol (E2) is the main form of estrogen and plays an essential role in regulating gene expression of several genes (i.e. BDNF) in neurons, astrocytes, and microglia, which influence the homeostasis of the brain. Low level of estradiol induces a significant change in gene transcription, altering the innate immune response (Sárvári et al. 2011). E2 is able to modulate microglia activation induced by an immune challenge, inhibiting the release of pro-inflammatory cytokines in-vivo (Soucy et al. 2005). Its activity is mediated by ERα that is the main receptor that regulates the expression of inflammatory genes.

Interestingly, a sex difference in response to LPS was reported, supporting the importance of estradiol in the inflammatory response. It was observed that estradiol was able to modulate the effects of LPS on microglia both *in vitro* and *in vivo* through ERα, inhibiting microglia activation as well as pro-inflammatory cytokines and NO expression (Wu et al., 2016, Soucy et al., 2005). Several studies revealed that a low levels of estrogens result in alterate innate immune response and enhance pro-inflammatory reactivity. These findings support the interest of the present study to look at sex difference in response to LPS.

1.7 AD preclinical animal models

To date, a number of transgenic mouse models of AD have been generated. Mice knock-out, knock-in and transgenic for familial AD genes have been used to better understand the underlying mechanism of AD (LaFerla and Green, 2012). Transgenic mice models with human APP and/or human tau transgene have been created to investigate in detail the correlation between the major neuropathlogical hallmarks of the disease and their impact on disease progression, memory and cognitive impairment. These animal models have been used to evaluate the potential of therapeutic compounds for AD. However, AD is not only characterized by accumulation of amyloid plaques and neurofibrillary tangles, but also by a widespread of synaptic loss, inflammation, oxidative damage and neuronal loss. None of the animal models developed so far exhibit the full neuropathological features of clinical AD.

Based on the amyloid cascade hypothesis Aβ accumulation occurs upstream tau pathology (Selkoe and Hardy, 2016). Thus, to study early stages of the disease, mice model with APP transgene have been widely used. The murine mice that overexpress mutant APP develop amyloid pathology similar to that found in the human brain, with an age related increase (LaFerla and Green, 2012). AD transgenic models have been used also to evaluate the inflammatory response and to investigate the inflammatory mediators upregulated by Aβ (Ruan et al., 2009). Thus, amyloid models, are widely used to understand the correlation between amyloid plaque deposition, reactive inflammatory response and cognitive impairment (Garcia-Alloza et al. 2006). However, these models do not develop NFTs

or increase in tau hyperphosphorylation (Yan et al., 2009b). A triple transgenic animal model (3xTg-AD) was also created with APPswe, $PS1_{M146V}$, and tau_{P301L} mutations, mainly to examine the relationship between plaques and tangles (Oddo et al., 2003).

These AD animal models have only been used to clarify pathological mechanisms related to gene mutations associated with the familial form of the disease, but it is unclear whether the same mechanisms occur in the sporadic form of AD.

1.7.1 APPswe/PS1ΔE9 mouse model

The mouse model used for this thesis is the APPswe/PS1ΔE9. This is a double transgenic mouse model that express both a human APP_{695} with a Swedish double mutation (K670N and M671L), and a mutation in PS1 with exon-9 deleted (Jankowsky et al. 2004). This mouse model shows plaque deposits from very early in age, compared to the other amyloid models (Garcia-Alloza et al., 2006; Jankowsky et al., 2004; Kamphuis et al., 2012; Ruan et al., 2009). Indeed, APP and PS1 mutations alter the processing of the APP protein by shifting the processing towards the amyloidogenic pathway leading to increase production of the highly toxic $A\beta_{42}$ peptides (Crouch et al., 2008). The APPswe/PS1ΔE9 mouse model exhibits Aβ deposition and plaques formation from 4-6 month of age, with an accelerated pathology development (Ruan et al., 2009, Jankowsky et al., 2004). There are also murine models that have the single APP transgene with the Swedish mutation, such as APP23 and Tg2576 models. These single transgenic mice develop extensive β-amyloid pathology from 6 month of age, with visible amyloid plaques from 11 months (Carrera et al., 2013), with cognitive and memory impairment observed before plaque formation (Taglialatela et al., 2009). Other animal model

with a single PS1 mutation show very limited Aβ pathology and cognitive impairment (Garcia-Alloza et al. 2006).

An *in vivo* study compared the plaque deposition and rate of plaque formation between the APP mice models (Tg2576, PDAPP, APP23, APPswe/PS1ΔE9, 3XTg-AD) (Lee and Han, 2013). This study reported that the APPswe/PS1ΔE9 model revealed a faster and more diffuse deposition of the plaques starting to appear in the hippocampus and cerebral cortex earlier than the other murine models (Lee and Han, 2013). German and Eisch also confirmed that the APPswe/PS1ΔE9 model showed an accelerated production of the amyloidogenic $A\beta_{42}$ form compared to the other transgenic amyloid models (German & Eisch 2004). The APPswe/PS1ΔE9 mouse model has the advantage to show inflammatory response, plaque deposition and cognitive impairment at early stage of life, compared to the other models (Ruan et al., 2009) and exhibit age-dependent amyloid deposition and appearance of dense-core plaques that characterize AD pathology (Elder et al., 2010, Carrera et al., 2013). Studies that fully characterized this model showed that amyloid deposition were associated with microglia and astrocytes clusters in the hippocampus and cortex from 4-6 months. A gene study revealed that plaque formation and build-up in the frontal cortex of APPswe/PS1dE9 mice was associated with an increased expression of genes involved in an immune response and in glial activation (Wirz et al., 2013). No changes in the genes associated with memory, synaptic transmission and plasticity were reported (Wirz et al., 2013). Behavioural characterization of the model showed that mice manifest memory deficit as early as 2 months of age (Bonardi et al., 2011), as well as spatial learning deficits and reduced anxiety at 7 months of age (Reiserer et al., 2007). Other

characteristics of this model include impaired contextual memory early as 6 months of age (Kilgore et al., 2010), affected nest-building and burrowing as well as age-dependent decline in cognitive behavior (Janus et al., 2015).

1.7.2 Sex differences in the APPswe/PS1ΔE9 mouse model

Sex specific differences have also been observed in the double transgenic animal model. A more severe Aβ pathology and higher levels of $A\beta_{42}$ in the hippocampus, were revealed in female mice from 4 months with an age, compared to males (Wang et al., 2003a). It was also reported that female APPSwe/PS1ΔE9 mice develop cognitive impairment before male (Savonenko et al. 2005). These data, suggests sex differences in this model of amyloidosis that strongly support a gender effect on the pathogenesis progression of AD, as seen in epidemiological studies in AD patients (Mielke et al., 2014b).

In conclusion APPswe/PS1ΔE9 animal model provide a useful tool to study the immune response and assess the impact of an immune challenge on amyloid plaque load, glial activation as well as behavioural changes. Indeed, the early formation of amyloid deposits in these mouse models separate AD pathology from ageing and allow to distinguish the effect of ageing and amyloid beta on microglia.

1.8 Hypothesis

In this thesis, I hypothesised that systemic inflammation, induced by acute LPS administration, would exacerbate a pro-inflammatory glial response and that APPswe/PS1ΔE9 mice would show higher response to the immune challenge than wild-type mice. Inflammation triggered by a systemic infection could influence amyloid pathology, thus I also hypothesised that systemic LPS would enhance amyloid plaque formation and growth. Finally, I hypothesised that LPS would affect the infiltration of peripheral macrophages into the brain in response to the increased amyloid plaque load.

1.9 Aims and objectives

The aim of the study was to investigate the impact of a systemic inflammation on hippocampal-dependent behaviour, central and peripheral immune response as well as amyloid plaque load, at an early stage of amyloid pathology, focusing on genotype and sex differences.

To address this aim:

- APPswe/PS1ΔE9 mouse model of AD was used to determine genotype susceptibility to a mild systemic infection of LPS (100µg/kg) and the immune response was compared to a wild-type mouse. Male and female mice were used to determine sex differences in the central and peripheral immune response to LPS
- Glial acute response and plasma cytokine response to LPS were investigated to determine genotype and sex susceptibility.

- Amyloid plaque load and glial activation were quantified in the hippocampus and cortex of APPswe/PS1ΔE9 mice to determine whether LPS affects amyloid aggregation and inflammatory response 7 days after the systemic infection.
- The presence of infiltrated macrophages into the hippocampus and cortex was established in response to the infection with a flow cytometry technique in order to distinguish these cells from resident microglia and determine whether single or multiple LPS challenges influence the transmigration.
- Pro-inflammatory and anti-inflammatory phenotypes of microglia and macrophages were determined by flow cytometry technique evaluating the expression of the surface markers CD80 (M1-phenotype), CD206 (M2-phenotype). Flow cytometry was also used to evaluate phagocytic activity of macrophages and resident microglia towards Aβ peptides and determine whether they express the receptor CCR2 in response to an increase amyloid beta production.

CHAPTER 2

Methodology

2.1 Animals

4.5 month-old APPswe/PS1ΔE9 and wild-type littermates, with C57BL/6 background, were used. Breeding stock was purchased from the Jackson laboratory (Sacramento, USA). The animals used in the studies were bred and maintained in the transgenic facility of the Bio Support Unit (BSU) at the University of Nottingham. Animals were group-housed by sex in individually ventilated cages (30 x 20 x 13cm) from weaning with unlimited access to food and water. Nesting material, a cardboard play tube and wooden sticks were provided in the cages. Mice were kept in a temperature-controlled room (21°C $\pm$ 1°C) with a 12:12h light-dark cycle. All procedures involving animals were regulated by the animals (Scientific Procedures) act 1986 and conducted under project licence number 40/3601, holder: Marie-Christine Pardon. The mice were euthanized at the indicated time points for tissue collection.

The ARRIVE (Animals in Research: Reporting In Vivo Experiments) guidelines were followed. Animals were randomizly assigned to tratment groups.

2.2 Drug Administration

Mice were injected intravenously (i.v.) in the lateral tail vein with lipopolysaccharide (LPS, Escherichia coli serotype, 0111:B4 lyophilized powder, Sigma-Aldrich, St. Louis, MO, USA) or vehicle (PBS, phosphate buffer saline solution)

at a dose of 100µg/kg. LPS was dissolved in PBS and stored at -20°C. Volume of 1µl per g of body weight was injected.

2.3 Behavioural tests

2.3.1 Food Burrowing

To study if the systemic administration of LPS impacts on the normal daily activities, the food burrowing task was performed. Burrowing was assessed as previously described (Deacon 2012). A pot with one open-end was filled with 30g of normal diet food pellet and the percentage of food displaced out (burrowed) was calculated. Mice spontaneously empty a pot full of food pellet or sand, gravel, even bedding material (R. Deacon, 2012). Mice tend to empty the pot overnight, and the burrowing task can distinguish between different mouse strains, lesion of the hippocampus and pre-frontal cortex, and effects of treatments (R.M.J. Deacon, 2009, Robert M J Deacon, 2006). Performing a baseline test is essential to reveal treatment effects in a clearer way. Mice were trained in group cages to burrow over a weekend, while the behaviour assessed was done overnight with mice individually caged for the duration of the burrowing task.

2.3.2 Spontaneous Alternation

The procedure used a plexiglass Y-maze that comprised 3 arms, each 45 cm long and 7.5 cm wide, surrounded by walls 14 cm high. The task considers the tendency of the animal to investigate new arms of the maze using working memory, according to what they have previously just visited (Deacon and Rawlins, 2006, Lalonde, 2002).

Mice were placed in the center of the maze and were allowed to freely explore the three arms for 5 minutes. Animals were tested both at baseline and post-injection.

The number of arm entries and the alternation rate between arms were recorded manually and were used as a measure of locomotor activity and spatial working memory, respectively. Mice that entered only one arm were excluded from the analysis of the alternation rate. For each group, alternation rate was compared to chance levels (50%) (Gerlai 2001), in order to determine the random chance of alternation. The alternation rate significantly above chance level is indicative of sustained cognition as the animals must remember which arm it entered previously (Bryan et al. 2009). The limbic system, including the hippocampus and pre-frontal cortex regions, is involved in this task (Lalonde 2002).

2.3.3 Open field

Locomotor activity was assessed in an open field using an arena with white floor and transparent walls in plexiglass (30 cm long × 35 cm wide × 30 cm high). Mice were moved from the holding room and left in the test room for at least 30 minutes to allow the animals to acclimatise to the room prior to testing. During the task mice were placed in the middle of the arena and allowed to move freely for 15 mins. The task was performed between 8 and 10am for baseline and post-injection data collection. The total distance moved in the whole arena was tracked automatically using the Ethovision software (v. XT7, Noldus, Wageningen, Netherlands) and used as a measure of locomotion. This test was performed to monitor the impact of the immune challenge on the exploratory drive and sickness behaviour, in addition to locomotion (Lau et al., 2008).

2.4 Immunohistochemistry

2.4.1 Animal euthanasia and tissue collection

Animals were euthanized by cervical dislocation, and the blood and the brains were collected immediately according to each experiment. Animals were then either transcardiac perfused with ice-cold heparinized saline solution (2U/ml of heparin in sterile PBS) first or their brains were dissected immediately after the dislocation and divided sagittally into 2 hemi-brains. Transcardic perfusion was performed manually following Gage et al protocol (Gage et al., 2012). Briefly the animals were fixed in a supine position, the rib cages was opened and the diafram was cut in order to expose the heart. Using a 50ml syringe the harinized saline solution was perfused through the heart until the the fluid exiting the right atrium is entirely clear. The animal was then decapitated and the brain collected.

For immunohistochemistry analysis one hemi-brain was post-fixed in 4% paraformaldehyde in PBS and stored at room temperature for 6h and transferred to 70% ethanol overnight. The second hemi-brain was dissected to collect the frontal cortex, hippocampus, cortex and striatum for further analysis. The tissue not used on the same day of the collection was immediately frozen in dry ice and stored at -80°C.

The tissue was dehydrated using a tissue processor (Leica TP1020) following sequestial incubation in 70% alcohol (for 90mins), 80% alcohol (for 90mins), 96% alcohol (for 90mins), 100% alcohol (for 3h), chloroform (for 6h) and paraffin (for 4h).Finally the tissue was paraffin embedded for immunostaining of glial markers and amyloid beta. 7µm-thick sagittal sections were cut throughout the hippocampus using a microtome (Microtome Slee Cut 4060), mounted on X-traTM Adhesive slides (26x76x10mm, Leica Biosystems) and dried overnight at 40°C.

Sections were stored at room temperature before the immunostaining analysis. Slides for immunostaining were selected in order to stain three levels of the hippocampus (Level 1: Lateral Bregma 1.08 -1.20, Level 2: Lateral Bregma 1.68-1.92 Level 3: Lateral Bregma 2.28-2.52).

2.4.2 Glial staining

Immunostaining of microglial marker Iba1 (ionized calcium binding adaptor molecules-1), and astrocyte marker GFAP (glial fibrillary acidic protein) was carried out using standard procedures at room temperature. An antigen retrieval protocol was used to expose the antigen from wax embedded tissue. All the solutions were freshly prepared before use. PBS-T [1% tween 80 (Sigma Aldrich, St. Louis, MO, USA) in phosphate buffer saline (Dulbecco A, OXOID)] was used to dilute all the solutions, except for DAB. Briefly, the tissue was rehydrated in consecutive rinses in xylene, 100% ethanol, 70% ethanol and distilled water (2 times for 5 minutes each) to deparaffinise the tissue. Antigen retrieval was performed by 20 minutes incubation in Tris-EDTA buffer solution, pH 9, at 98-100°C to expose the antigen and disrupting the covalent bonds formed by formalin in tissue. Once the solution was cooled down to 70°C under running tap water, sections were washed in PBS, incubated in 1% hydrogen peroxide H_2O_2 (Sigma Aldrich, St. Louis, MO, USA) for 10min to inhibit endogenous peroxidase activity. After washes in PBS the tissue was blocked in 5% goat serum (Vector Laboratories Inc. Burlingame, CA) for 30min. The tissue was then incubated with rabbit anti-Iba1 (WAKO Chemicals, VA, USA, diluted 1:2000) for 90 mins, or rabbit anti-GFAP (Biogenix, CA, U.S.A, diluted 1:3000) for 90 mins, washed in PBS, and incubated with biotinylated secondary anti-rabbit (Vector

Laboratories Inc. Burlingame, CA, diluted 1:200) for 30min. After washing, sections were incubated for 30 minutes with ABC from Vectastain Elite Rabbit ABC Kit (Vector Laboratories Inc. Burlingame, CA) and labelled for 4-5 minutes with DAB peroxidase substrate (Vector Laboratories, Burlingame, CA), prepared according to manufacturer's instructions. All dilution were done in PBS.

Sections were then counterstained with haematoxylin to visualize nuclei and brain sections underwent intermediate washing in warm tap water between each step. Then sections were dehydrated in increasing percentage of ethanol solution for 10sec each and twice in xylene for 2 min. Cover slips were glued with DPX-mounting media over the sides to protect the tissue and the staining.

2.4.3 Amyloid beta staining

Immunostaining for β-Amyloid was also carried out at room temperature. Briefly, 20 minutes antigen retrieval incubation was performed using 10mM EDTA, pH6 buffer solution at 95-100°C. Once finished, the solution was cooled down until 70°C, slides were then washed in PBS and incubated for 1min with 98% formic acid. After washing, sections were incubated with 3% hydrogen peroxide H_2O_2 (Sigma Aldrich, St. Louis, MO, USA) for 10 mins and 5% horse serum for 1h. The tissue was then incubated with monoclonal Anti-β-Amyloid antibody produced in mouse (A5213 , Sigma Aldrich, St. Louis, MO, USA, diluted 1:2000) for 1h, washed in PBS, and incubated with biotinylated secondary anti-mouse (Vector Laboratories Inc. Burlingame, CA, diluted 1:200) for 1h. The following incubation with ABC, DAB and haematoxylin steps were carried out as described above.

2.5 Immunohistochemistry quantification method

Quantification of Iba-1, GFAP and Aβ was performed using a semi-automated method, detailed and explained below, to quantify the area stained, the number of microglia somas and amyloid plaques, the number of microglia clusters and the size of microglia somas and amyloid plaques. Number of GFAP-clusters in the cortex was manually quantified by the experimenter. Blind quantification was performed.

2.5.1 Semi-automated immunostaining quantification

Brain tissue was slices at different levels of the hippocampus and immunostaining was analysed with a semi-automated software that was validated in house (Ding et al., 2017). Digital focused photo-scanning images were then acquired using a Hamamatsu NanoZoomer-XR 2.0-RS C10730 digital scanning system with TDI camera technology a NanoZoomer (Hamamatsu Photonics K.K. Systems, Japan) at 20x magnification and visualised using NDP.view2 (NanoZoomer Digital Photography). Images were exported individually at 1.63x magnification and saved as Jpeg images with a resolution of 15360*8640. A custom made software (Matlab) was used for the immunostaining quantification of the cortex and the hippocampus (with subfields cornu ammonis CA1, CA2, CA3 and dentate gyrus (DG)). This software allows the operator to isolate the entire region of interest and to delete artefacts, providing the area stained by glial markers, number of microglia cells and microglial soma size, as well as the number of amyloid plaques and plaques area. The percentage of area stained by Iba1 and the number of Iba1 positive cells were used as markers of microglial density, while the percentage of stained area marked by GFAP was used as a marker of astrocytes density. Plaques area was used to

discriminate between small (area<400µm2), medium (400µm^2< area< 700µm^2) and large plaques (area>700µm^2) (Scheffler et al., 2011). All analysis was performed blind to the treatment group to ensure unbiased results.

Validation of the semi-automatic quantification method.

For the validation of the semi-automatic quantification method, manual and automatic quantification using a Matlab code were compared. Percentage of area stained by Iba1, the number of soma and the size of the cell soma were analysed. The manual quantification was repeated twice by the experimenter and another individual (identified as Manual A and Manual B for semplicity).

20 images from brain slices taken from animals in the study described in chapter 3 were analysed using ImageJ (win-32bit, National Institutes of Health), for the manual quantification and a Matlab code (Ding et al., 2017) for the authomatic segmentation. Hippocampal subfields of the images randomply selected were cropped using NDP.view2 (NanoZoomer Digital Photography) tool to draw a rectangular region of interests (ROIs) with an area of 0.2 mm^2 for CA1, CA3 and DG and 0.1mm^2 for CA2 (Figure 11). For the manual analysis, the soma size was analysed drawing a line around the microglia soma using the freehand line tool in NDP.view2 at a magnification of 40X. The number of somas per ROIs was counted manually and the data collected. For the percentage of area stained, ROIs were exported at 20x and saved as JPEG images for subsequent analysis using ImageJ. Images were split into red, green and blue using the RGB stack command, prior to thresholding. The blue stack was chosen to eliminate non-specific highlighting of the neuronal nuclei. The threshold level was adjusted manually to highlight the

soma and processes (Figure 11.F), and the percentage area stained extracted. Manual analysis was performed blind from treatment conditions to ensure unbiased results.

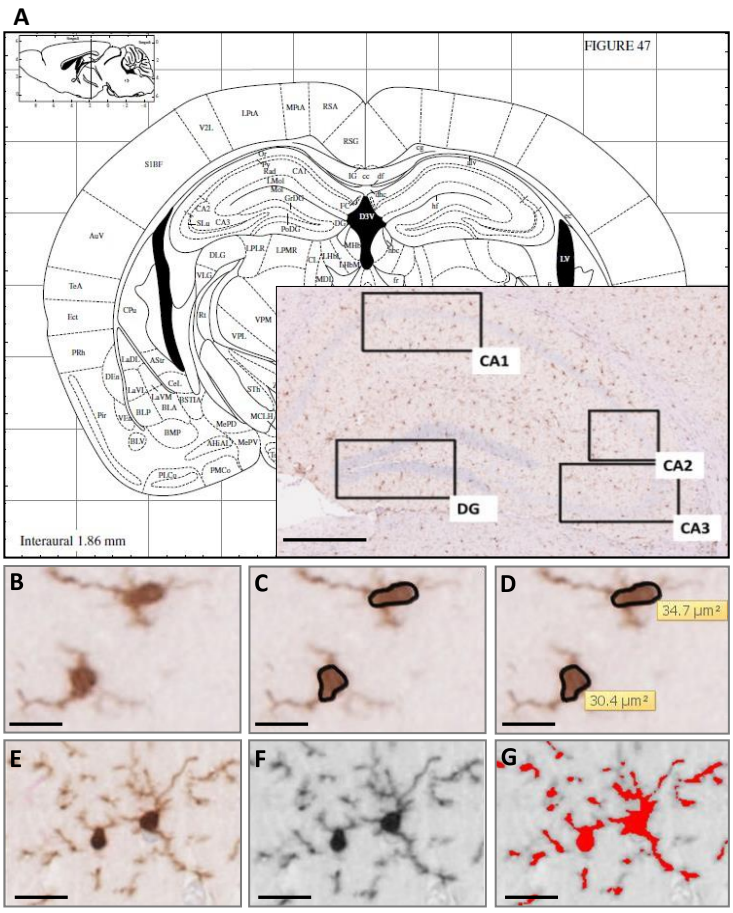

Figure 11. **Manual quantification steps.** The hippocampal subfields were identified using the Franklin and Paxinos Altlas (**A**). Examples of soma area quantification using NDP.view2 (**B**-**D**) and the quantification of the percentage of the area stained measured using Image J (**E**-**G**). Iba-1 positive microglial cells in unprocessed images (**B**)(**E**). Freehand delineation of microglial somas (**C**). Annotation of the Area size calculated by NDP.viewer2. software (**D**). Image converted to blue RBG stack in ImageJ (**E**). Example of manually adjusted threshold level for the estimation of the percentage of area stained by Iba-1 (**G**). Scale bar of 0.5mm (**A**) and 0.025mm (**B**-**G**).

All the data were analysed using the paired T-test with InVivoStat 2.0 (Clark et al., 2012) statistical software. The paired t-test analysis showed a significantly lower area stained by Iba1 quantified by the automatic method than the manual

quantifications (p<0.0001). Moreover, Manual A quantified significantly less stained area (p= 0.0011) compared to Manual B and significantly smaller soma size compared to the automatic method (p<0.0001) and Manual B (p<0.0001).

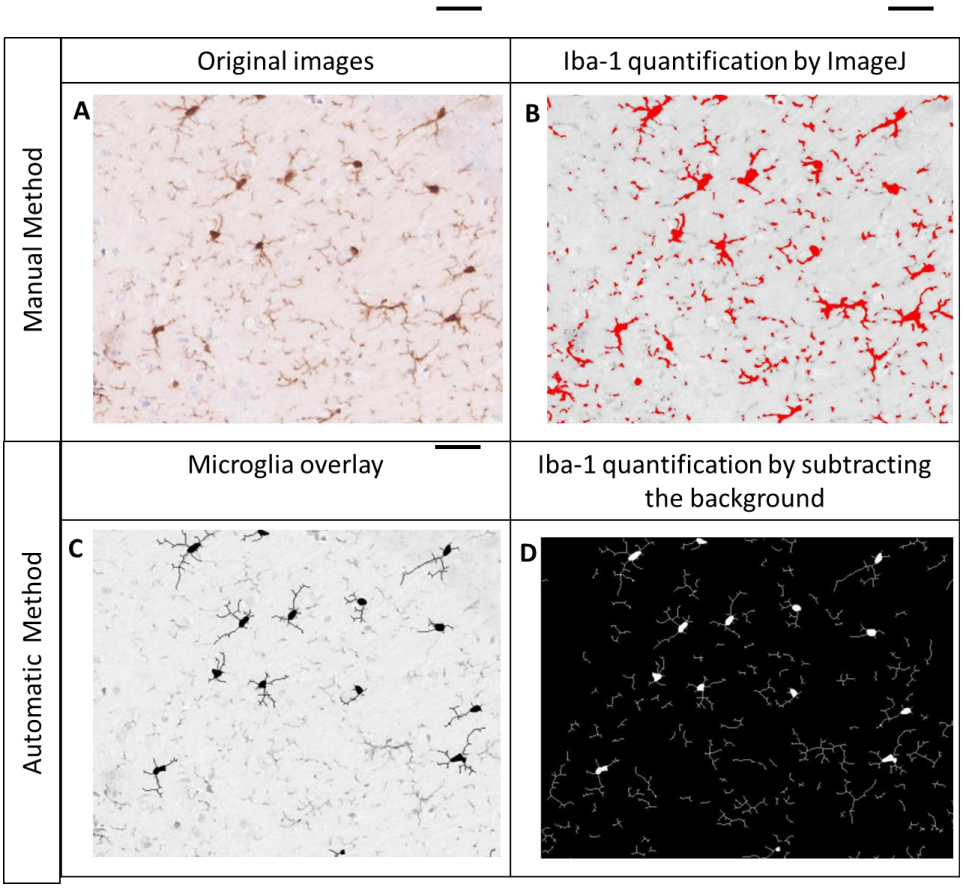

Figure 12. **Visual comparison of manual and automatic cell quantification of microglia**. Image that was analysed with both methods (**A**). Quantification of Iba-1 staining (red highlighted part) with ImageJ (**B**). Illustration of automated quantification of microglia only (**C**). Illustration that shows the automated quantification of the all area stained by Iba-1 (in white) (**D**). Scale bar, 0.05mm.

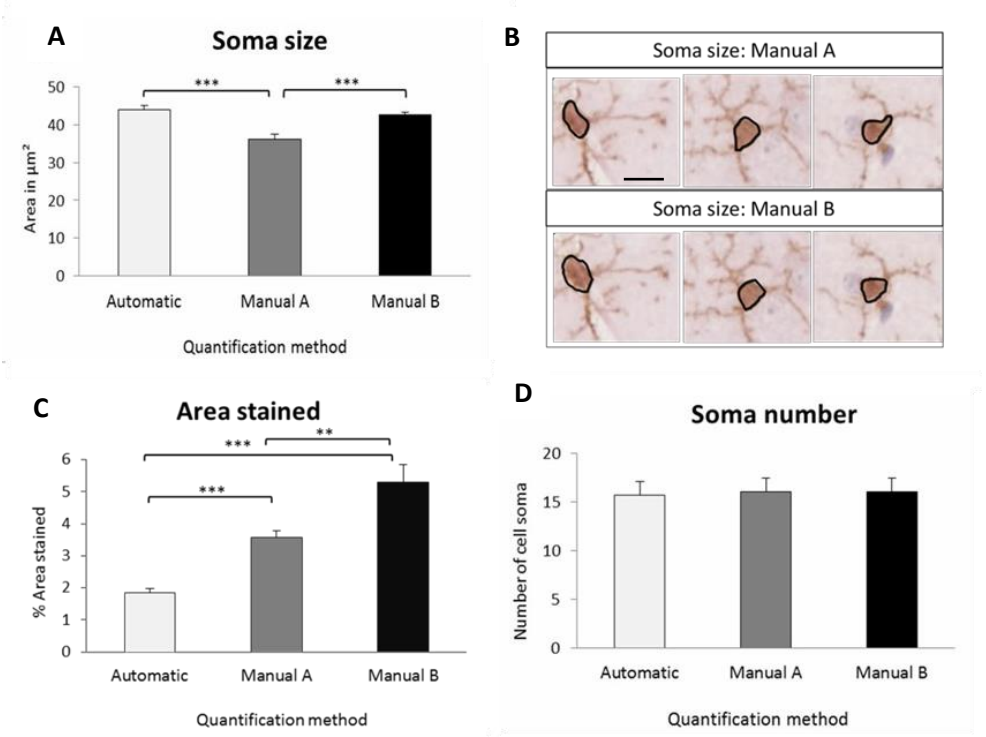

Figure 13. **Comparison of manual and authomatic method.** Percentage of area stained by Iba-1, the microglia soma size and the number of microglia soma, were analysed by manual and automatic methods. Manual A and Manual B identify two different individuals that performed the analysis by ImageJ. The analysis done by Matlab has been named Automatic in the graphs. There were no differences in the number of cells analysis between the methods (**D**). However, the percentage of area stained was smaller with Manual A than Manual B ($p=0.001$) but still higher than the automatic method ($p<0.0001$) (**C**). Thus, Manual B showed a significant higher area stained quantified, than the automatic method ($p<0.0001$) (**C**) and a bigger soma size measured than manual A ($p<0.0001$) (**A**). The automatic method considered a larger somas than Manual A as well ($p<0.0001$) even if it quantified the lowest percentage of area stained ($p<0.0001$) An example of the different manual measure of soma size is illustrated in (B) to visually compare the two manual quantifications. Data are shown as mean $\pm$ S.E.M. [**$p<0.005$, ***$p<0.0001$]. Scale bar, 12.5µm^2.

The comparison of the methods clearly showed how the manual quantification is strongly influenced by subjective criteria, while the automatic analysis is more objective. In fact, the analysis made by the two manual quantifications differed significantly in both the percentage of the area stained and the size of microglia soma. Quantify the percentage of area stained by ImageJ needs a compromise

between excluding artefacts (as blue nuclei) and maintaining the right soma size, or including all the staining, increasing the change to consider artefacts as stained area. In both cases the analysis is compromised.

While the automatic method gives more accurate quantification with the possibility to exclude artefacts and obtaining thinner processes with more precise soma size. This accuracy is achieved by subtracting the background and highlighting the brown staining (Figure 12).

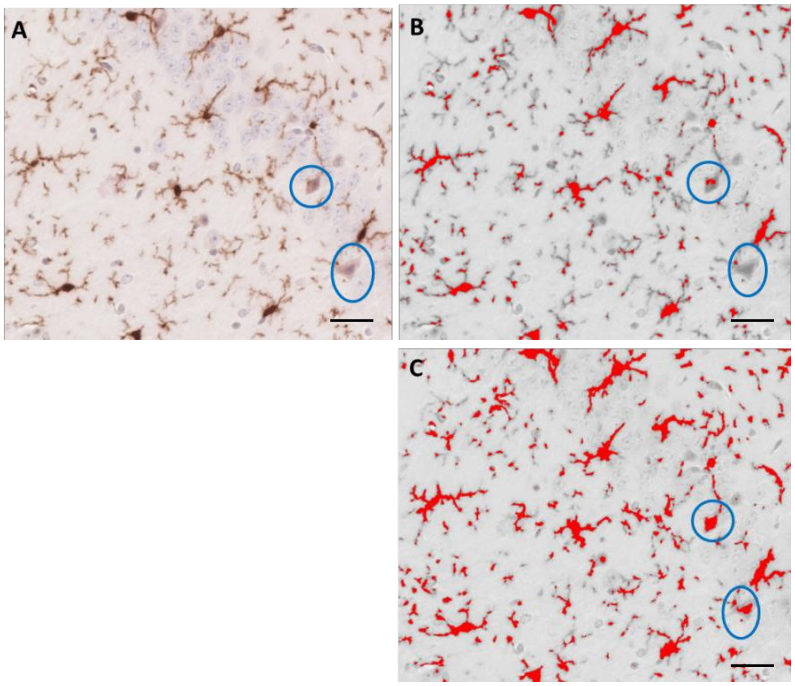

Figure 14. **Illustration of the different criteria for manual quantification**. The original image (**A**) is analysed by ImageJ with two different criteria used by the two examiners: excluding some staining and artefacts and including the all microglia (**B**), or including all the Iba-1 staining but also artefacts that are not stained by Iba-1 (as the blue nuclei circled in blue). Scale bar, 0.05mm.

The analysis of the soma size by the automatic method is based on a previous study of Kozlowski and Weimer that defined a cell soma a contiguous area larger than

16.7 μm^2 (Kozlowski and Weimer 2012). This value was considered as the minimum soma size. While the soma size quantified manually has a subjective criteria: a small soma can be considered microglia or a thick ramification.

2.5.2 Matlab code used for immunostaining analysis

The Matlab code (Ding et al., 2017) was the end result of a collaborative work, written by Yuchun Ding, a computer scientists, and constantly validated by me against ImageJ quantification method.

The code, itself consists of 6 steps run by the experimenter, who need to manually crop the regions of interest and delete the artefacts. Each steps take different time to run, but overall the analysis takes 80 minutes per image. Images from slices immunostained in the same day were analysed at the same time in order to maintain an equal staining threshold.

Briefly the steps of the code are:

- **Step 1**: Reduce image size

Automatically produce small images for each of the exported images. It's essential to decrease the size of the images to speed up the analysis as each image is too large to be managed on Matlab in a short timescale. For example it can change the size from 15.7MB, size of the exported image with a resolution of 16776x9408, to 189KB with a resolution of 1677x940.

- **Step 2**: Cropping subfield

The region of interests are cropped manually. Cortex and hippocampal subfields were identified using the Franklin and Paxinos altlas (Figure 15). Each cropped subfields are then saved in a separate folder automatically.

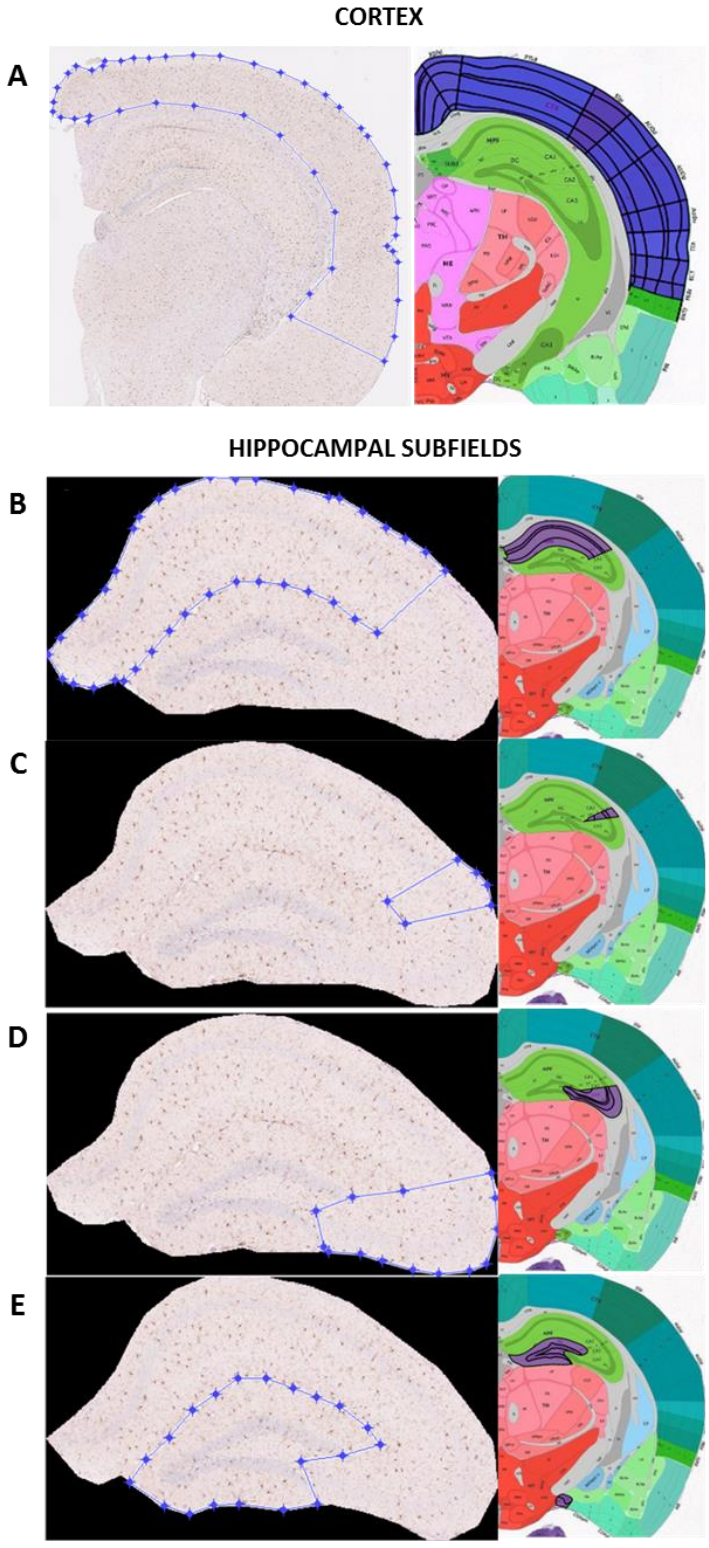

Figure 15. **Illustration of cropping cortex, hippocampus and hippocampal subfields**. Cortex (**A**) and the hippocampal subfields Cornu ammonis CA1 (**B**), CA2 (**C**), CA3 (**D**) and dentate gyrus (DG) (**E**) were identified using the Franklin and Paxinos Altlas as illustrated on the right of each cropped images. Mouse brain atlas images were taken from http://mouse.brain-map.org/static/atlas.

- **Step 3**: Create overlay

Automatic overlay of the cropped area with the original image.

- **Step 4**: Export single microglia soma

Automatic generation of small images for each of the microglia soma in a single folder and manually removal of artefacts and non-specific staining from the folder. Excluded staining were not considered in the final analysis. In particular, in the quantification of Iba-1 stained cells, cell somas in tissue holes or stained in a non-specific way were excluded. (Figure 16). Before the removal of the artefacts is essential to set the optimal threshold suitable for the specific staining in order to reduce the variability between stained batches.

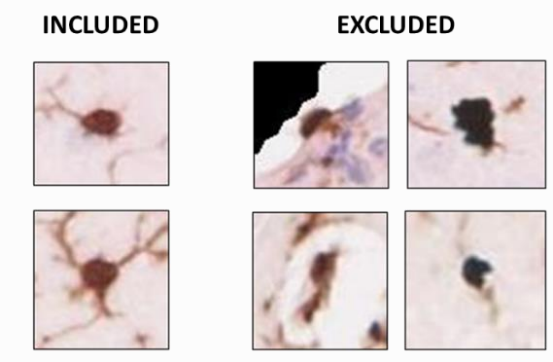

Figure 16. **Illustration of artefact elimination.** Example of included (on the left) and excluded microglia soma (on the right).

- **Step 5**: Staining Segmentation

Automatic generation of images after artefact removal (Figure 17).

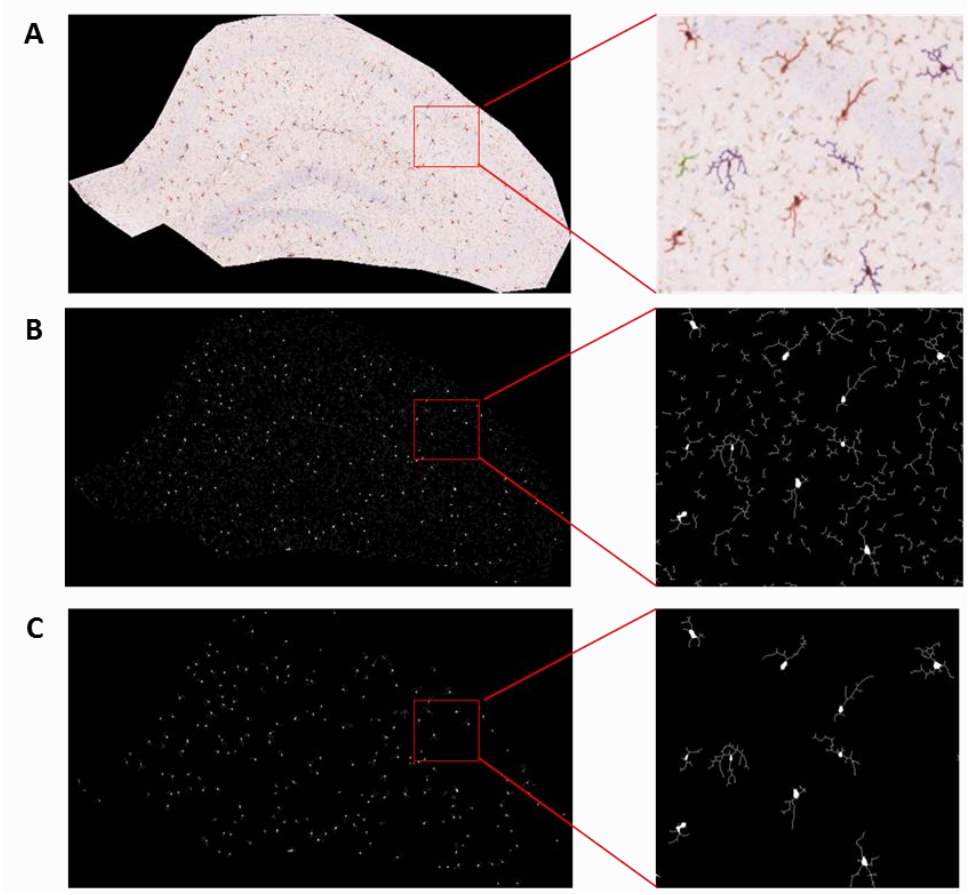

Figure 17. **Illustration of segmented staining.** Hippocampus with coloured microglia with its ramifications (**A**). Hippocampus with subtracted background highlighting full microglia and isolated processes (**B**). Hippocampus with subtracted background highlighting full microglia only (**C**).

- **Step 6**: Analytical output

Analytical output is generated into an excel file. Data are expressed in pixels and then converted into micrometres using pixel size for the analysis. Data for number of cell somas or plaques, soma/plaque density, average of soma/plaque size, area cropped, percentage of area stained and the number of Iba-1 stained cells clusters

were automatically generated from the software for each cropped ROI. The final analysis has been done converting the pixel in the base unit of length, metre.

2.6 Peritoneal macrophages collection

The mice were anesthetized by intraperitoneal injection of pentobarbital 30 mg/kg and peritoneal macrophages isolation was performed according to Ray and Dittel protocol (Ray and Dittel, 2010). The peritoneal cavity provides an easily accessible site for harvesting moderate numbers of resident macrophages and generally provides mature quiescent macrophages (Zhang et al., 2008).

After cleaning the peritoneal area with 70% ethanol a cut of the outer skin of the peritoneum is needed to expose the inner skin lining the peritoneal cavity. With a 30G needle 5ml of ice-cold saline solution containing 3% of fetal bovine serum was injected into the peritoneal cavity and 2ml of the peritoneal fluid was collected using a 25G needle and keept on ice. The collected cell suspension was centrifuged at 800 RCF for 10 minutes at 4°C and the pellet re-suspend in FACS buffer for flow cytometry analysis.

Peritoneal macrophages were collected in order to analyse the espression of surface receptors, to distinguish between M1 and M2 macrophages, and the presence of Aβ peptides intracellularly.

2.7 Animal preparation and brain cell isolation

Mice underwent transcardiac perfusion with cold heparinized saline solution (2U/ml of heparin in sterile PBS) in order to remove circulating blood and inhibit

blood clot formation. Transcardic perfusion was performed manually following Gage et al protocol (Gage et al., 2012). Briefly the animals were fixed in a supine position, the rib cages was opened and the diafram was cut in order to expose the heart. Using a 50ml syringe the harinized saline solution was perfused through the heart until the the fluid exiting the right atrium is entirely clear. The animal was then decapitated and the brain rapidly collected. The brain was divided into the two hemispheres: one hemisphere was collected for further immunohistochemistry analysis, while the other hemisphere were collected for brain cell isolation. The hemisphere was freed from meninges, then cortex and hippocampus were dissected and analyzed separately.

Each tissue collected was placed into 3 mL of ice-cold HBSS to preserve the tissue. The tissue was dissociated first mechanically using a pre-sterilized single-edged blade and then incubated at 37°C for 30 minutes in an enyymatic cocktail. The enzymatic cocktail used in 10ml/g of tissue was made from 5 USP units/ml of neutral protease (Dispase) (Worthington Biochemical Corporation, LS2104), 500 USP units/ml collagenase Type I (Worthington Biochemical Corporation, LS004194), 4000 USP units/ml DNase Type I (Worthington Biochemical Corporation, LS002139) and 30K USP units/ml of hyaluronidase (Worthington Biochemical Corporation, LS002592). After the incubation, the suspension of cells was passed through a 100-µm and then 70µm nylon cell strainer to exclude brain cells bigger than 70µm. The collected cells were centrifuged at 1000g for 10 minutes at room temperature. The pellet was washed and re-suspended in 100µl of FACS buffer (5mM EDTA, 5% fetal bovine serum 0.2% mouse serum in PBS solution) into a minimum cell concentration of 1×10^6 for flow cytometric analysis.

2.8 Flow Cytometry analysis

Samples were incubated with 2% of mouse serum (Vector Laboratories Inc. Burlingame, CA) for 30mins at 4°C to avoid non-specific bindings. Brain cells were then incubated with the LIVE/DEAD™ Fixable Near-IR Dead Cell Stain Kit (L10119 supplied by ThermoFisher Scientific, 1:1000) for 30min on ice. After washes with FACS buffer, samples were incubated with primary antibodies at a concentration of 1 µg/ml for 60 min at 4 °C as followed (see Figure 18 for the schematic protocol):

- Brain cells were incubated with Hoechst and labelled for extracellular markers using APC anti-mouse CD45 [cat number 147708, BioLegend, San Diego (USA)], Brilliant Violet 650™ anti-mouse/human CD11b [cat number 101259, BioLegend, San Diego (USA)], Brilliant Violet 421™ anti-mouse CD206 [cat number 141717, BioLegend, San Diego (USA)], PE anti-mouse CD80 [cat number 104708, BioLegend, San Diego (USA)], PE/Cy7 anti-mouse CD192 (CCR2) [cat number 150612, BioLegend, San Diego (USA)].
- Peritoneal macrophages were incubated with Alexa Fluor® 488 anti-mouse F4/80 [cat number 123120, BioLegend, San Diego (USA)], Brilliant Violet 421™ anti-mouse CD206 [cat number 141717, BioLegend, San Diego (USA)], PE anti-mouse CD80 16-10A1 200UG GBP [cat number 104708, BioLegend, San Diego (USA)], PE/Cy7 anti-mouse CD192 (CCR2) [cat number 150612, BioLegend, San Diego (USA)].

After fixation in 2% PFA for 15mins at room temperature and permeabilization in 0.1% Tween 20 in PBS for 15mins, samples were incubated with endogenous biotin-blocking kit (ca number E21390) as instructed for 30 mins at room temperature

(Figure 18). Cells were finally incubated with biotin anti-β-amyloid 6E10 antibody specific for the 1–16 fragment of the human Aβ protein [cat number 803007, Biolegend, San Diego (USA)] at a concentration of 1 µg/ml for 60 mins (Figure 18). Isotype control and negative control, sample with no staining, were prepared in parallel. After washes in FACS buffer cells were left in the buffer overnight at 4 °C before the analysis. Flow Cytometric analysis was performed with a Beckman Coulter MoFlo Astrios EQ Cells Sorter with the Summit™ Software System. Data were analyzed using Kaluza Analysis 1.5a software. Twenty thousand events were collected for each sample.

See Figure 19 and Figure 20 for the gating strategy used for brain cells and peritoneal macrophages respectively. Briefly, to identify the cells of interest, debris (Figure 19. A-B, Figure 20. A,B), doublets (Figure 19. C, Figure 20.C) and dead cells (Figure 19.D, Figure 20.D) were excluded before gating for microglia and infiltrated macrophages from brain tissue or peritoneal macrophages.

Microglia were identified by the surface expression of CD11b and by low or intermediate expression of CD45 (CD11b+ CD45+Low) (Martin et al., 2017), while infiltrated macrophages also positive for CD11b but show high expression of (CD45 CD11b+ CD45+Hi) (Manitz et al., 2016). Peritoneal macrophages were identified gating for F4/80 (Zhang et al., 2008). Pro-inflammatory (M1) and anti-inflammatory phenotype (M2) where analysed by staining for CD80 and CD206 (Jablonski et al., 2015). To investigate the migratory and infiltration capacity of macrophages, cells were stained for CCR2 (Yang et al., 2014). Finally, cells were stained for Aβ intracellularly to investigate the possibility of an internalization of both microglia and macrophages of the peptide (Lai and McLaurin, 2012).

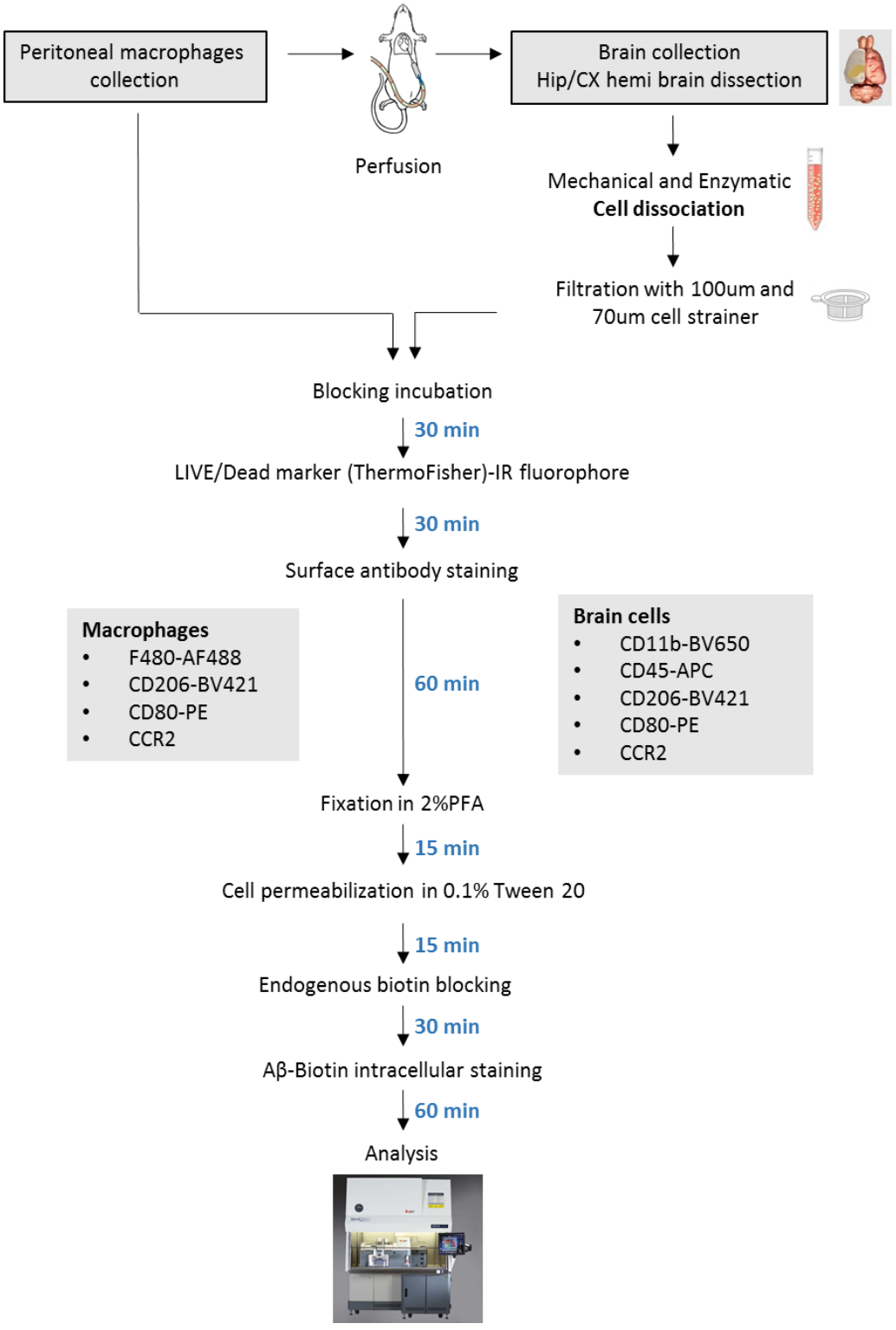

Figure 18. Protocol used to prepare cells for flow cytometry analysis.

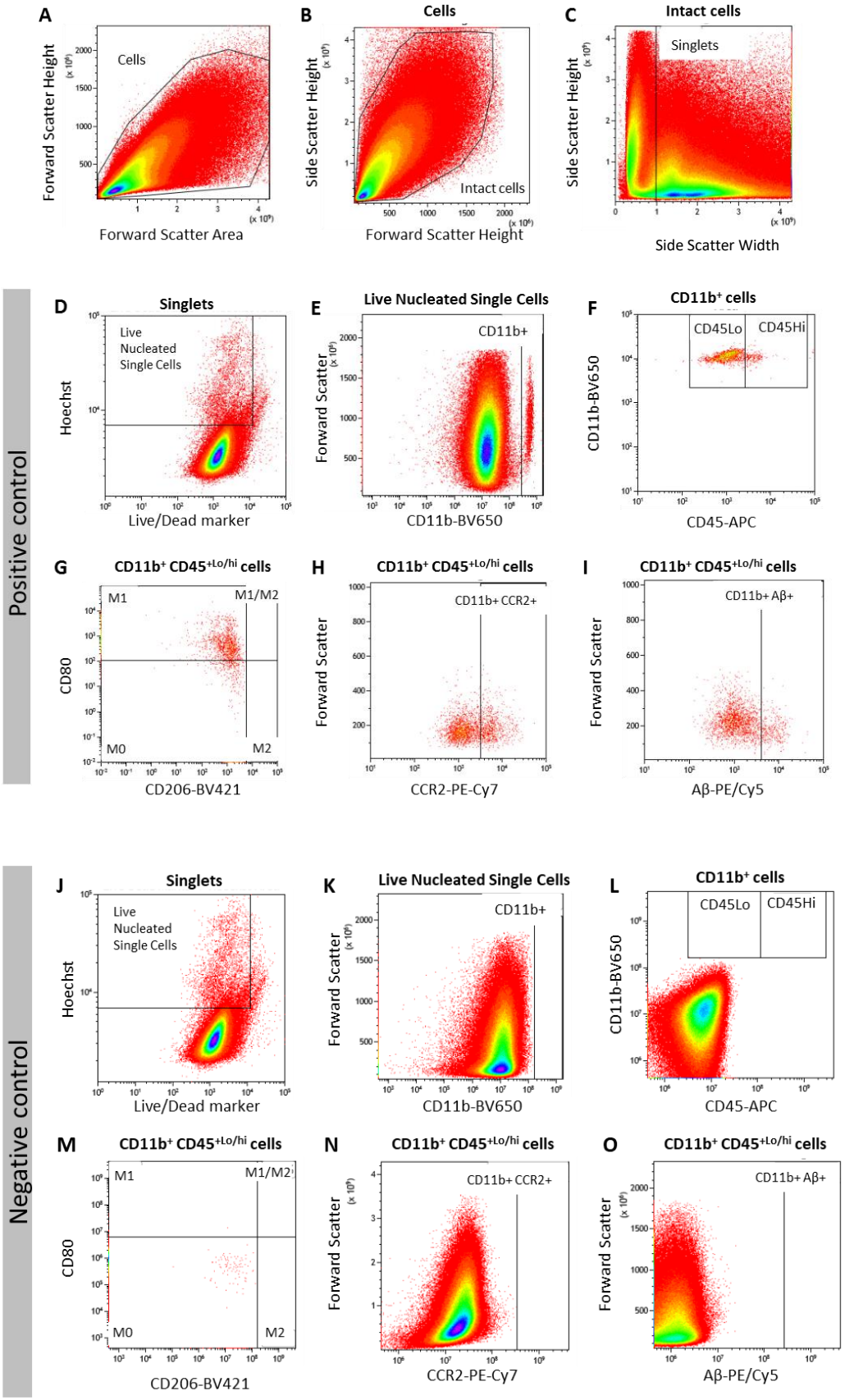
A
Cells
Forward Scatter Height
Forward Scatter Area
B
Cells
Intact cells
Side Scatter Height
Forward Scatter Height
C
Intact cells
Singlets
Side Scatter Height
Side Scatter Width
Positive control
D
Singlets
Live
Nucleated
Single Cells
Hoechst
Live/Dead marker
E
Live Nucleated Single Cells
CD11b+
Forward Scatter
CD11b-BV650
F
CD11b+ cells
CD45Lo
CD45Hi
CD11b-BV650
CD45-APC
G
CD11b+ CD45+Lo/hi cells
M1
M1/M2
M0
M2
CD80
CD206-BV421
H
CD11b+ CD45+Lo/hi cells
CD11b+ CCR2+
Forward Scatter
CCR2-PE-Cy7
I
CD11b+ CD45+Lo/hi cells
CD11b+ Aβ+
Forward Scatter
Aβ-PE/Cy5
Negative control
J
Singlets
Live
Nucleated
Single Cells
Hoechst
Live/Dead marker
K
Live Nucleated Single Cells
CD11b+
Forward Scatter
CD11b-BV650
L
CD11b+ cells
CD45Lo
CD45Hi
CD11b-BV650
CD45-APC
M
CD11b+ CD45+Lo/hi cells
M1
M1/M2
M0
M2
CD80
CD206-BV421
N
CD11b+ CD45+Lo/hi cells
CD11b+ CCR2+
Forward Scatter
CCR2-PE-Cy7
O
CD11b+ CD45+Lo/hi cells
CD11b+ Aβ+
Forward Scatter
Aβ-PE/Cy5

Figure 19. **Gating strategy for brain cells flow cytometry analysis.** After the exclusion of debris (**A**,**B**), doublets (**C**) and dead cells (**D**) by Hoechst and Live/Dead cell staining, the gating strategy for each staining had been identified using a negative and a positive staining. Microglia and infiltrated macrophages were identified by CD11b and CD45 staining, gating for CD11b first (**E**) and then identifying $CD45^{low}$ and $CD45^{hi}$ (**F**). To identify the inflammatory profile, cells were stained and gated for CD80 and CD206 (**G**), as well as CCR2 (**H**). To identifying the presence of intracellular amyloid-beta, cells were also stained for Aβ (**I**). Antigen expression was analyzed considering only $CD11b^{+}$ $CD45^{+}$ cells. Negative control is respectively rapresented from gating J to O.

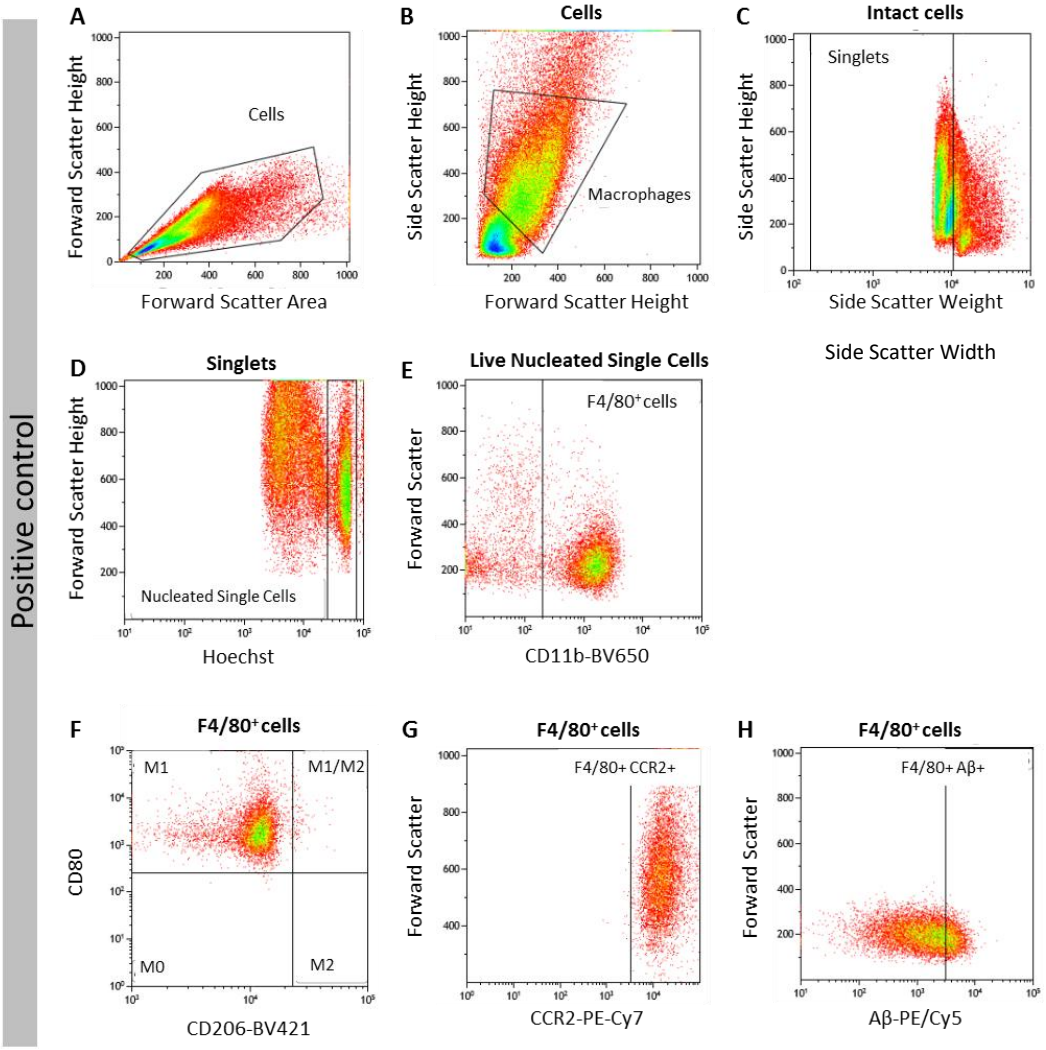

Figure 20. **Gating strategy for peritoneal macrophages analysis.** Representation of flow cytometry analysis of the peritoneal macrophages isolated: after the exclusion of debris (**A**), it was gated for the macrophages population (**B**) and identified singlets (**C**) and nucleated cells by Hoechst (**D**). Macrophages were identified by F4/80 staining. After gating for F4/80 (**E**), cells were stained and gated for CD80 and CD206 (**F**), to identify their inflammatory profile, as well as CCR2 (**G**). To analyse the presence of intracellular Aβ cells were also stained for Aβ (**H**).

2.9 Multiplex Cytokine Assay

Blood was collected into anti-coagulant test tubes. Blood was kept at 4 °C until separation into plasma. Blood was then centrifuged at 3000g for 10mins at 4°C. Samples were then frozen at −80 °C until testing.

On the day of the analysis, samples were defrosted and centrifuged at 10000g for 10 min and the supernatant collected. Samples were tested using a 96-magnetic bead well plate Bio-Plex ProTM Mouse Cytokine 23-Plex, Group I, an immunoassay where a soluble analyte is captured between two antibodies. Samples were processed according to the assay instructions (see Figure 21 for the illustrated protocol). Firstly the plate was incubated with the beads provided by the kit and washed using the magnetic bead separator in order to keep the beads at the bottom of the plate during the washing. The plate was then incubated with standards, samples (1:2 dilution in sample diluent provided in the kit), or the blank control for 30 mins at 850 RPM at room temperature. After the washes, samples were incubated with the biotinylated antibodies for 30 mins at 850 RPM. After washing away the unbounded biotinylated antibodies, the beads were incubated with a reporter streptavidin-phycoerythrin conjugate (SA-PE) for 10 min. Following the removal of excess SA-PE, Levels of cytokines were determined by the Bio-Plex array reader, a bead-based suspension microarray technology (Bio-Plex Pro™ Cytokine immunoassay), which measures the fluorescence of the beads and of the bound SA-PE. During the incubation step, the plate was protected from light and to avoid plate-to-plate variation all samples from the same experiment were analyzed in one plate. Cytokines which were undetected for a sample were assigned

a value of zero. The results were expressed in picograms per milligram of protein and analyzed by two-way ANOVA. $P < 0.05$ was considered statistically significant.

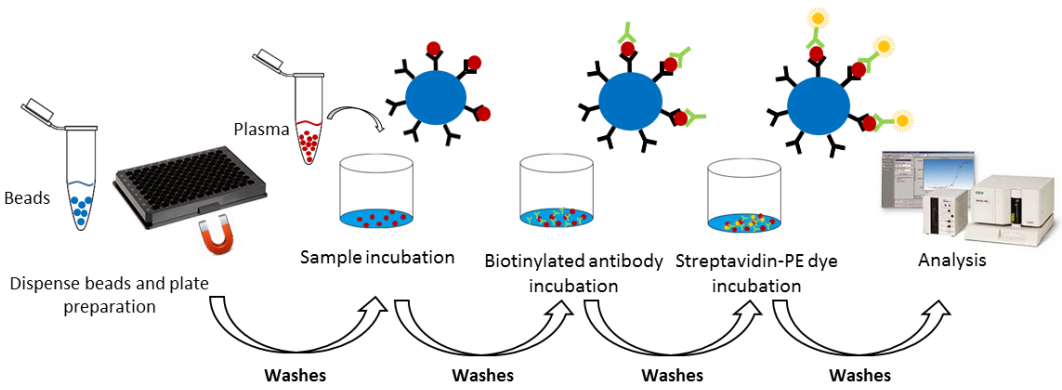

Figure 21. Illustration of the Bioplex bead-based immunoassay protocol.

2.9.1 Statistical Analysis

All the data are expressed as mean + S.E.M. (standard error of the mean) and are analysed using InVivoStat 2.0 statistical software (Clark et al., 2012) and SPSS statistics 22 (Maric et al., 2015). Data were analysed by three-way Analysis of variance (ANOVA) or three-way ANOVAs with repeated measures analysis considering the interaction between sex (female vs male) genotype (wild-type vs APPswe/PS1ΔE9) and treatment (PBS vs LPS). Two-way ANOVA was used to analysed immunostaining of Aβ. In the analysis of behaviour the number of arm entries were used as a covariate for the spatial working memory because results showed it could significantly impact the alternation rate. In the quantification of microglia staining, number of Iba-1 clusters were also used as a covariate for glial analysis as could significantly impact the microglia soma size quantification. Indeed, microglia clustering around amyloid plaques in the APPswe/PS1ΔE9 transgenic

mouse model is well documented (Cartier et al. 2014). ANOVAs were followed by post-hoc multiple pairwise comparisons when appropriate within each experimental group. One-sample t-test were used to determine whether an animal's alternation performance was significantly above the 50% chance level. Paired t-test were used to see any treatment effects and whether post-injection performance differs from the baseline.

A three-way ANOVA has three factors (independent variables) and one dependent variable. The present thesis investigated the interaction between genotype, sex and treatment, considered the three independent variables. Furthermore, a more stringent p-value threshold for the declaration of statistical significance was used, $p<0.0001$, in order to ensure the reproducibility of the study and decrease the rate of false positive.

CHAPTER 3

Gliosis response to an acute systemic infection in 4.5 months old Appswe/PS1ΔE9 mice after 4h

3.1 Introduction

The purpose of the studies described in this chapter was to investigate the acute immune response to LPS (100 µg/kg) in microglial and astrocyte cell populations in 4.5 month old wild-type and APPswe/PS1ΔE9 males and female mice, 4 hours after the treatment. Immune challenges, such as LPS administration, are associated with cognitive impairments, exaggerated sickness behaviour and enhanced glial response due to the release of inflammatory cytokines both peripherally and centrally (Henry et al., 2009). These changes are likely to be exaggerated and prolonged in AD patients and AD mouse models, where microglia have been seen to be more sensitive to immune challenges (Cunningham et al., 2009, Perry et al., 2010). Therefore, I hypothesized that, upon LPS administration, transgenic animals would be more susceptible to the immune challenge with a stronger pro-inflammatory phenotype than the wild-type littermates.

Behavioural, glial and cytokines inflammatory response have been analyzed. Behavioural results will not be reported here as they were part of my MRes project. In brief, behaviour was assessed before and 4h after the treatment using food burrowing and spontaneous alternation tests in order to monitor the LPS-induced sickness syndrome. The results showed overall suppression of daily living (food burrowing) and locomotor activity mediated by LPS, similarly in both genotypes and sexes, while an improvement of spatial working memory was evident in LPS-treated

APPswe/PS1ΔE9 females (see Figure 75 in the appendix). In the present chapter, I will focus instead, on brain changes and cytokine responses associated with these behavioural effects, quantifying microglia and astrocyte densities in hippocampal and cortical regions, as well as peripheral cytokine levels in the plasma.

Based on disease stage and level of inflammation, glial cells show a waxing and waning of numbers, activation state and cytokine expression levels. Indeed, systemic LPS injection has been widely used to trigger a transient acute neuroinflammatory reaction (Yang et al., 2014, Glass, Saijo, Winner, Marchetto, & Gage, 2010) in a variety of diseases and time-points and at different concentrations. Previous research found a significant increase in microglial proliferation in the hippocampus after a single systemic administration of LPS (1 mg/kg) for one week (Fukushima et al., 2015), indicating the hippocampus as a region with high proliferative microglial capability against LPS-induced inflammation. However, a high dose of LPS can result in exaggerated sickness symptoms that can lead to sepsis and confuse cognitive and performance assessments (Sparkman, Kohman, Garcia, & Boehm, 2005, Kondo, Kohsaka, & Okabe, 2011). On the other hand, a mild dose of LPS has been used to mimic systemic infections without impacting on behavioural sickness effects (Couch et al., 2016). Systemic injection of LPS, at 100 µg/kg, had been reported to induce a transient reduction in locomotor activity and acute systemic inflammation with a greater increase in plasma levels of pro-inflammatory mediators IL-6, IL-1β and TNFα (Skelly et al., 2013). Indeed, cytokines are important regulators of humoral and cell-mediated immune responses, and pro-inflammatory cytokines have been seen significantly increased in response to LPS, independently of the dose used. In particular, previous studies have reported

an acute release of pro-inflammatory cytokines that peaked between 2 and 6 hours after a single administration of 100 µg/kg of LPS (Teeling and Perry 2009, Teeling, Cunningham et al. 2010), while anti-inflammatory cytokines peaked after 2 hours and have been detectable until 8 hours post administration (Pardon, 2015). In particular, in transgenic mice models of AD, LPS was found to induce exacerbation of intracellular accumulation of APP and Aβ peptide, as well as tau pathology (Kitazawa et al., 2005, Sheng et al., 2003).

Overall, the present study was designed to investigate genotype susceptibility and sex differences in response to LPS. We used APPswe/PS1ΔE9 mice at 4.5 months old in order to study the inflammatory response at an early stage of the disease in relation to early plaque accumulation, as Aβ plaques start to accumulate from the age of 4 months in the this model used (Malm et al., 2011).

3.2 Study design

Forty-four experimental 4.5 month-old mice were used to assess glial response 4h after LPS injection. 22 APPswe/PS1dE9 transgenic mice (10 males with mean weight: 32.4 ± 0.8 g; and 12 female with mean weight: 23.7 ± 0.4g) and 22 wild-type littermates (12 male mean weight: 32.5 ± 0.4g; and 10 female with mean weight: 26.8 ± 1.1g). Animals were euthanized by cervical dislocation, blood was collected from the neck and the brain was removed immediately. Half of the brain was used to analyze the microglia and astrocytes response by immunohistochemical staining for Iba-1 and GFAP respectively, in the hippocampus and cortex. Eight sections per brain were immunostained at different levels of the hippocampus. The second half was dissected and hippocampus sent to our collaborators for metabolite analysis (data not reported here). Plasma was collected and stored at -80°C. Once samples from all animals were ready, the cytokine assays was performed as described in chapter 2. An illustrated study design is showed in Figure 22.

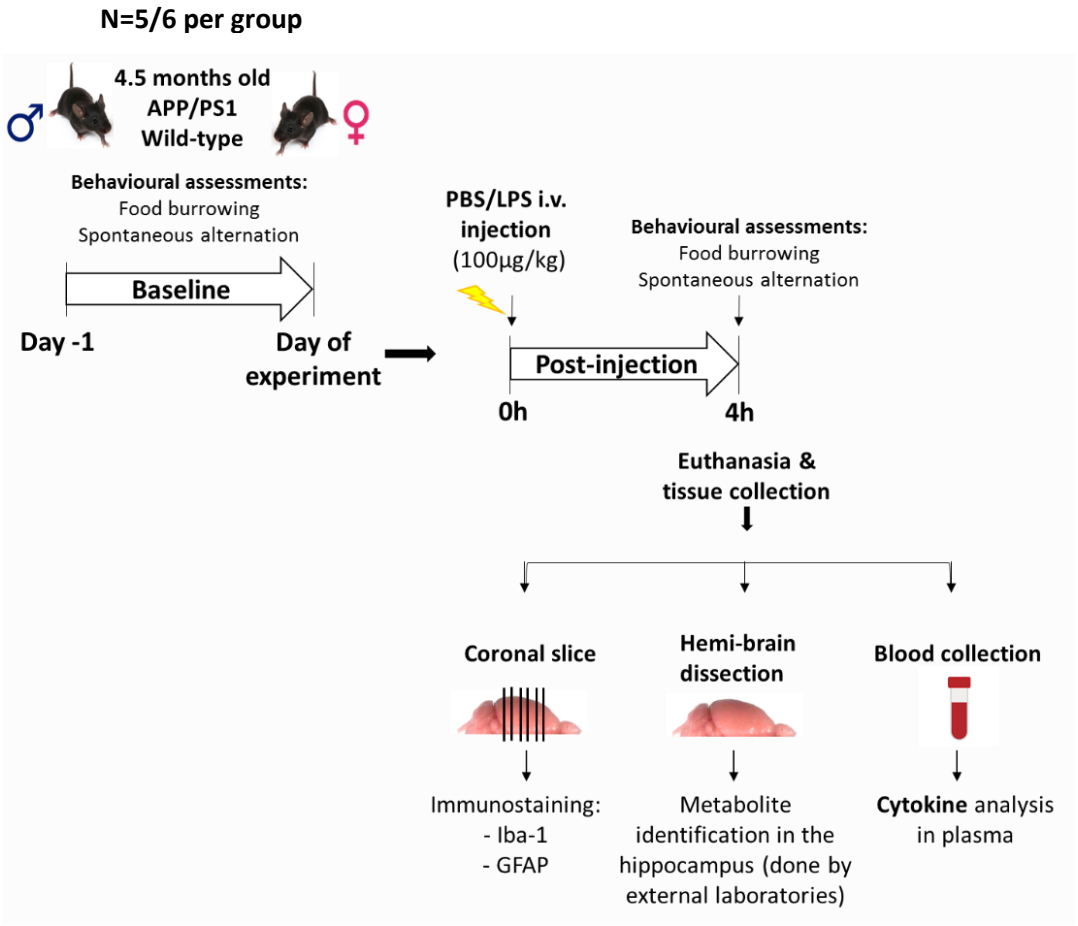

Figure 22. **Schematic experimental timeline**.

3.3 Results

3.3.1 Cytokine Analysis

Cytokine plasma concentration have been quantified using the multiplex array described in the method chapter. Quantification of IL-6 levels (Figure 23.C) in plasma showed overall treatment effects ($F_{(1,37)}$=157.84, p<0.0001), with LPS-injected mice showing elevated protein levels in plasma compared to PBS-treated littermates (p<0.0001), as well as sex X treatment ($F_{(1,37)}$=4.61, p=0.0385) and genotype X treatment interaction effect ($F_{(1,37)}$=7.32, p=0.0102), where LPS-treated wild-type females revealed an higher IL-6 increase than APPswe/PS1 females (p=0.006) and wild-type males (p=0.012). Analysis of IL-10 levels (Figure 23.C) showed an overall treatment effect ($F_{(1,37)}$=36.71, p<0.0001), where a greater concentration of IL-10 was seen in LPS-treated transgenic female (p=0.0016), transgenic males (p=0.029) and wild-type female (p<0.0001) compared to the vehicle-treated counterparts. Sex X treatment interaction ($F_{(1,37)}$=5.82, p=0.021) and sex ($F_{(1,37)}$=4.48, p=0.041) effect was also observed in IL-10 quantification, where LPS-treated wild-type females had significantly greater levels of IL-10 than wild-type males (p=0,002). An overall treatment effect was also seen for TNF-α levels ($F_{(1,37)}$=10.34, p=0.027, Figure 23.E) with LPS-challenged female showing significantly higher TNF-α concentrations than PBS-treated female mice, both in the wild-type (p=0.016) and transgenic (p=0.035) group. No LPS effects were revealed for IL-1β and IFN-γ concentration (Figure 23.A-B).

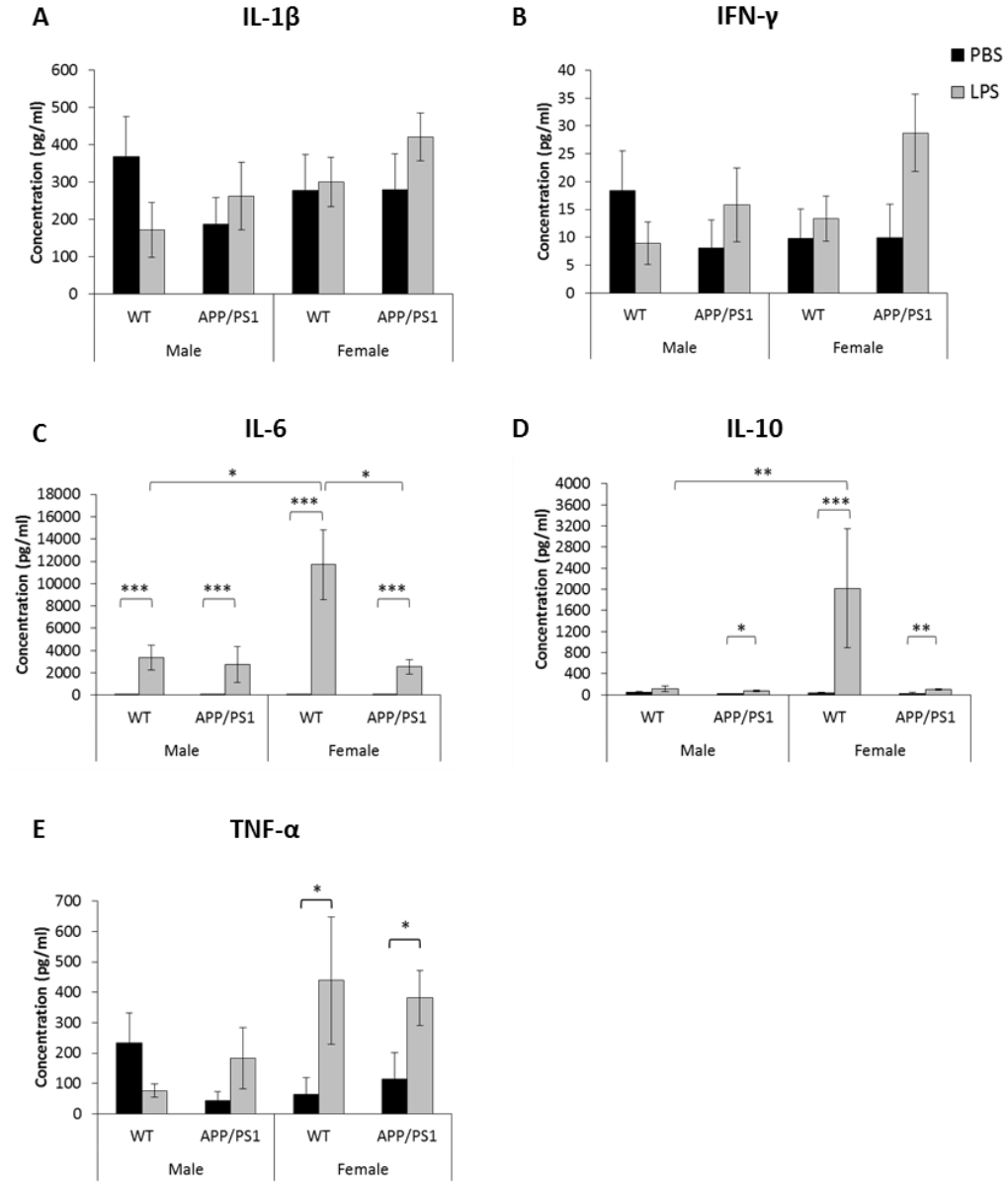

Figure 23. **Cytokines expression in plasma**. 4.5 months old male and female mice APPswe/PS1ΔE9 (APP/PS1) and wild-type (WT) (n=5/6 per group) were treated with LPS or vehicle (PBS) and plasma collected 4h after the challenge. No significant difference observed in IL-1β (**A**) and IFN-γ (**B**) plasma concentration between groups. LPS-injected animals showed higher IL-6 expression than PBS-injected controls: in particular LPS-treated wild-type female revealed higher IL-6 levels than APP/PS1 females (p=0.006) and wild-type males (p=0.012) (**C**). Expression of IL-10 significantly increased in LPS-injected transgenic females (p=0.003) and males (p=0.024) and mostly in wild-type females (p<0.0001) compared to the controls: in particular LPS-challenged wild-type females had higher IL-10 levels than wild-type males (p=0.002) (**D**). A significant increase in TNF-α expression was revealed in females transgenic (p=0.035) and wild-type (p=0.016) only (**E**). Data are shown as mean ± S.E.M. [* p< 0.05, ** p< 0.005 *** p< 0.0001].

3.3.2 Glial response to LPS in the hippocampus 4 hours after the challenge

Analysis of glial activation with the semi-automated method revealed a genotype difference showing a significantly higher percentage of area stained by GFAP and Iba-1, and a significantly increased number of microglial cells and microglial clusters per mm^2 in APPswe/PS1ΔE9 mice compared to wild-type, especially in females. Sex differences were also observed: a significantly higher number of microglia clusters per mm^2 and bigger microglia soma in APPswe/PS1ΔE9 females compare to males, while a significantly lower percentage of area stained by Iba-1 and number of microglia cells/mm^2 in wild-type females compared to males. The number of microglia cells/mm^2 calculated as a measure of the cells density. The percentage of area stained by GFAP and Iba-1 was quantified as a measure of area occupied by microglia and astrocytes respectively.

An overall genotype effect was observed in the percentage of area stained by GFAP in the whole hippocampus ($F_{(1,36)}$=5.04, p=0.031) (Figure 24) and 2 subfields [CA1 ($F_{(1,36)}$=6.16, p=0.032), DG ($F_{(1,36)}$ =5.26, p=0.033)] (Figure 28) with APPswe/PS1ΔE9 females' showing a higher density of GFAP immunoreactivity than wild-type females, being significant in the whole hippocampus (p=0.035) (Figure 24) and DG (p=0.017) (Figure 28).

For the percentage of area stained by Iba-1, an overall significant genotype X sex interaction effect was observed in CA2 ($F_{(1,35)}$=4.65, p=0.038) only, with wild-type females having less area stained than transgenic females (p=0.025) and wild-type male (p=0.035) (Figure 25). For the number of microglial cells/mm2, a significant overall genotype effect was revealed in CA3 ($F_{(1,35)}$ =4.31, p=0.045), where APPswe/PS1ΔE9 mice showed significantly higher microglia density than wild-type

animals (Figure 26). A significant genotype X sex interaction effect was shown in CA2 ($F_{(1,35)}$=4.13, p=0.049), CA3 ($F_{(1,35)}$ =4.36, p=0.044) and DG ($F_{(1,35)}$ = 6.12, p=0.0184) subfields, with wild-type females showing fewer microglia cells per mm^2 compared to transgenic females in CA2 (p=0.026, Figure 25), CA3 (p=0.006) (Figure 26) and DG (p=0.018) (Figure 26) and to wild-type males in CA2 (p=0.018) (Figure 25), CA3 (p=0.0.31) (Figure 26) and DG (p=0.011) (Figure 26). The number of microglial clusters per mm^2 in APPswe/PS1ΔE9 was also significantly elevated in the whole hippocampus ($F_{(1,36)}$ =12.86, p=0.001), CA1 ($F_{(1,36)}$ =6.55, p=0.015) and DG ($F_{(1,36)}$=11.95, p=0.0014) subfields, compared to wild-type mice. In particular APPswe/PS1ΔE9 females showed significantly higher number of microglia clusters than wild-type females in the whole hippocampus (p<0.0001) (Figure 24), CA1 (p=0.01) (Figure 25), CA3 (p=0.023) (Figure 26) and DG (p=0.0073) (Figure 26). APPswe/PS1ΔE9 males also presented greater number of clusters compared to wild-type males in DG (p=0.048) (Figure 26). A significant genotype X sex interaction effect was seen in the whole hippocampus ($F_{(1,36)}$ =7.16, p=0.011) with transgenic females having a greater number of clusters than transgenic males (p=0.037) (Figure 24). An overall sex effect was observed in the analysis of the microglia soma size in CA2 ($F_{(1,36)}$=6.36, p=0.016), CA3 ($F_{(1,36)}$ =9.62, p=0.004) and DG ($F_{(1,36)}$ =5.5, p=0.025) with females showing larger soma compared to their male counterparts. In particular, transgenic females showed larger somas than transgenic males in CA2 (p=0.032) (Figure 25) and CA3 (p=0.007) (Figure 26). The number of microglia clusters used as a covariate did significantly influenced the soma size quantification in the all hippocampus (p=0.015) and CA1 subfield (p=0.0241), but did not influence the percentage of area stained by Iba-1 or the number of microglial cells/mm^2.

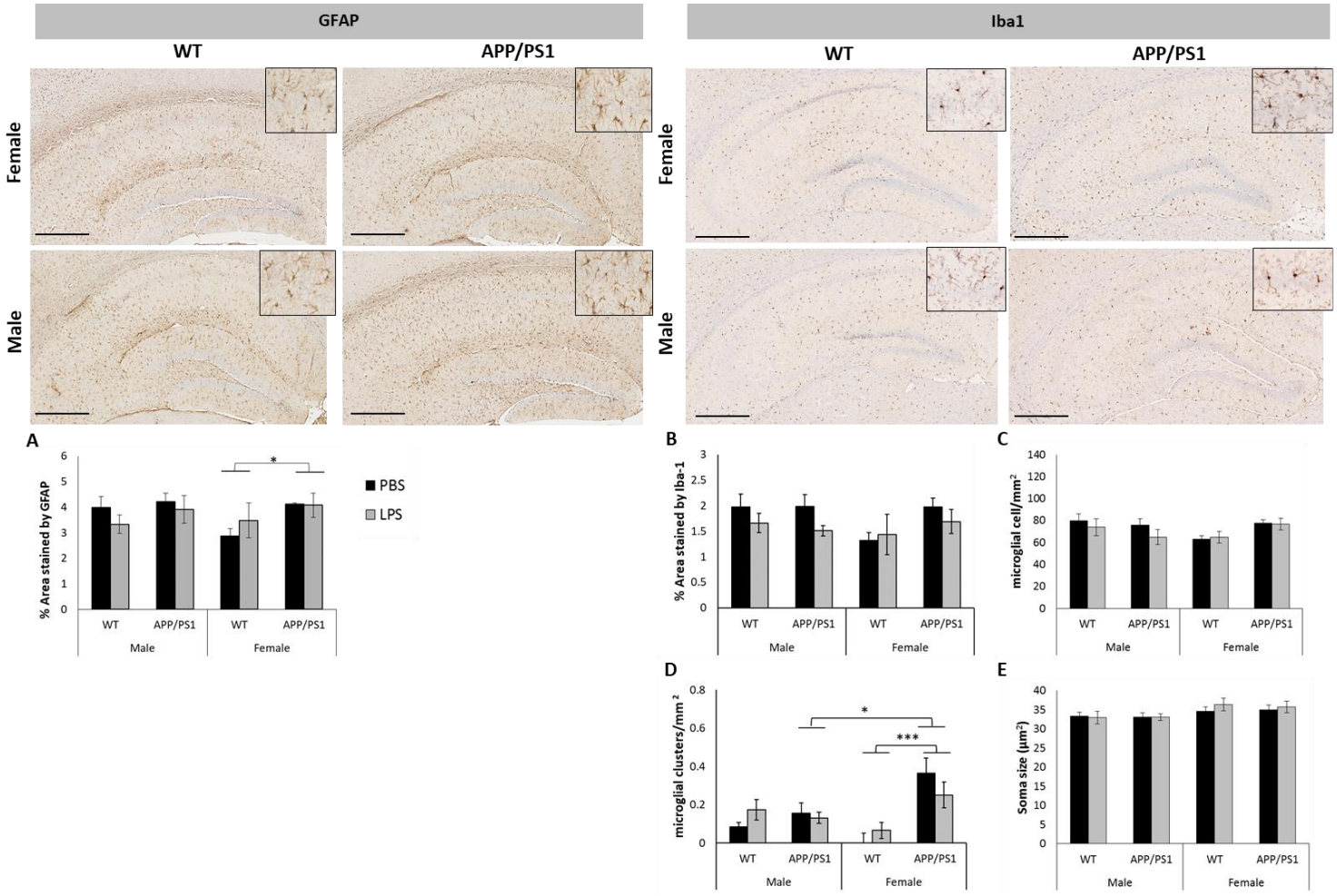
GFAP
Iba1
WT
APP/PS1
Female
Male
A
B
C
D
E
PBS
LPS
% Area stained by GFAP
% Area stained by Iba-1
microglial cell/mm²
microglial clusters/mm²
Soma size (µm²)
Male
Female

Figure 24. **Area occupied by GFAP and Iba-1 in the hippocampus**. 4.5 months old male and mice APPswe/PS1ΔE9 (APP/PS1) and wild-type (WT) (n=5/6 per group) were treated with LPS or vehicle (PBS) and their brain was collected 4h after the challenge. Wild-type female showed lower percentage of area stained by GFAP compared to transgenic female (p=0.035) (**A**), while no significant difference was observed in the percentage of area stained by Iba-1 (**B**) and in the number of microglial cells/mm^2 (**C**). Transgenic females showed higher number of microglia clusters/mm^2 than wild-type littermates (p<0.0001) and transgenic male (p=0.006) (**D**). No significant difference observed in the soma size between groups (**E**). Scale bar, 0.5mm. Data are presented as mean $\pm$ S.E.M. [* p< 0.05, *** p< 0.0001].

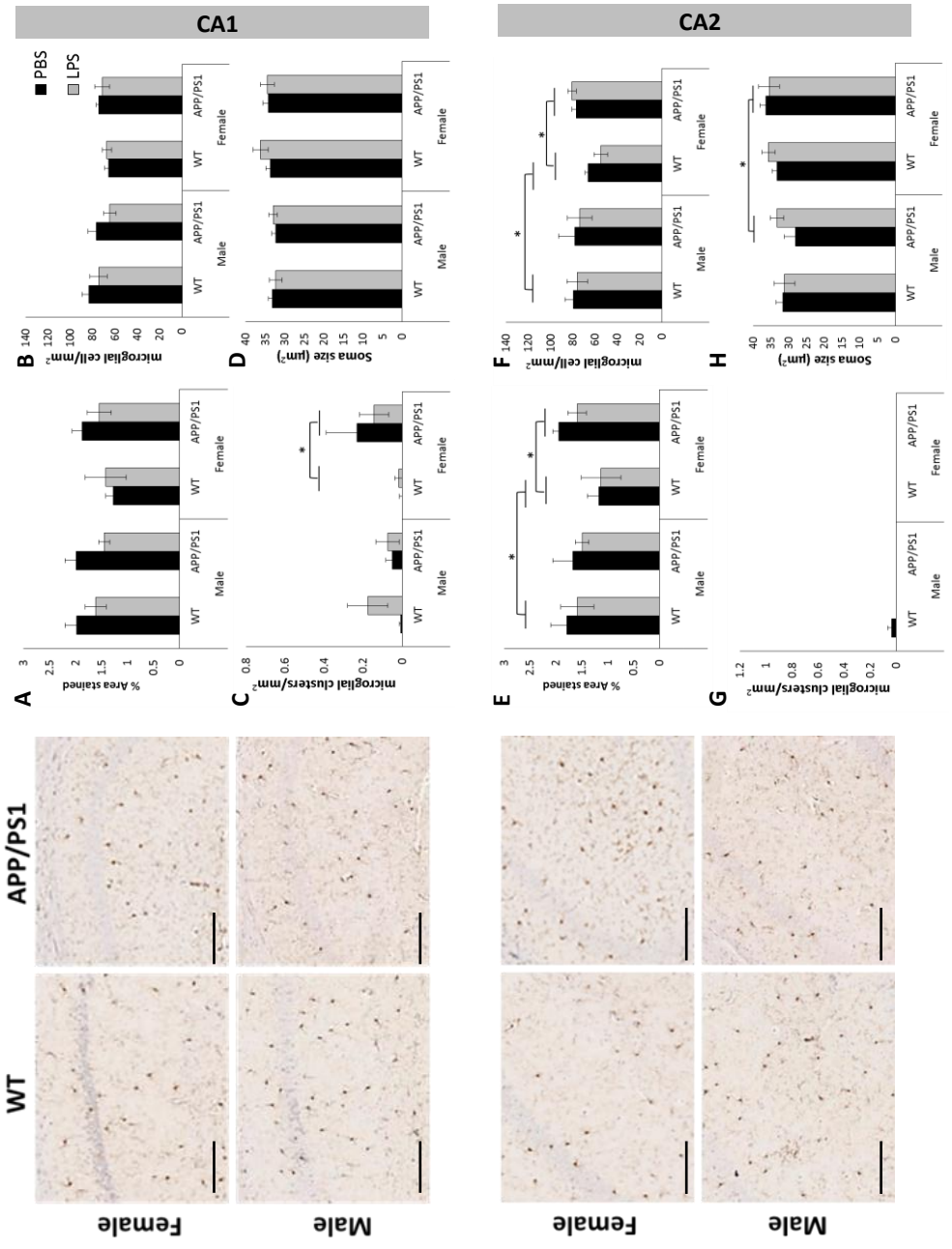
CA1
CA2
PBS
LPS
WT
APP/PS1
Male
Female
% Area stained
microglial cell/mm²
microglial clusters/mm²
Soma size (µm²)
A
B
C
D
E
F
G
H
WT
APP/PS1
Female
Male

Figure 25. **Area occupied by Iba-1 in the hippocampal subfields.** 4.5 months old male and female APPswe/PS1ΔE9 (APP/PS1) and wild-type (WT) (n=5/6 per group) were treated with LPS or vehicle (PBS) and their brain was collected 4h after the challenge. No significant difference was observed in the percentage of area stained by Iba-1 in CA1 (**A**), while in CA2 wild-type females showed less area stained by Iba-1 compared to transgenic females (p=0.025) and wild-type males (p=0.035) (**E**). No significant difference was observed in the number of microglial cells/mm^2 in CA1 (**B**) while wild-type females showed less number of microglial cells/mm^2 compared to transgenic females (p=0.026) and wild-type males (p=0.018) in CA2 (**F**). Higher number of microglial clusters/mm^2 was revealed in transgenic females compared to wild-type females in CA1 (p=0.01) (**C**). Transgenic female revealed a bigger microglia soma size than transgenic male in CA2 (p=0.032) (**G**). Scale bars, 0.25mm. Data are presented as mean $\pm$ S.E.M. [* $p< 0.05$, ** $p<0.005$].

CA3
DG
PBS
LPS
A
B
C
D
E
F
G
H
% Area stained
microglial cell/mm²
microglial clusters/mm²
Soma size (µm²)
WT
APP/PS1
Male
Female
WT
APP/PS1

Figure 26. **Area occupied by Iba-1 in the hippocampal subfields.** 4.5 months old male and female mice APPswe/PS1ΔE9 (APP/PS1) and wild-type (WT) (n=5/6 per group) were treated with LPS or vehicle (PBS) and their brain was collected 4h after the challenge. No significant difference was observed in the percentage of area stained by Iba-1 in CA3 (**A**) and DG (**E**). Wild-type females showed less number of microglial cells/mm^2 compared to transgenic females in CA3 (p=0.006) (**B**) and DG (p=0.018) (**F**) and also compared to wild-type males in CA3 (p=0.031) (**B**) and DG (p=0.010) (**F**). Higher number of microglial clusters/mm^2 was revealed in transgenic females compared to wild-type females in CA3 (p=0.023) (**C**) and in DG (p=0.0073) (**G**) and in transgenic males compared to wild-type males in DG (p=0.048) (**G**). Transgenic female revealed a bigger microglia soma size than transgenic male in CA3 (p=0.0068) (**D**). in DG, overall, females showed a bigger microglia soma size than males (p=0.025) (**H**).Scale bars, 0.25mm. Data are presented as mean $\pm$ S.E.M. [* $p < 0.05$].

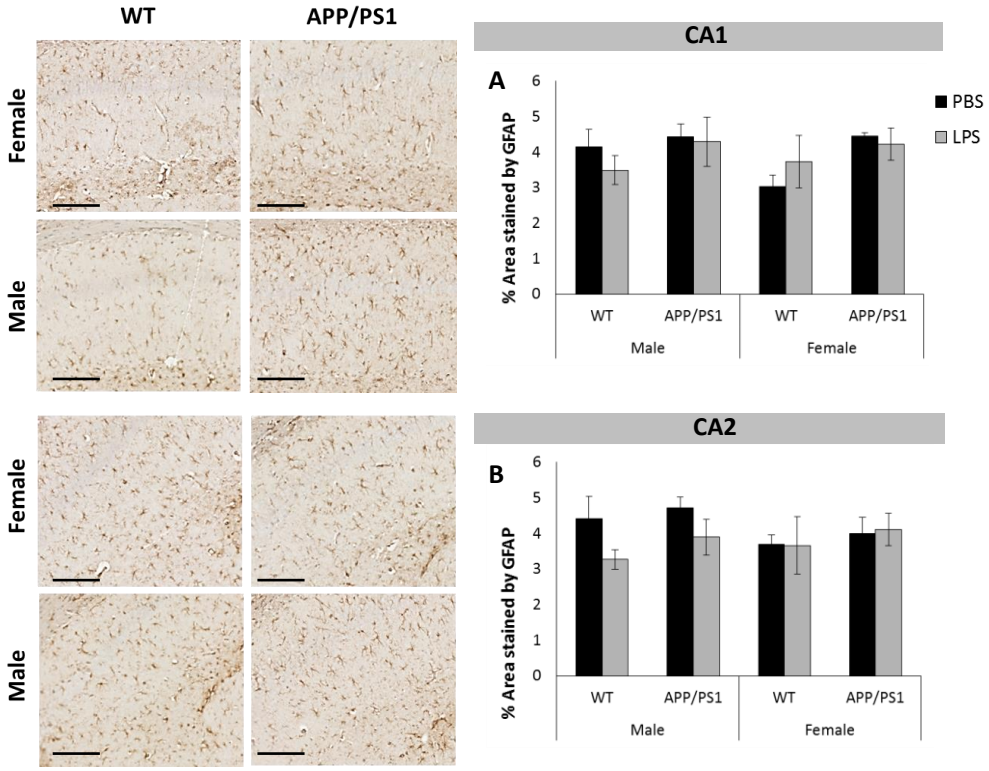

Figure 27 **Area occupied by GFAP in the hippocampal subfields.** 4.5 months old male and female mice APPswe/PS1ΔE9 (APP/PS1) and wild-type (WT) (n=5/6 per group) were treated with LPS or vehicle (PBS) and their brain was collected 4h after the challenge. No significant difference was observed in the percentage of area stained by GFAP in CA2 (**B**), while a lower percentage of area stained by GFAP was observed in wild-type females compared to transgenic females in both CA1 (p=0.03) (**A**). Scale bars, 0.25mm. Data are presented as mean ± S.E.M.

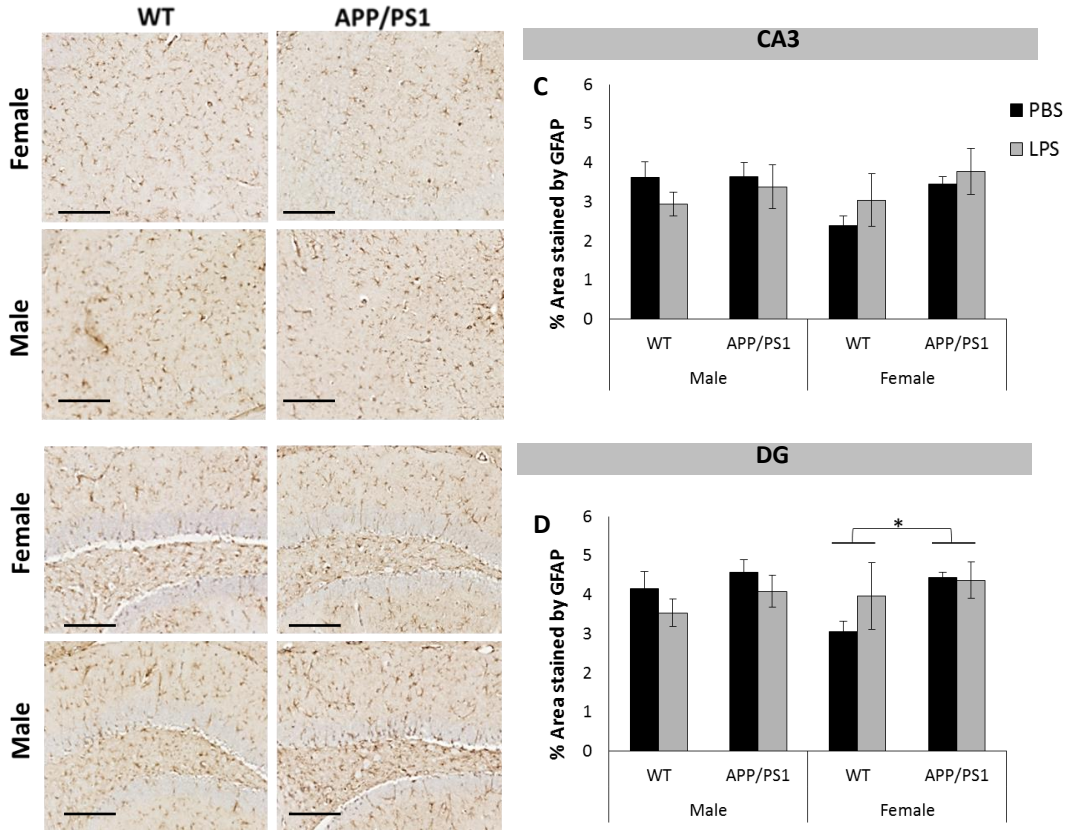

Figure 28 **Area occupied by GFAP in the hippocampal subfields.** 4.5 months old male and female mice APPswe/PS1ΔE9 (APP/PS1) and wild-type (WT) (n=5/6 per group) were treated with LPS or vehicle (PBS) and their brain was collected 4h after the challenge. No significant difference was observed in the percentage of area stained by GFAP in CA3 (**C**), while a lower percentage of area stained by GFAP was observed in wild-type females compared to transgenic females in DG (p=0.017) (**D**). Scale bars, 0.25mm. Data are presented as mean ± S.E.M. [* p< 0.05].

3.3.3 Microglia response to LPS in the cortex.

Analysis of microglial activation in the cortex revealed an overall sex effect in the number of cells per mm^2 ($F_{(1,36)}$ = 7.04, p=0.012) with wild-type female showing less microglial cells/mm^2 than wild-type males (p=0.027, Figure 29.B). A genotype X sex interaction effect was also observed in the number of microglial clusters per mm^2 ($F_{(1,36)}$ = 5.94, p=0.012) with lower number observed in wild-type female compared to transgenic female (p=0.0065) and transgenic males (p=0.016) (Figure 29.C). The number of microglia clusters used as a covariate did significantly influence both percentage of area stained by Iba-1 ($F_{(1,35)}$ = 4.82, p=0.0348) and the soma size ($F_{(1,35)}$ = 4.67, p=0.038).

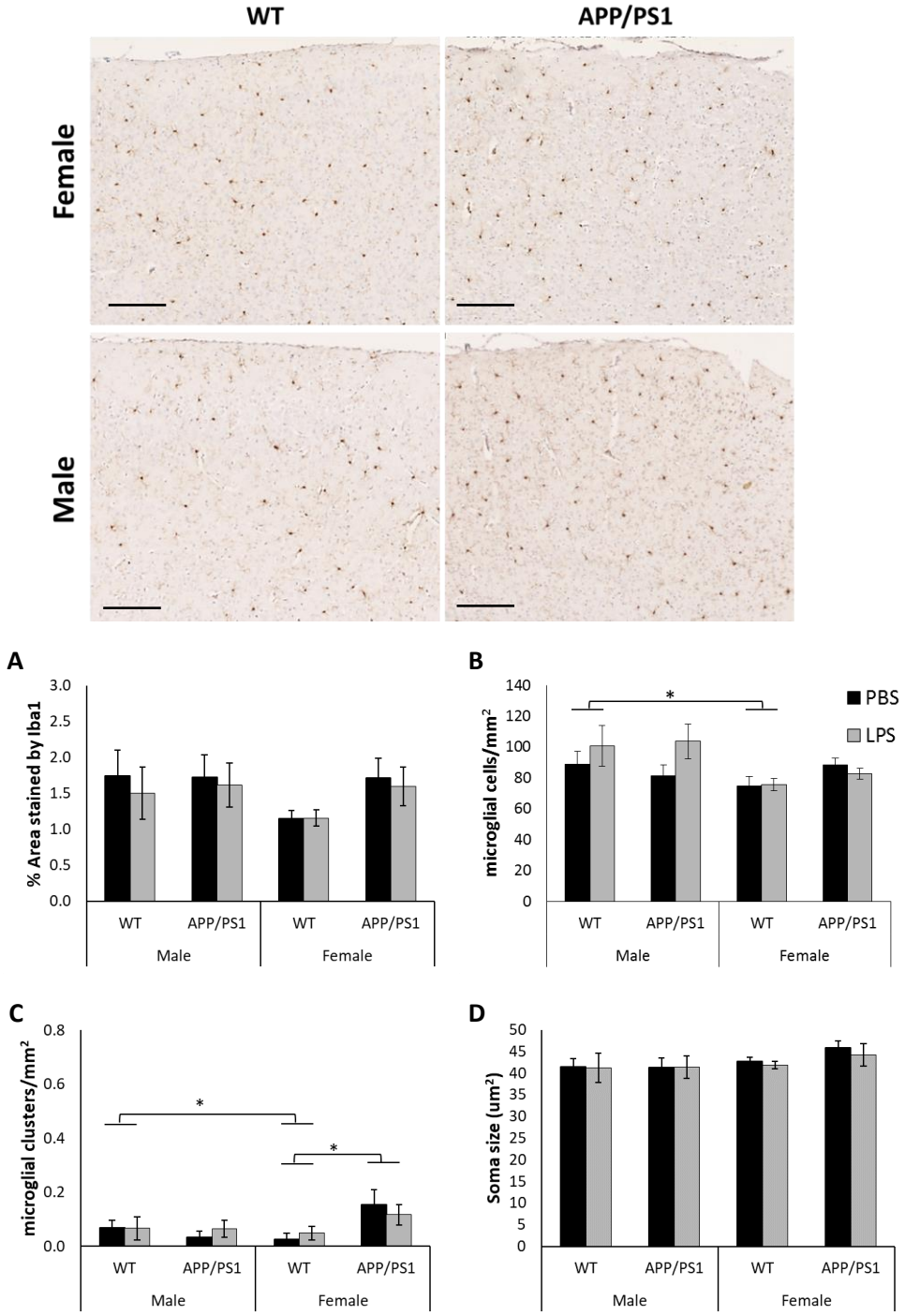

Figure 29 **Area occupied by Iba-1 in the cortex**. 4.5 months old male and female mice APPswe/PS1ΔE9 (APP/PS1) and wild-type (WT) (n=5/6 per group) were treated with LPS or vehicle (PBS) and brain collected 4h after the challenge. No significant difference was observed in the percentage of area stained by Iba-1 (**A**). Wild-type female also presented lower number of microglial cells/mm^2 compared to wild-type male (p=0.027) (**B**). Higher number of microglial clusters/mm^2 was revealed in transgenic female compared to wild-type female (p=0.016) and transgenic male (p=0.0065) (**C**). No difference observed in the soma size between groups (**D**). Scale bars, 0.25mm. Data are presented as mean $\pm$ S.E.M. [* p< 0.05].

3.4 Discussion

In the present study, lipopolysaccharide was administered systemically to test the hypothesis that 4.5 months old APPswe/PS1ΔE9 mice were more susceptible to an immune challenge than wild-type mice, and to determine if the susceptibility was sex-dependent. The data supported the hypothesis showing, only in transgenic female mice higher susceptibility to the immune challenge compared to wild-type mice. These findings highlited also a sex differences with transgenic male not being more susceptible to LPS compared to wild-type littermated. LPS was used as an immune modulator at a dose of 100µg/kg of animal body weight to determine the effect of an acute systemic immune challenge on both male and female 4 hours later. Behavioural changes (results shown in the appendix, Figure 75), as well as plasma cytokines and central glial response to LPS, were analyzed to assess susceptibility. LPS induced an increase in the concentration of pro-inflammatory cytokines IL-6 and TNF-α, as well as the anti-inflammatory IL-10 in plasma. In particular, wild-type females had greater increase of cytokines than transgenic female (IL-6) and wild-type males (IL-6 and IL-10). On the other hand, LPS did not affect glial response in the brain, but a sex difference was revealed, where wild-type females showed a reduction in astrocytes and microglia densities compared to the transgenic females and to wild-type males.

Investigation of plasma cytokines levels revealed a pro-inflammatory response to the peripheral immune challenge. A significant increase in circulating pro-inflammatory cytokines IL-6, and TNF-α and the anti-inflammatory mediator IL-10 was found in LPS-treated animals. However, LPS did not affect pro-inflammatory IL-

1β and IFN-γ levels, contrary to what was found in previous reports of acute LPS responses. LPS-treated mice did not show an increase in IFN-γ levels, which were expected. Data from a previous study observed just a transient elevation of IFN-γ serum concentrations peaking 4–5 hours after LPS administration (Lauw et al., 2000). An LPS-induced increase of IL-1β was also expected as several studies reported high levels of pro-inflammatory cytokines in association with microglia activation (Shaftel et al., 2007). LPS-enhancement of IL-1β was reported both *in vitro* (John et al., 2005, de Souza et al., 2009) as well as *in vivo* in mice (Cunningham and Sanderson, 2008) and humans (Wynne et al., 2010, Chen et al., 2008). Interestingly, LPS-treated mice did not show higher levels of IL-1β 4 hours after treatment. Various reasons could explain this contradictory finding: one could be that the dose given was not high enough to enhance the secretion of IL-1β. The second reason for the lack in IL-1β response to LPS can be related to the stress caused by the handling of the mice during the behavioural tests performed both before and after LPS administration. Indeed, stress is known to decrease pro-inflammatory cytokines expression via glucocorticoid induction (Propes and Johnson, 1997). The third reason might be that the timelines for sampling collection needed to be optimized, allowing longer or shorter time after LPS injection. Moreover, IL-1β expression could be suppressed by high levels of IL-10, known to play an essential part in controlling the overproduction of pro-inflammatory cytokine, in order to contain the spread of the immune response (Saraiva and O'Garra, 2010, Bachstetter et al., 2014). However, in the present study, a significant elevation in levels of IL-10 was mainly observed in LPS-treated females, with a greater increase in the anti-inflammatory cytokine seen in wild-type females compared to wild-type males. These high levels of IL-10 in wild-type females could

elicit a protective effect. Indeed, IL-10 is known to play a role in controlling excessive inflammation, inhibiting the production and secretion of pro-inflammatory cytokines in the periphery (Lauw et al., 2000) as well as downregulating activation of microglia in the brain (Lobo-Silva et al., 2016).

However, an LPS-induced increase in TNF-α and IL-6 was also seen here and this can be explained by the distinct cytokine time-course induced by the challenge: TNF-α peaks before the other pro-inflammatory mediators and IL-6 was reported to be the most responsive pro-inflammatory cytokines among the others (Pardon, 2015). In particular, plasma levels of TNFα peak at 2-hour post LPS injection and returned to baseline after 5 hours, as well as levels of IL-6 peak at 2-hour and remain measurable for several hours after the challenge (Ventura et al., 2010). Interestingly, TNF-α levels were found to be significantly higher in both wild-type and transgenic LPS-treated females, but not in male mice. A difference between sexes was also revealed in IL-6 quantifications where wild-type female mice had significantly higher levels of IL-6 than transgenic females and wild-type males. It is important to consider that LPS is indeed a potent inducer of TNF-α expression in both monocytes and macrophages (Lee and Sullivan, 2001) as well as IL-6, that can also be indirectly induced via TNF-α signaling pathways (Ghezzi et al., 2000). However, in contrast with the findings reported here, previous in-vitro (Santos-Galindo, Acaz-Fonseca et al. 2011) and in-vivo (Kuo, 2016) studies found the opposite, revealing higher TNF- α levels in males compared to control females. Santos-Galindo et al. observed a significantly higher increase in mRNA levels of TNFα in astrocytes derived from male or androgenized females after 5 hours incubation with LPS (Santos-Galindo, Acaz-Fonseca et al. 2011). Kuo revealed a

significantly higher level of the pro-inflammatory cytokines in plasma starting at 3 hours after peritoneal injection of LPS in ten-week-old mice, reporting also that the difference was independent of the level of endotoxin dosage and the genotype (Kuo, 2016). The levels of IL-6 was also seen to be higher in males compared to females, suggesting greater vulnerability of males to infection and inflammation (Everhardt Queen et al., 2016).

Interestingly, data from a clinical study on pain sensitization revealed a more pronounced LPS-induced cytokine increase in plasma samples of women compared to men (Wegner et al., 2015), with significantly higher TNFα levels up to 4 hours post-injection. TNFα is known to play a central role in the perpetuation of inflammation in chronic diseases (Parameswaran and Patial, 2010). Together with the finding of elevated IL-6 levels seen in females only in response to LPS, our data could suggest that, peripherally, females might be more susceptible to inflammation, leading to the expectation of a higher glial response in the brain of female mice compared to males. The analysis of the central immune response showed a lower microglia density in wild-type females compare to transgenic females and wild-type males, with no effects mediated by LPS.

Indeed, our findings did not reveal a higher susceptibility of APPswe/PS1ΔE9 mice to LPS compared to control mice, as was expected, but a genotype and sex difference was observed. Regarding the glial response, I measured glial density, microglial soma size, used as a marker of activation, and the number of microglia clusters, known to be related to amyloid plaques, in both the hippocampus and cortex. Our study revealed a lower microglial density in wild-type females compared to APPswe/PS1ΔE9 females in CA2, CA3, and DG hippocampal subfields

and compared to wild-type males in the cortex. Microglia response to an immune challenge was positively associated with alterations in the number of microglial cells and their distribution in the brain (Kim et al., 2000). In particular, Kim's laboratories showed that the difference in the number of microglial cells in distinct brain areas was based on region-specific differential susceptibility to LPS, leading to the hypothesis that lower numbers of microglia cells can be associated with a lower susceptibility to an immune challenge. An in-vitro study also demonstrated that high density of microglial cultured is associated to a pronounced pro-inflammatory response, whereas a low microglial density could be associated to an anti-inflammatory response (Pintado et al., 2011). Thus, the lower density of microglia seen in our wild-type female compared to transgenic female or the male counterpart suggests that wild-type female are less susceptible to the immune stimulation, possibly associated with anti-inflammatory response. Indeed, this hypothesis is also supported by the data here showing a greater increase in the peripheral anti-inflammatory cytokine IL-10 in wild-type females compared to males.

Looking at microglia activation, I expected a higher cell activation in transgenic mice than wild-type mice treated with LPS, as increasing lines of evidence indicate that microglia develop a pro-inflammatory phenotype (primed) in AD mouse models, characterized by a lower threshold to inflammatory stimuli and a higher inflammatory response (Wirz et al., 2013). Indeed, in-vitro experiments showed how the presence of inflammation at early stage of the disease might be exaggerated by a mild immune challenge (Perry, Cunningham, and Holmes 2007), and also an in-vivo studies revealed higher Iba-1 immunoreactive microglia in young

APPswe/PS1ΔE9 mice after intra-hippocampal injections of LPS, compared to wild-type mice (Go et al., 2016a). These previous data support our hypothesis that APPswe/PS1 mice are more susceptible compared to wild-type animals, but current data do not support this hypothesis. It is likely that the increased number of microglial cells that I found is due to a change in microglia proliferation, and not mediated by the immune challenge itself. However, we need to consider that LPS does not cross the blood-brain barrier and the amount that reaches the brain after intravenous administration is estimated to be only 0.025% (Banks and Robinson, 2010). Thus, immune response in the CNS is not mediated through direct activation of TLR4, as it is unlikely that enough LPS, administered systemically, enters the brain at a low dose. The CNS and immune system interact through cytokine signaling that might act directly or indirectly with brain cells (Hasegawa-Ishii et al., 2016, Dunn, 2002). This could be the reason for our lack of clear glial susceptibility to LPS. Another reason would be the short time-point chosen, as peripheral cytokines need to be synthesized and then cross the BBB or interact with endothelial receptors that indirectly mediate the signaling (McCusker and Kelley, 2013). A recent review showed that a single-dose LPS challenge activates microglia 6 hours after challenge and the activation remains for up to 3 days (Hoogland et al., 2015). However, I decided to select a 4-hour time point based on a previous experiment conducted by my research group revealing higher microglia activation in wild-type mice 4 hours after an acute challenge using the same low dose of LPS (Pardon et al., 2016). In this study, though, I haven't seen a significant increase of microglia density or microglia soma size mediated by LPS. This lack of microglia response to LPS seen here can be due to the difference in the study design as Pardon et al., kept the mice under anesthesia for the duration of the experiment before collecting the brain.

Indeed, the anesthetic itself can increase susceptibility to infections (Kelbel and Weiss, 2001) possibly promoting BBB permeability to the LPS, as it was found that anesthesia was able to increase BBB permeability to small molecules in 2 hours (Yang et al., 2017)

Interestingly, here, wild-type female mice showed a lower microglia density and number of cells/mm^2 compared to males. Studies on brain development in both males and females rodent have seen a shift in microglia density and microglia phenotype from the neonatal period to adulthood, possibly based on the different exposure to sex steroids (McCarthy et al., 2015). A gender difference in the endotoxin and pathogen-induced inflammation had been reported in both humans and animals. It is known that estrogens modulate the immune response by influencing gene transcription via it's α and β receptors: on one hand 17β-estradiol in young females can induce the production of pro-inflammatory mediators, inhibiting expression of anti-inflammatory cytokines, through the activation of NF-κB (García-Gómez et al., 2013, Gosselin and Rivest, 2011). On the other hand 17β-estradiol can have anti-inflammatory properties, particularly towards microglia, interfering with the LPS signal transduction, inhibiting the transcription of inflammatory genes (Vegeto et al., 2008, Vegeto et al., 2001, Pozzi et al., 2006). Estrogen's effects vary based on its concentration levels, the type of cells and tissue involved in the immune response, as well as the microenvironment (Straub, 2007). The greater increase in pro- and anti-inflammatory cytokines, mediated by LPS, was revealed here in wild-type females, suggesting a higher susceptibility to the infection in these animals. However, this increase was not reflected in the brain.

In particular, quantification of hippocampal microglia in previous studies revealed higher microglia density and more activated amoeboid morphology in adult females than adult males, while in neonatal development males showed higher microglia density than females (Villa et al., 2018, Loram et al., 2012b). However, the finding of the present study doesn't reflect the literature. Microglia are known to regulate brain development by modulating many physiological processes such as neurogenesis, survival, phagocytosis and of neuronal circuits, that distinguish the two sexes after puberty (Arnold and Gorski, 1984, MacLusky and Naftolin, 1981, Lenz et al., 2013).

Susceptibility of transgenic female to infection, revealed by the analysis of microglia density, is reflected in the reactivity of microglia as well. The present study showed that transgenic females had bigger microglial soma than transgenic males in CA2 and CA3, as well as in DG where the females had larger cell soma than the males. Indeed, changes in microglia soma size are correlated to changes in cell morphology and cell activation (Torres-Platas et al., 2014). However, cell body size was not affected by the immune challenge itself, probably because 4 hours was not enough to induce morphological changes. A time-lapse two-photon microscopy study showed that 48h were required to detect microglia process motility and response to an acute injury (Avignone et al., 2015). Study on sex differences in brain development showed that microglia phenotype shifts during the development differently in males and females (McCarthy et al., 2015). Neonatal microglia cells from male mice appeared to have a more amoeboid-shaped soma than females, while females showed a more branched-resting phenotype (McCarthy et al., 2015). In more detail, males exhibited a greater number of microglia and a predominant activated amoeboid state early in development, especially at P4, while females

have a reverse pattern where microglia exhibited a more activated morphology throughout adulthood, rendering females more susceptible to inflammatory disease (Schwarz et al., 2012, Lenz et al., 2013).

To investigate microglia reactivity in relation to amyloid plaques, the numbers of Iba-1 positive clusters were quantified. Indeed, several studies have showed microglia cluster around amyloid-β deposits (Zhao et al., 2017a, Jung et al., 2015, Yuan et al., 2016), suggesting that these cells are important for amyloid plaque formation, maintenance or clearance. I found that the number of microglial clusters was higher in transgenic mice compared to wild-type littermates, in most regions of interest, as expected. Aβ plaque formation had never been described in wild-type animals and clusters of microglia were not seen in non-transgenic mice (Hellwig et al., 2015). I have also shown higher number of clusters in females, similar to a previous study that reported sex-differences on plaque formation and growth where female mice presented heavier amyloid burden and higher plaque numbers compared to age-matched males (Wang et al., 2003b). Particularly, amoeboid activated microglia have been seen surrounding Aβ plaques (Zhao et al., 2017a, Stalder et al., 1999). The observation here of larger microglia soma size in transgenic females, compared to males, can be correlated to the number of plaques, known to higher in females compared to males. Effects of LPS on amyloid plaque load will be described at longer time-points in the next chapters.

Another major player in the inflammatory response are the astrocytes. Quantification of astrocytes density revealed higher cell density in transgenic females compared to their wild-type littermates. The genotype difference revealed by this study is in accordance with a clinical study that showed an increase in GFAP-

immunoreactive astrocytes, in the hippocampus of AD patients (Lu et al., 2003). Here, I did not see the same difference in male mice, but there is limited literature that investigates the immune responses of astrocytes in both sexes. However, studies on the impact of estrogen on astrocytes inflammatory response reported contradictory results where estrogens increased mRNA of the astrocytes marker GFAP on one hand (Lewis et al., 2008), but inhibited astrogliosis and accumulation of reactive astrocytes in response to injury, on the other hand (García-Estrada et al., 1999, Lu et al., 2003). It needs to be considered that astrocyte reactivity and density can be influenced by the presence of the plaques and occur early in AD stages (Loram et al., 2012a), as we observed in our transgenic females at 4.5 months of age.

Overall the present data revealed higher microglia and astrocyte susceptibility to LPS in APPswe/PS1ΔE9 females compare to wild-type females. Indeed, we showed that transgenic females had a significant increase in microglia density and activation, as well as astrocytes density, compared to wild-type females. In the periphery, we revealed a higher pro-inflammatory response to LPS in all animals that was stronger in females compared to males. Differences seen between our study and the literature, using the same stimulating immune modulator, could be due to the different experimental methods used to quantify glial or protein levels. However, since LPS did not affect brain response to infection within the 4 hours' time point, in the next chapter, I investigated later time points to determine if the differences in susceptibility do reveal also with time.

CHAPTER 4

A single systemic challenge with LPS increased microglia proliferation in the hippocampus of 4.5-month old APPswe/PS1ΔE9 7-days post-treatment but did not affect amyloid plaque load.

4.1 Introduction

The present study investigated whether an acute systemic immune challenge with LPS (100µg/kg) induced changes in amyloid plaque load and immune response in 4.5 months old wild-type and APPswe/PS1ΔE9 males and females mice at seven days post stimulation. To investigate the central immune response I analyzed glial density and activation in hippocampus and cortex, as well as the putative presence of brain infiltrating monocytes. The peripheral immune response was also examined by quantifying circulating cytokine levels in plasma, and by characterizing the peritoneal macrophage populations. Immune cell infiltration from the periphery to the CNS is believed to be more functional in clearing excessive Aβ peptides than resident microglia (Lai and McLaurin, 2012). Therefore, here I investigated the possibility of monocytes infiltrating the brain and their phagocytic activity towards Aβ by staining for intracellular Aβ, as well as evaluating the expression of the chemokine receptor CCR2. CCR2 and its main ligand CCL2 (also known as MCP-1) have been reported to be involved in the altered metabolism and clearance of Aβ (Westin et al., 2012), playing a critical role in monocyte mobilization (E. Hirbec et al., 2017).

The seven days' time point was chosen to analyze a longer-term effect of a single systemic LPS injection on the deposition of Aβ plaques and monocytes recruitment

into the CNS. Previous studies have reported an increase in Aβ expression levels in the hippocampus 7 days after LPS administration that was not seen at earlier time points (Zhu et al., 2014). This increase was associated with an enhanced RNA level of the pro-inflammatory cytokines IL-1β, IL-6, TNF-α in the hippocampus and enhanced cognitive dysfunction (Zhu et al., 2014). Moreover, previous data revealed an increased production and intracellular accumulation of Aβ peptide in a mouse model of AD, induced by a systemic administration of LPS (10 µl/g, i.p) (Sheng et al., 2003). Other types of infections have been studied in correlation with Aβ deposition in animal models of AD. A recent report showed that infection with *C. pneumonia* induced Aβ aggregation as a result of the neuroinflammatory response (Bibi et al., 2014), supporting the significant role that inflammation plays, as a risk factor, in AD pathogenesis (Azizi et al., 2015, Zotova et al., 2010, Eikelenboom et al., 2012).

The presence of amyloid plaques has seen to prime microglia in AD brains (Norden et al., 2015a). An *in vivo* study on a 5XFAD mouse model, characterized by plaques deposition from 2 months of age, reported that microglia exposure to soluble Aβ early on in life could affect their response to a secondary stimulation such as bacterial infections (Jawhar et al., 2012). Microglia priming is associated with a pro-inflammatory phenotypic shift and a consequent increase in the pro-inflammatory surface markers (Cameron and Landreth, 2010) that contribute to a rapid loss in cognitive function and memory (Cagnin et al., 2001).

Therefore, I hypothesized that inflammation induced by LPS could contribute to the progression of AD pathology, triggering a pro-inflammatory response that would impact amyloid plaque aggregation and infiltration of peripheral macrophages, with transgenic animals being more susceptible to the immune challenge than their

wild-type littermates. Furthermore, higher susceptibility to LPS was expected in APPswe/PS1ΔE9 females, compared to males, as it has been seen that APPswe/PS1dE9 female have higher numbers of amyloid plaques and Aβ burden compared to age-matched males (Wang et al., 2003a).

Recruitment of mononuclear phagocytes from the periphery to Aβ deposits in the brain was seen to be dependent on CCR2 expression, with high expression levels of Aβ in the brain associated with increased expression of CCR2 in infiltrating macrophages (Mildner et al., 2011). In this study, Mildner's group showed that APPswe CCR2-deficient mice had impaired Aβ clearance and amplified vascular Aβ deposition compared to $CCR2^{+/+}$, with no effect on parenchymal plaque deposition (Mildner et al., 2011). Another in-vivo study reported that CCR2 deficiency in an AD mouse model accelerated disease progression as a consequence of decreased monocyte accumulation in the brain (El Khoury et al., 2007b). A growing body of evidence suggests that bone-marrow and blood-derived monocytes take part in the neuroinflammatory response seen in AD brains. Indeed, an in-vivo study that used a chimeric mouse model with eGFP-labelled bone-marrow macrophages showed enhanced engraftment of bone marrow-derived monocytes cells in response to Aβ deposition in transgenic AD mice, with a higher density of these cells in the brain of AD mice compared with wild-type mice (Malm et al., 2005). Migration of these cells into the brain has been related not only to the process of Aβ deposition, but also to the activation and proliferation of glial cells that trigger the release of chemoattractant mediators and cytokines (Malm et al., 2005).

Peritoneal monocytes were also investigated in this study as increasing evidence are suggesting that these cells may contribute to cerebral amyloid angiopathy by

releasing Aβ into the vessel walls following apoptosis (Malm et al., 2010, Zaghi et al., 2009). Moreover, a recent observation, done in both humans and APPswe/PS1dE9 transgenic mice, suggested that the clearance of Aβ from the brain through blood vessels play an important role, preventing amyloid burden that characterized the AD pathogenesis (Xiang et al., 2015).

Overall, genotype susceptibility and sex differences were examined here in response to the same dose of LPS used in my previous study (chapter 3), but with a focus on the longer-term consequences both in the brain and the periphery. APPswe/PS1dE9 and wild-type mice aged 4.5 months at the time of the injection were used to investigate the inflammatory response in relation to early plaque accumulation. The age of the animals is the same used in the previous study described in chapter 3. Infiltrating monocytes were identified by the surface expression of CD11b with high expression of CD45 ($CD11b^{+}$ $CD45^{+Hi}$) (Manitz et al., 2016), distinguished by microglia that have CD11b with low or intermediate CD45 expression ($CD11b^{+}$ $CD45^{+Low}$) (Martin et al., 2017). Peritoneal macrophages were identified as positive for F4/80 (Zhang et al., 2008). Pro-inflammatory (M1) and anti-inflammatory phenotype (M2) were analyzed by staining for CD80 and CD206 respectively (Jablonski et al., 2015). To investigate the capacity of macrophages to infiltrate the CNS, brain cells were stained for CCR2 (Yang et al., 2014). Finally, cells were stained for Aβ intracellularly to investigate the possibility of an internalization of the peptide from both microglia and macrophages (Lai and McLaurin, 2012). To monitor the sickness syndrome induced by the infection, behavioural changes in daily living and locomotor activity, as well as spatial working memory were also assessed.

4.2 Study design

Sixty-four 4.5 month-old mice were used to assess the behavioural and glial response, as well as peripheral cytokine response and macrophages infiltration into the brain 7 days after LPS injection. 32 APPswe/PS1dE9 transgenic mice (16 males with mean weight: 30.5 ± 1.1 g; and 16 females with mean weight: 23.9 ± 0.4g) and 32 wild-type littermates (16 males mean weight: 32.8 ± 1 g; and 16 females with mean weight: 24 ± 0.8g) were tested. See Figure 30 for a schematic timeline of the experiment.

Mice were subjected to food burrowing, spontaneous alternation and open field in order to assess daily living activity, spatial working memory and locomotor activity both before and 7 days after treatment. After a food burrowing training for 3 days, baseline data were collected. Mice were tested for spontaneous alternation the day before the injection (day -1). The open field task was performed the day of the injection (day 0), in the morning, with an overnight food burrowing assessment between the two days. On day 0 mice were injected with either LPS (100µg/kg, i.v) or vehicle (PBS) in the afternoon, after the open field test. On days 6 and 7 mice underwent the same behavioural tests to collect post-injection data. Body weight of each mouse was recorded daily throughout the experiment in order to monitor their recovery from LPS-induced sickness. On day 7 mice were anesthetized to collect macrophages from the peritoneal area and blood by heart puncture before being perfused with ice-cold PBS. Brain tissue was collected and sagittally separated into two hemibrains. One half of the brain was sagittally sliced and destined to analyze the microglia, astrocytes and amyloid response in the hippocampus and cortex, by immunostaining for Iba-1, GFAP and Aβ respectively. Two brains from

the same genotype and sex, but with different treatment, were fixed in the same block to minimize staining variability. Nine sections per brain were immunostained at different levels of the hippocampus. The second half of the brain was used for two different purposes: brain tissue from n=4 mice/group was dissociated in cells and analysed by flow cytometry to investigate brain infiltrating macrophages, while the tissue from the other n=4 mice/group was further dissected into frontal cortex, hippocampus, cortex and striatum and stored at -80°C, but not used in this study. Plasma was collected and stored at -80°C for cytokines analysis.

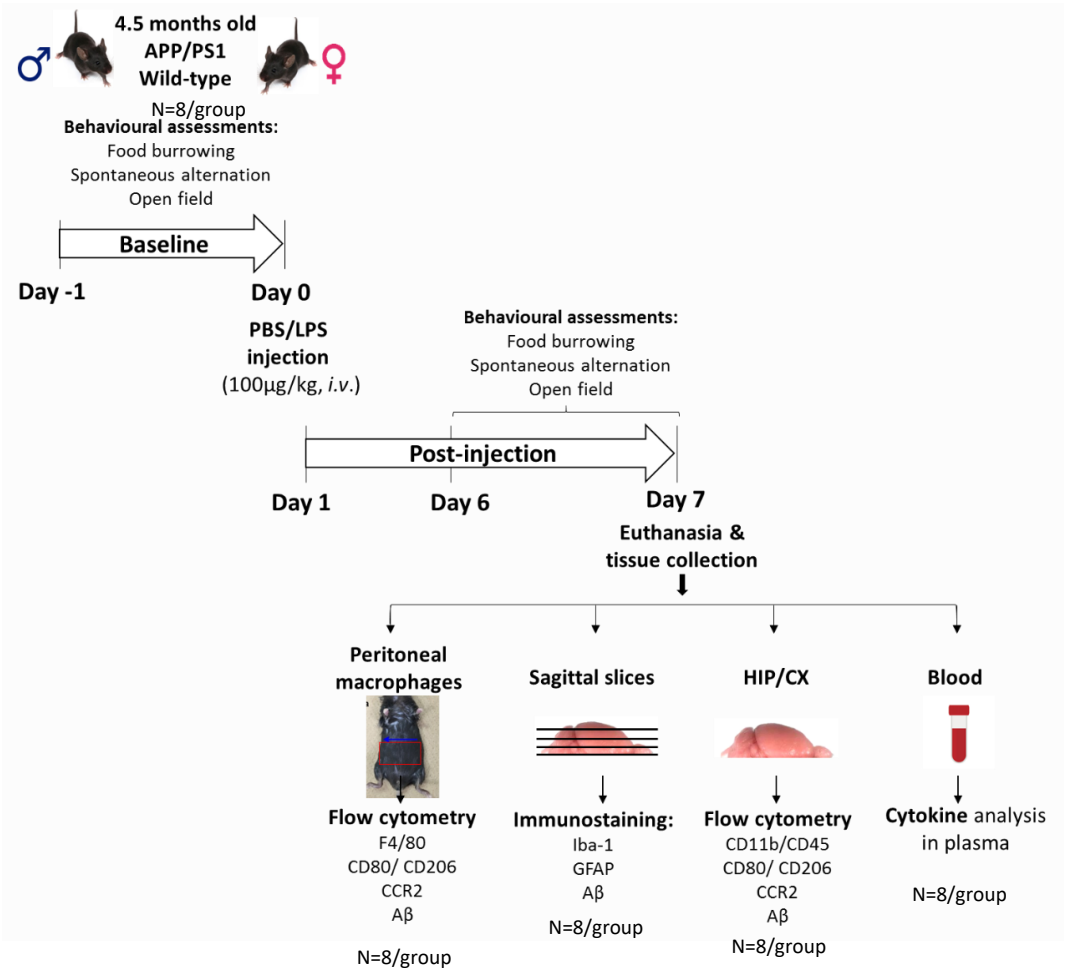

Figure 30. **Schematic experimental timeline.**

4.3 Results

4.3.1 Behavioural response to the immune challenge after 7 days

Body weight

Results showed an overall significant sex effect at baseline ($F_{(1,57)}$=963.2, p<0.0001), with males being heavier than females (Figure 31.A). Repeated measure ANOVA used to analyse post-injection data revealed overall significant effects of sex ($F_{(1,57)}$=75.83, p<0.0001) and time ($F_{(1,57)}$=16,94, p<0.0001) and a significant sex X time interaction effects ($F_{(1,57)}$=5,03, p<0.0001). Males showed higher body mass than females from day 1 to day 7 post-injection in both wild-type (p<0.0001) (Figure 31.B) and transgenic (LPS-treated mice p<0.0001; PBS-treated mice p<0.05) groups (Figure 31.C). A treatment X time interaction effect ($F_{(1,57)}$=31,52, p<0.0001) was also observed with a greater loss in body mass in LPS-treated wild-type females compared to the control animals (p=0.021)(Figure 31.B).

To investigate the recovery of the animals after the challenge, body weight changes were calculated by subtracting post-injection data from the baseline data and expressed as a percent change from baseline. Results showed that all LPS-treated animals lost weight significantly, but females seemed to recover faster than males, reaching their baseline weight by day 3 (Figure 32.B), while males did not return to baseline weight within the 7 days (Figure 32.A). PBS-treated APPswe/PS1ΔE9 females significantly gained weight on days 2 (p=0.039) and 3 (p=0.001) (Figure 32.B), and wild-type males on day 2 (p=0.042) (Figure 32.A) post-administration, compared to the baseline weight.

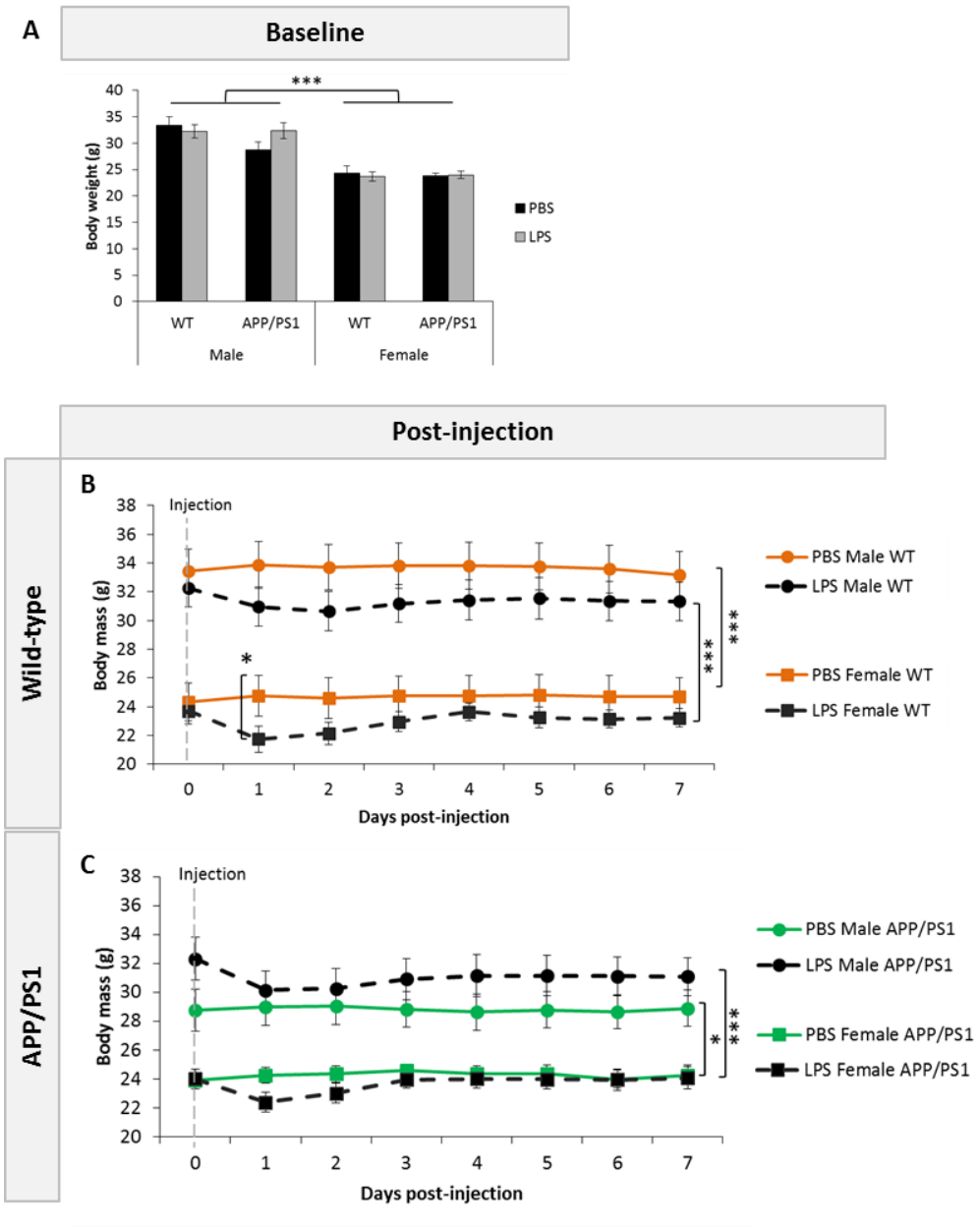

Figure 31. **Body weight at baseline and post-injection**. 4.5 months old male and female mice APPswe/PS1ΔE9 (APP/PS1) and wild-type (WT) (n=8 per group) were treated with LPS or vehicle (PBS). Body weight was recorded before the injection and every day after the treatment. Males were significantly heavier than females before the injection ($p<0.0001$) (**A**) and post-injection ($p<0.05$) (**B-C**). The day after the challenge LPS-treated WT females showed a significantly lower body mass than PBS-treated control ($p=0.021$) (**B**). Data are shown as mean ± S.E.M. 3-way and 2-way ANOVA were used. [* $p< 0.05$, *** $p< 0.0001$].

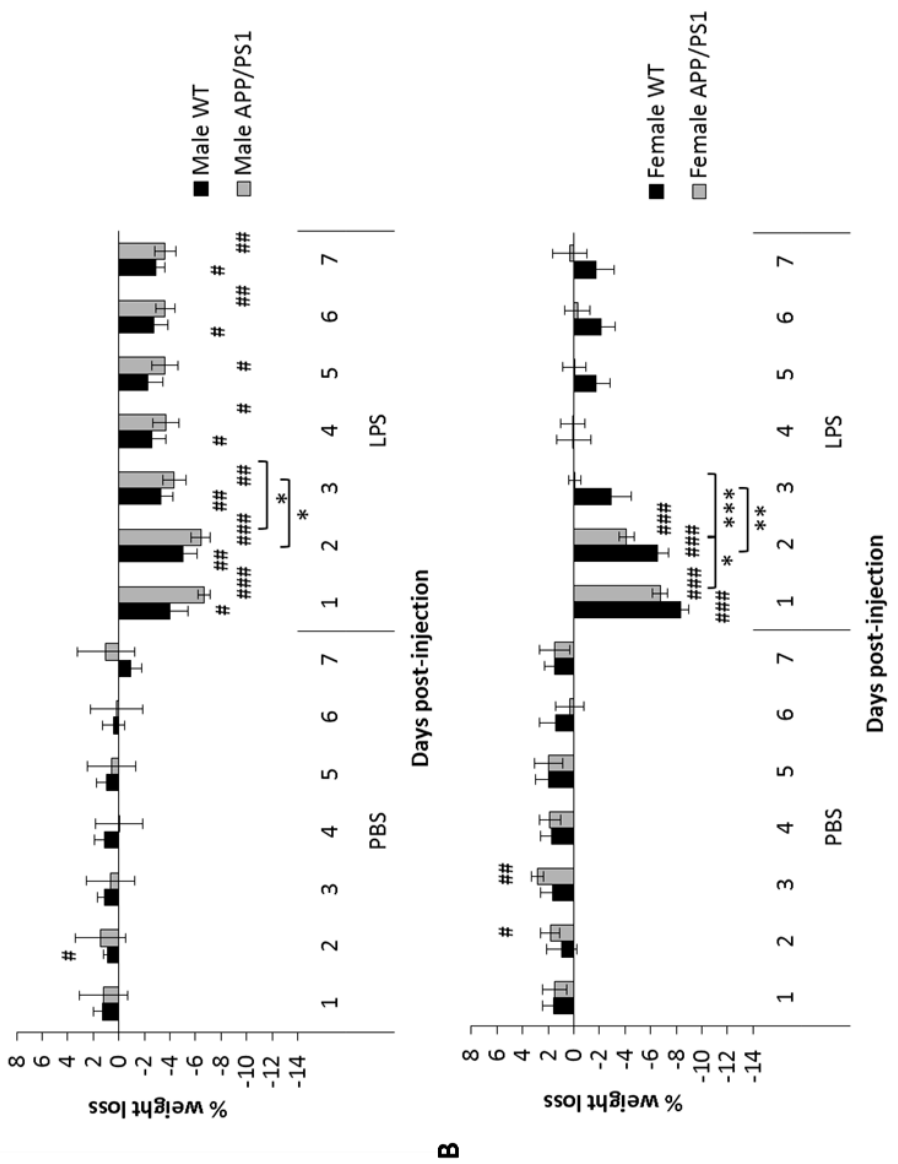

Figure 32. **Body weight recovery from the treatment**. 4.5 months old male and female APPswe/PS1ΔE9 (APP/PS1) and wild-type (WT) (n=8 per group) were treated with LPS or vehicle (PBS). Body weight was recorded before the injection and every day after the injection. PBS-treated males (**A**) and females (**B**) did not lose weight after the injection. LPS-treated animals lost a significant amount of weight on day 1, after the treatment, seen in males WT ($p=0.024$) and APP/PS1 ($p<0.0001$) (**A**), as well as in females WT ($p<0.0001$) and APP/PS1 ($p<0.0001$) (**B**). 7 days after the injection, LPS-treated WT ($p=0.005$) and APP/PS1 ($p=0.003$) males still showed body weight loss, compared to baseline (**A**). LPS-treated females showed increase in body weight by day 3 in both APP/PS1 ($p<0.0001$) and WT ($p=0.0004$) mice, compared to day 2, reaching the baseline weight (**B**). Data are shown as mean ± S.E.M. [the * was used for the statistical significance shown by the pairwise comparisons analysis between the days: **p< 0.005]; [the # was used used for the statistical significance shown by the one-sample t-test compared to the baseline: #p< 0.05, ##p<0.005, ###p< 0.0001].

Food Burrowing

To study if the systemic administration of LPS impacts on the normal daily activities, the food burrowing task was performed. There were no differences in performance between treatment groups at baseline and post-injection assessments. An overall significant effect of genotype was observed at baseline ($F_{(1,57)}$=7.33, p=0.009) (Figure 33A) with wild-type females burrowing more food than APPswe/PS1ΔE9 females (p=0.007) and wild-type males (p=0.026). An overall genotype effect was also seen post-injection ($F_{(1,57)}$=11.1, p=0.002) (Figure 33.B) with wild-type females burrowing more food than APPswe/PS1ΔE9 females (p=0.002). Analysis of the changes in the amount of food burrowed from baseline revealed that LPS-treated APPswe/PS1ΔE9 male burrowed significantly more food than prior the treatment (p=0.01) (Figure 33.C).

Spatial working memory

There were no differences in performance between the experimental groups at baseline and seven days after the injection. The number of arm entries was recorded and used as a covariate. Results revealed that number of arm entries significantly impacted the alternation rate both at baseline (p=0.0067) and post-injection (p=0.029). One sample t-test showed that all wild-type males (PBS-treated, p<0.0001; LPS-treated p=0.004), APPswe/PS1ΔE9 males (PBS-treated, p=0.001; LPS-treated p=0.002) and APPswe/PS1ΔE9 females (PBS-treated, p=0.001; LPS-treated p=0.006) alternated significantly above the 50% random choice rate at baseline (Figure 33.D). Seven days after the treatment all experimental groups, except PBS-treated wild-type males, alternated significantly above the chance level ($p < 0.05$ compared to 50% choice rate) (Figure 33.E). In addition, PBS-treated transgenic males showed improvement in spatial working memory (p=0.014)

(Figure 33.F). Therefore these results suggests that the treatment did not impact spatial working memory.

Locomotor activity

No differences in locomotor activity were observed at baseline and post-injection between experimental groups. An overall genotype effect was observed on the distanced moved both at baseline ($F_{(1,57)}$=11.55, p=0.001) (Figure 33.G) and post-injection ($F_{(1,57)}$=12.73, p=0.001) (Figure 33.H). Wild-type females moved less than APPswe/PS1ΔE9 females (p=0.032 at baseline; p=0.012 post-treatment) and with wild-type males did cover shorter distances than APPswe/PS1ΔE9 males (p=0.011 at baseline; p=0.017 post-treatment).

Investigating the effect of the injection over the performance, all animals, except LPS-treated APPswe/PS1ΔE9 females showed a significant decrease in the distanced moved between baseline and post-treatment test (p<0.05) (Figure 33.I).

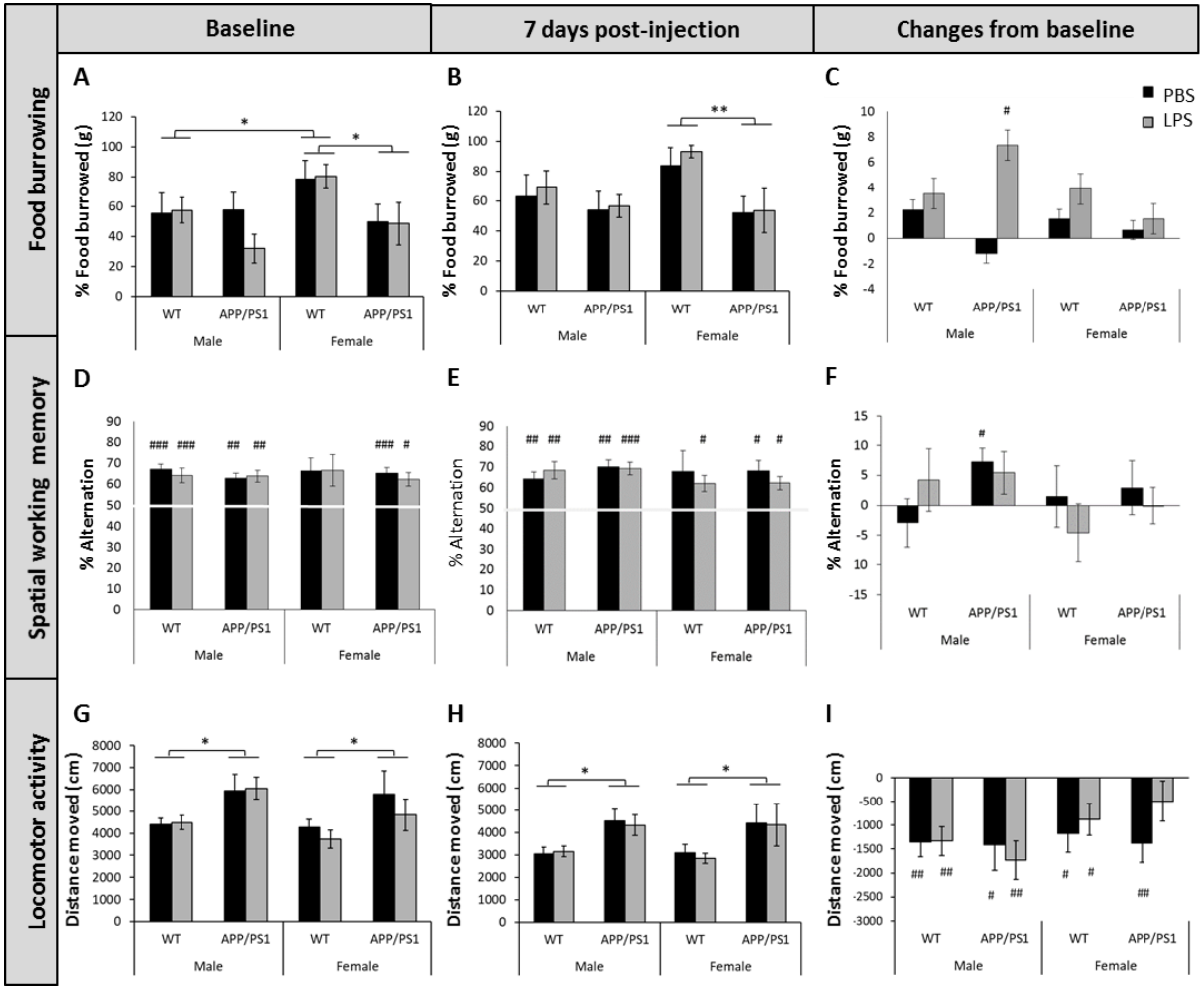
Baseline
7 days post-injection
Changes from baseline
Food burrowing
Spatial working memory
Locomotor activity
A
B
C
D
E
F
G
H
I
PBS
LPS
% Food burrowed (g)
% Alternation
Distance moved (cm)
WT
APP/PS1
Male
Female

Figure 33. **LPS effects on behaviour at baseline and 7 days post-injection**. 4.5 months old male and female mice APPswe/PS1ΔE9 (APP/PS1) and wild-type (WT) (n=8 per group) were treated with LPS or vehicle (PBS). Behaviour was assessed before and 7 days post-treatment. A white line in D and E represent the 50% chance level. No significant differences were seen between experimental groups in the effect of treatment, in the food burrowed (**C**), alternation rate (**F**) and locomotor activity (**I**) regardless of sex and genotype. Wild-type females burrowed more food than transgenic females both at baseline (p=0.007) (**A**) and post-injection (p=0.002) (**B**), and than wild-type males at baseline (p=0.0262) (**A**). APP/PS1 animals showed higher locomotor activity than WT littermates in both females and males at baseline (p=0.032 in females, p=0.0114 in males) (**G**) and post-injection (p=0.0123 in females, p=0.017 in males) (**H**). However, comparing the treatment effect to baseline data (represented by the Y-axis) it was revealed a significant increase in food burrowed in LPS-treated APP/PS1 males (p=0.01) (**C**), an increase in the alternation rate in PBS-treated APP/PS1 males (**F**) and a decrease in locomotor activity in all the groups (p<0.05), except LPS-treated transgenic female (**I**). Data are shown as mean ± S.E.M [ANOVA:* p< 0.05, **p< 0.005]. [# was used used for the statistical significance shown by the one-sample t-test compared to the baseline: $^{\#}$p<0.05, $^{\#\#}$p<0.005, $^{\#\#\#}$p< 0.0001].

4.3.2 Cytokine response to LPS 7 days after the challenge

Plasma cytokine concentrations were quantified using the multiplex array described in the method chapter 2. There were no significant effects of LPS treatment after 7 days. An overall sex effect was revealed for IFN-γ ($F_{(1,57)}$=7.05, p=0.0103) (Figure 34.B) and TNF-α ($F_{(1,57)}$=9.31, p=0.0049) levels (Figure 34.E) with wild-type females showing elevated protein levels in plasma compared to wild-type males [IFN-γ (p=0.015), TNF-α (p=0.004)]. No significant differences were seen for IL-1β (Figure 34.A), IL-6 (Figure 34.C) and IL-10 (Figure 34.D).

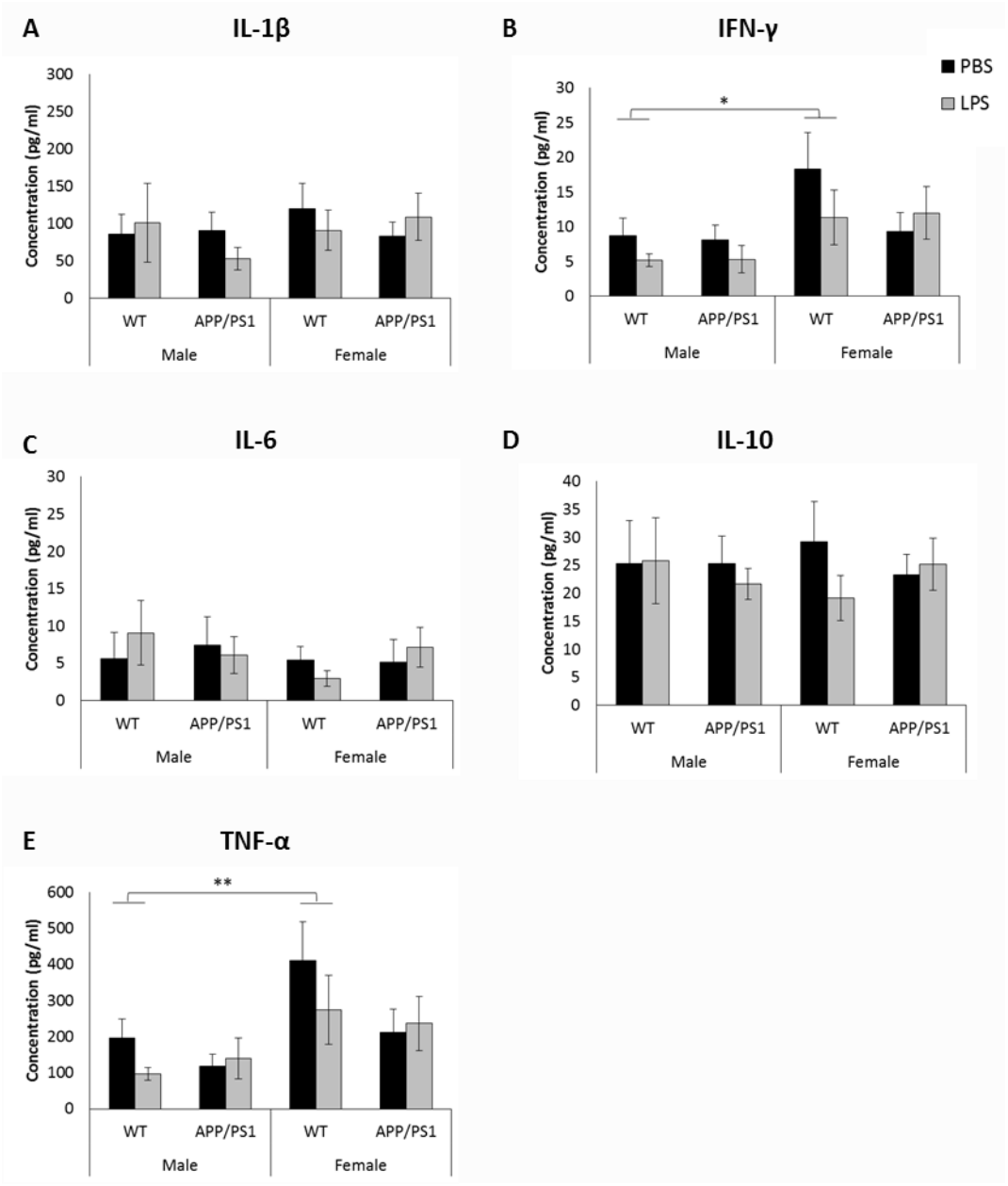

Figure 34. **Cytokines levels in plasma**. 4.5 months old male and female APPswe/PS1ΔE9 (APP/PS1) and wild-type (WT) (n=8 per group) were treated with LPS or vehicle (PBS) and plasma collected 7 days after the challenge. No significant differences observed in IL-1β (**A**), IL-6 (**C**) and IL-10 (**D**) plasma levels between groups. Wild-type females showed higher concentration of IFN-γ (p=0.015) (**B**) and TNF-α (p=0.004) (**E**) than wild-type males. Data are shown as mean ± S.E.M. [* p< 0.05, ** p< 0.005].

4.3.3 Changes in amyloid plaque load in the hippocampus and cortex 7 days after LPS challenge.

An overall sex effect was revealed in both hippocampus ($F_{(1,28)}$=92.19, p<0.0001) (Figure 35.A) and cortex ($F_{(1,28)}$=37.58, p<0.0001) (Figure 36.A), with females showing higher number of amyloid plaques compared to males. Analysis of the size of the plaques revealed a sex effect for small ($F_{(1,28)}$=71.39, p<0.0001) medium ($F_{(1,28)}$=41.89, p<0.0001) and large ($F_{(1,28)}$=41.01, p<0.0001) plaques in the hippocampus, as well as small ($F_{(1,28)}$=28.99, p<0.0001), medium ($F_{(1,28)}$=19.71, p<0.0001) and large ($F_{(1,28)}$=39.58, p<0.0001) plaques in the cortex. A significant sex X treatment interaction effect ($F_{(1,28)}$=5.81, p=0.023) was found in the total number of plaques in the hippocampus, but no significant differences were seen between the experimental groups.

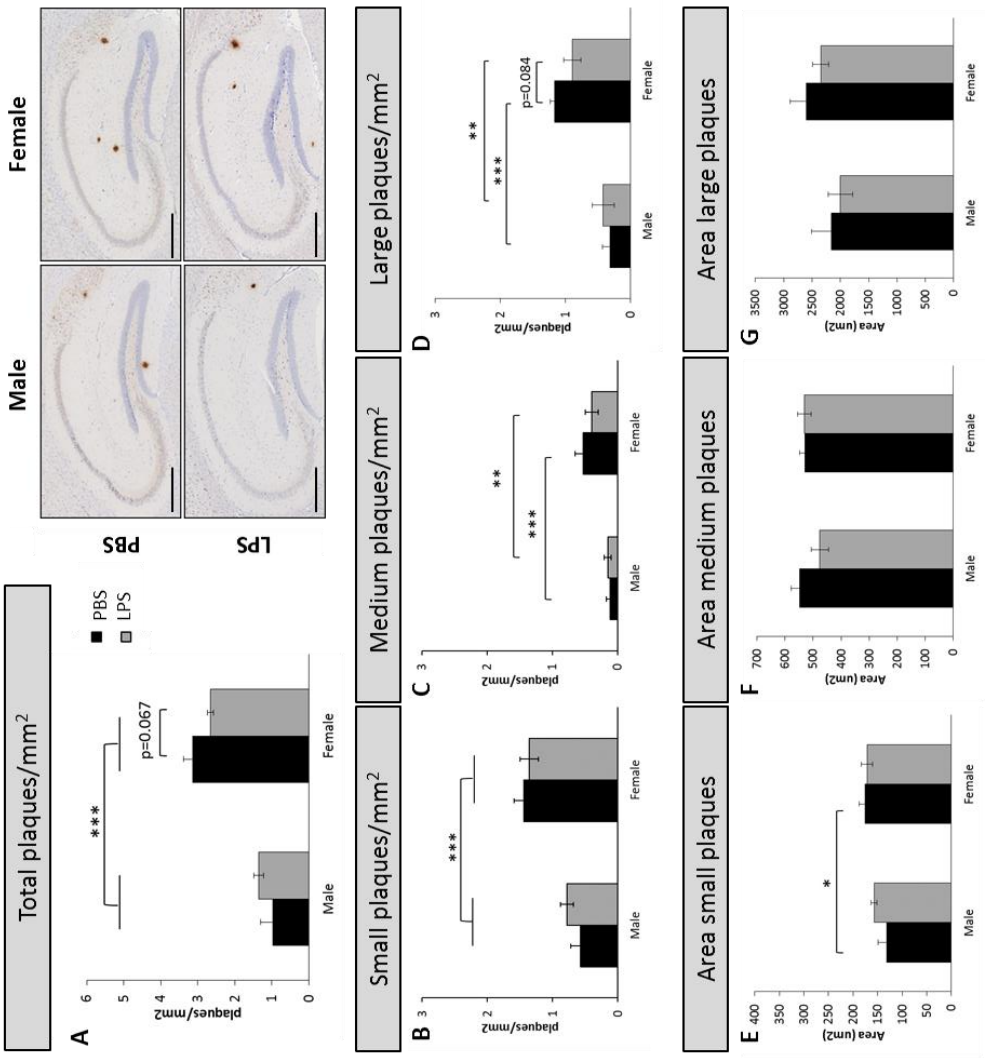

Figure 35. **Amyloid plaque load in hippocampus 7 days after LPS challenge**. 4.5 months old male and female mice APPswe/PS1ΔE9 (APP/PS1) and wild-type (WT) (n=8 per group) were treated with LPS or vehicle (PBS) and their brain was collected 7 days after the challenge. Females showed higher number of total amyloid plaques per mm^2 ($p<0.0001$) (**A**) and small plaques per mm^2 ($p<0.0001$) (**B**) compared to males. In addition, PBS-treated females showed higher number of medium plaques/mm^2 ($p<0.0001$) (**C**) and large plaques/mm^2 ($p<0.0001$) (**D**) compared to PBS-treated males. Moreover LPS-treated females showed higher number of medium plaques/mm^2 ($p=0.002$) (**C**) and large plaques/mm^2 ($p=0.004$) (**D**), compared to LPS-treated males. PBS-treated females showed larger small plaques than PBS-treated males ($p=0.0003$) (**E**), but no significant difference was found between the experimental groups in medium (**F**) and large plaques (**G**). Scale bars, 0.5mm. Data are presented as mean ± S.E.M. [* $p< 0.05$, **$p< 0.005$ *** $p < 0.0001$].

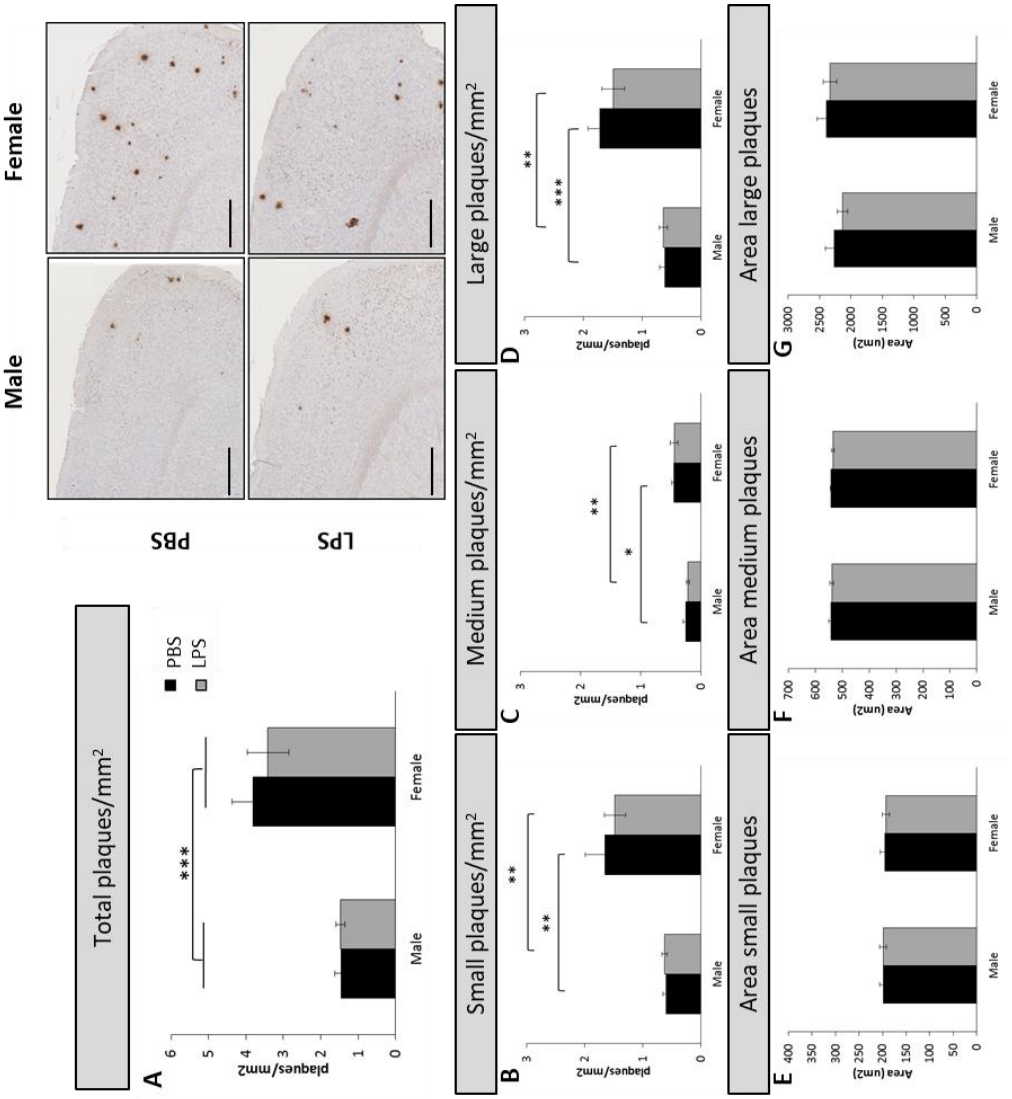

Figure 36. **Amyloid plaque load in cortex 7 days after LPS challenge**. 4.5 months old male and female mice APPswe/PS1ΔE9 (APP/PS1) and wild-type (WT) (n=8 per group) were treated with LPS or vehicle (PBS) and their brain was collected 7 days after the challenge. Females showed higher number of total amyloid plaques per mm^2 ($p<0.0001$) (**A**) compared to males. In addition PBS-treated females showed higher number of small ($p=0.0002$), medium ($p=0.0072$) (**C**) and large ($p<0.0001$) (**D**) plaques per mm^2, compared to PBS-treated males. Moreover LPS-treated females showed higher number small ($p=0.002$), medium ($p=0.002$) (**C**) and large ($p=0.0006$) (**D**) plaques/mm^2. No significant differences were found between the experimental groups in the size of small, medium and large plaques (**E**-**G**). Scale bars, 0.5mm. Data are presented as mean $\pm$ S.E.M. [* $p< 0.05$, **$p< 0.005$ *** $p < 0.0001$].

4.3.4 Glial response to LPS in the hippocampus and cortex

Astrocytes response in the hippocampus and cortex 7 days after LPS challenge

LPS did not affect astrocyte density in the whole hippocampus and no significant differences were observed between experimental groups (Figure 37). An overall sex effect was shown in the CA3 hippocampal subfield ($F_{(1,57)}$=9.33, p=0.003) with males having a higher astrocyte density compared to females (Figure 39.A). An overall genotype ($F_{(1,56)}$=233.98, p<0.0001), sex ($F_{(1,56)}$=7.58, p=0.0079) effects and a genotype X sex interaction effect ($F_{(1,56)}$=13.56, p=0.0005) was revealed in astrocytes clusters in the cortex (Figure 37). APPswe/PS1ΔE9 female showed more clusters than transgenic males (p<0.0001) and wild-type females (p<0.0001). APPswe/PS1ΔE9 males presented higher number of clusters than their wild-type littermates (p<0.0001).

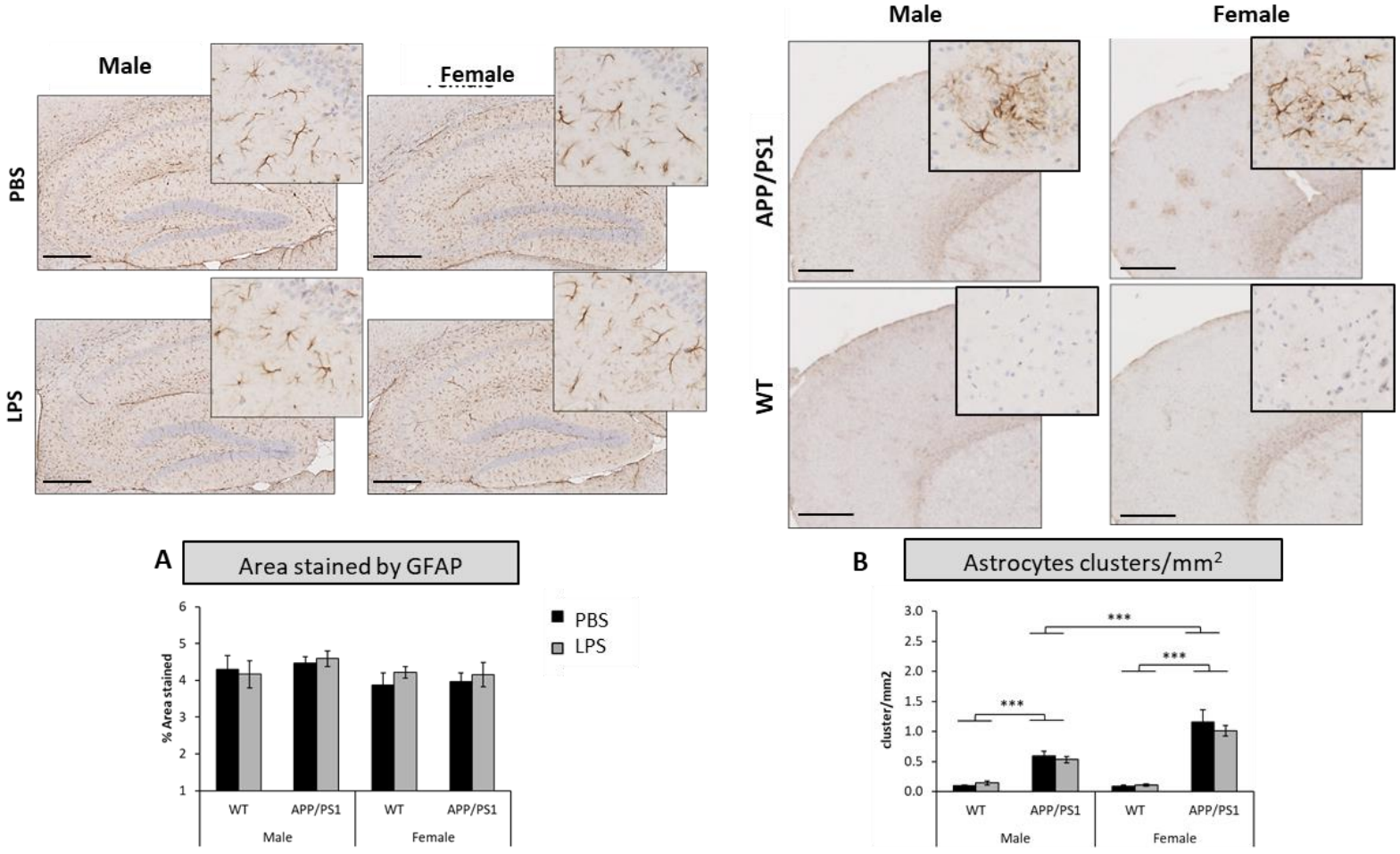
Male
Female
PBS
LPS
Male
Female
APP/PS1
WT
A
Area stained by GFAP
% Area stained
PBS
LPS
WT
APP/PS1
WT
APP/PS1
Male
Female
B
Astrocytes clusters/mm2
cluster/mm2
***
***
***
WT
APP/PS1
WT
APP/PS1
Male
Female

Figure 37. **Area occupied by GFAP in the hippocampus and cortex.** 4.5 months old male and female mice APPswe/PS1ΔE9 (APP/PS1) and wild-type (WT) (n=8 per group) were treated with LPS or vehicle (PBS) and their brain was collected 7 days after the challenge. No significant differences were found in the percentage of area stained by GFAP between the experimental groups (**A**). APP/PS1 females showed a higher number of clusters than WT females ($p<0.0001$) and APP/PS1 males ($p<0.0001$) (**B**). APP/PS1 males revealed higher number of GFAP clusters compared to WT littermates ($p<0.0001$) (**B**). Scale bars, 0.5mm. Data are presented as mean ± S.E.M. [***$p<0.0001$].

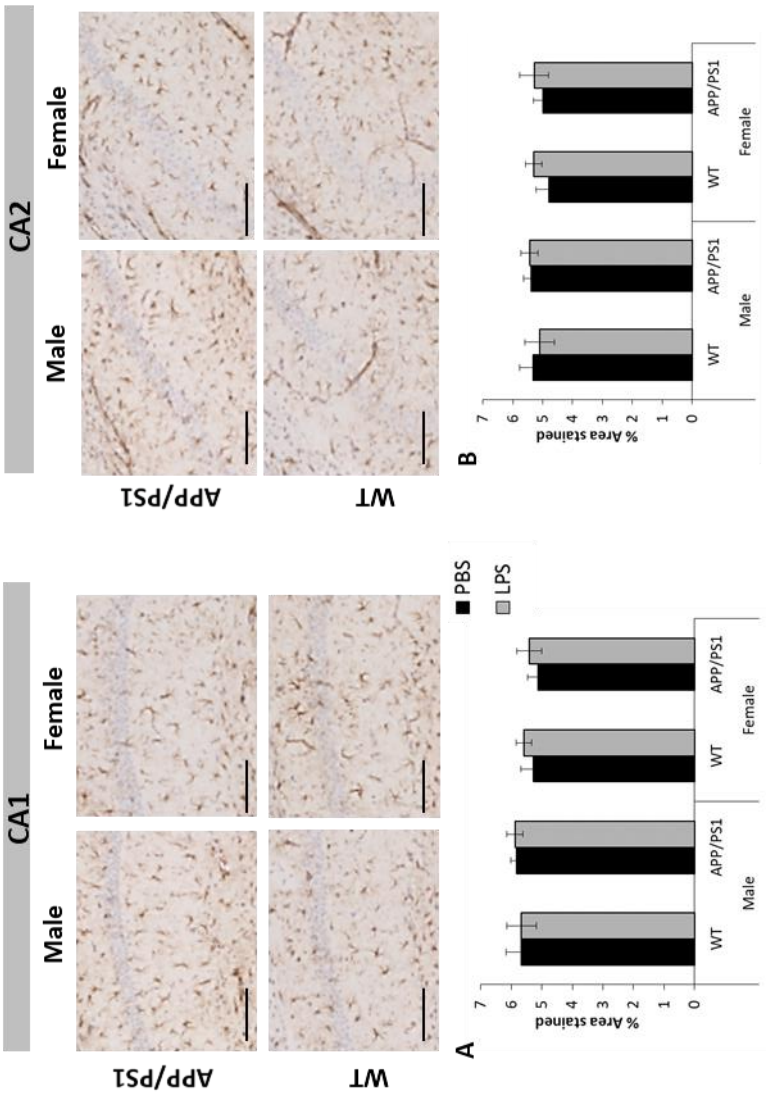

Figure 38. **Area occupied by GFAP in the hippocampal subfields**. 4.5 months old male and female mice APPswe/PS1ΔE9 (APP/PS1) and wild-type (WT) (n=8 per group) were treated with LPS or vehicle (PBS) and their brain was collected 7 days after the challenge. No significant differences were observed in the percentage of area stained by GFAP in CA1 (**A**), CA2 (**B**) Scale bars, 0.25mm. Data are presented as mean ± S.E.M. [* $p < 0.05$].

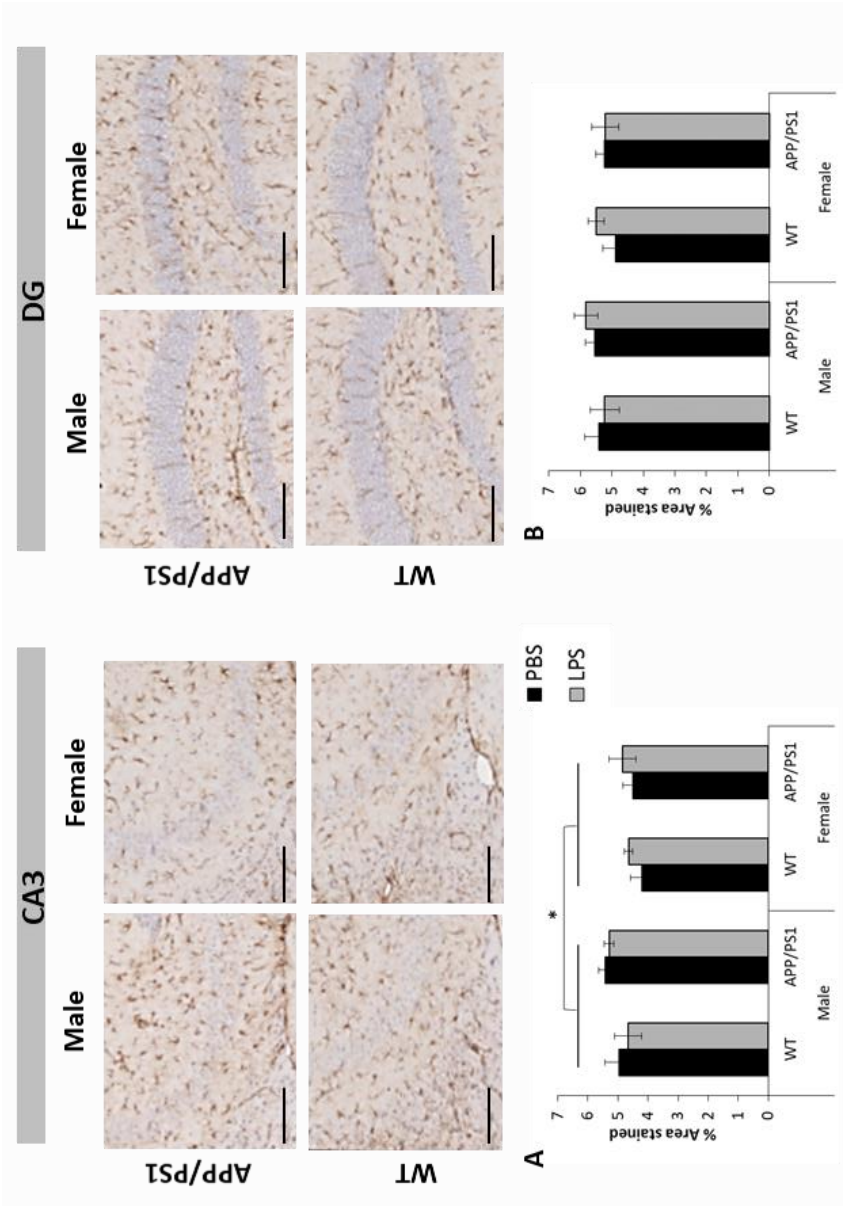

Figure 39. **Area occupied by GFAP in the hippocampal subfields**. 4.5 months old male and female mice APPswe/PS1ΔE9 (APP/PS1) and wild-type (WT) (n=8 per group) were treated with LPS or vehicle (PBS) and their brain was collected 7 days after the challenge. No significant differences were observed in the percentage of area stained by GFAP in DG (**B**), while a lower percentage of area stained by GFAP was observed in female compared to the male group in CA3 (p=0.04) (**A**). Scale bars, 0.25mm. Data are presented as mean ± S.E.M. [* p< 0.05].

Microglia response to LPS in the hippocampus and cortex

An overall sex effect was observed in the percentage of area stained by Iba-1 in the cortex ($F_{(1,55)}$=5.46, p=0.023) (Figure 41.A) and in 3 hippocampal subfields [CA1 ($F_{(1,55)}$=4.65, p=0.036) (Figure 42.A), CA2 ($F_{(1,55)}$=4.04, p=0.049) (Figure 42.B), CA3 ($F_{(1,55)}$ =5.74, p=0.020) (Figure 43.C)] with females showing higher density of Iba-1 than males. In particular, wild-type females revealed higher microglia density than wild-type males in CA2 (p=0.039) (Figure 42.B). An overall treatment effect was observed for the number of microglia cells per mm^2 in the whole hippocampus ($F_{(1,55)}$=8.71, p=0.005) (Figure 40.B) and the 4 hippocampal subfields [CA1 ($F_{(1,55)}$=4.81, p=0.033), CA2 ($F_{(1,55)}$=10.98, p=0.002) (Figure 42.E-F), CA3 ($F_{(1,55)}$ =13.71, p=0.0005) and DG ($F_{(1,55)}$ =7.96, p=0.0066)] (Figure 43 G-H) with LPS-treated animals showing higher number of cells compared to PBS-treated counterpart, in particular in APPswe/PS1ΔE9 males in CA2 (p=0.031) (Figure 42.F) and CA3 (p=0.016) (Figure 43.G), and in APPswe/PS1ΔE9 female in CA3 (p=0.018) (Figure 43.F) and DG (p=0.0315) (Figure 43.H).

An overall genotype effect in the number of microglia clusters per mm^2 (density) was revealed in the cortex ($F_{(1,56)}$=122.99, p<0.0001) (Figure 41.C), the whole hippocampus ($F_{(1,56)}$=20.87, p<0.0001) (Figure 40.C), and 2 hippocampal subfields [CA1 ($F_{(1,56)}$=5.36, p=0.024) (Figure 42.I) and DG ($F_{(1,56)}$=24.94, p<0.0001) (Figure 43.L)]. Transgenic animals showed more clusters than wild-type, in both males and females (p<0.005). In addition, an overall genotype X sex ($F_{(1,56)}$=5.36, p=0.021) and genotype X sex X treatment ($F_{(1,56)}$=7.08, p=0.010) interaction effects was seen in CA1 (Figure 42.I), where transgenic females presented more clusters than transgenic males. Moreover, an overall sex effect was observed in the size of microglia soma in the whole hippocampus ($F_{(1,55)}$=6.56, p=0.013) (Figure 40.D), in the cortex ($F_{(1,55)}$=5.46, p=0.023) (Figure 41.D), and in 3 hippocampal subfields [CA1

($F_{(1,55)}$=4.06, p=0.049) (Figure 42.M), CA3 ($F_{(1,55)}$=6.11, p=0.016) (Figure 43.O) and DG ($F_{(1,55)}$=4.1, p=0.048)] (Figure 43.P). Indeed, females showed larger microglia soma than males. The number of microglia clusters was found to be a significant covariate in the analysis of microglia soma size in DG ($F_{(1,55)}$=5.43, p=0.023) (Figure 43.P).

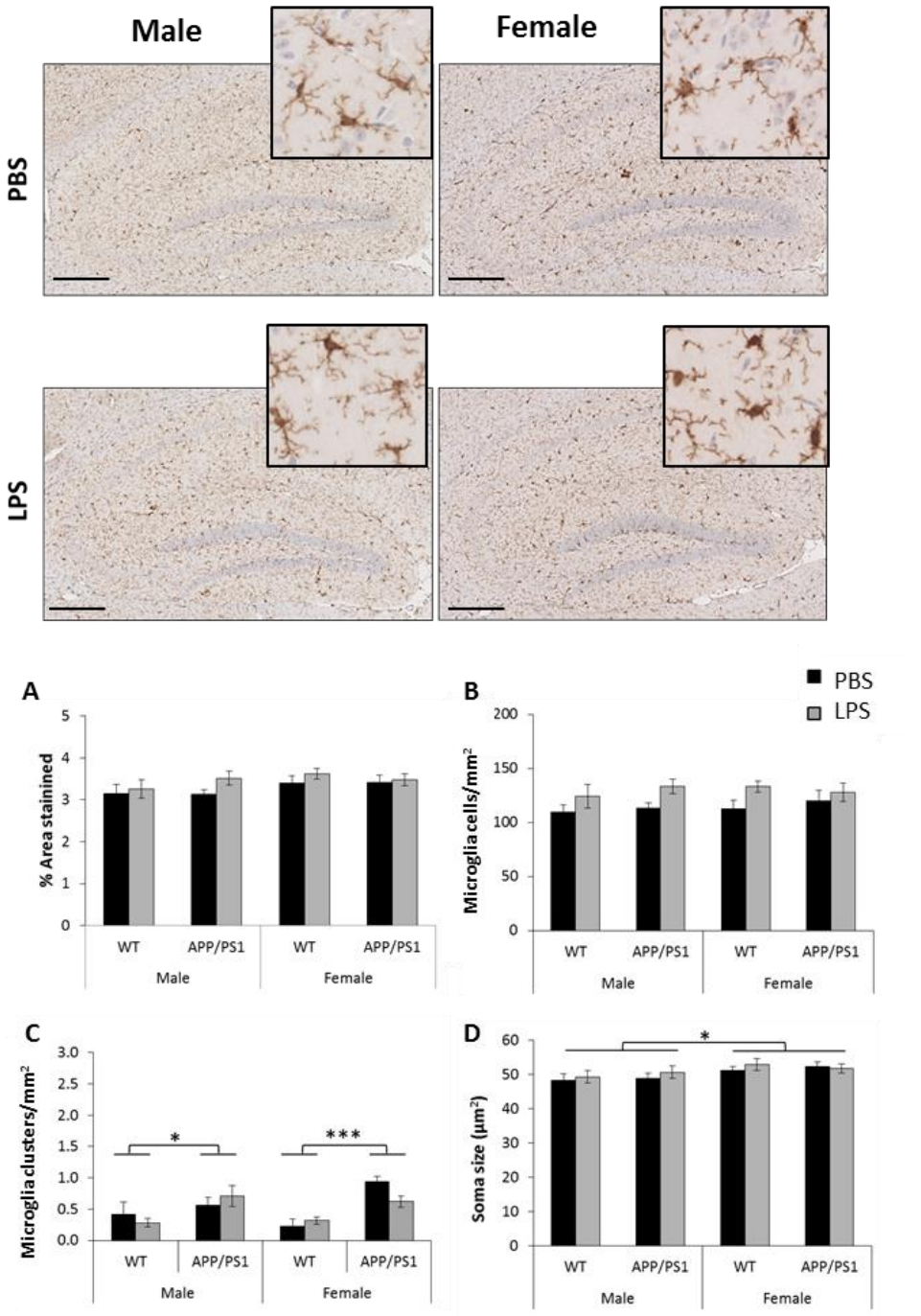

Figure 40. **Area occupied by Iba-1 in the hippocampus**. 4.5 months old male and female mice APPswe/PS1ΔE9 (APP/PS1) and wild-type (WT) (n=8 per group) were treated with LPS or vehicle (PBS) and their brain was collected 7 days after the challenge. No significant difference between groups was observed in the percentage of area stained by Iba-1 (**A**) and in microglia cells per mm2 (**B**). A higher number of microglial clusters/mm^2 was revealed in APP/PS1 female compared to WT female ($p<0.0001$) and in APP/PS1 male compared to their WT littermates ($p=0.006$) (**C**). A sex difference was observed for the soma size where females showed larger microglia soma than males ($p=0.0132$) (**D**). Scale bars, 0.5mm. Data are presented as mean ± S.E.M. [ANOVA: * $p< 0.05$, *** $p< 0.0001$].

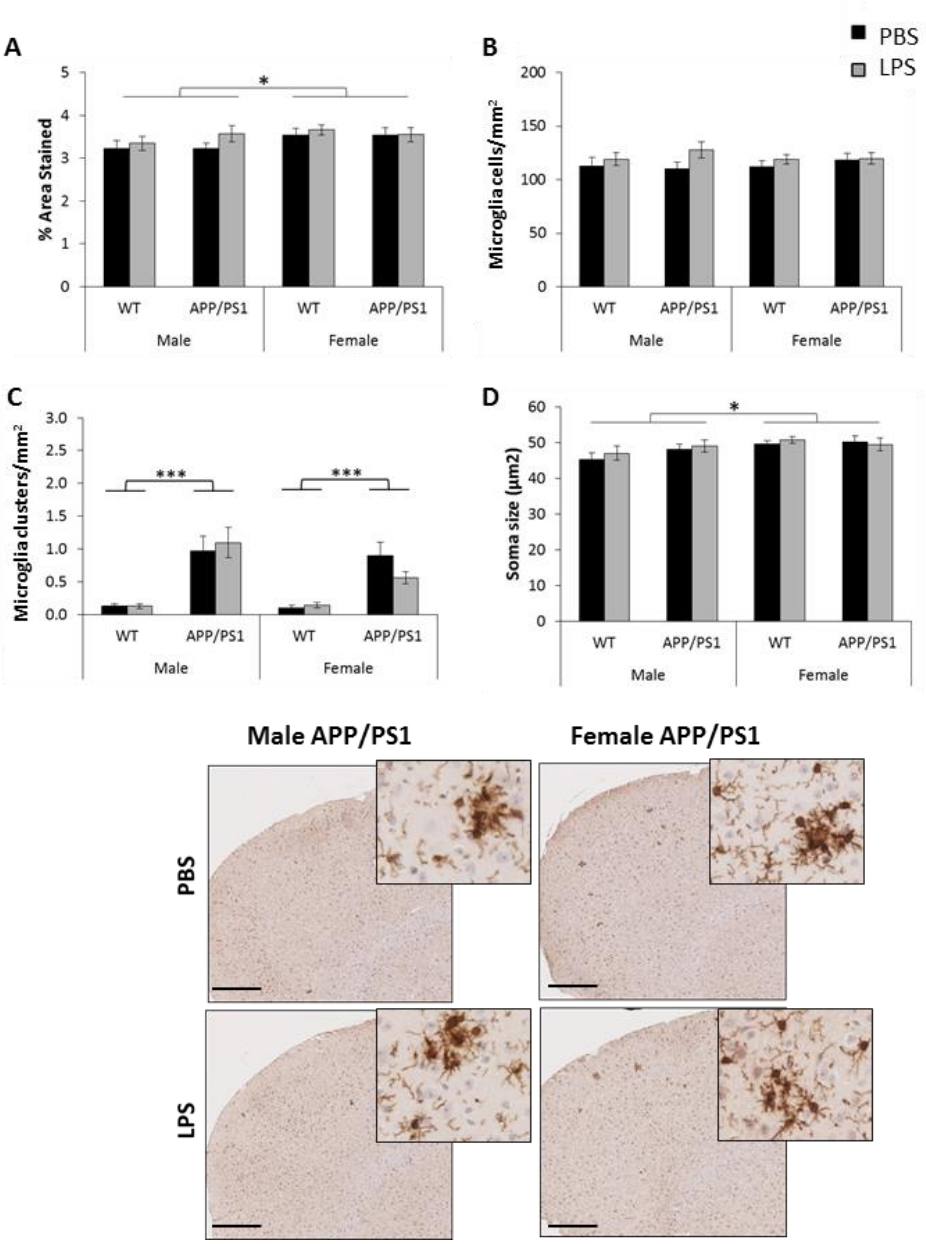

Figure 41. **Area occupied by Iba-1 in the cortex.** 4.5 months old male and female mice APPswe/PS1ΔE9 (APP/PS1) and wild-type (WT) (n=8 per group) were treated with LPS or vehicle (PBS) and their brain was collected 7 days after the challenge. Females showed a significant higher percentage of area stained by Iba-1 (p=0.023) (**A**) and larger microglia soma size (p=0.023) (**D**) than males. No significant difference observed in microglia cells per mm2 (**B**). A higher number of microglial clusters/mm^2 was revealed in APP/PS1 female compared to WT female (p<0.0001) and in APP/PS1 male compared to WT littermates (p<0.0001) (**C**). Scale bars, 0.5mm. Data are presented as mean ± S.E.M. [* p< 0.05].

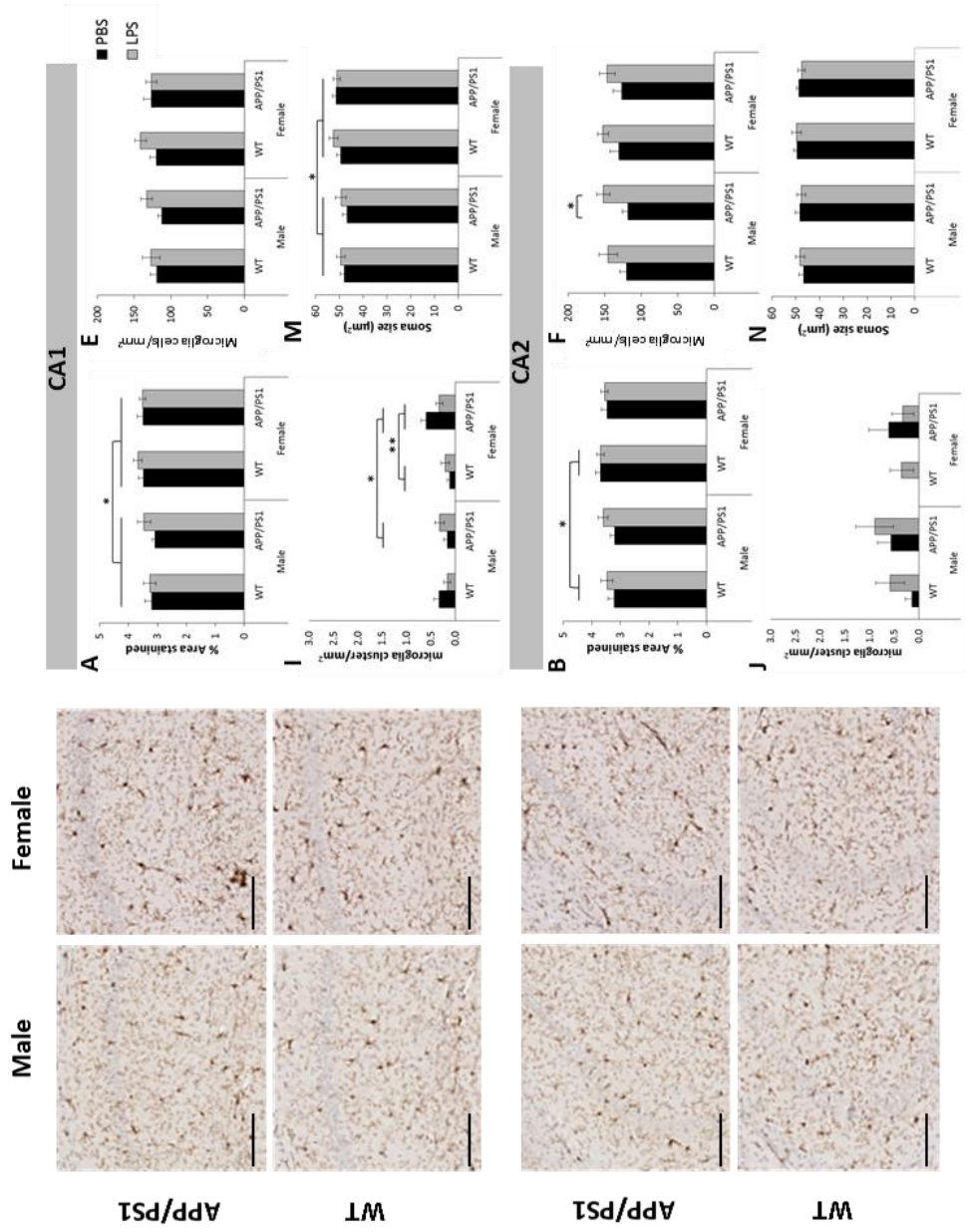

Figure 42. **Area occupied by Iba-1 in the CA1 and CA2 hippocampal subfields.** 4.5 months old male and female mice APPswe/PS1ΔE9 (APP/PS1) and wild-type (WT) (n=8 per group) were treated with LPS or vehicle (PBS) and their brain was collected 7 days after the challenge. Females showed higher percentage of area stained by Iba-1 in CA1 (p-0.036) (**A**) than males, with higher percentage of area stained in WT females compared to WT males in CA2 (p=0.039) (**B**). No significant difference was observed in the number of microglial cells/mm^2 in CA1 (**E**), while LPS-treated APP/PS1 males showed higher number of microglial cells/mm^2 compared to PBS-treated counterparts in CA2 (p=0.031) (**F**). A higher number of microglial clusters/mm^2 was revealed in APP/PS1 females compared to WT females (p=0.001) and compared to APP/PS1 males in CA1 (p=0.023) (**I**). Females revealed a larger microglia soma size than males in CA1 (p=0.013) (**M**). Scale bars, 0.25mm. Data are presented as mean $\pm$ S.E.M. [* p< 0.05, **p<0.005].

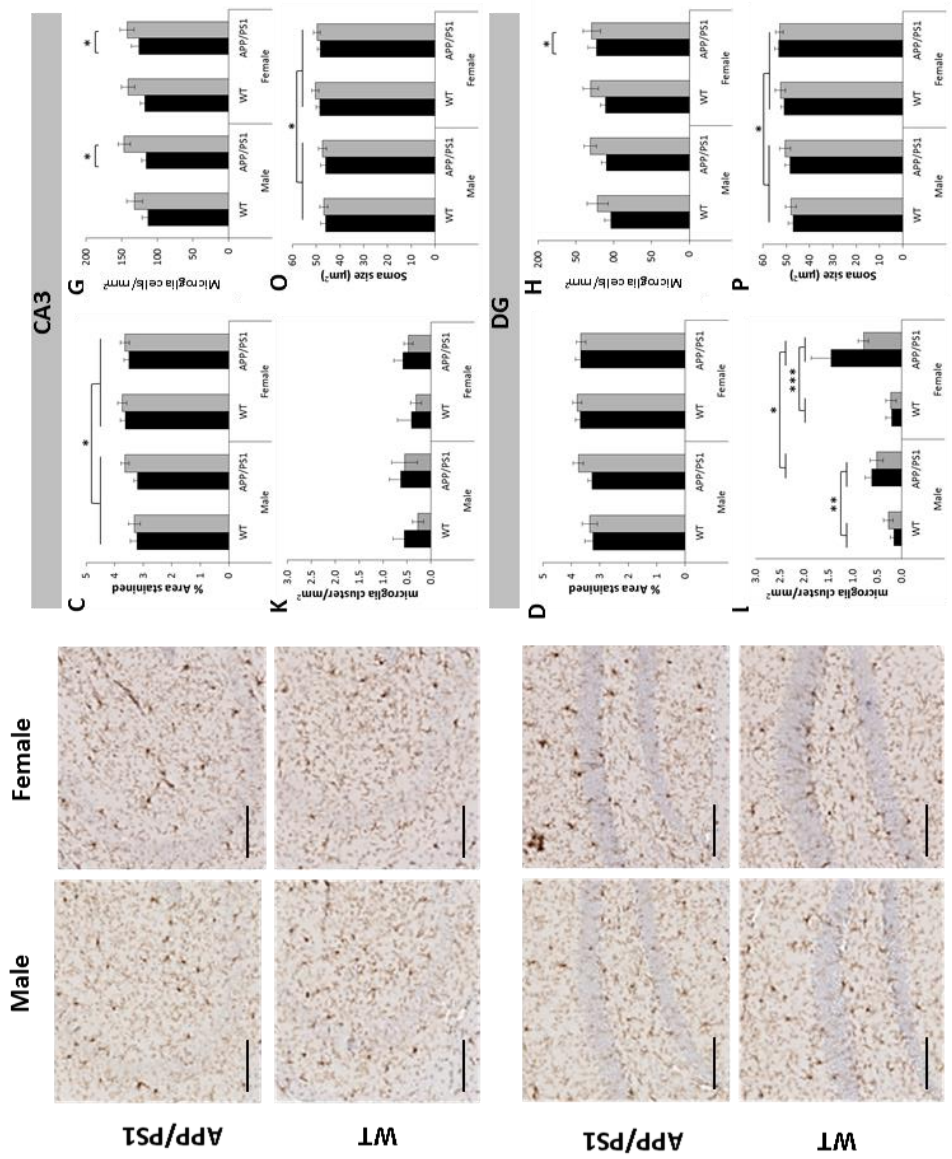

Figure 43. **Area occupied by Iba-1 in the CA3 and DG hippocampal subfields.** 4.5 months old male and female mice APPswe/PS1ΔE9 (APP/PS1) and wild-type (WT) (n=8 per group) were treated with LPS or vehicle (PBS) and their brain was collected 7 days after the challenge. Females showed higher percentage of area stained by Iba-1 in CA3 (p=0.02) (**C**), compared to males. LPS-treated APP/PS1 males showed greater number of microglial cells/mm^2 compared to PBS-treated counterparts in CA3 (p=0.016) (**G**), and LPS-treated APP/PS1 females revealed more number of microglial cells/mm^2 compared to PBS-treated group in CA3 (p=0.018) and DG (p=0.036) (**H**). In DG, higher number of microglial clusters/mm^2 was revealed in APP/PS1 females compared to WT females (p<0.0001) (**L**) and compared to APP/PS1 males (p=0.036). APP/PS1 male showed also higher number of microglial clusters/mm^2 than wild-type males (p=0.003) (**L**). Females revealed a larger microglia soma size than males in CA3 (p=0.049) (**O**) and DG (p=0.048) (**P**). Scale bars, 0.25mm. Data are presented as mean $\pm$ S.E.M. [* p< 0.05, **p<0.005, ***p<0.0001].

4.3.5 Infiltration of peripheral monocytes into the CNS and characterization of their immune profile

To detect macrophages that infiltrated the brain 7 days after the immune challenge, brain tissue was collected and cells were dissociated, stained and analysed using flow cytometry as described in the method chapter (chapter 2). The percentage of gated cells relative to the total number of cells were stained with $CD11b^{+}CD45^{+Lo}$ and $CD11b^{+}CD45^{+Hi}$ to distinguish between resident microglia and infiltrating monocytes respectively. Analysis of the proportion of infiltrating monocytes in the brain showed no significant differences between the experimental groups in the hippocampus (Figure 44), while in the cortex an overall sex effect was revealed ($F_{(1,20)}$= 6.47, p=0.019), with wild-type males showing a lower number of infiltrating macrophages than wild-type females (p=0.006) (Figure 46.A). An overall effect of sex was also revealed in the microglia analysis the hippocampus ($F_{(1,20)}$= 6.17, p=0.022) (Figure 45) and cortex ($F_{(1,20)}$= 11.73, p=0.003) (F igure 47.A), where wild-type males showed higher number of resident microglia compare to wild-type females (p<0.05).

To further identify the subpopulation distribution among the infiltrated macrophages and resident microglia, expression of CCR2 and intracellular Aβ staining was analysed to characterize the chemotactic phenotype and the presence of intracellular amyloid beta peptide, respectively. An overall sex effect was seen in the hippocampus ($F_{(1,20)}$= 7.53, p=0.0125) (Figure 44.B) and in the cortex ($F_{(1,20)}$= 22.53, p=0.0001) (Figure 46.B). Wild-type males showed a higher number of infiltrated macrophages expressing CCR2 compared to wild-type females (p=0.038) in the hippocampus, and compared to females wild-type (p=0.035) and transgenic (p=0.0002) in the cortex. An overall sex effect was also seen in the percentage of microglia expressing CCR2 in the hippocampus ($F_{(1,20)}$= 38.56, p<0.0001) (Figure

45.B), and cortex ($F_{(1,20)}$= 8.36, p=0.009) (Figure 47.B), with males having more microglia cells expressing CCR2 than females (p<0.05). Intracellular Aβ analysis showed an overall genotype ($F_{(1,20)}$= 7.32, p=0.014) and sex ($F_{(1,20)}$= 18.3, p=0.0004) effect in the hippocampus (Figure 44.C), with APPswe/PS1ΔE9 females showing higher number of infiltrated macrophages positive for Aβ compared to transgenic males (p-=0.0084), and APPswe/PS1ΔE9 males having more infiltrated macrophages positive for Aβ compared to wild-type males (p=0.041). Moreover also wild-type females showed more infiltrated macrophages with intracellular Aβ compared to wild-type males (p=0.053) (Figure 44.C). An overall genotype effect was seen in the cortex ($F_{(1,20)}$= 5.11, p=0.035) (Figure 46.C), with higher number of infiltrating macrophages presenting intracellular Aβ in transgenic females compare to transgenic males (p=0.028). An overall sex effect was indeed observed in the hippocampus ($F_{(1,20)}$= 12.94, p=0.002) (Figure 45.C), with higher number of resident microglia presenting intracellular Aβ in transgenic (p=0.018) and wild-type females (p=0.021) compared to wild-type males.

To characterize the immune phenotype of the brain-infiltrating macrophages and resident microglia cells, analysis of the expression of M1 (CD80) and M2 (CD206) was performed through flow cytometry (detailed protocol in the method chapter). From the analysis of M1 expression, an overall sex effect was revealed in the hippocampus in infiltrated macrophages ($F_{(1,21)}$= 20.76, p=0.0002) (Figure 44.D) and in microglia ($F_{(1,21)}$= 7.78, p=0.011) (Figure 45..D) expressing CD80, with wild-type males showing higher M1 expression than wild-type females. No significant difference emerged between the experimental groups in the cortex (Figure 46.D-Figure 47.D).

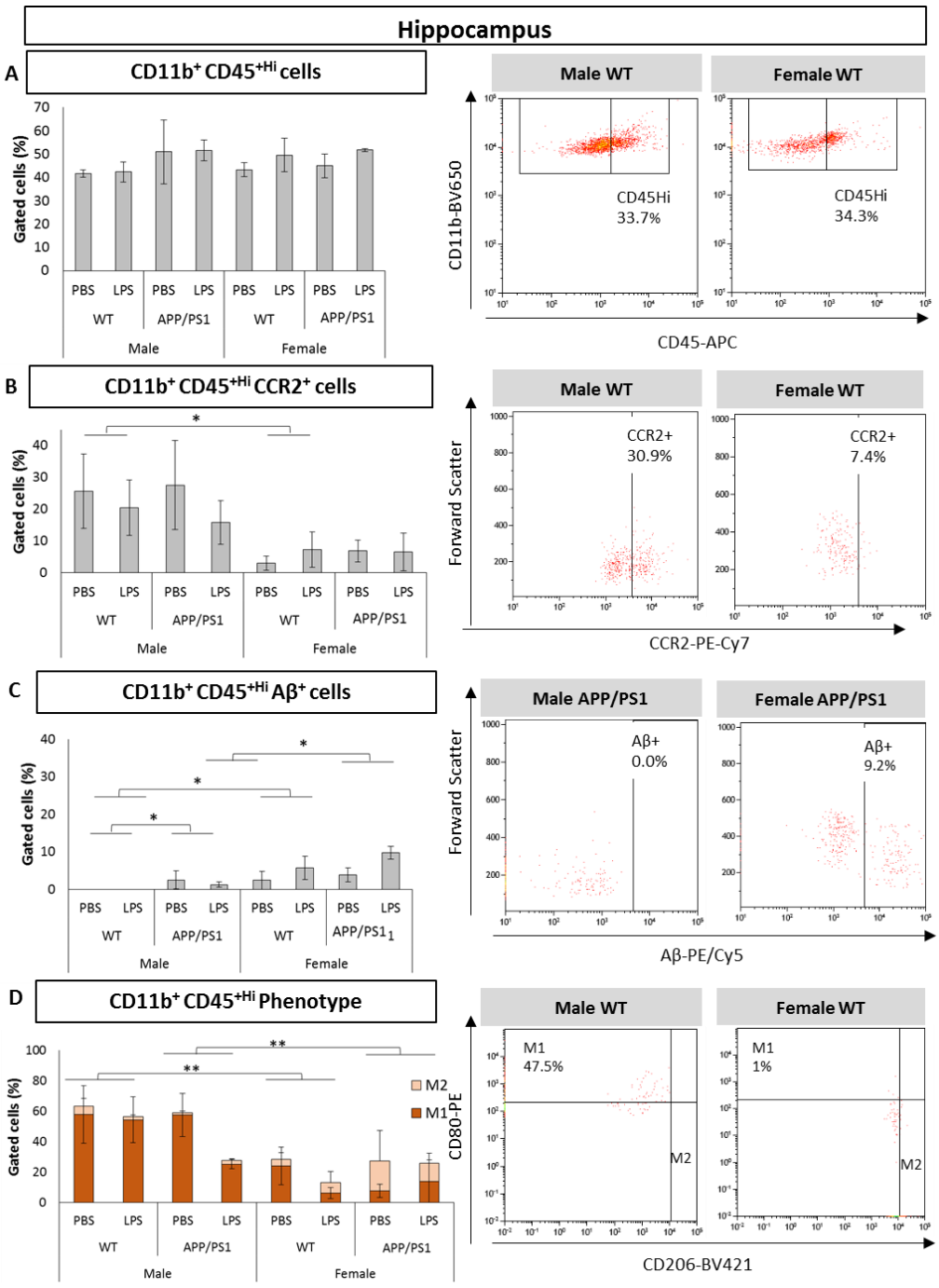
Hippocampus
A
CD11b+ CD45+Hi cells
Gated cells (%)
PBS LPS PBS LPS PBS LPS PBS LPS
WT APP/PS1 WT APP/PS1
Male Female
Male WT
Female WT
CD11b-BV650
CD45Hi
33.7%
CD45Hi
34.3%
CD45-APC
B
CD11b+ CD45+Hi CCR2+ cells
Gated cells (%)
Male WT
Female WT
Forward Scatter
CCR2+
30.9%
CCR2+
7.4%
CCR2-PE-Cy7
C
CD11b+ CD45+Hi Aβ+ cells
Gated cells (%)
Male APP/PS1
Female APP/PS1
Forward Scatter
Aβ+
0.0%
Aβ+
9.2%
Aβ-PE/Cy5
D
CD11b+ CD45+Hi Phenotype
Gated cells (%)
M2
M1
Male WT
Female WT
CD80-PE
M1
47.5%
M2
M1
1%
M2
CD206-BV421

Figure 44 **Infiltrated macrophages analysis with flow cytometry in the hippocampus.** 4.5 months old male and female mice APPswe/PS1ΔE9 (APP/PS1) and wild-type (WT) (n=3/4 per group) were treated with LPS or vehicle (PBS) and their brain was collected 7 days after the challenge. Flow cytometry analysis revealed no significant differences regarding the $CD11b^{+}$ $CD45^{+Hi}$ cells (**A**). Analysis of $CCR2^{+}$ expression in $CD11b^{+}$ $CD45^{+Hi}$ cell population revealed lower percentage of cells having the CCR2 receptor in WT females compared to WT males (p=0.038) (**B**). Higher number of $CD11b^{+}CD45^{+Hi}A\beta^{+}$ cells was seen in APP/PS1 females compared to APP/PS1 males (p=0.008), in WT females compared to WT males (p=0.005), and in APP/PS1 males compared to WT males (p=0.041) (**C**). Moreover, lower expression of CD80, the M1 marker, was seen in WT females compared to WT males (p=0.004) and in APP/PS1 females compared to APP/PS1 males (p=0.004) (**D**). Data are shown as mean $\pm$ S.E.M. [*p< 0.05, **p<0.005].

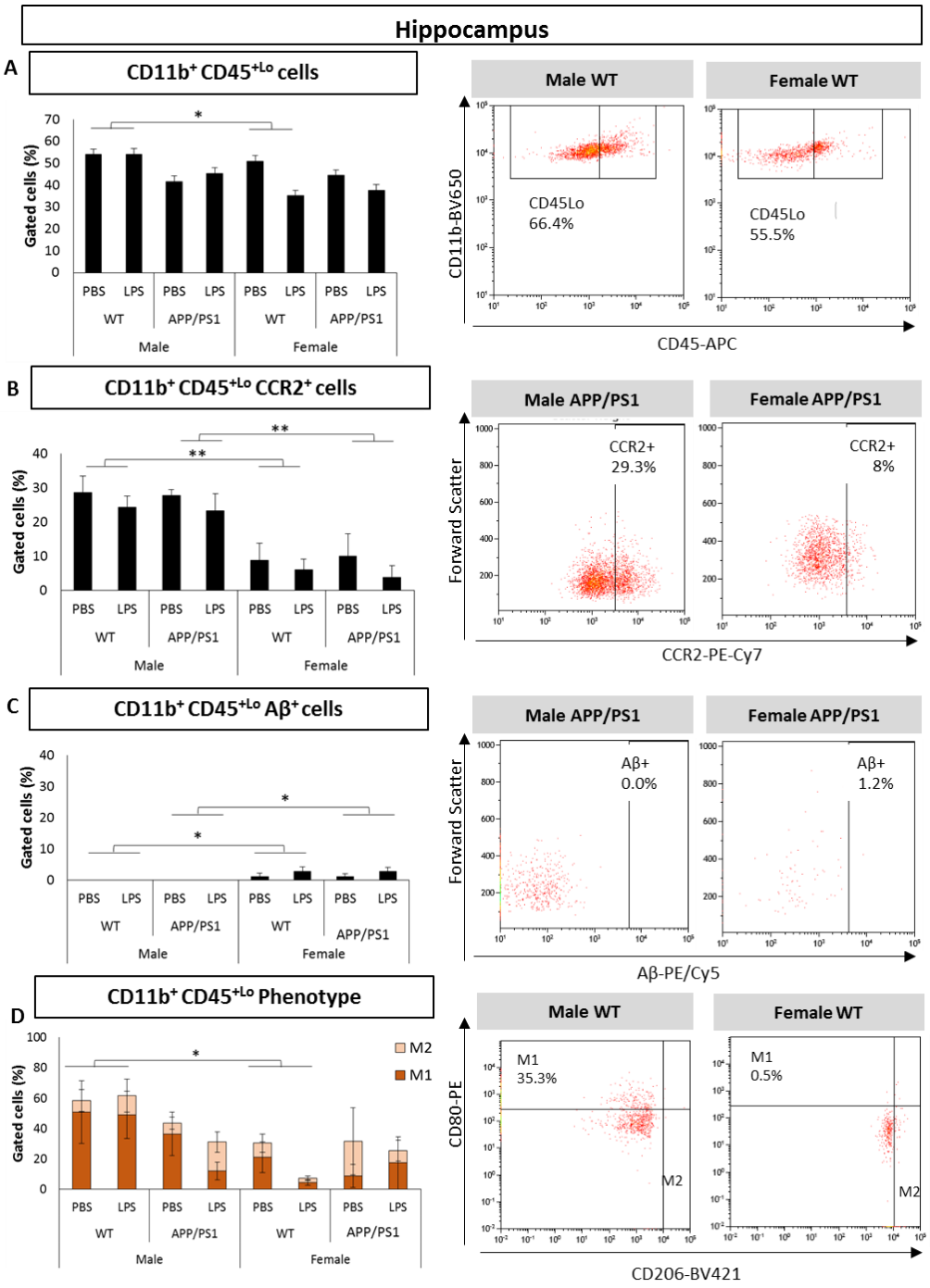
Hippocampus
A
CD11b+ CD45+Lo cells
Gated cells (%)
PBS LPS PBS LPS PBS LPS PBS LPS
WT APP/PS1 WT APP/PS1
Male Female
Male WT
Female WT
CD45Lo
66.4%
CD45Lo
55.5%
CD11b-BV650
CD45-APC
B
CD11b+ CD45+Lo CCR2+ cells
Male APP/PS1
Female APP/PS1
CCR2+
29.3%
CCR2+
8%
Forward Scatter
CCR2-PE-Cy7
C
CD11b+ CD45+Lo Aβ+ cells
Aβ+
0.0%
Aβ+
1.2%
Aβ-PE/Cy5
D
CD11b+ CD45+Lo Phenotype
M2
M1
M1
35.3%
M1
0.5%
M2
CD80-PE
CD206-BV421

Figure 45**. Microglia analysis with flow cytometry in the hippocampus.** 4.5 months old male and female mice APPswe/PS1ΔE9 (APP/PS1) and wild-type (WT) (n=3/4 per group) were treated with LPS or vehicle (PBS) and their brain was collected 7 days after the challenge. Flow cytometry analysis revealed lower percentage of $CD11b^{+}$ $CD45^{+Lo}$ cells in WT females compared to WT males (p=0.023) (**A**). Analysis of $CCR2^{+}$ expression in $CD11b^{+}$ $CD45^{+Lo}$ cell population revealed lower percentage of cells having the CCR2 receptor in WT females compared to WT males (p=0.0002) and in APP/PS1 females compared to APP/PS1 males (p=0.0004) (**B**). Higher number of $CD11b^{+}CD45^{+Lo}A\beta^{+}$ cells was observed in APP/PS1 females compare to APP/PS1 males (p=0.018) and in WT females compared to WT males (p=0.021) (**C**). Moreover, lower expression of CD80, the M1 marker was seen in WT females compared to WT males (p=0.003) (**D**). Data are shown as mean $\pm$ S.E.M. [* p< 0.05, **p<0.005].

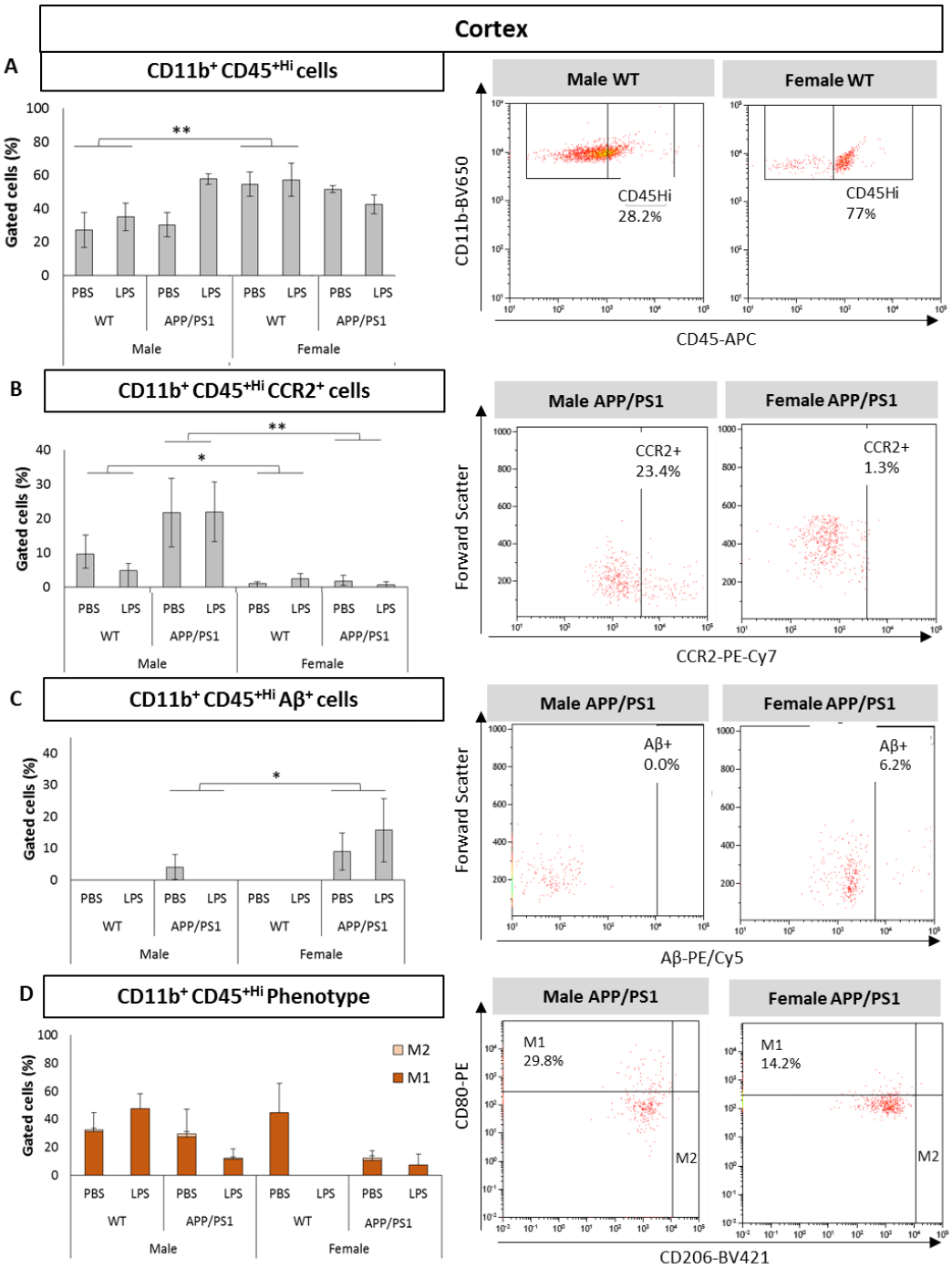
Cortex
A
CD11b+ CD45+Hi cells
Gated cells (%)
PBS LPS PBS LPS PBS LPS PBS LPS
WT APP/PS1 WT APP/PS1
Male Female
Male WT
Female WT
CD11b-BV650
CD45Hi
28.2%
CD45Hi
77%
CD45-APC
B
CD11b+ CD45+Hi CCR2+ cells
Male APP/PS1
Female APP/PS1
Forward Scatter
CCR2+
23.4%
CCR2+
1.3%
CCR2-PE-Cy7
C
CD11b+ CD45+Hi Aβ+ cells
Aβ+
0.0%
Aβ+
6.2%
Aβ-PE/Cy5
D
CD11b+ CD45+Hi Phenotype
M2
M1
CD80-PE
M1
29.8%
M1
14.2%
CD206-BV421

Figure 46. **Infiltrated macrophages analysis with flow cytometry in the cortex.** 4.5 months old male and female mice APPswe/PS1ΔE9 (APP/PS1) and wild-type (WT) (n=3/4 per group) were treated with LPS or vehicle (PBS) and their brain was collected 7 days after the challenge. Flow cytometry analysis of the cellular staining revealed lower percentage of $CD11b^{+}$ $CD45^{+Hi}$ cells in WT males compared to WT females (p=0.006) (**A**). Analysis of $CCR2^{+}$ expression in $CD11b^{+}$ $CD45^{+Hi}$ cell population revealed lower percentage of cells having the CCR2 receptor in WT females compared to WT males (p=0.034) and in APP/PS1 females compared to APP/PS1 males (p=0.0002) (**B**). Higher number of $CD11b^{+}CD45^{+Hi}A\beta^{+}$ cells was observed in APP/PS1 females compared to APP/PS1 males (p=0.028) (**C**). No significant differences were seen in the analysis of the cellular markers CD80 and CD206 (**D**). Data are shown as mean $\pm$ S.E.M. [* p< 0.05, **p<0.005].

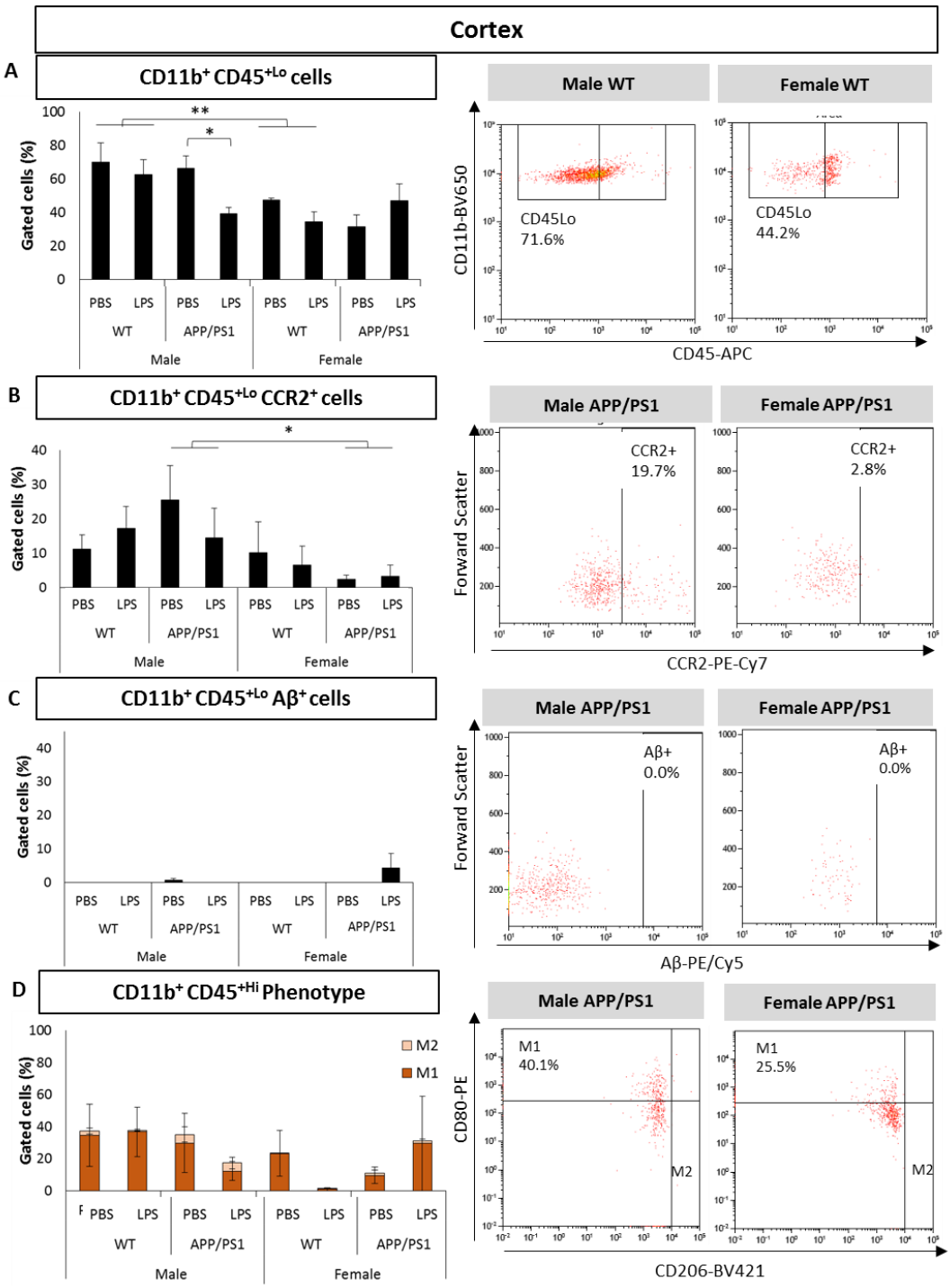
Cortex
A
CD11b+ CD45+Lo cells
Gated cells (%)
PBS LPS PBS LPS PBS LPS PBS LPS
WT APP/PS1 WT APP/PS1
Male Female
Male WT
Female WT
CD11b-BV650
CD45Lo
71.6%
CD45Lo
44.2%
CD45-APC
B
CD11b+ CD45+Lo CCR2+ cells
Male APP/PS1
Female APP/PS1
Forward Scatter
CCR2+
19.7%
CCR2+
2.8%
CCR2-PE-Cy7
C
CD11b+ CD45+Lo Aβ+ cells
Aβ+
0.0%
Aβ+
0.0%
Aβ-PE/Cy5
D
CD11b+ CD45+Hi Phenotype
M2
M1
CD80-PE
M1
40.1%
M1
25.5%
M2
CD206-BV421

Figure 47. **Microglia analysis with flow cytometry in the cortex.** 4.5 months old male and female APPswe/PS1ΔE9 (APP/PS1) and wild-type (WT), (n=3/4 per group), were treated with LPS and vehicle (PBS) and their brain was collected 7 days after the challenge. Flow cytometry analysis of the cellular staining revealed lower percentage of $CD11b^{+}$ $CD45^{+Lo}$ cells in WT females compared to WT males (p=0.0049) and in PBS-treated compared to LPS-treated mice (p=0.006)(**A**). Analysis of $CCR2^{+}$ expression in $CD11b^{+}$ $CD45^{+Lo}$ cell population revealed lower percentage of cells having the CCR2 receptor in WT females compared to WT males (p=0.021)(**B**). No significant differences were observed in the analysis of intracellular Aβ (**C**), and the surface phenotypic markers CD80 and CD206 (**D**). Data are shown as mean $\pm$ S.E.M. [* $p< 0.05$, ** $p<0.005$].

4.3.6 Characterizing peritoneal macrophages 7 days after LPS treatment

To characterize the phenotype of peritoneal macrophages in 4.5 months old mice wild-type and APPswe/PS1ΔE9, 7 days after LPS/vehicle injection, flow cytometry analysis was performed as described in the method chapter (chapter 2). Peritoneal macrophages, identified as $F4/80^+$ cells, were characterized by staining for CCR2, to analyse the chemotactic phenotype, for CD80 and CD206, to investigate the inflammatory phenotype, and for Aβ, to show the intracellular presence of the amyloid peptide as an indicator of their phagocytic activity. No significant differences between the experimental groups were observed in the analysis of CCR2 (Figure 48.A), and in the M1 (CD80) and M2 (CD206) (Figure 48.C) expression. From the analysis of the intracellular Aβ, an overall genotype effect was revealed ($F_{(1,20)}$= 4.78, p=0.041), with wild-type males showing a lower number of peritoneal macrophages positive for Aβ compared to transgenic males (p=0.006), and wild-type females (p=0.019) (Figure 48.B).

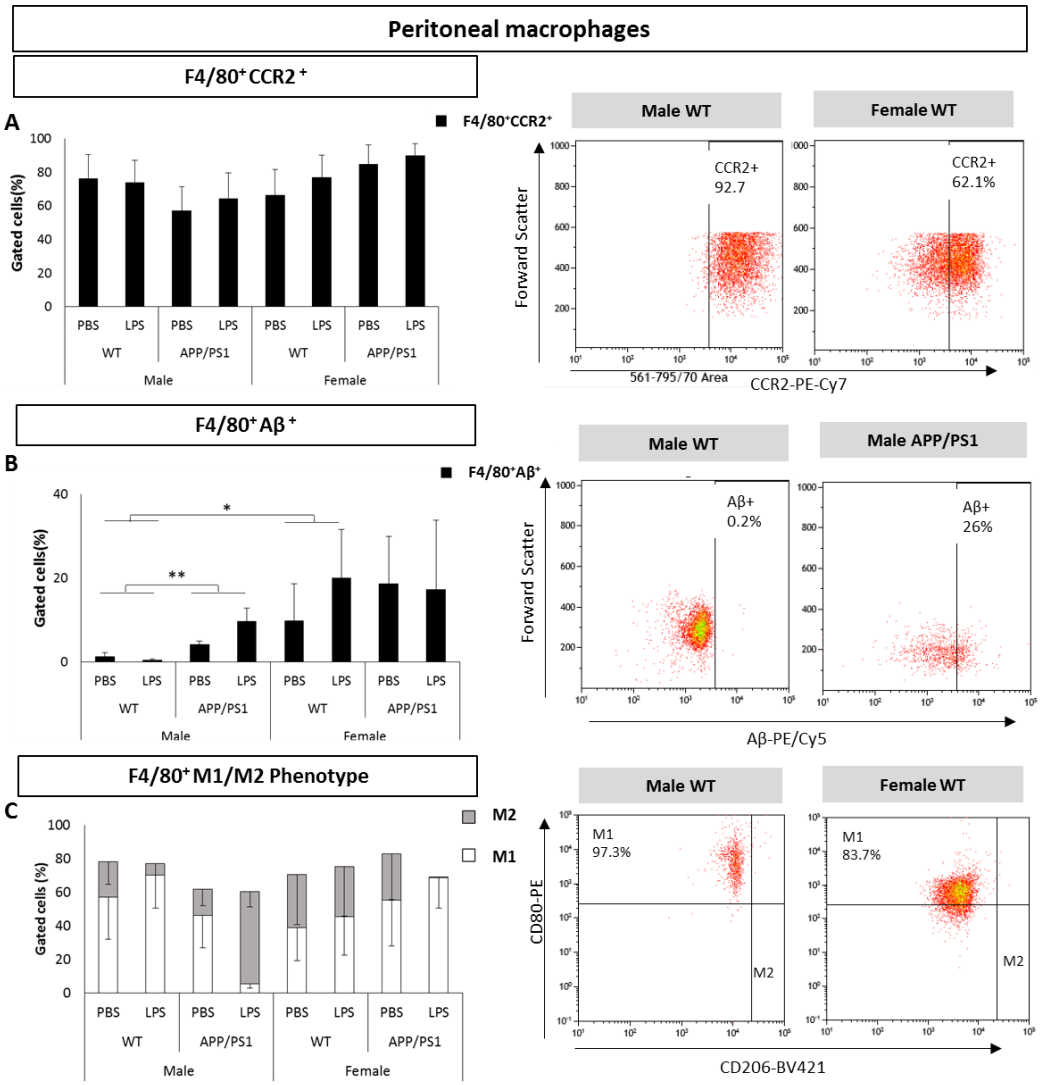

Figure 48. **Peripheral macrophages analysis with flow cytometry**. 4.5 months old male and female mice APPswe/PS1ΔE9 (APP/PS1) and wild-type (WT) (n=3/4 per group) were treated with LPS and vehicle (PBS) and peritoneal macrophages were collected 7 days after the challenge. No significant differences were seen between the experimental groups in the analysis of CCR2 expression (**A**), as well as in the M1 or M2 marker expression (**C**). F4/80^{+} cells in WT males showed lower intracellular Aβ staining than APP/PS1 males (p=0.002) and WT females (p=0.005) (**B**). Data are presented as mean + S.E.M. Data are shown as mean $\pm$ S.E.M. [*p< 0.05, **p<0.005].

4.4 Summary of the main findings

In summary, the present study revealed that LPS affected the number of microglia cells per mm^2, with LPS-treated APPswe/PS1ΔE9 animals showing a higher number of iba-1-immunoreactive cells per mm^2 than vehicle-treated animals in both males and females (Table 3). In particular, flow cytometry analysis showed that LPS decreased the number of resident microglia, marked as $CD11b^{+}CD45^{+Lo}$ positive cells, in LPS-treated APPswe/PS1ΔE9 males compared to the control (Table 4). No effects of LPS were seen 7 days after the treatment on the behavioural assessments (Table 2), cytokines quantification in plasma (Table 2), amyloid plaque load and GFAP-immunoreactive cells (Table 3). No effects of LPS were observed in the analysis of the brain-infiltrated and peritoneal macrophages (Table 4) 7 days after the treatment.

Nevertheless, differences between sexes and genotypes have been revealed. Females showed a faster body weight recovery from LPS administration, associated with a smaller area covered by GFAP-immunoreactive cells and larger area covered by Iba-1 immunoreactive cells, compared to males. In particular, transgenic females presented a higher number of extracellular amyloid plaques and intracellular Aβ staining, as well as higher number of Iba-1 and GFAP clusters, compared to transgenic males. Characterization of the cellular phenotype of infiltrated macrophages and resident microglia revealed a lower expression of CCR2 and CD80 in females, associated with a higher presence of intracellular Aβ stained by flow cytometry, compared to males. In particular, APPswe/PS1ΔE9 females showed more intracellular Aβ than APPswe/PS1ΔE9 males in infiltrated and peritoneal macrophages, as well as resident microglia.

Table 2. Summary of the main findings on behaviour and cytokines levels

	BEHAVIOURAL AND CYTOKINES ANALYSIS		
	TREATMENT	**GENOTYPE**	**SEX**
BODY WEIGHT RECOVERY	–	–	Females recover faster than males.
FOOD BURROWING	–	WT females burrowed more food than APP/PS1 females both at baseline and post-injection.	–
SPATIAL WORKING MEMORY	–	–	–
LOCOMOTOR ACTIVITY	–	APP/PS1 mice moved more than WT mice in both sexes.	–
CYTOKINES	–	–	WT females showed higher **TNF-α** and **IFN-γ** levels than WT males.

Table 3. Summary of the main immunostaining analysis.

	IMMUNOSTAINING ANALYSIS		
	TREATMENT	**GENOTYPE**	**SEX**
AMYLOID PLAQUE LOAD	–	N/A	Higher **number of plaques** in females compared to males.
GFAP-IMMUNOREACTIVITY	–	Higher number of **GFAP clusters** in APP/PS1 compared to WT mice.	Higher **% area stained** in males compared to females. Higher number of **GFAP clusters** in females compared to males APP/PS1.
IBA-1-IMMUNOREACTIVITY	LPS-treated APP/PS1 mice showed a greater density of **iba-1-immunoreactive cells** than PBS-treated APP/PS1 animals in both males and females.	Higher number of **Iba-1 clusters** in APP/PS1 compared to WT mice.	Higher **% area stained** in females compared to males. Larger **microglia soma** in females compared to males. Higher number of **Iba-1 clusters** in females compared to males.

Table 4. Summary of the main flow cytometry analysis.

	FLOW CYTOMETRY ANALYSIS		
	TREATMENT	**GENOTYPE**	**SEX**
BRAIN INFILTRATING MACROPHAGES $CD11b^{+}CD45^{+HI}$	–	Higher number in APP/PS1 females compared to WT females.	Higher number in WT females compared to WT males in the cortex only.
MICROGLIA $CD11b^{+}CD45^{+LO}$	Lower number in LPS-treated APP/PS1 males compared to vehicle-treated animals, in the cortex.	–	Lower number in WT females compared to WT males.
CCR2 EXPRESSION	–	–	Lower in females compared to males in infiltrated macrophages and resident microglia, regardless of the genotype. **$F4/80^{+}$:** no changes.
INTRACELLULAR Aβ	–	Higher in APP/PS1 males compared to WT males in **infiltrated** (hippocampus) and **peritoneal macrophages.**	Higher in females compared to males in **infiltrated and peritoneal macrophages, and resident microglia.**
M1/M2 IMMUNE PHENOTYPE	–	–	Lower expression of M1 marker in females compared to males in **infiltrated macrophages and resident microglia** from the hippocampus only. **$F4/80^{+}$**: no changes

4.5 Discussion

In the present study, I tested the hypothesis that a single systemic LPS challenge would exacerbate glial response and amyloid plaque load in 4.5 months old APPswe/PS1ΔE9 mice, seven days after the treatment. Increased levels of pro-inflammatory mediators and recruitment of peripheral monocytes into the brain were expected, as a consequence of increased Aβ accumulation.

LPS, administered at a low dose of 100μg/kg, was used to modulate the immune response, and to determine the effect of an acute systemic immune challenge on both male and female. Behavioural changes, as well as cytokines and glial response, were analyzed to assess susceptibility to LPS, and the impact on amyloid plaque load. The presence of infiltrating monocytes and the characterization of their phenotype and phagocytic activity was investigated to determine if LPS would increase recruitment of peripheral immune cells in APPswe/PS1ΔE1 more than in wild-type animals.

Immunostaining analysis revealed that LPS did not increase amyloid plaque load, as expected. LPS affected the density of microglia cells after 7 days in the hippocampus, with LPS-treated APPswe/PS1ΔE9 animals showing a higher number of cells compared to vehicle-treated mice, in both males and females. However, analysis of microglia by flow cytometry, as $CD11b^{+}CD45^{+Lo}$ positive cells, revealed that LPS-treated APPswe/PS1ΔE9 males had a lower percentage of microglia cells, compared to the vehicle-treated mice. These contradictory findings can be explained by the consideration that Iba-1, used to immunostain microglia cells in this study, is known to stain also macrophages (Bennett et al., 2016), suggesting

that the higher number of Iba-1 positive cells observed in transgenic males can be both microglia and macrophages, as reflected by the flow cytometry analysis.

LPS did not affect spatial working memory, daily living activity and locomotor activity, 7 days after the treatment. Previous evidence showed that systemic LPS administration induced sickness syndrome lasting up to 48 hours (Biesmans et al., 2013), suggesting a possible return to baseline behaviour after one week. Contrary, a previous in-vivo study in a 3xTg-AD mouse model showed that a single intraperitoneal injection with LPS had a long-term impact affecting memory performance associated to AD pathology, 6 weeks after the treatment, associated with decreasing hippocampal neurogenesis (Valero et al., 2014). However, a reduction in locomotor activity was seen in this study in all the experimental groups, regardless of treatments, can be due to the habituation of the animals to the already familiar environment that reduced the tendency to explore the open space. Indeed novelty of the open field had been considered a motivational influence on locomotor activity, that would otherwise decrease without novelty stimuli (Engeland et al., 2001).

Females and males were both tested to elucidate the difference in amyloid burden and etiopathology. Sex difference in amyloid deposit, revealed in this study, was already reported in AD mice models, showing higher amyloid burden and plaque numbers in females compared to males with an age-dependent increase (Wang et al., 2003b, Callahan et al., 2001, Sykova et al., 2005). Previous investigators revealed increased expression of amyloid precursor protein and increased generation of Aβ, following systemic LPS administration between 4 hours and 12

weeks after the challenge (Lee et al., 2008, Sheng et al., 2003). A reduction of Aβ was only observed after intra-hippocampal injection of LPS in 11 and 16 months old mice, 7 days after the challenge (DiCarlo et al., 2001, Herber et al., 2004). The experimental conditions of these previous reports vary, including the age and the animal model used, as well as the dose, the route of administration, the number of injections and the time-point of the study. For example, Sheng, Bora et al, injected LPS intraperitoneally and at a higher dose than the one used in this study (10µl/g of body weight), in older mice (11±4 months old) and revealed LPS-increase of Aβ production (Sheng et al., 2003). Indeed, high dose of the bacterial infection can exacerbate the immune response activating pro-inflammatory mechanism (Cunningham, 2013). Effects of inflammation are also age-dependent, indicating that inflammation can affect disease progression differently in old and young animals. It is well documented in aged animals that the immunomodulatory response is compromised and microglia are primed (Norden and Godbout, 2013, Williams et al., 2015), linked to age-dependent reduction of the association between microglia and amyloid plaques (Wyss-Coray, 2006). Thus, even moderate doses of LPS could exacerbate the existing pathology in old animals. Furthermore, the route of administration can also modulate the response differently as an intrahippocampal administration of LPS does not involve the cross-talk between the periphery and the brain, overcoming the BBB, while a systemic injection activates immune pathways that transduce the peripheral signal into the brain (Rivest, 2003). Indeed, systemic injection of LPS better mimic the clinical conditions where infections are more likely to induce brain inflammation via indirect mechanisms, rather than crossing the BBB (Mallard, 2012).

Higher number of amyloid plaques observed in females, compared to males, are associated with a higher number of microglia and astrocytes clusters in females' hippocampal and cortical regions. It demonstrates, once again, the strong correlation between amyloid plaques and glial cells. Previous evidence also observed GFAP and Iba-1 clusters in close association with dense plaques, in hippocampus and cortex (Ruan et al., 2009, Ising and Heneka, 2018, Tsai-Teng et al., 2016).

Astrocytes and microglia activation were not affected by the treatment in all the experimental groups. Lack of astrocytes activation can be explained by a a previous report that showed an increase in GFAP density that peaked at 6 h, after systemic LPS injection, indicating that astrocytes respond might have an early and short-lasting response to a peripheral immune stimulation (Biesmans et al., 2013), that return to normal after 7 days. Furthermore, here I didn't observe an effect in microglia soma size, used as a marker of activation, suggesting lack of activation of microglia 7 days after LPS. Indeed, microglia were seen activated 6 h after LPS administration, remaining activated for at least 3 days (Hoogland et al., 2015). A significant increase in microglia activation at 7 days was only seen after an intrahippocampal injection of LPS and lasted 28 days (Herber et al., 2006).

Microglia density analysis revealed a higher number of microglia cells in LPS-treated transgenic mice. Previous literature showed that the number of proliferating cells in the cortex of APPswe/PS1dE9 mice significantly increased in association to the widespread deposition of amyloid plaques (Marlatt et al., 2014). This finding was also confirmed in-vitro where cultured microglia were seen proliferating in response to Aβ application (Kamphuis et al., 2012). Our transgenic mice showed higher microglia density after LPS injection in accordance to a study done by

Puntener et al., where moderate microglial activation was found 7 days after the challenge (Puntener et al., 2012).

Quantification of cytokines in plasma revealed that LPS did not induce an increase in the concentration of pro- and anti-inflammatory cytokines, 7 days after the treatment. However, higher levels of TNF-α and IFN-γ were detected in wild-type females compared to wild-type males, regardless of treatment. AD progression is associated with an immune disorder, enhanced production of pro-inflammatory cytokines and free radicals, such as NO. IFN-γ and TNF-α are involved in NO production and their levels were reported higher in patients with AD (Belkhelfa et al., 2014). Therefore, higher levels of these cytokines were expected in the transgenic animals and not in the wild-type littermates, as I observed. Indeed, levels of TNF-α in the periphery and central nervous system of healthy adults are maintained at very low levels, while the levels of this cytokine are significantly elevated peripherally and centrally in patients with AD (Chang et al., 2017). Nonetheless, a significant up-regulation of mRNA and protein levels of the pro-inflammatory cytokines TNFα and IL-1β was seen in hippocampal tissue 1 week after a single systemic dose of LPS (2 mg/kg, i.p), but not in serum where TNFα and IL-1β were seen acutely increased up to 6 hours following LPS-injection (Fu et al., 2014). This finding suggested a long-lasting neuroinflammatory response in the CNS, but this was not reflected in the levels of cytokines in the serum. Indeed, one study correlated the responses of the pro-inflammatory cytokines TNF- α, MCP-1 and IL-1β in liver, serum and brain after LPS (3 mg/kg, i.p.) and suggested that these cytokines are transported from the serum into the brain 1 hour after the challenge,

with their levels returning to normal in liver and serum after one week (Qin et al., 2008).

Flow cytometry analysis of brain cells showed a higher number of infiltrated macrophages in the cortex of wild-type females compared to wild-type males. Both infiltrated macrophages and microglia had lower expression of CCR2 and higher presence of Aβ in females compared to males, regardless of the genotype. Higher expression of CCR2 was observed in a previous report, in association with the pro-inflammatory phenotype (Yrlid et al., 2006), suggesting that the lower expression of CCR2 is associated to the anti-inflammatory phenotype. Several studies have demonstrated that Aβ stimulates transmigration of the immune cell across the BBB (Rezai-Zadeh et al., 2009, Gate et al., 2010, Naert and Rivest, 2013), promoting the expression of adhesion molecules (Hohsfield and Humpel, 2015). In particular, mononuclear phagocyte accumulation in the area of the AD brain with high Aβ levels was CCR2-dependent, suggesting that the gathering of these cells at sites of Aβ deposition, is an initial attempt to clear these aggregates (Hickman and El Khoury, 2010). Indeed, experimental models using microglial ablation (Grathwohl, Kälin et al. 2009) or using *in vivo* two-photon microscopy (Krabbe, Halle et al. 2013), revealed that microglia motility and phagocytic activity towards Aβ were reduced and impaired with increased deposition of amyloid plaques and progression of the AD pathology (Grathwohl et al., 2009, Krabbe et al., 2013).

Higher numbers of amyloid plaques observed in our transgenic females, as shown from the immunostaining analysis, was expected to be associated with increased levels of the chemotactic receptor CCR2 that would stimulate higher movement of monocytes into the brain. Previous studies in rodent models have seen that CCR2-

expressing monocytes are recruited in response to inflammation and amyloid plaque accumulation (Naert and Rivest, 2013), acquiring a pro-inflammatory phenotype and the ability to phagocyte Aβ (Hohsfield and Humpel, 2015, Malm et al., 2010, Town et al., 2008). In a particular study on APPswe/PS1E9 mice, revealed that both endogenous and injected Aβ induced an activation of microglial cells, leading to the release of CCL2, and the recruitment of peripheral monocytes, which are able to significantly phagocyte aggregated Aβ, contrary to resident microglia (Simard et al., 2006a). Moreover, transgenic mice deficit for CCR2 showed an increase in Aβ deposits, compared to the controls (El Khoury et al., 2007a). These findings were in accordance with a recent study on mice where the chemokine receptor CCR2 was expressed in pro-inflammatory monocytes transmigrating into the brain, also expressing the surface receptor CD80 (Jiang et al., 2016). However, here, I didn't observe a pro-inflammatory shift in phenotype as low levels of CCR2 and CD80 (M1 marker) was seen on both infiltrated monocytes and resident microglia cells in females.

Higher presence of intracellular Aβ was reported in transgenic females, compared to transgenic males. Whereas, higher intracellular levels of Aβ were seen in transgenic males compared to wild-type males was observed in the peritoneal macrophages and hippocampal infiltrated macrophages. Unexpectedly, higher intracellular staining of Aβ was observed also in wild-type females, limiting the interpretation of the data. This can be explained by an observation made on post-mortem human brain tissue samples that showed that the 6E10 anti-Aβ antibody was unable to distinguish intracellular Aβ from AβPP (intracellular APP) and it was detected in all subjects independent of the disease state or presence of

extracellular Aβ aggregates (Aho et al., 2010). An additional report, that used 6E10 anti-Aβ antibody in a western blot experiment showed a similar band pattern in tissue from wild-type and 4–8-month-old APP transgenic mice, with 6E10 also cross-reacting with the full-length APP (Teich et al., 2013). Teich et al showed also that 6E10 binds in a non-specific way, concluding that this antibody might also detect proteins that are not derived from APP (Teich et al., 2013). A solution was proposed by Aho et al to overcome the non-specificity of this antibody, suggesting that an antibody directed to the C-terminal of the Aβ peptide (i.e., Aβ40, Aβ42, and 12F4), instead of the N-terminal, would better identify intracellular Aβ and distinguish patients with Alzheimer's disease (Aho et al., 2010).

Investigating the phenotype and expression of M1 and M2 surface markers in the hippocampus, females showed lower M1 expression on infiltrating monocytes and resident microglia than males, with no differences in the expression of the M2 marker. This may suggest that phagocytic activity of Aβ could be associated with an intermediate state between M1 and M2. It needs to be considered that a previous study, investigating microglia cells' phenotype using CD206 as an M2 marker, reported CD206 immunoreactivity only in macrophages present in vessels, but not in resident microglia cells (Peferoen et al., 2015). Peritoneal macrophages did not show differences in the expression of CD80 and CD206, maybe due to differences in tissue and related functions for Aβ internalization. In a previous study, higher levels of CCR2 in the peritoneal macrophages were seen in LPS-treated rodents after 6h from the injection (Bachstetter et al., 2014). Therefore, the lack of LPS effect in the present study may reflect the longer time point chosen.

In conclusion, the present study showed that inflammation, due to bacterial infection, did not affect amyloid plaque load, cytokines levels and astrocytes activation after 7 days. Increase in the number of microglia cells per mm^2 was significantly affected in LPS-treated transgenic mice, leading to the hypothesis that microglia proliferate in response to the presence of plaques. To clarify the mechanism involved in Aβ response, analysis of brain infiltrating macrophages was assessed and higher internalization of amyloid peptide was seen in females compared to males. This may be linked to the higher presence of Aβ plaques in the brain regions investigated. Further study needs to clarify how the peripheral inflammation leads to a neuroinflammatory response and how to beneficially modulate the response.

CHAPTER 5

A second systemic challenge of LPS increased the number of microglia cells, limiting the growth of small amyloid plaques in APPswe/PS1ΔE9 female mice.

5.1 Introduction

The present study investigated the impact of a single and double systemic challenge of LPS (100µg/kg) 7 days after the last injection, in wild-type and APPswe/PS1ΔE9 mice, males and females, at 4.5 months of age. To determine the effect of LPS on the central and peripheral immune response, glial activity and amyloid plaque load in the brain, as well as cytokines levels in the plasma were analysed. In particular, microglia and astrocytes density and activation were analysed in hippocampus and cortex, and both pro-inflammatory (IL-1β, IL-6, IFN-γ, TNF-α) and anti-inflammatory (IL-10) cytokines were quantified in the plasma.

The behavioural response was also assessed in order to monitor the recovery of the mice from the infection and to examine the effect of the treatment on spatial working memory, daily living and locomotor activity.

LPS has often been acutely administered to exacerbate the pro-inflammatory response and induce cognitive impairments (Cunningham et al., 2009, Murray et al., 2012). However, many investigations reported that repeated exposure to LPS created a state of unresponsiveness to the infection, called endotoxin tolerance, characterized by decreased febrile response, reduction of pro-inflammatory cytokines (as TNF-α, IL-6 and IFN-γ) and increase in anti-inflammatory cytokines (as IL-10 and TNF-β) (Cavaillon et al., 2003, Dawicki and Marshall, 2007, Freudenberg et al., 2001, Nomura et al., 2000). Thus, an increase in pro-inflammatory cytokines

and activation of microglia was expected after the single systemic injection, while attenuation of the pro-inflammatory cytokines was expected after repeated LPS exposures.

In all these studies on endotoxin tolerance (Cavaillon et al., 2003, Dawicki and Marshall, 2007, Freudenberg et al., 2001), LPS was administered within few hours or days of the first exposure, while, in the present study, a second LPS injection was performed 2 weeks after the first challenge. A recent study done by Samira Parhizkar, from my research group, (Personal Communication) that investigated changes in body temperature induced by systemic LPS (100µg/kg, *i.v*) in both wild-type and APPswe/PS1ΔE9 males and females at 4.5 month old (data not published), showed that 2 weeks were necessary for the complete recovery of the animals from the infection. Another group also reported that 14 days were necessary for wild-type mice to regain normal responsiveness to infections after a tolerant state induced by intraperitoneal injection of LPS, (Lu et al., 2008). Moreover, having weeks between the first and second exposure to LPS is a better way to mimic real-life infections.

The effect of the treatments on amyloid plaque load was investigated as an increase in Aβ levels in response to a systemic administration of LPS was reported in more than one study (Sly et al., 2001, Sheng et al., 2003). In particular, an in-vivo experiment showed that repeated injections of LPS (250 µg/kg) induced accumulation of Aβ in the hippocampus and cerebral cortex of mice brains (Lee et al., 2008).

Since the innate immune system is a major target of LPS, the possible infiltration of peripheral macrophages into the brain in response to the treatment were analysed, and immune phenotype of infiltrated and peritoneal macrophages, as well as

resident microglia, were characterized. Macrophages, infiltrate the brain in response to inflammation and have been shown to be more functional to phagocyte Aβ peptides, compared to resident microglia (Lai and McLaurin, 2012). Therefore, here I also analysed the intracellular Aβ in infiltrated macrophages ($CD11b^{+}$ $CD45^{+Hi}$), resident microglia ($CD11b^{+}$ $CD45^{+Low}$) and peritoneal macrophages ($F4/80^{+}$). The chemokine receptor CCR2 play an important role in the recruitment of macrophages (Mack et al., 2001, E. Hirbec et al., 2017) and the clearance of Aβ (Westin et al., 2012). For this reason, the immune phenotype of infiltrated macrophages, resident microglia, and peritoneal macrophages was also characterized, quantifying the expression of CCR2, as well as the phenotypic markers M1 (pro-inflammatory, CD80) and M2 (anti-inflammatory, CD206). Indeed, investigation of the impact of repeated exposure to LPS on gene transcript in macrophages revealed that LPS induced an increase in M2-genes transcription, silencing most of the M1 genes (O'Carroll et al., 2014).

Therefore I hypothesize that 1) a second LPS injection would attenuate the immune response, reducing the levels of peripheral pro-inflammatory cytokines associated with reduced infiltration of macrophages into the brain and further accumulation of amyloid plaque in the APPswe/PS1ΔE9 mouse model. Moreover, I hypothesised that 2) a single systemic injection would induce accumulation of amyloid plaques in the brain and exacerbation of the pro-inflammatory response and infiltration of peripheral macrophages during the early stage of plaque deposition, with transgenic animals more susceptible to the immune challenge than the wild-type littermates.

5.2 Study design

One-hundred-and-nine mice, at 4.5 months of age, were used to assess the behavioural and glial response one week after the second challenge. Circulating cytokines and infiltrated macrophages into the brain were also quantified. The following mice were tested: 54 APPswe/PS1dE9 transgenic mice (27 males with mean weight: 32.4 $\pm$ 0.6g; and 27 females with mean weight: 23.4 $\pm$ 0.5g) and 55 wild-type littermates (28 males mean weight: 33 $\pm$ 0.5g; and 27 females with mean weight: 23.1 $\pm$ 0.4g).

Mice were subjected to food burrowing, spontaneous alternation and open field in order to assess daily living activity, spatial working memory and locomotor activity (see chapter 2 for method details) both at baseline and 7 days after the second challenge. Mice underwent 3 days of food burrowing training, then mice were assessed to collect baseline data: spontaneous alternation was performed the day before the first injection (day -1) and open field was done the day of the injection (day 0), in the morning, with an overnight food burrowing assessment between the two days. Mice were injected with either LPS (100µg/kg, *i.v*) or vehicle (PBS) in the afternoon, after the open field test: the first injection was performed at day 0, and a second injection was given 2 weeks later, on day 14, yielding to the experimental groups PBS-PBS, PBS-LPS, LPS-LPS (see experimental timeline in Figure 49).

Between day 13 and day 14, two weeks after the first injection, mice daily living activity was assessed to monitor the sickness syndrome and food burrowing test was performed. Subsequently on day 20 and 21 post-injection behavioural data were collected and mice underwent the same behavioural tests performed at baseline, in the same order and time of day.

Body weight of each mouse was recorded daily throughout the experiment in order to monitor the recovery of the animals after the treatment and compare the recovery from the first and second injection. On day 21 mice were anesthetized to collect peritoneal macrophages, then blood was collected by heart puncture before the animals were perfused with ice-cold PBS. Brain tissue was finally collected and sagittally separated into two hemibrains. One half of the brain was sagittally sliced and used to analyse the microglia, astrocytes and amyloid response in the hippocampus and cortex, by immunostaining for Iba-1, GFAP and Aβ respectively. Nine sections per brain were immunostained at different levels of the hippocampus and cortex. Three brains from the same genotype and sex, but different treatment, were fixed in the same block to minimize immunostaining variability. The second half of the brain was destined for two different purposes: brain tissue from n=4 mice/group was used for cells dissociation and analysis of brain infiltrating macrophages, while the tissue from the other n=4 mice/group was further dissected into frontal cortex, hippocampus, cortex and striatum but not used in this study. Plasma was collected and stored at -80°C. Once all the samples were ready, cytokines levels were quantified using a multiplex assay (see chapter 2 for details).

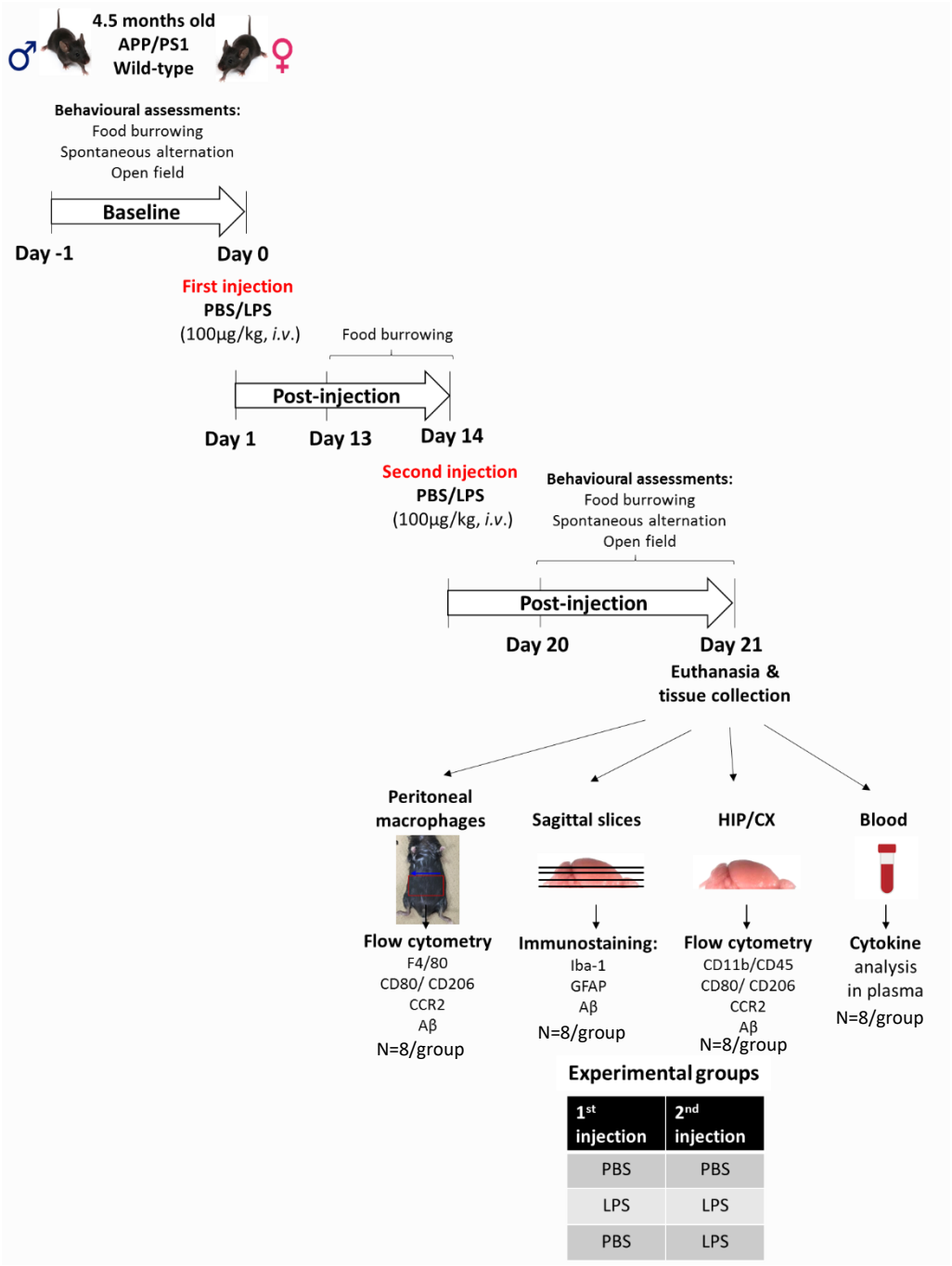

Figure 49. **Schematic experimental timeline.**

5.3 Results

5.3.1 Behavioural response to LPS, 7 days after the 2nd challenge

Body weight

Results showed an overall significant sex effect at the baseline ($F_{(1,97)}$=357.34, p<0.0001), with males being heavier than females (Figure 50.A). Post-injection data analysis revealed overall significant effects of sex ($F_{(1,97)}$=300.59, p<0.0001), time ($F_{(1,97)}$=15.53, p<0.0001) and a significant sex X time interaction effects ($F_{(1,97)}$=3,03, p<0.0001) with males showing higher body mass than females regardless of genotype and treatment (p<0.0001) (Figure 50.B-C). A treatment X time interaction effect ($F_{(1,97)}$=17.67, p<0.0001) was also observed with a greater loss in body mass the day after the first injection in LPS-LPS treated wild-type females (p=0.046) (Figure 50.B), and APP/PS1 males (p=0.041) (Figure 50.C) compared to PBS-LPS treated control. A significant loss in body mass was also seen the day after the 2nd challenge in PBS-LPS treated WT males (p=0.017) and LPS-LPS treated WT females (p=0.045) (Figure 50.B), as well as LPS-LPS-treated APP/PS1 males (p=0.019) and PBS-LPS treated APP/PS1 females (p=0.044) (Figure 50.C) compared to PBS-PBS treated littermates.

Body weight changes were calculated by subtracting post-injection data from the baseline data and expressed as a percent change from baseline. Analysis of the body weight recovery after the first challenge revealed that all LPS-LPS treated animals lost a significant amount of weight the day after the injection (p<0.0001). Wild-type males significantly gained weight by day 7 (p=0.033), while transgenic males by day 3 (p=0.045). Wild-type males did not return to baseline weight 7 days post-1st injection, while transgenic males returned to the pre-injection weight by day 7 (p<0.0001) (Figure 51.A). However, females seemed to recover faster than males from the first injection, with wild-type females gaining weight by day 3

(p=0.0024) and transgenic females gaining weight by day 2 (p=0.0026), compared to day 1 (Figure 51.B). Wild-type males unexpectedly lost weight in the PBS-PBS-treated groups (p=0.049) the day after the injection, and the PBS-LPS treated group (p=0.021) at day 2 (Figure 51.A). PBS-PBS treated transgenic females gained a significant body mass on day 2 (p=0.024) (Figure 50.B) compared to their baseline weight.

Analysis of the body weight recovery after the second challenge (Figure 52) showed that LPS-LPS treated wild-type male (p<0.0001), APPswe/PS1ΔE9 males (p=0.020) and wild-type females (p=0.023) lost a significant amount of weight the day after the injection. All LPS-LPS treated animals gained weight by day 17, compared to the day after the 2nd injection (p<0.05). All PBS-LPS treated animals lost weight after the 2nd injection (p<0.05), with wild-type males (p=0.022), APPswe/PS1ΔE9 males (p=0.025), and APPswe/PS1ΔE9 females (p=0.034) gained weight by day 16, while WT females by day 17 (p=0.0005).

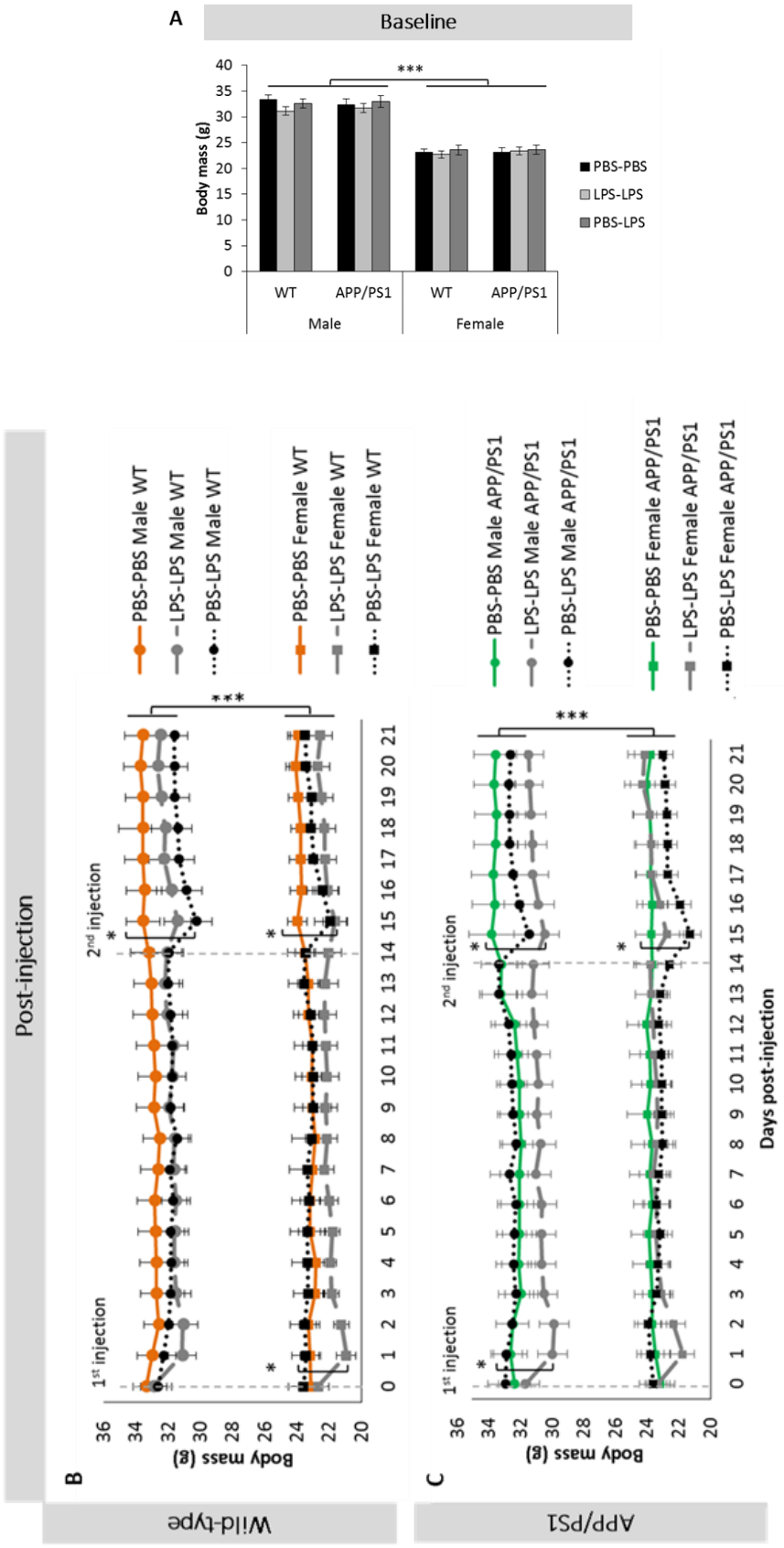
A
Baseline
Body mass (g)
***
PBS-PBS
LPS-LPS
PBS-LPS
WT
APP/PS1
Male
Female
Post-injection
PBS-PBS Male WT
LPS-LPS Male WT
PBS-LPS Male WT
PBS-PBS Female WT
LPS-LPS Female WT
PBS-LPS Female WT
PBS-PBS Male APP/PS1
LPS-LPS Male APP/PS1
PBS-LPS Male APP/PS1
PBS-PBS Female APP/PS1
LPS-LPS Female APP/PS1
PBS-LPS Female APP/PS1
1st injection
2nd injection
Body mass (g)
Days post-injection
B
C
Wild-type
APP/PS1

Figure 50. **Body weight at baseline and post-injection**. 4.5 months old males and females APPswe/PS1ΔE9 (APP/PS1) and wild-type (WT) (n=8 per group) were treated with LPS or vehicle (PBS) and body weight recorded daily before and after the injections. Males were significantly heavier than females before the injection ($p<0.0001$) (A) and post-injection ($p<0.0001$) (B-C). The day after the 1st challenge LPS-LPS-treated WT females ($p=0.046$) (B) and APP/PS1 males ($p=0.041$) (C) showed a significantly lower body mass than PBS-LPS- treated control. The day after the 2nd challenge PBS-LPS-treated WT males ($p=0.017$) and LPS-LPS-treated WT females ($p=0.045$) (B), as well as LPS-LPS-treated APP/PS1 males ($p=0.019$) and PBS-LPS-treated APP/PS1 females ($p=0.044$) (C) revealed a significant lower body mass than the control littermates. Data are shown as mean $\pm$ S.E.M. 3-way and 2-way ANOVA were used [* $p< 0.05$, *** $p< 0.0001$].

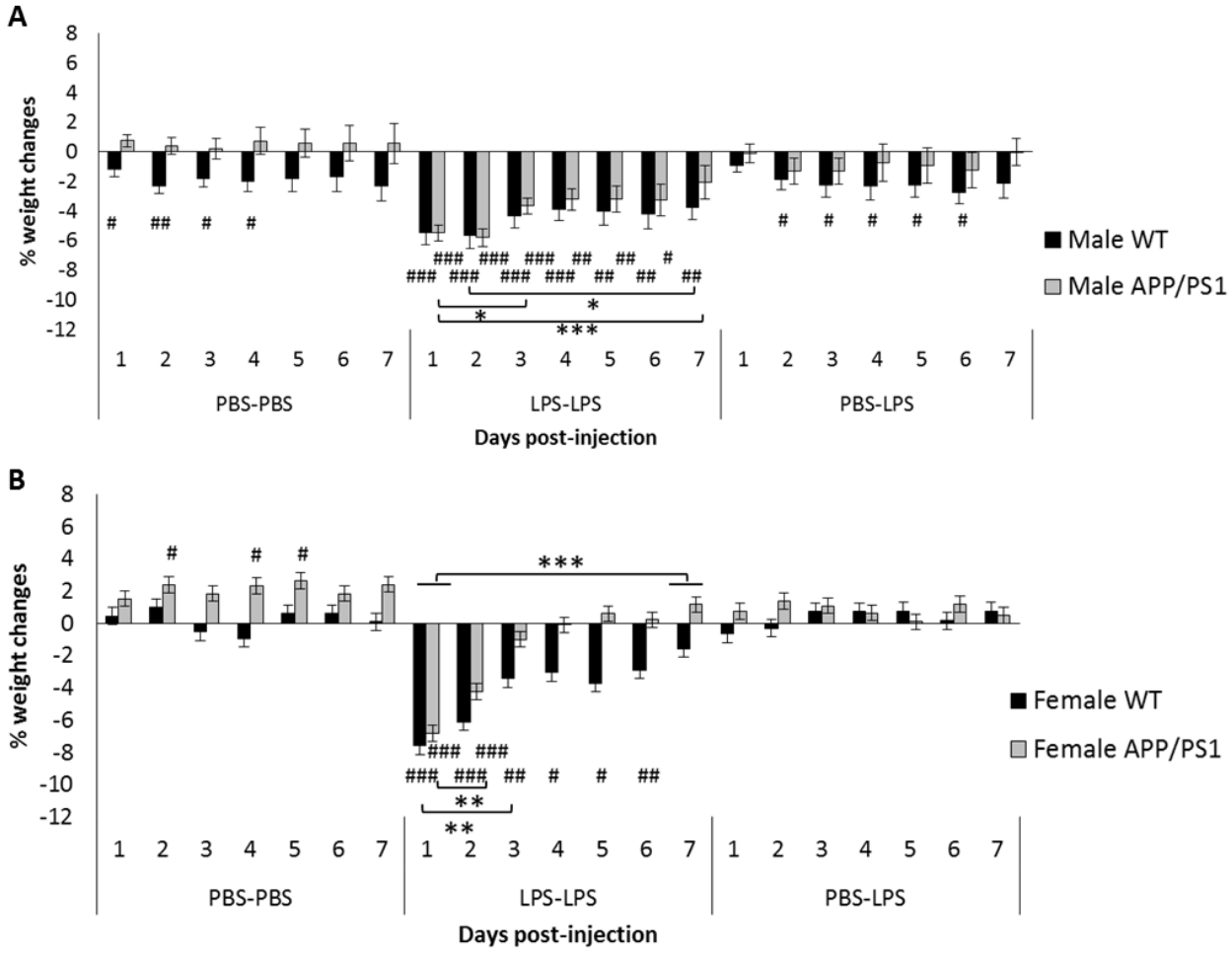
A
% weight changes
8
6
4
2
0
-2
-4
-6
-8
-10
-12
PBS-PBS
LPS-LPS
PBS-LPS
Days post-injection
Male WT
Male APP/PS1
B
% weight changes
Days post-injection
Female WT
Female APP/PS1

Figure 51. **Recovery from LPS-induced weight loss after 1st injection**. 4.5 months old males and females mice APPswe/PS1ΔE9 (APP/PS1) and wild-type (WT) (n=8 per group) were treated with LPS or vehicle (PBS) and body weight recorded daily after the 1st injection. PBS-PBS treated WT males lost weight the day after the injection ($p=0.049$) (**A**), while PBS-PBS- treated APP/PS1 females gained weight from day 2 ($p=0.024$) All LPS-LPS-treated animals lost a significant amount of weight the day after the treatment ($p<0.0001$) (**A**) (**B**). LPS-LPS-treated APP/PS1 males significantly gained weight, and return to baseline weight by day 7 ($p<0.0001$, compared to day 1), while LPS-LPS-treated WT males, did not return to baseline weight within 7 days. (**A**). LPS-LPS-treated APP/PS1 and WT females reached a complete body weight recovery by day 7 for both genotypes ($p<0.0001$) (**B**). PBS-LPS-treated WT males lost weight the day after the injection with PBS (**A**), while APP/PS1 males and all females did not show a significant change in body weight. Data are shown as mean $\pm$ S.E.M. [the * was used for the statistical significance shown by the pairwise comparisons analysis between the days:*$p<0.05$,**$p< 0.005$,***$p<0.0001$]; [the # was used used for the statistical significance shown by the one-sample t-test compared to the baseline: #$p< 0.05$, ##$p<0.005$, ###$p< 0.0001$].

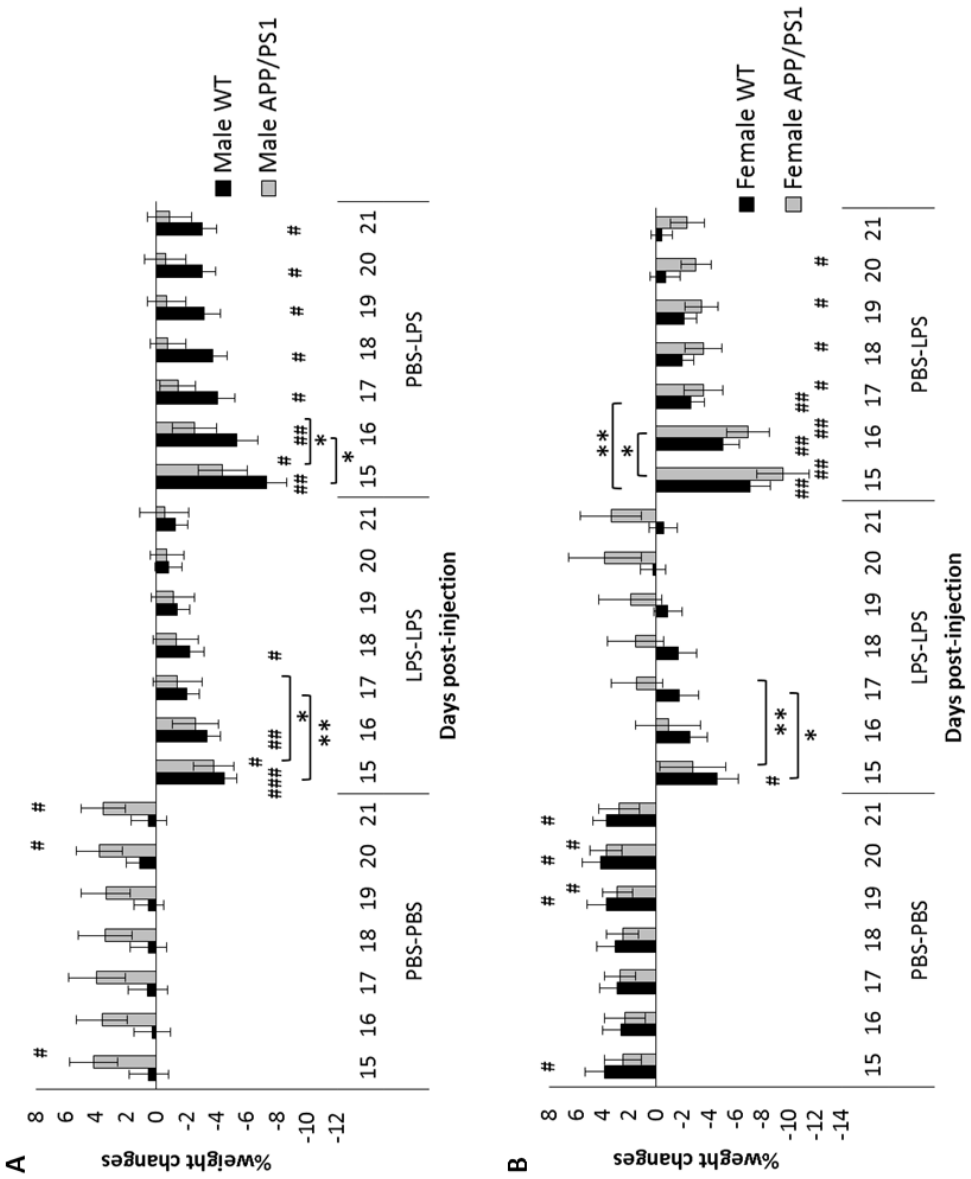

Figure 52 **Recovery from LPS-induced weight loss after 2nd injection.** 4.5 months old males and females mice APPswe/PS1ΔE9 (APP/PS1) and wild-type (WT) (n=8 per group) were treated with LPS or vehicle (PBS) and body weight recorded daily after the 2nd injection. PBS-PBS-treated animals did not show a decrease in body weight after the 2nd challenge, compared to the baseline weight ($p<0.05$) (**A**) (**B**). LPS-LPS-treated males [WT males ($p<0.0001$), APP/PS1 males ($p=0.020$)] (**A**) and WT females ($p=0.023$) (**B**) lost a significant amount of weight after the 2nd injection. All LPS-LPS-treated males (**A**) and females (**B**) gained weight by day 17, compared to the day after the 2nd injection ($p<0.05$). PBS-LPS-treated animals lost weight after the 2nd injection [in WT males ($p=0.001$), APP/PS1 males ($p=0.026$) (**A**), WT females ($p=0.002$) APP/PS1 females ($p=0.002$)(**B**)]. PBS-LPS-treated WT males ($p=0.022$), APP/PS1 males ($p=0.025$), and APP/PS1 females ($p=0.034$) gained weight by day 16, while WT females by day 17 ($p=0.0005$). Data are shown as mean ± S.E.M. [*$p<0.05$, **$p< 0.005$], [#$p< 0.05$, ##$p<0.005$, ###$p< 0.0001$].

Food Burrowing

There were no differences in performance between treatment groups at baseline and post-injection. An overall significant effect of sex was observed on the amount of food burrowed at baseline ($F_{(1,96)}$=9.34, p=0.003) (Figure 53.A), with females burrowing more than males (p=0.007). An overall sex effect was also showed 7 days after the 1st injection ($F_{(1,96)}$=13.43, p=0.0004) (Figure 53.B), and after the 2nd injection ($F_{(1,96)}$=16.1, p=0.0001) (Figure 53.C), with wild-type females burrowing more than wild-type males post 1st injection (p=0.0013) and post-2nd injection (p=0.003), as well as transgenic females burrowing more than transgenic males after the 2nd injection (p=0.001). An overall genotype effect was revealed after the 1st injection ($F_{(1,96)}$=5.12, p=0.026), with wild-type females burrowing more than transgenic females (p=0.024) (Figure 53.B). Analysis of the changes in the amount of food burrowed from baseline revealed that PBS-treated wild-type males and all the females burrowed significantly more food than prior the treatment ($p<0.05$) (Figure 53.D).

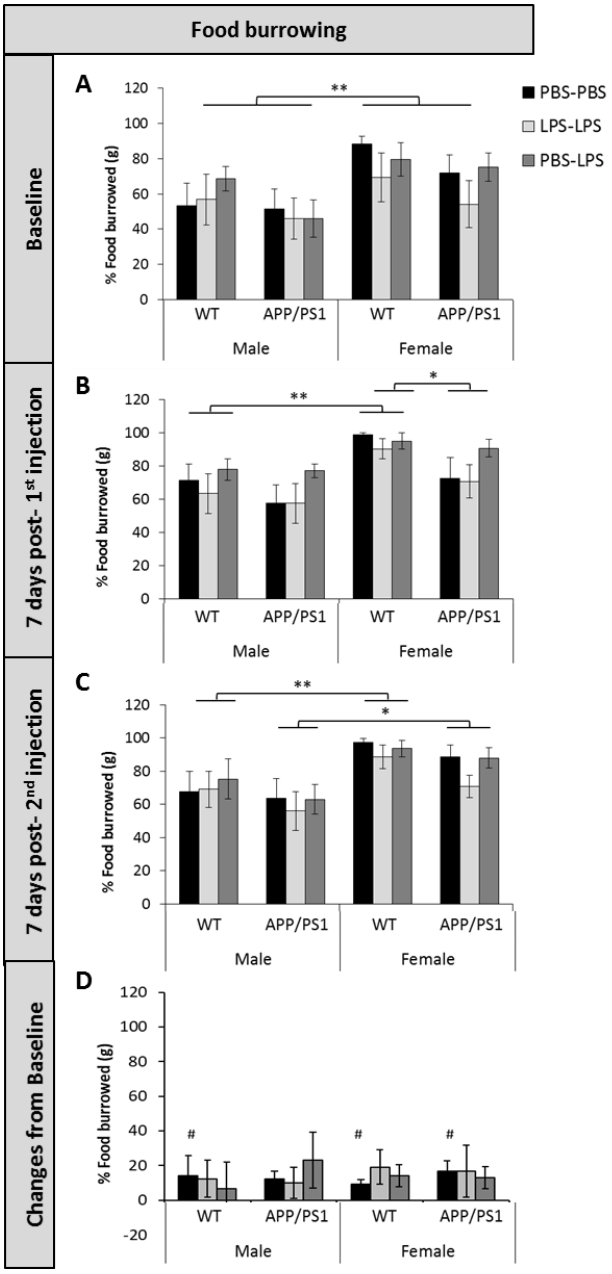

Figure 53. **LPS effects on food burrowing at baseline and post-injection**. 4.5 months old males and females mice APPswe/PS1ΔE9 (APP/PS1) and wild-type (WT) (n=8 per group) were treated with LPS or vehicle (PBS) and food burrowing was assessed at baseline, 7 days post- 1st injection and 7 days post- 2nd injection. Females burrowed more food than males at baseline (p=0.003) (**A**). In particular WT females burrowed more food than WT males both 7 days post- 1st injection (p=0.013) (**B**) and 7 days post- 2nd injection (p=0.003) (**C**), and than APP/PS1 females 7 days post-1st injection (p=0.024) (**B**). APP/PS1 females burrowed more than APP/PS1 males 7 days after the 2nd injection (p=0.01) (**C**). No significant differences were seen in the effect of treatment between experimental groups, regardless of genotype and sex (**D**). Data are presented as mean ± S.E.M. [* p< 0.05, **p< 0.005] [#p<0.05].

Spatial working memory

Results revealed that the number of arm entries significantly impacted the alternation rate both at baseline (p=0.009) and post-injection (p=0.0003). There were no differences in performance between the experimental groups at baseline. Post-injection analysis revealed an overall sex X treatment ($F_{(1,95)}$=5.42, p=0.006) and genotype X sex X treatment ($F_{(1,95)}$=5.73, p=0.004) interaction effects, with PBS-PBS treated wild-type females having lower percentage of alternation rate compared to LPS-LPS treated (p=0.0003) and PBS-LPS treated (p=0.0011) groups (Figure 54.B). Moreover, LPS-LPS-treated APPswe/PS1ΔE9 females showed a higher percentage of alternation rate compared to the PBS-LPS-treated counterpart (p=0.004) (Figure 54.B).

One sample t-test showed that all experimental groups alternated significantly above the 50% random choice rate both at baseline (p<0.05) (Figure 54.A) and post-injection (p<0.05) (Figure 54.B). Effects of treatment showed improvement in spatial working memory in PBS-PBS-treated wild-type males (p=0.005), and LPS-LPS-treated transgenic males (p=0.047) and females (p=0.038) (Figure 54.C).

Locomotor activity

An overall genotype effect was observed on the distanced moved both at baseline ($F_{(1,93)}$=23.87, p<0.0001) (Figure 54.D) and post-injection ($F_{(1,93)}$= 31.79, p<0.0001) (Figure 54.E). APPswe/PS1ΔE9 females (p=0.0001 at baseline; p<0.0001 post-injection) and APPswe/PS1ΔE9 males (p=0.004 at baseline; p=0.0003 post-treatment) moved more than the wild-type counterpart. Moreover LPS-LPS-treated transgenic males showed higher locomotor activity at baseline compared to PBS-PBS treated (p=0.049) and PBS-LPS treated (p=0.041) transgenic males (Figure 54.D).

Analysis of the effect of treatment over the performance was calculated by subtracting post-injection data from baseline data. Results did not show significant differences between experimental groups in the alternation rate (Figure 54.C), while a decrease in locomotor activity was observed almost all the groups ($p<0.05$), except in transgenic male group and PBS-PBS-treated wild-type males. Transgenic females moved also significantly less compared to transgenic male ($p=0.03$) (Figure 54.F).

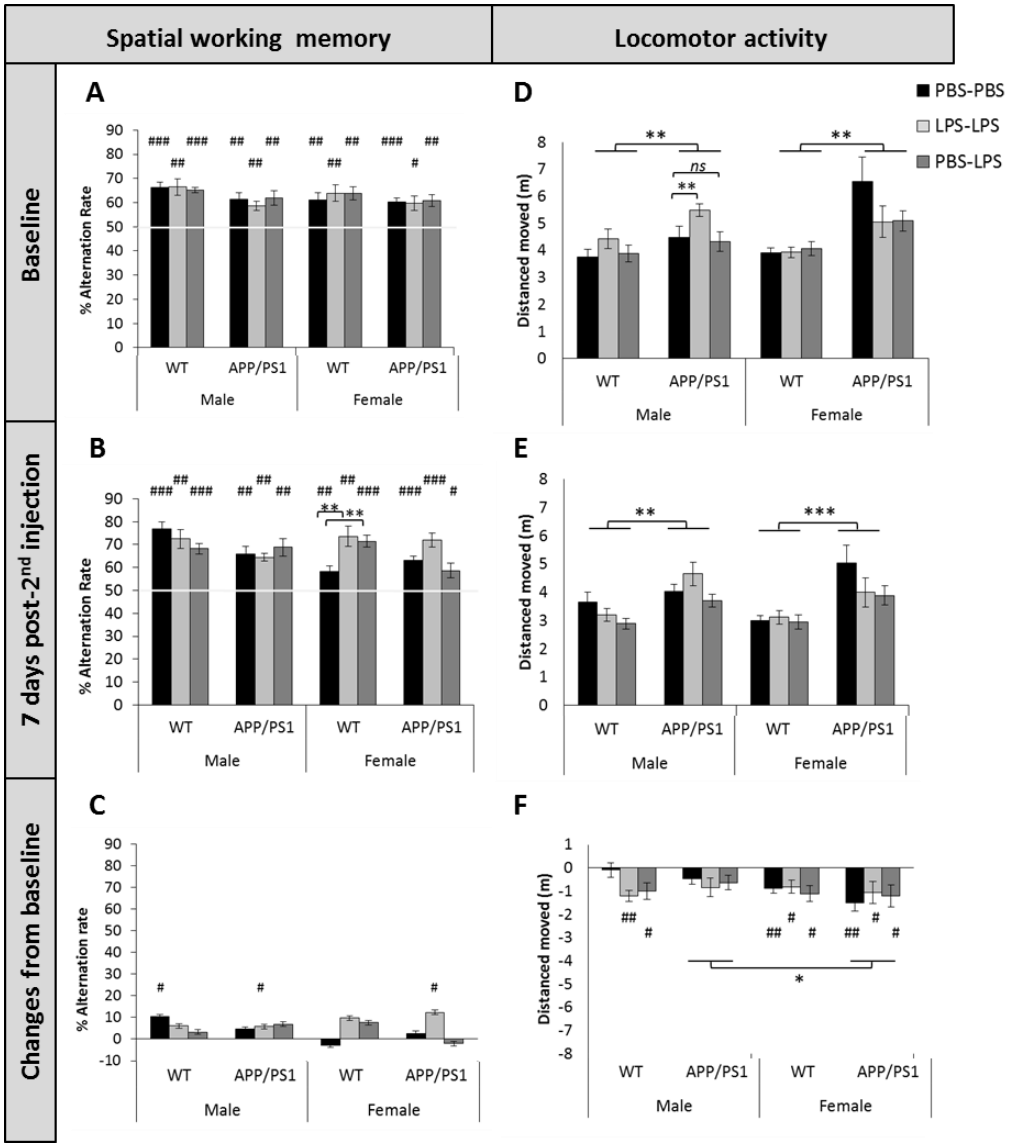

Figure 54. **LPS effects on behaviour at baseline and 7 days post-2nd injection**. 4.5 months old males and females mice APPswe/PS1ΔE9 (APP/PS1) and wild-type (WT) (n=8 per group) were treated with LPS or vehicle (PBS) and behaviour was assessed at baseline and 7 days after the 2nd injection. The alternation rate observed in all animals was statistically different from the random 50% chance level (shown with a line) both at baseline (**A**) and post-injection (**B**) ($p<0.05$). Post-treatment, PBS-PBS-treated WT females mice revealed a lower percentage of alternation rate compared to LPS-LPS-treated ($p=0.0003$) and PBS-LPS-treated ($p=0.001$) counterparts (**B**). APP/PS1 mice showed higher locomotor activity than WT both at baseline (**D**) and post-injection (**E**) ($p<0.05$). At baseline, LPS-LPS-treated APP/PS1 males showed higher locomotor activity compared to the PBS-PBS-treated group ($p=0.049$) (**D**). Changes in the locomotor activity from baseline revealed that APP/PS1 females decreased the activity after the treatment, compared to the male counterpart ($p=0.03$) (**F**). No significant differences were seen in the alternation rate changes from baseline between experimental groups, regardless of sex and genotype (**C**). Mean ± S.E.M. [ANOVA: * $p< 0.05$, ** $p< 0.005$].[# was used used for the statistical significance shown by the one-sample t-test compared to the baseline: $^{\#}p<0.05$, $^{\#\#}p<0.005$].

5.3.2 Cytokine response to LPS 7 days after the 2nd challenge

A multiplex assay was used to quantify the concentration of cytokines in the plasma. All samples were analysed in one plate to minimized variability. An overall sex effect was revealed for IL-6 ($F_{(1,75)}$=6.57, p=0.012) (Figure 55Figure 34.B), IFN-γ ($F_{(1,75)}$=6.68, p=0.012) (Figure 55.C), IL-10 ($F_{(1,75)}$=15.13, p=0.0002) (Figure 55.D) levels, with wild-type females showing lower protein levels in plasma than wild-type males. An overall genotype X treatment interaction effect was observed for IFN-γ ($F_{(1,75)}$=3.63, p=0.031) (Figure 55.C) with PBS-PBS-treated transgenic females having greater IFN-γ concentration than LPS-LPS-treated (0.026), and PBS-LPS-treated (p=0.005) animals, and also compared to PBS-PBS-treated wild-type females (p=0.029) (Figure 55.C). No significant differences were seen in IL-1β (Figure 55.A) and TNF-α (Figure 55.E).

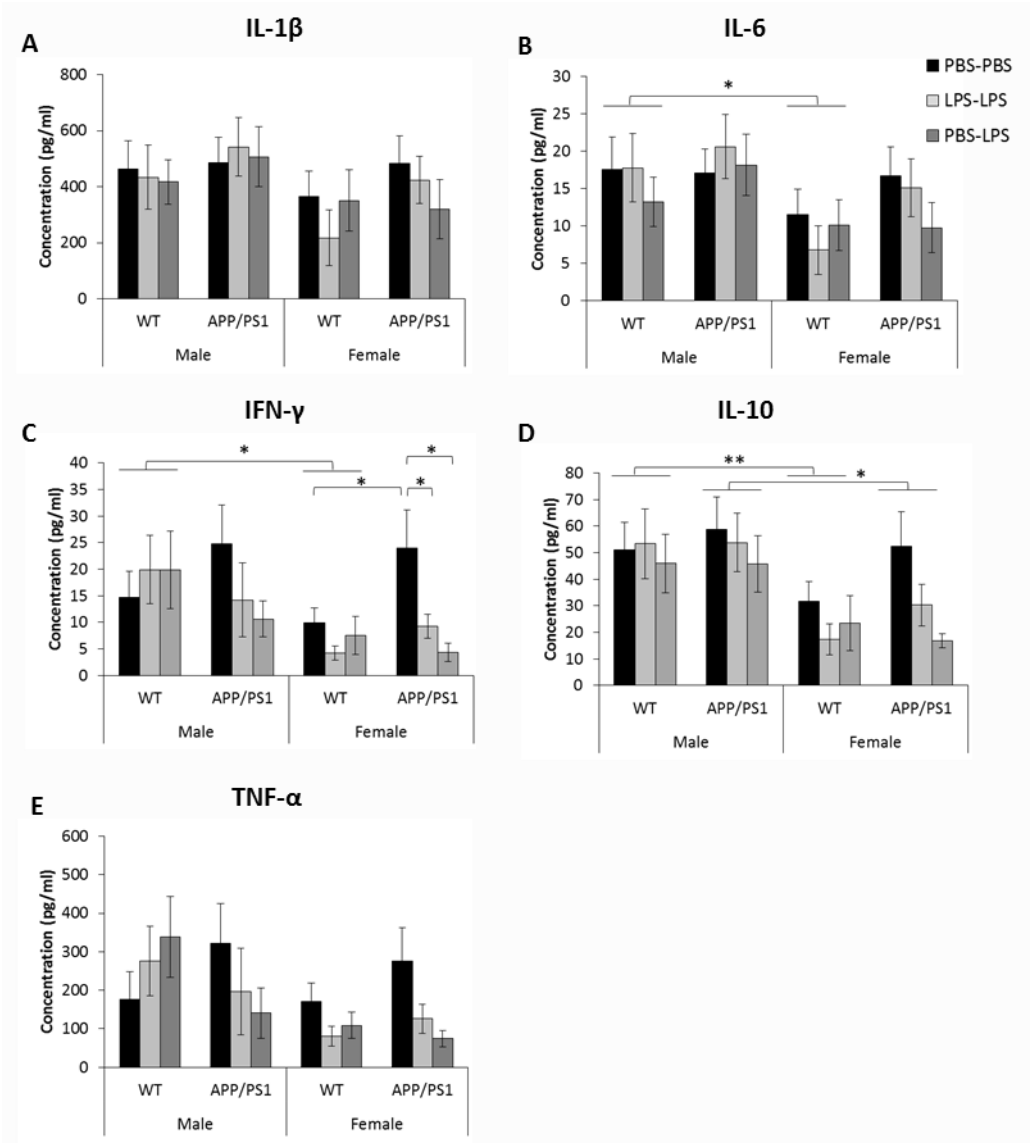

Figure 55. **Cytokines expression in plasma**. 4.5 months old males and females mice APPswe/PS1ΔE9 (APP/PS1) and wild-type (WT) (n=6/8 per group) were treated with LPS or vehicle (PBS) and plasma collected 7 days after the 2nd injection. No significant differences were observed in IL-1β (**A**) and TNF-α (**E**) plasma concentration between groups. WT females showed lower expression of IL-6 (p=0.037) (**B**), IFN-γ (p=0.009) (**C**) and IL-10 (0.0024) (**D**) than WT males. APP/PS1 females also revealed lower IL-10 levels than APP/PS1 males (p=0.021) (**D**). The effect of treatment was observed in APP/PS1 females where PBS-PBS-treated mice showed higher INF-γ levels than LPS-LPS-treated (0.026), and PBS-LPS-treated (p=0.005) animals, as well as compared to PBS-PBS-treated wild-type females (p=0.029) (**C**). Data are shown as mean ± S.E.M. [* p< 0.05, ** p< 0.005].

5.3.3 Changes in amyloid plaque load in the hippocampus and cortex 7 days after the 2nd challenge

Analysis of amyloid plaque load revealed a higher number of total amyloid plaques in females compare to males showing an overall sex effect in both hippocampus ($F_{(1,43)}$=35.98, p<0.0001) (Figure 56) and cortex ($F_{(1,43)}$=39.36, p<0.0001) (Figure 58). An overall sex effect was also revealed in the number of small ($F_{(1,43)}$=47.3, p<0.0001), medium ($F_{(1,43)}$=21.21, p<0.0001, and large ($F_{(1,43)}$=18.86, p<0.0001) plaques in the hippocampus (Figure 57), as well as small ($F_{(1,43)}$=47.97, p<0.0001), medium ($F_{(1,43)}$=42.75, p<0.0001) and large ($F_{(1,43)}$=18.86, p<0.0001) plaques in the cortex (Figure 59). Analysis of the area of the plaques, males showed larger area of small plaques compared to females in the LPS-LPS-treated (p=0.011) and PBS-LPS-treated (p=0.006) treated groups in the cortex (Figure 58), but not in the hippocampus. No significant difference was found in the area of medium and large plaques between the treated groups, regardless of sex, in both the regions of interests (Figure 56. and Figure 58).

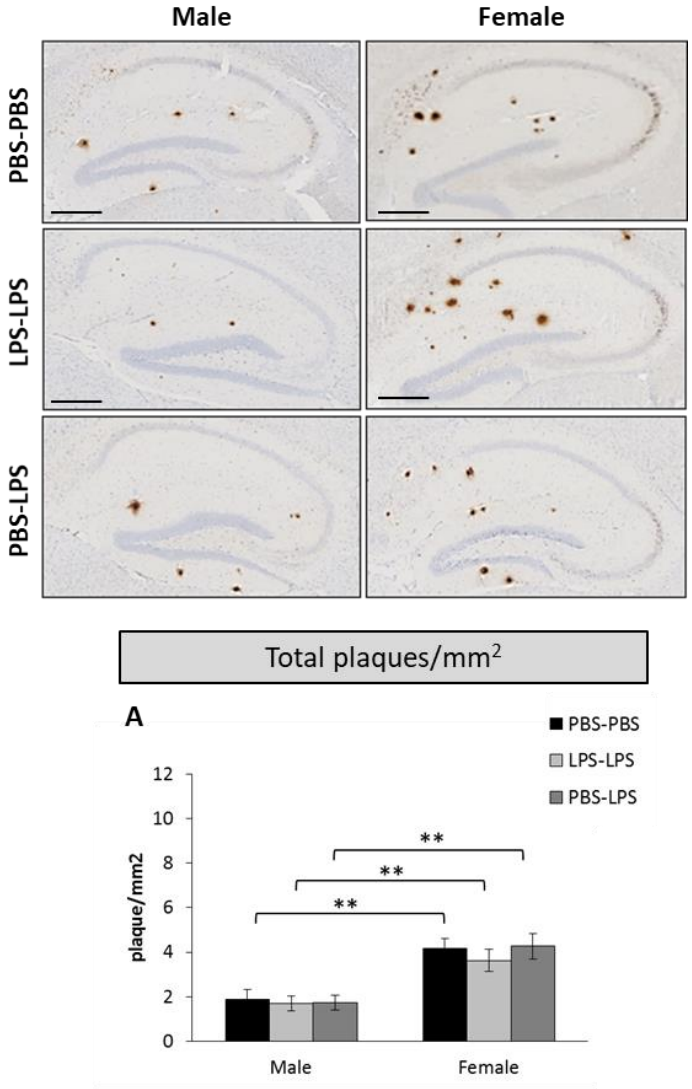

Figure 56. **Amyloid plaque load in the hippocampus.** 4.5 months old males and females mice APPswe/PS1ΔE9 (APP/PS1) and wild-type (WT) (n=8 per group) were treated with LPS or vehicle (PBS) and their brain collected 7 days after the 2nd injection. Females showed higher numbers of total (p=0.001). In particular higher numbers of total plaques per mm^2 (p=0.002) was observed in LPS-LPS-treated females compared to the male counterpart. Moreover PBS-LPS-treated females revealed higher numbers of total plaques per mm^2(p=0.0007) compared to PBS-LPS-treated males. Data are presented as mean ± S.E.M. [* p< 0.05, **p< 0.005 *** p < 0.0001].

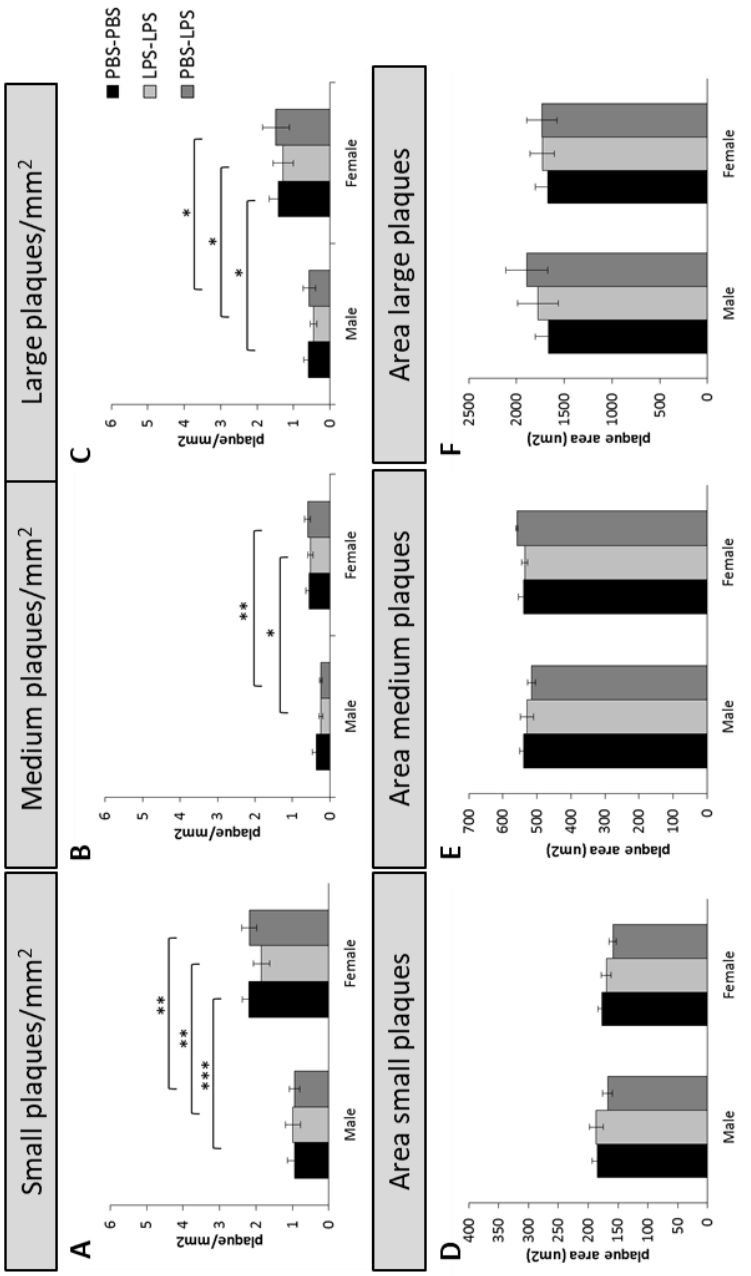

Figure 57. **Amyloid plaque load in the hippocampus.** 4.5 months old males and females mice APPswe/PS1ΔE9 (APP/PS1) and wild-type (WT) (n=8 per group) were treated with LPS or vehicle (PBS) and their brain collected 7 days after the 2nd injection. Females showed higher numbers of small ($p<0.0001$) (**A**) and large ($p=0.017$) (**C**) amyloid plaques per mm^2 compared to vehicle-treated males. Higher numbers of total small ($p=0.002$) (**A**), medium ($p=0.006$) (**B**) and large ($p=0.013$) (**C**) plaques per mm^2 was also observed in LPS-LPS-treated females compared to the male counterpart. Moreover PBS-LPS-treated females revealed higher numbers of small ($p=0.0001$) (**A**), medium ($p=0.024$) (**B**) and large ($p=0.018$) (**C**) plaques per mm^2 compared to PBS-LPS-treated males. No significant differences were found in the area of the plaques between the treated groups, regardless of sex (**D**-**F**). Data are presented as mean ± S.E.M. [* $p< 0.05$, ** $p< 0.005$ *** $p < 0.0001$].

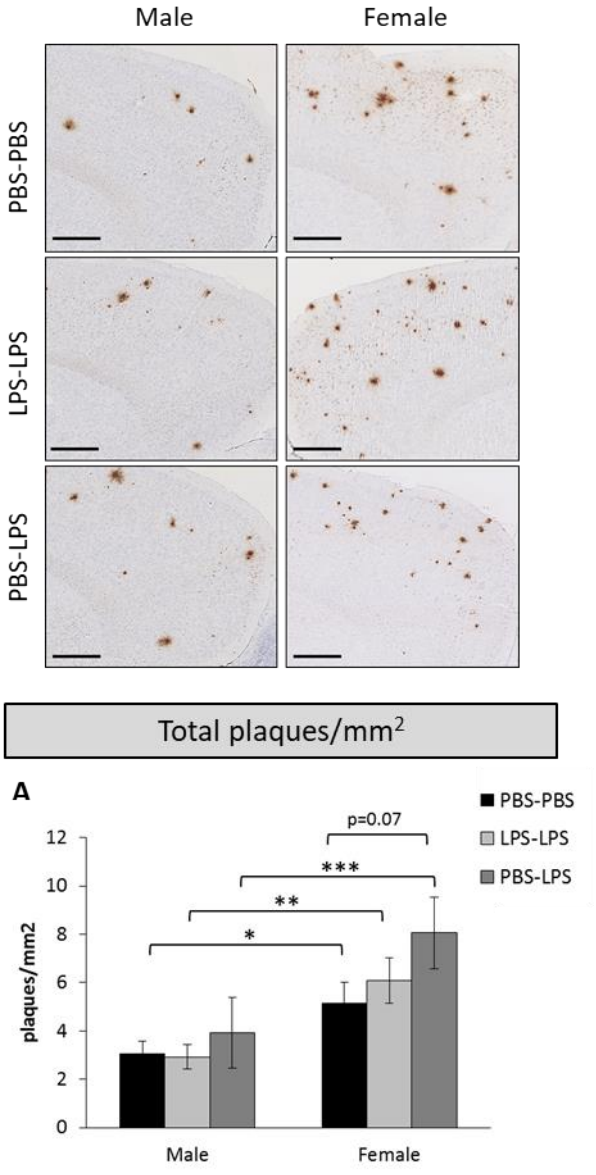

Figure 58. **Amyloid plaque load in the cortex**. 4.5 months old males and females mice APPswe/PS1ΔE9 (APP/PS1) and wild-type (WT) (n=8 per group) were treated with LPS or vehicle (PBS) and their brain collected 7 days after the 2nd injection. Females showed higher number of total amyloid plaques/mm^2 compared to males in the PBS-PBS (p=0.012), LPS-LPS (p=0.0004) and PBS-LPS (p<0.0001) treated groups (**A**)**.** Data are presented as mean ± S.E.M. [* p< 0.05, **p< 0.005 *** p < 0.0001].

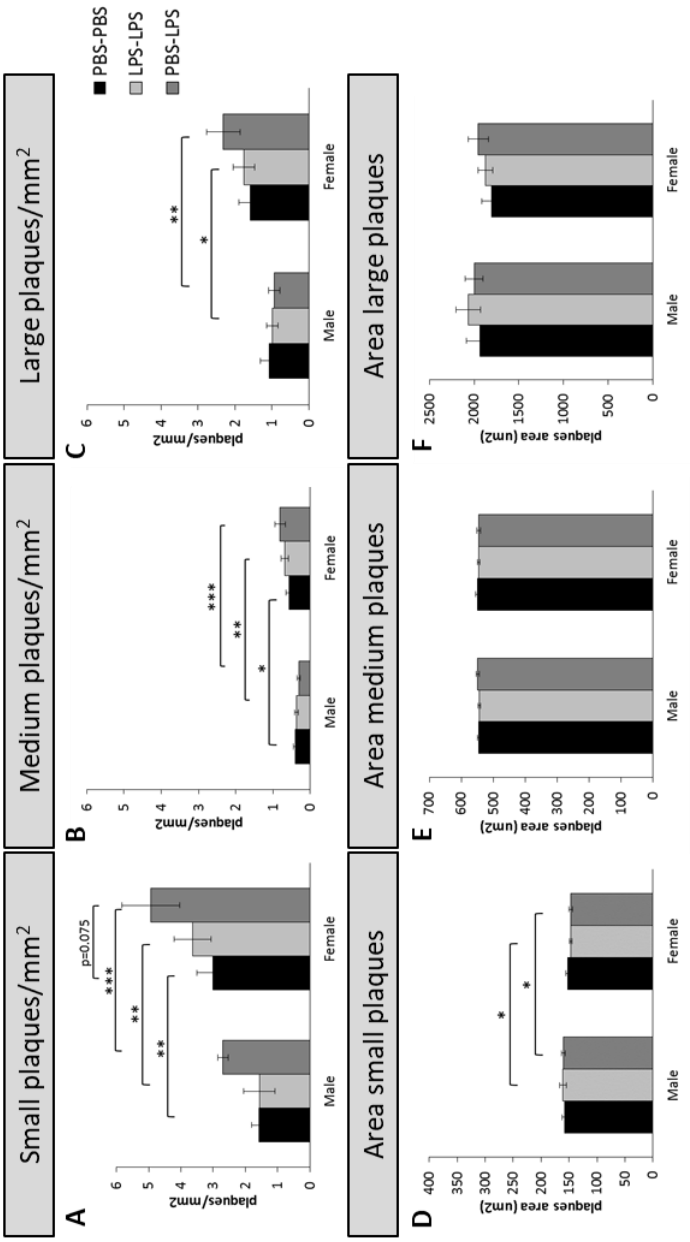

Figure 59. **Amyloid plaque load in the cortex**. 4.5 months old males and females mice APPswe/PS1ΔE9 (APP/PS1) and wild-type (WT) (n=8 per group) were treated with LPS or vehicle (PBS) and their brain collected 7 days after the 2nd injection. Higher number of amyloid plaques was also observed in LPS-LPS treated females compared to LPS-LPS treated males regarding small (p=0.0001) (**B**), medium (p=0.0002) (**C**) and large (p=0.0016) (**D**) plaques/mm^2. PBS-LPS-treated females showed higher number of plaques compared to PBS-LPS-treated males in the small (p<0.0001) (**B**), medium (p<0.0001) (**C**) and large (p=0.0006) (**D**) plaques/mm^2. Moreover, PBS-PBS treated females showed higher number of small plaques/mm^2 compared to the vehicle-treated mice (p=0.004). Males showed a larger area of small plaques compared to females in the LPS-LPS-(p=0.011) and PBS-LPS (p=0.006) treated groups (**E)**. No significant difference was found in the area of medium and large plaques between the treated groups, regardless of sex (**F**-**G**)**.** Data are presented as mean ± S.E.M. [* p< 0.05, **p< 0.005 *** p < 0.0001].

5.3.4 Glial response to LPS in the hippocampus and cortex 7 days after the 2nd challenge

Astrocytes response in hippocampus and cortex

Analysis of astrocytes density did not show a significant difference in the whole hippocampus (Figure 60), in CA1 (Figure 62.A), CA2 (Figure 62.B), CA3 (Figure 63.A) and DG (Figure 63.B). An overall genotype ($F_{(1,87)}$=339.17, p<0.0001) and sex ($F_{(1,87)}$=9.98, p=0.002) effects were revealed in the analysis of the GFAP clusters in the cortex (Figure 60.B), with APPswe/PS1ΔE9 females showing more GFAP clusters wild-type females (p<0.0001) and with APPswe/PS1ΔE9 males presenting higher number of GFAP clusters than their wild-type littermates (p<0.0001). An overall genotype X sex interaction effect ($F_{(1,87)}$=12.69, p=0.0006) was also observed in the cortex (Figure 61), with APPswe/PS1ΔE9 females showing more GFAP clusters than transgenic males (p<0.0001).

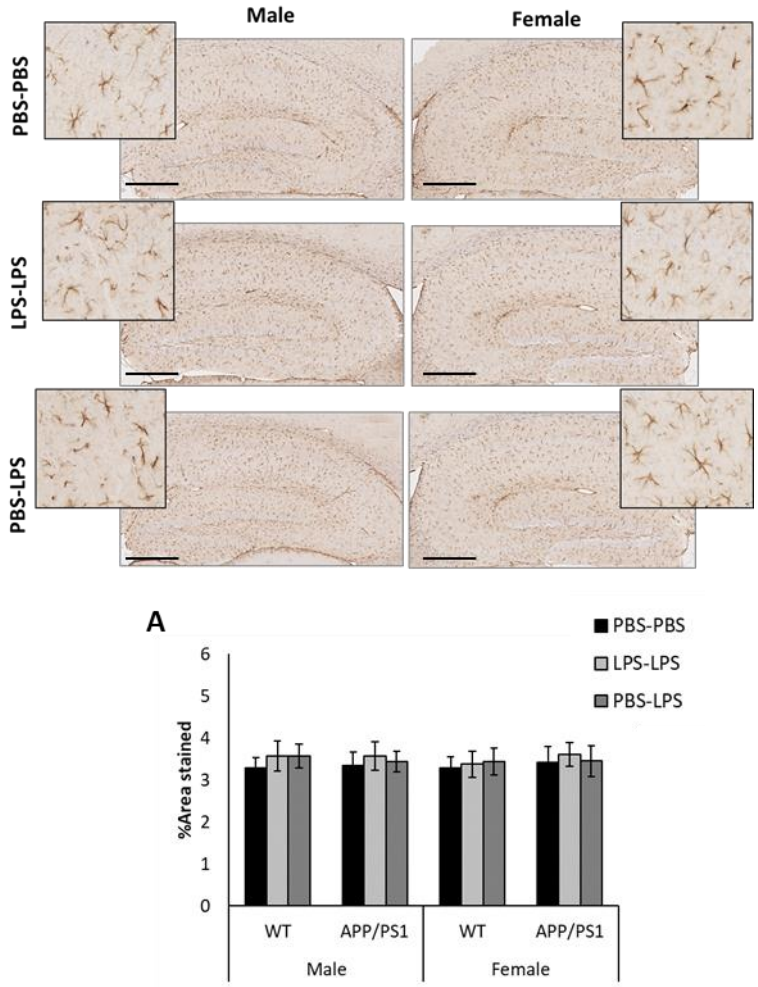

Figure 60 **Area occupied by GFAP in the hippocampus**. 4.5 months old males and females mice APPswe/PS1ΔE9 (APP/PS1) and wild-type (WT) (n=8 per group) were treated with LPS or vehicle (PBS) and their brain was collected 7 days after the 2nd injection. No significant differences found in the percentage of area stained by GFAP between the experimental groups in the hippocampus (**A**). Scale bars, 0.5mm. Data are presented as mean ± S.E.M.

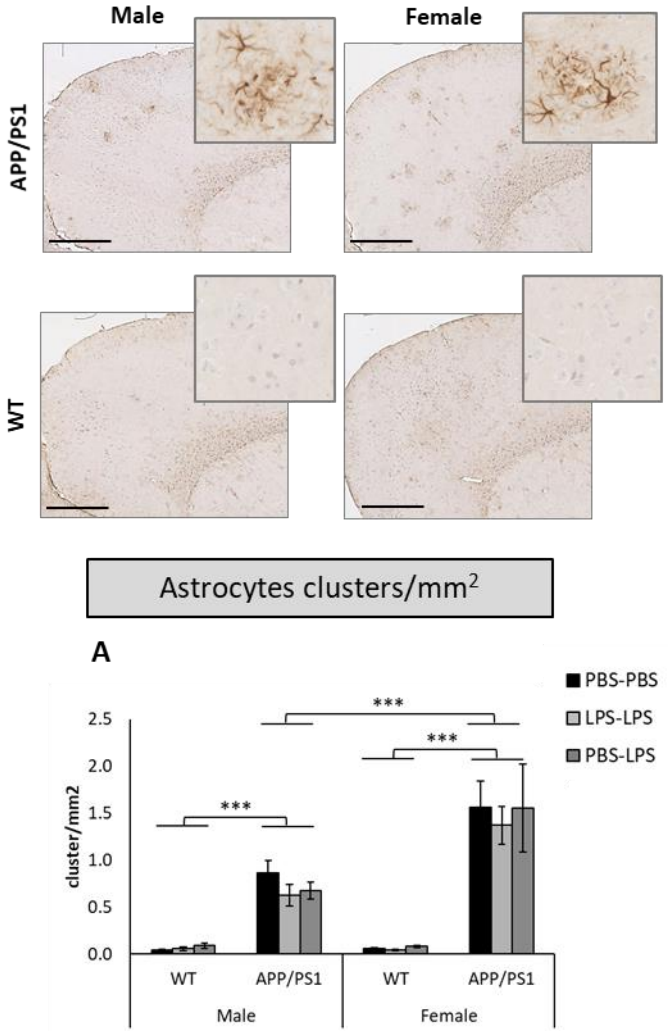

Figure 61. **Area occupied by GFAP in the cortex**. 4.5 months old males and females mice APPswe/PS1ΔE9 (APP/PS1) and wild-type (WT) (n=8 per group) were treated with LPS or vehicle (PBS) and their brain was collected 7 days after the 2nd injection. APP/PS1 females showed a higher number of clusters than WT females ($p<0.0001$) and APP/PS1 males ($p<0.0001$), as well as APP/PS1 males had higher number of GFAP clusters compared to WT littermates ($p<0.0001$) (**B**). Scale bars, 0.5mm. Data are presented as mean ± S.E.M. [***$p<0.0001$].

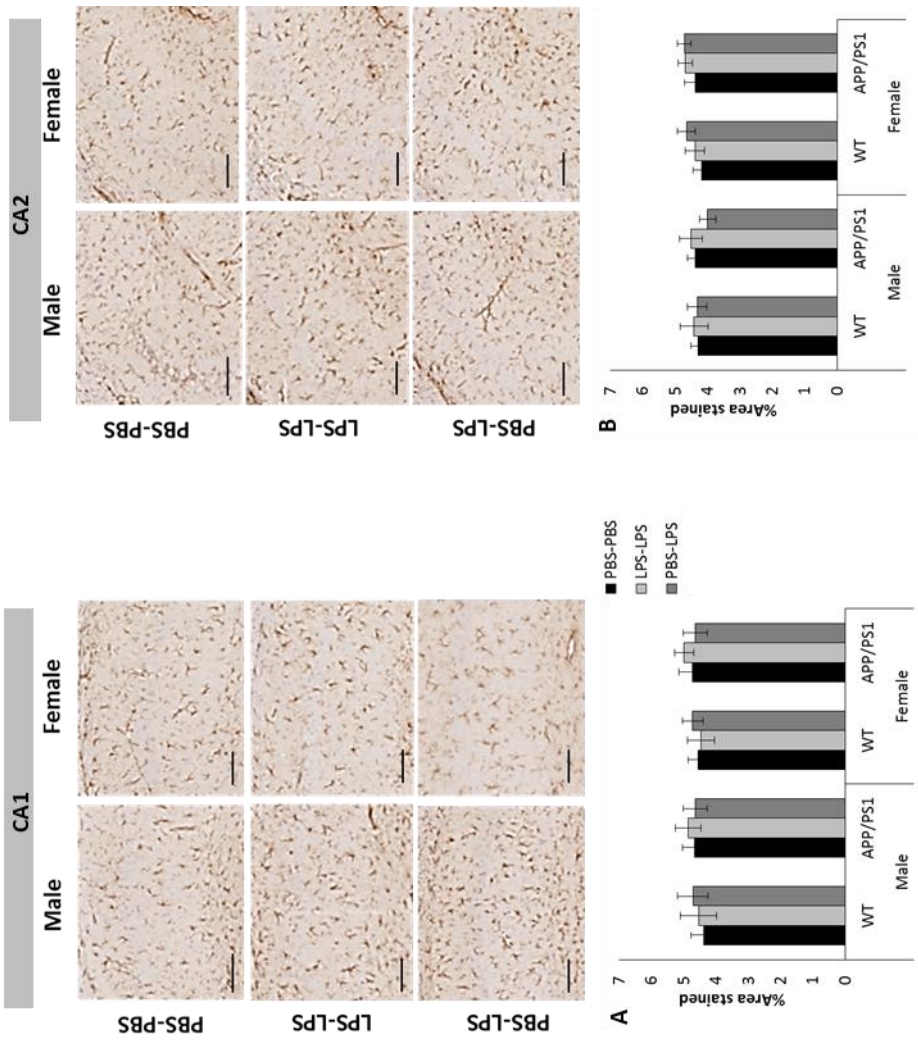

Figure 62. **Area occupied by GFAP in the CA1 and CA2 hippocampal subfields.** 4.5 months old males and females mice APPswe/PS1ΔE9 (APP/PS1) and wild-type (WT) (n=8 per group) were treated with LPS or vehicle (PBS) and their brain was collected 7 days after the 2nd injection. No significant differences were observed in the percentage of area stained by GFAP in CA1 (**A**) and CA2 (**B**). Scale bars, 0.25mm. Data are presented as mean ± S.E.M.

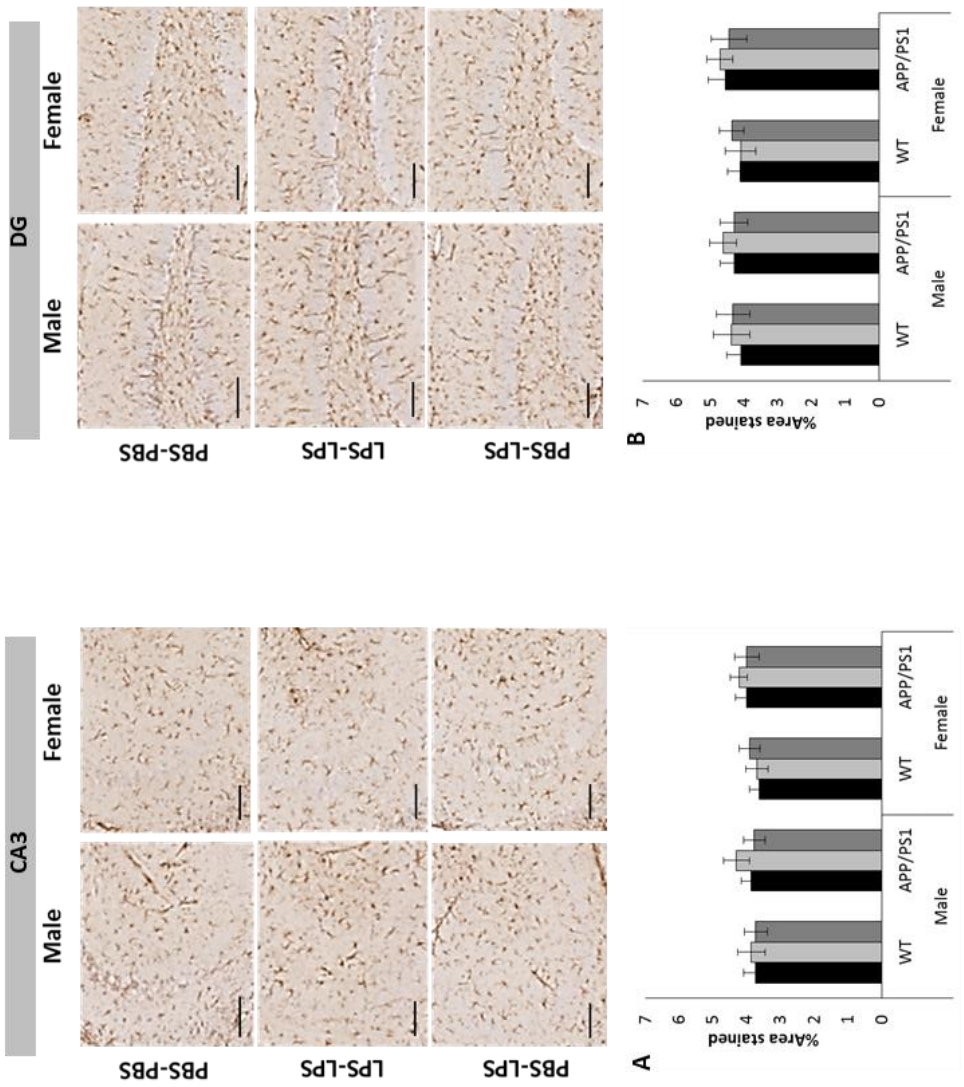

Figure 63. **Area occupied by GFAP in the CA3 and DG hippocampal subfields.** 4.5 months old males and females mice APPswe/PS1ΔE9 (APP/PS1) and wild-type (WT) (n=8 per group) were treated with LPS or vehicle (PBS) and their brain was collected 7 days after the 2nd injection. No significant differences were observed in the percentage of area stained by GFAP in CA3 (**A**) and DG (**B**). Scale bars, 0.25mm. Data are presented as mean ± S.E.M.

Microglia response to LPS in the hippocampus and cortex

An overall genotype X sex interaction effect was observed in the percentage of area stained by Iba-1 in the whole hippocampus ($F_{(1,89)}$=7.85, p=0.006) (Figure 64) and CA3 hippocampal subfield ($F_{(1,89)}$=6.82, p=0.011) (Figure 68), with APPswe/PS1ΔE9 females showing lower microglia density than wild-type females [in hippocampus (p=0.003) and CA3 (p=0.006)], and than APPswe/PS1ΔE9 males in the whole hippocampus only (p=0.015). An overall genotype effect ($F_{(1,89)}$=8.86, p=0.004) was seen in the percentage of area stained by Iba-1 in the cortex (Figure 65), with APPswe/PS1ΔE9 males having higher microglia density than the wild-type littermates (p=0.0053).

Analysis of the number of microglia cells per mm^2 revealed an overall treatment effect in the whole hippocampus ($F_{(1,89)}$=3.77, p=0.027) (Figure 64), in CA1 ($F_{(1,89)}$=3.87, p=0.025) (Figure 66), in DG ($F_{(1,89)}$=4.36, p=0.015) (Figure 69) and in the cortex ($F_{(1,89)}$=8, p=0.0006) (Figure 65), with PBS-PBS-treated APPswe/PS1ΔE9 females showing fewer microglia cells/mm^2 than LPS-LPS-treated APPswe/PS1ΔE9 females [in hippocampus (p=0.0236); CA1 (p=0.029); DG (p=0.038); and cortex (p=0.044)]. Moreover PBS-PBS-treated wild-type males and females revealed fewer microglia cells/mm^2 compared to PBS-LPS-treated wild-type littermates in the cortex (p<0.05). An overall genotype X sex interaction effect was also observed in the analysis of the number of microglia cells per mm^2 in the whole hippocampus ($F_{(1,89)}$=5.17, p=0.025) (Figure 64), in CA2 ($F_{(1,89)}$=4.12, p=0.045) (Figure 67) and in CA3 ($F_{(1,89)}$=5.50, p=0.021) (Figure 68.G), with wild-type males showing fewer microglia cells/mm^2 than wild-type females [in hippocampus (p=0.023); CA2 (p=0.009); and CA3 (p=0.007)], and than APPswe/PS1ΔE9 males [in CA2 (p=0.034)]. Analysis of the number of microglia clusters revealed an overall genotype effect in the whole hippocampus ($F_{(1,89)}$=39.9, p<0.0001) (Figure 64), in the cortex

($F_{(1,89)}$=36.76, p<0.0001) (Figure 65), and in all the 4 hippocampal subfields [CA1 ($F_{(1,89)}$= 10.31, p=0.002) (Figure 66), CA2 ($F_{(1,56)}$=4.34, p=0.04) (Figure 67), CA3 ($F_{(1,89)}$=23.86, p<0.0001) (Figure 68), and DG ($F_{(1,89)}$=121.41, p<0.0001) (Figure 69)], with transgenic animals showing more clusters than wild-types, in both males and females (p<0.05). In addition, an overall genotype X sex interaction effect was seen in the whole hippocampus ($F_{(1,89)}$=5.71, p=0.018) (Figure 64), in the cortex ($F_{(1,89)}$=4.77, p<0.032) (Figure 65), and in 2 hippocampal subfields [CA3 ($F_{(1,89)}$=7.18, p=0.009) (Figure 68), and DG ($F_{(1,89)}$=12.11, p=0.0008) (Figure 69)], where transgenic females presented more clusters than transgenic males (p<0.05). Analysis of the size of microglia soma showed an overall genotype X sex interaction in CA3 ($F_{(1,89)}$=6.01, p=0.018) (Figure 68), with APPswe/PS1ΔE9 females having smaller microglia soma than wild-type females. The number of microglia clusters, used as a covariate, was found to be a significant in the analysis of microglia density, number of microglia cells per mm^2 and microglia soma size (p<0.05).

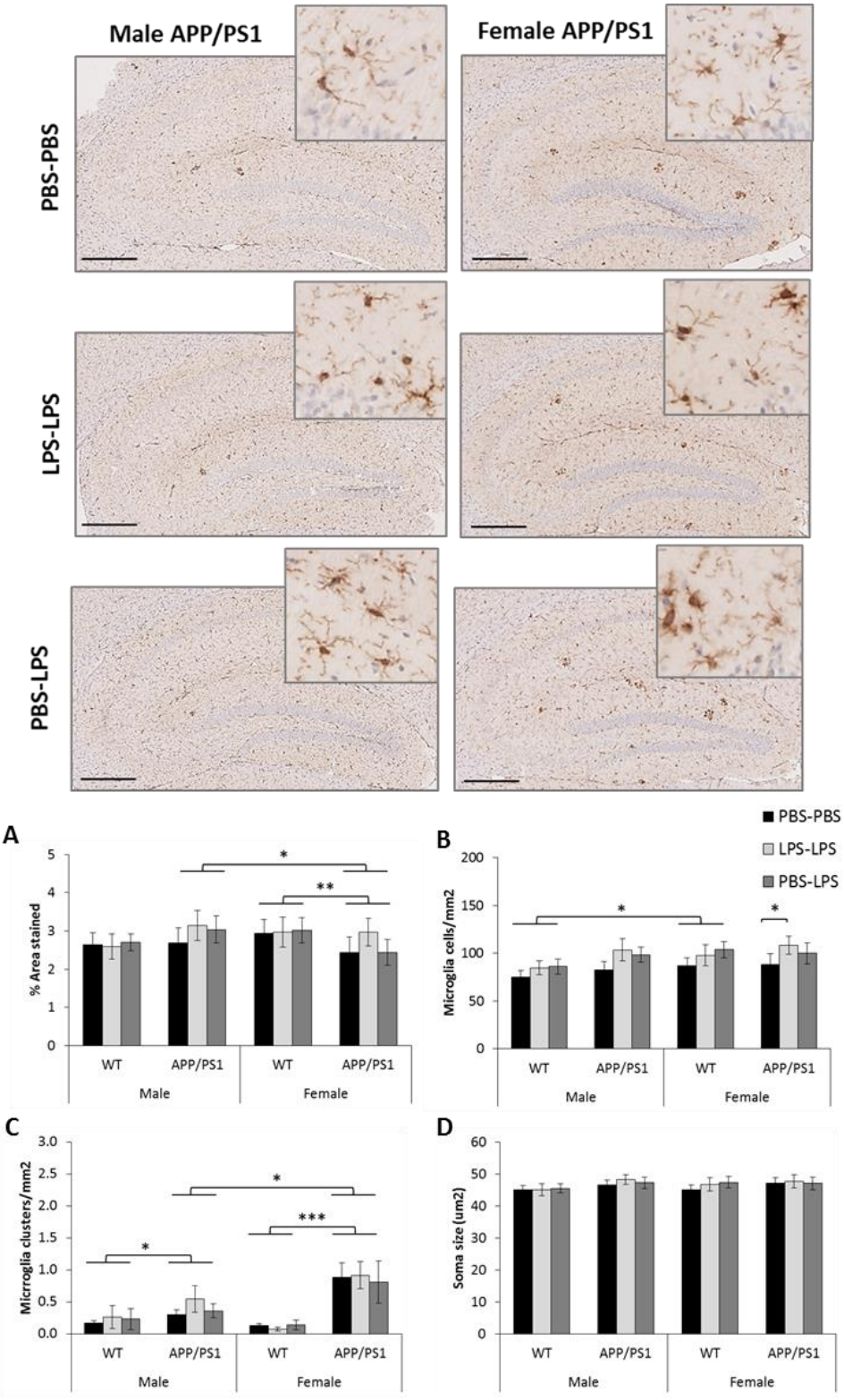
Male APP/PS1
Female APP/PS1
PBS-PBS
LPS-LPS
PBS-LPS
A
% Area stained
B
Microglia cells/mm2
C
Micrroglia clusters/mm2
D
Soma size (um2)
PBS-PBS
LPS-LPS
PBS-LPS
WT
APP/PS1
Male
Female

Figure 64. **Area occupied by Iba-1 in the hippocampus**. 4.5 months old males and females mice APPswe/PS1ΔE9 (APP/PS1) and wild-type (WT) (n=8 per group) were treated with LPS or vehicle (PBS) and their brain was collected 7 days after the 2nd injection. APP/PS1 females showed lower percentage of Iba-1 compared to WT females (p=0.003) and APP/PS1 males (p=0.015) (**A**). A higher number of microglia cells per mm^2 was observed in WT females compared to WT males (p=0.023), and in LPS-LPS-treated APP/PS1 females compared to PBS-PBS-treated APP/PS1 females (p=0.023) (**B**). A higher number of microglial clusters/mm^2 was revealed in APP/PS1 female compared to WT female (p<0.0001) and APP/PS1 males (p=0.013), and in APP/PS1 male compared to their WT littermates (p=0.007) (**C**). No significant differences were seen for the soma size (**D**). Scale bars, 0.5mm. Data are presented as mean ± S.E.M. [* p< 0.05, **p<0.005, ***p<0.0001].

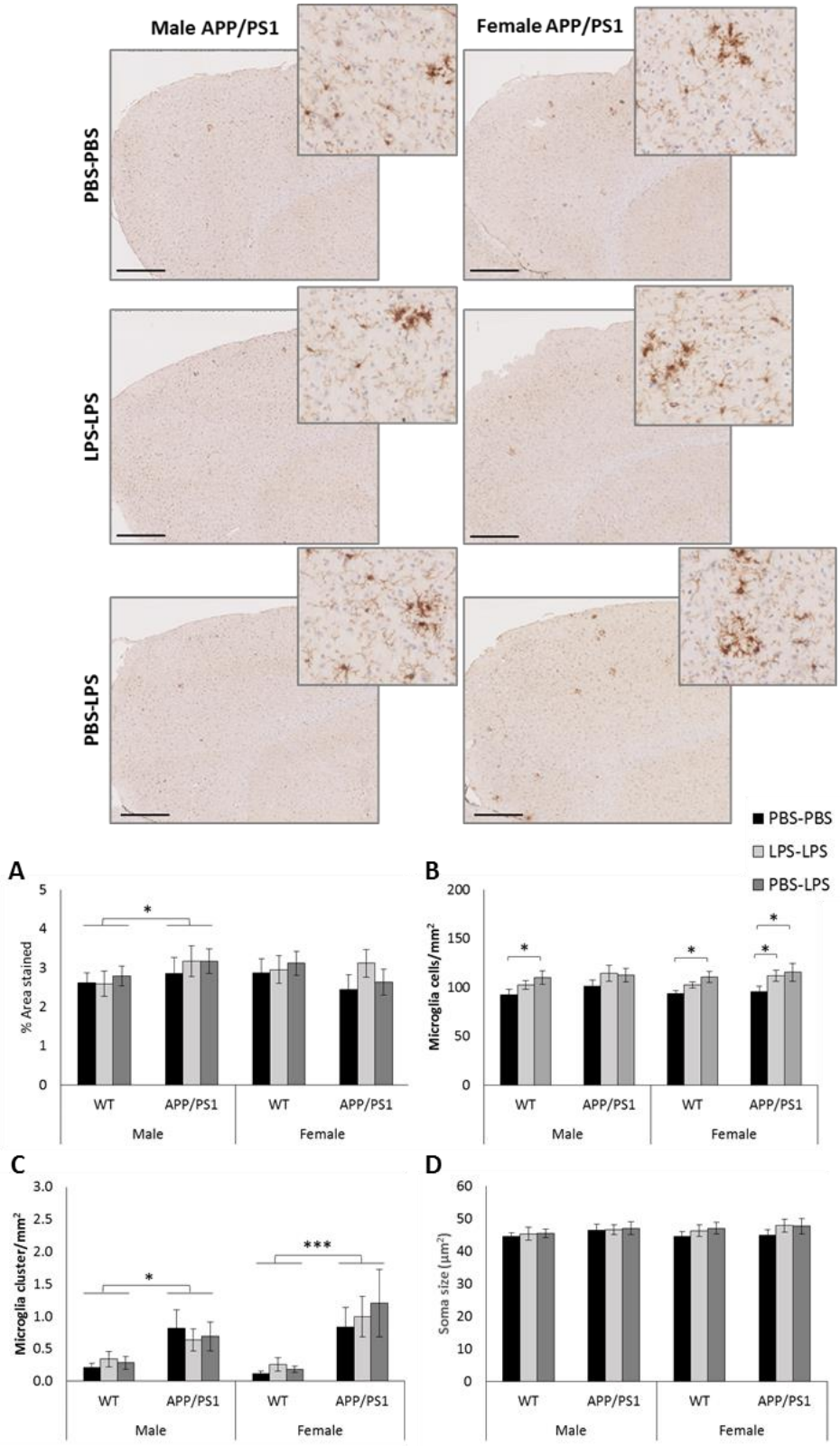
Male APP/PS1
Female APP/PS1
PBS-PBS
LPS-LPS
PBS-LPS
PBS-PBS
LPS-LPS
PBS-LPS
A
% Area stained
B
Microglia cells/mm²
C
Microglia cluster/mm²
D
Soma size (µm²)
WT
APP/PS1
Male
Female

Figure 65. **Area occupied by Iba-1 in the cortex.** 4.5 months old males and females mice APPswe/PS1ΔE9 (APP/PS1) and wild-type (WT) (n=8 per group) were treated with LPS or vehicle (PBS) and their brain was collected 7 days after the 2nd injection. APP/PS1 males showed higher percentage of area occupied by Iba-1 compared to WT males (p=0.005) (**A**). A higher number of microglia cells per mm^2 was observed in LPS-LPS-treated APP/PS1 females compared to PBS-PBS-treated APP/PS1 females (p=0.044), in PBS-LPS-treated APP/PS1 females (p=0.05), WT females (p=0.043) and WT males (p=0.033) compared to their PBS-PBS-treated counterpart (**B**). A higher number of microglial clusters/mm^2 was revealed in APP/PS1 female compared to WT female (p<0.0001) and in APP/PS1 male compared to WT males (p=0.007) (**C**). No significant differences were seen for the soma size (**D**). Scale bars, 0.5mm. Data are presented as mean ± S.E.M. [* p< 0.05, **p<0.005, ***p<0.0001].

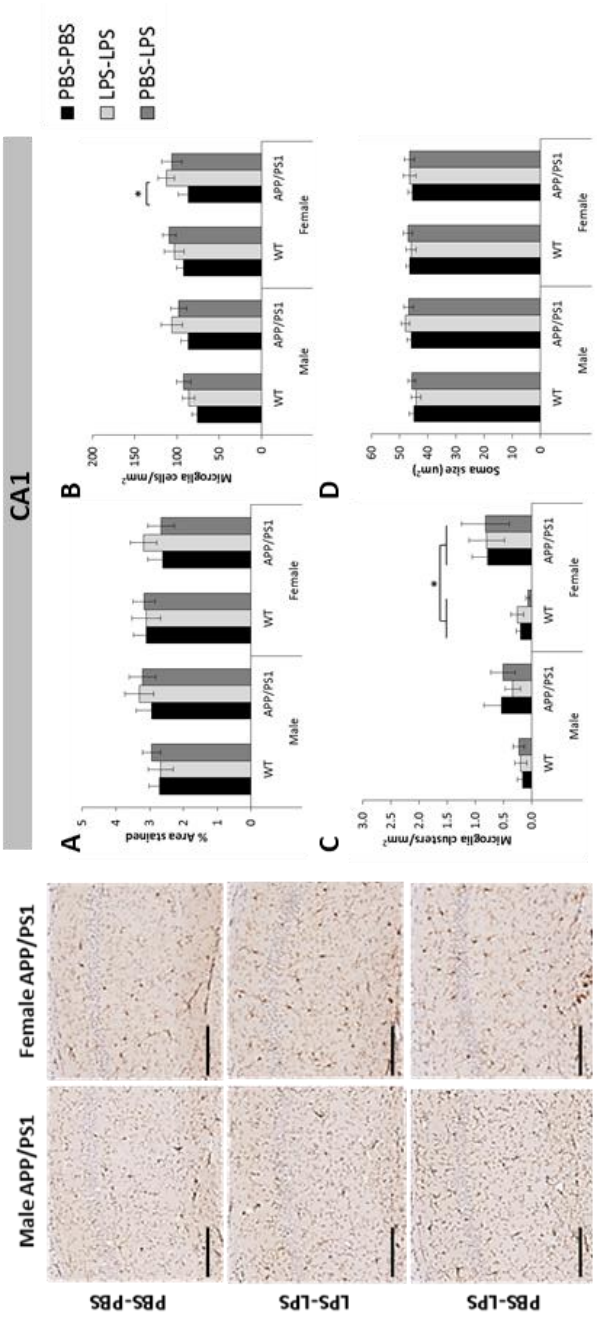

Figure 66. **Area occupied by Iba-1 in the CA1 hippocampal subfield.** 4.5 months old males and females mice APPswe/PS1ΔE9 (APP/PS1) and wild-type (WT) (n=8 per group) were treated with LPS or vehicle (PBS) and their brain was collected 7 days after the 2nd injection. No significant difference was observed in the percentage of area stained by Iba-1 in CA1 (**A**). LPS-LPS-treated APP/PS1 females showed higher numbers of microglial cells/mm^2 compared to PBS-PBS-treated females in CA1 (**B**). A higher number of microglial clusters/mm^2 was revealed in APP/PS1 females compared to WT females (p=0.006) (**C**). No significant differences were observed in the microglia soma size (**D**). Scale bars, 0.25mm. Data are presented as mean ± S.E.M. [* p< 0.05].

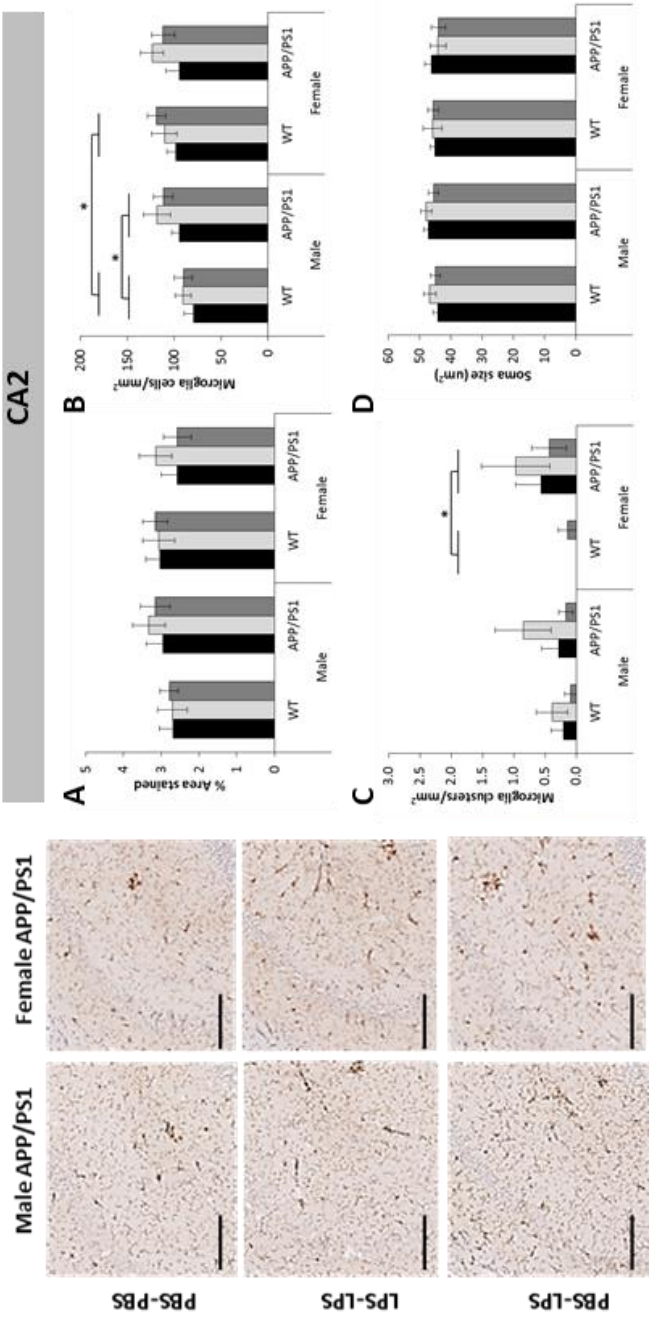

Figure 67. **Area occupied by Iba-1 in CA2 hippocampal subfield.** 4.5 months old males and females mice APPswe/PS1ΔE9 (APP/PS1) and wild-type (WT) (n=8 per group) were treated with LPS or vehicle (PBS) and their brain was collected 7 days after the 2nd injection. No significant difference was observed in the percentage of area stained by Iba-1 in CA2 (**A**). Lower numbers of microglial cells/mm^2 was revealed in wild-type males compared to wild-type females (p=0.009) and APPswe/PS1ΔE9 males (p=0.034) (**B**). A higher number of microglial clusters/mm^2 was revealed in APP/PS1 females compared to WT females in CA2 (p=0.021) (**C**). No significant differences were observed in the microglia soma size (**D**). Scale bars, 0.25mm. Data are presented as mean ± S.E.M. [* p< 0.05].

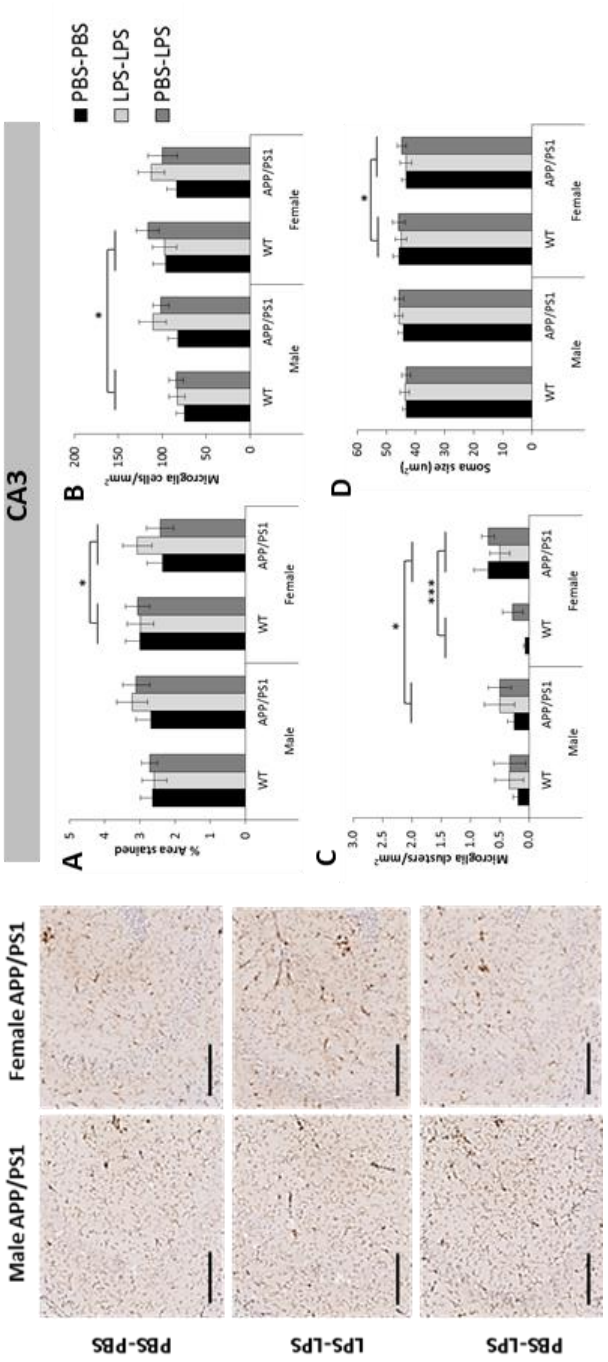

Figure 68. **Area occupied by Iba-1 in the CA3 hippocampal subfield.** 4.5 months old males and females mice APPswe/PS1ΔE9 (APP/PS1) and wild-type (WT) (n=8 per group) were treated with LPS or vehicle (PBS) and their brain was collected 7 days after the 2nd injection. Lower percentage of area stained by Iba-1 was seen in APP/PS1 females compared to WT littermates (p=0.006) in CA3 (**A**). Lower numbers of microglial cells/mm^2 was revealed in wild-type males compared to wild-type females (p=0.007) (**B**). A higher number of microglial clusters/mm^2 was revealed in APP/PS1 females compared to WT females (p<0.0001) (**C**), and compared to APP/PS1 males (p=0.018) (**C**). APP/PS1 females showed smaller microglia soma than WT males (p=0.019) (**C**). Scale bars, 0.25mm. Data are presented as mean ± S.E.M. [*p< 0.05, ***p<0.0001].

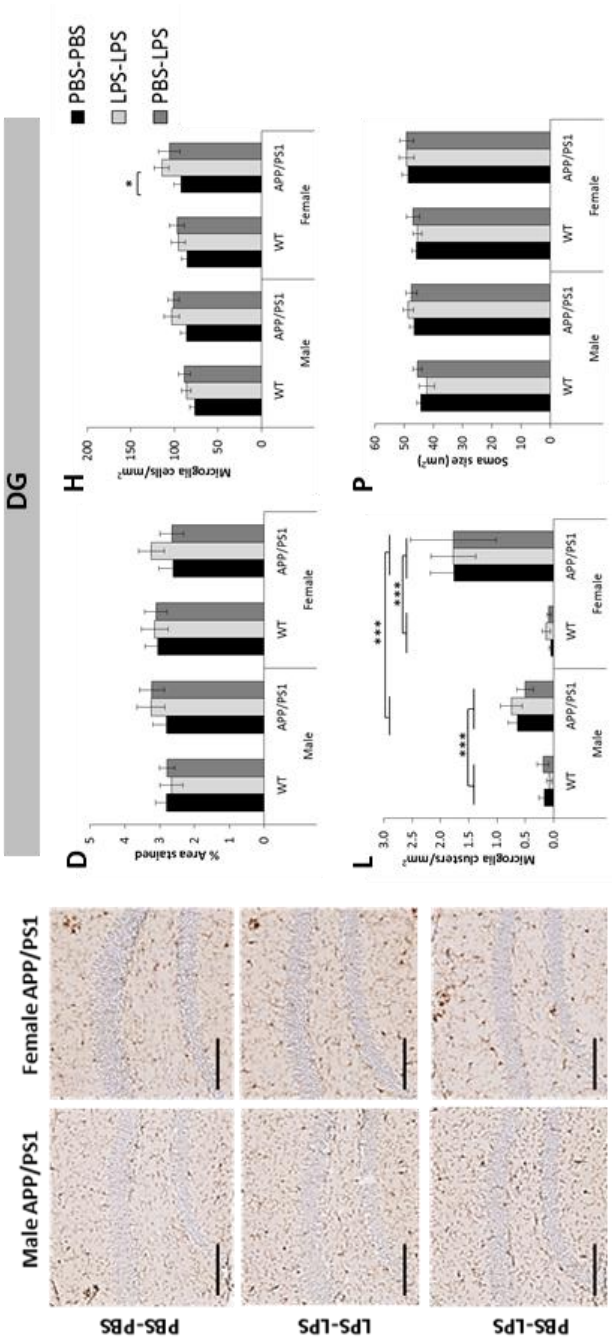

Figure 69. **Area occupied by Iba-1 in the DG hippocampal subfield.** 4.5 months old males and females mice APPswe/PS1ΔE9 (APP/PS1) and wild-type (WT) (n=8 per group) were treated with LPS or vehicle (PBS) and their brain was collected 7 days after the 2nd injection. LPS-LPS-treated APP/PS1 females showed higher numbers of microglial cells/mm^2 compared to PBS-PBS-treated females (p=0.037) (**B**). A higher number of microglial clusters/mm^2 was revealed in APP/PS1 females compared to WT females (p<0.0001) (**C**), and compared to APP/PS1 males (p<0.0001) (**C**). APP/PS1 males also showed higher numbers of microglia clusters/mm^2 compared to WT littermates (**C**). Scale bars, 0.25mm. Data are presented as mean ± S.E.M. [**p< 0.0001].

5.3.5 Infiltration of peripheral monocytes into the CNS and characterization of their immune profile

To detect macrophages that infiltrated the brain, flow cytometry analysis was performed as described in the method chapter (chapter 2). The percentage of gated cells relative to the total number of cells were stained with $CD11b^{+}CD45^{+Lo}$ and $CD11b^{+}CD45^{+Hi}$ to distinguish between resident microglia and infiltrating monocytes respectively.

No significant differences were observed in the number of macrophages that infiltrated the hippocampus (Figure 70.A) and the cortex (Figure 72.A). An overall effect of sex was revealed in the analysis of microglia cell population in the hippocampus ($F_{(1,40)}$=4.36, p=0.043) (Figure 71.A), with wild-type females showing fewer microglia cells than wild-type males (p=0.023). An overall effect of sex was also observed in the analysis of microglia in the cortex ($F_{(1,40)}$= 19.22, p<0.0001) (Figure 73.A), where females showed fewer cells than males (p<0.05., regardless of genotype.

To further identify the subpopulation distribution among the infiltrated macrophages and resident microglia, expression of CCR2 was analysed to characterize the chemotactic phenotype. An overall sex effect was seen in the hippocampus ($F_{(1,40)}$= 5.52, p=0.0239) (Figure 70.B), with females having higher numbers of infiltrated macrophages expressing CCR2 compared to males (p=0.024). An overall sex effect was also seen in resident microglia in the cortex ($F_{(1,40)}$= 5.61, p=0.023) (Figure 72.B), with wild-type females having higher numbers of cells expressing CCR2 than wild-type males (p=0.032).

Investigating the phagocytic activity, intracellular Aβ staining was quantified to analyse the presence of intracellular amyloid beta peptide. Analysis of the infiltrating macrophages revealed an overall sex effect in the hippocampus ($F_{(1,40)}$=

5.52, p=0.0239) (Figure 70.C), with APPswe/PS1ΔE9 females showing higher numbers of infiltrated macrophages positive for Aβ compared to transgenic males (p-=0.0081). An overall sex effect was also observed in the hippocampal resident microglia ($F_{(1,40)}$= 4.45, p=0.0411) (Figure 71.C), with a higher number of microglia presenting intracellular Aβ in females compared to males (p=0.041).

To characterize the immune phenotype of the infiltrated macrophages and resident microglia, the expression of CD80 (M1 marker) and CD206 (M2 marker) were analysed. From the analysis of M1 expression, an overall sex effect was revealed in the hippocampal resident microglia ($F_{(1,40)}$= 9.29, p=0.004) (Figure 71.D), with APPswe/PS1ΔE9 females showing higher CD80 expression than transgenic males (p=0.014).

No significant differences emerged between the experimental groups in the analysis of intracellular Aβ staining (Figure 72.C-Figure 73.C) and CD80/CD206 expressions (Figure 72.D-Figure 73.D) in the cortex.

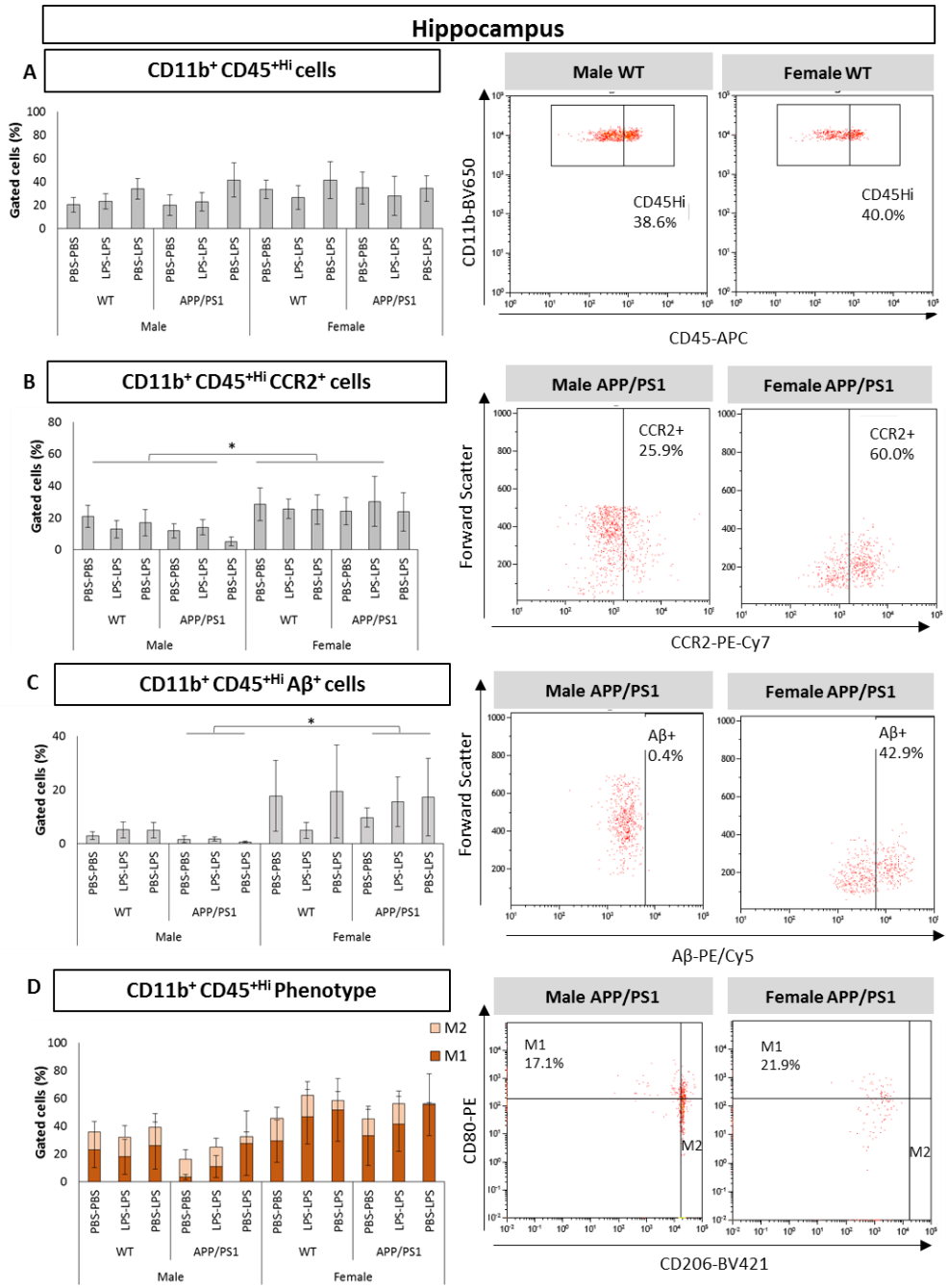

Figure 70 **Infiltrated macrophages analysis with flow cytometry in the hippocampus.** 4.5 months old males and females mice APPswe/PS1ΔE9 (APP/PS1) and wild-type (WT) (n=3/4 per group) were treated with LPS or vehicle (PBS) and their brain was collected 7 days after the 2nd injection. Flow cytometry analysis revealed no significant differences regarding the $CD11b^{+}$ $CD45^{+Hi}$ cells (**A**). Analysis of $CCR2^{+}$ expression in $CD11b^{+}$ $CD45^{+Hi}$ cell population revealed higher percentage of cells having the CCR2 receptor in females compared to males (p=0.024) (**B**). Higher numbers of $CD11b^{+}CD45^{+Hi}A\beta^{+}$ cells were seen in APP/PS1 females compared to APP/PS1 males (p=0.008) (**C**). Moreover, higher expression of CD80 was seen in females compared to males (p=0.041) (**D**). Data are shown as mean ± S.E.M. [*p< 0.05].

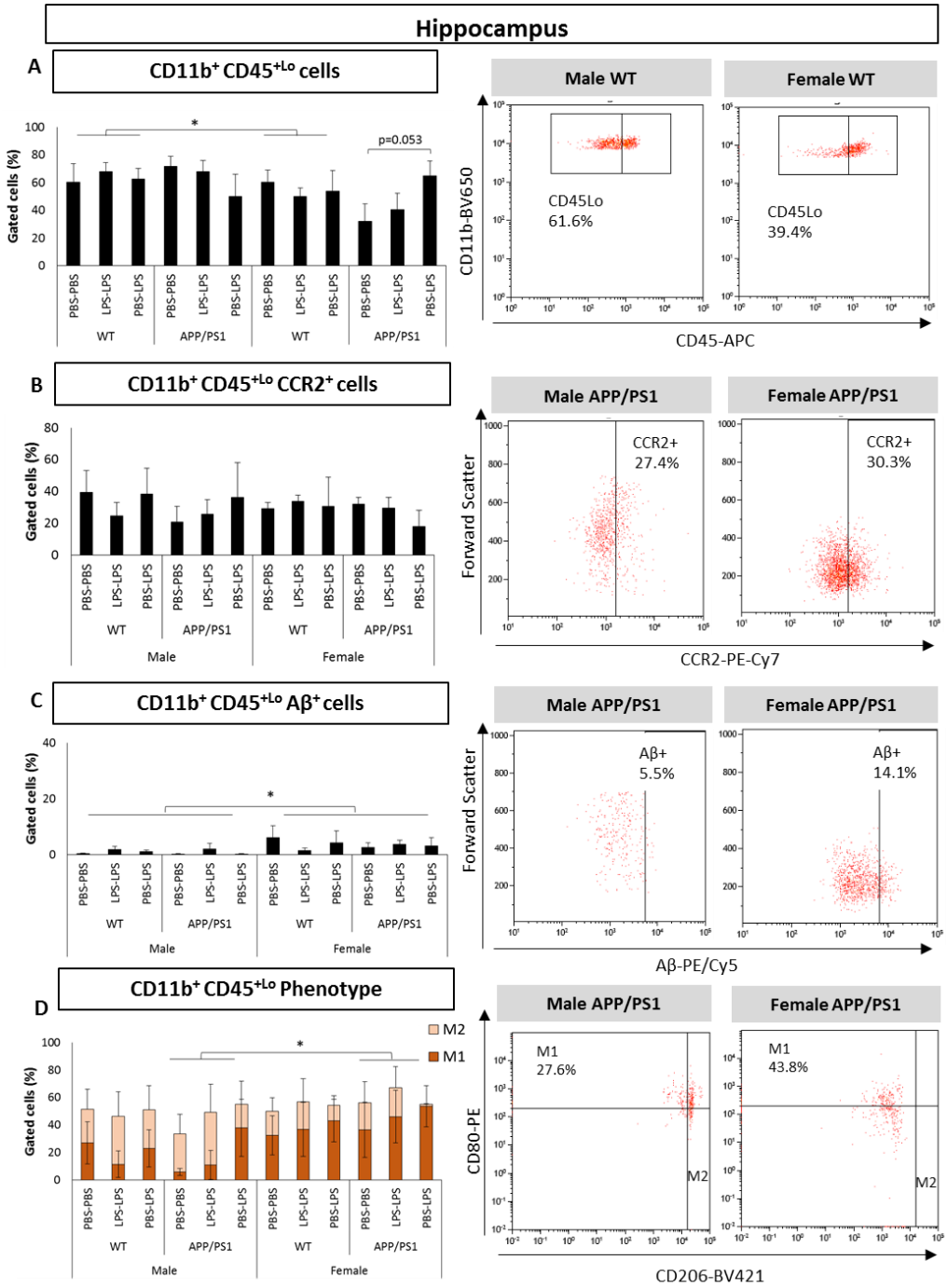

Figure 71**. Microglia analysis with flow cytometry in the hippocampus.** 4.5 months old males and females mice APPswe/PS1ΔE9 (APP/PS1) and wild-type (WT) (n=3/4 per group) were treated with LPS or vehicle (PBS) and their brain was collected 7 days after the 2nd injection. Flow cytometry analysis revealed lower percentage of $CD11b^{+}$ $CD45^{+Lo}$ cells in WT females compared to WT males (p=0.023) (**A**). No significant differences were seen in the analysis of $CCR2^{+}$ expression (**B**). A higher number of $CD11b^{+}CD45^{+Lo}A\beta^{+}$ cells was observed in females compare to males (p=0.041) (**C**). Moreover, higher expression of CD80 was seen in APP/PS1 females compared to APP/PS1 males (p=0.014) (**D**). Data are shown as mean ± S.E.M. [* p< 0.05].

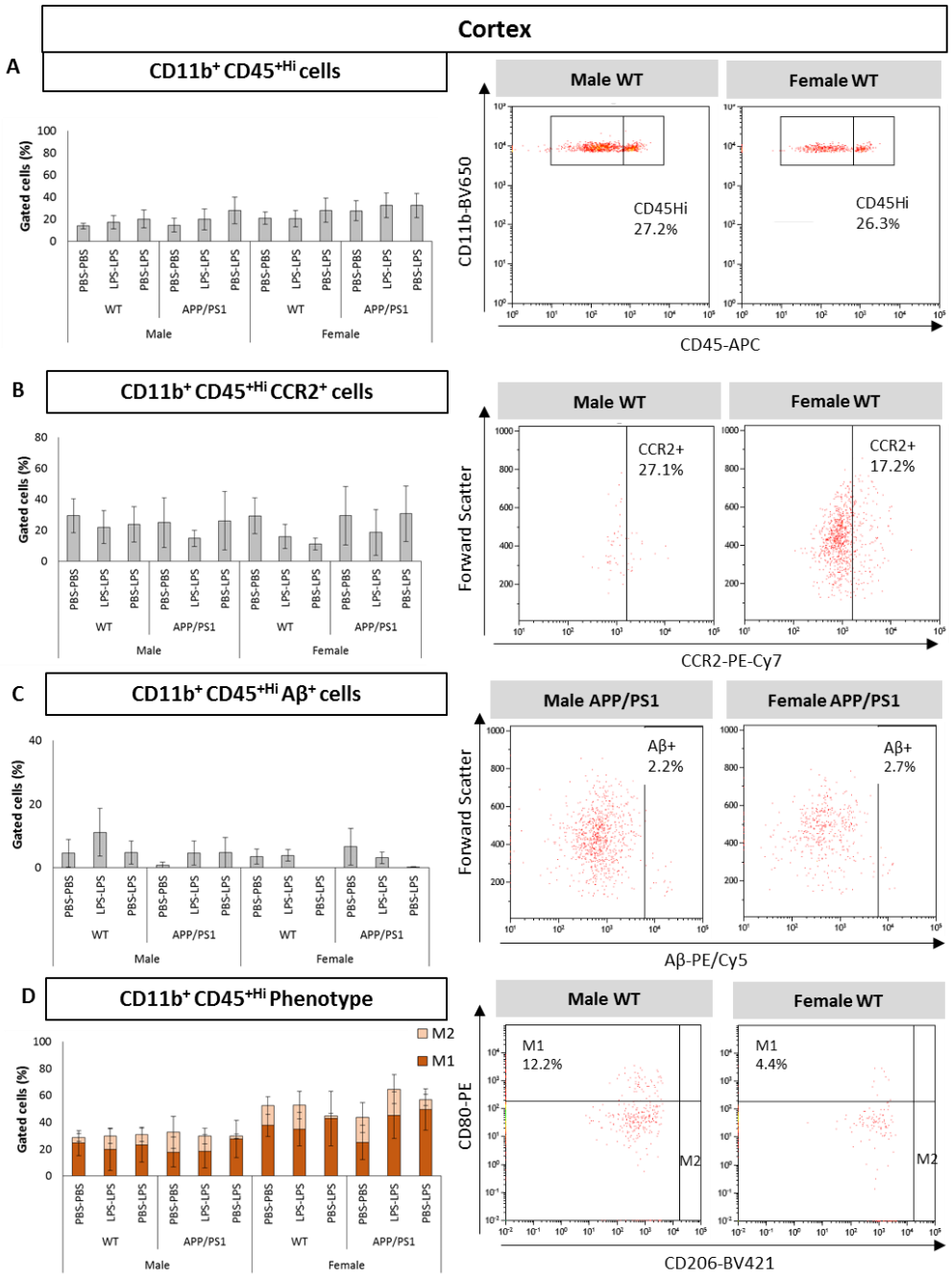

Figure 72. **Infiltrated macrophages analysis with flow cytometry in the cortex.** 4.5-months-old male and female mice APPswe/PS1ΔE9 (APP/PS1) and wild-type (WT) (n=3/4 per group) were treated with LPS or vehicle (PBS) and their brain was collected 7 days after the 2nd injection. Flow cytometry analysis revealed no significant differences between experimental groups in the number of CD11b+ CD45+Hi (**A**), in the expression of CCR2 (**B**), in the intracellular Aβ staining (**C**) and in the expression of CD80 (M1) and CD206 (M2) (**D**). Data are shown as mean ± S.E.M.

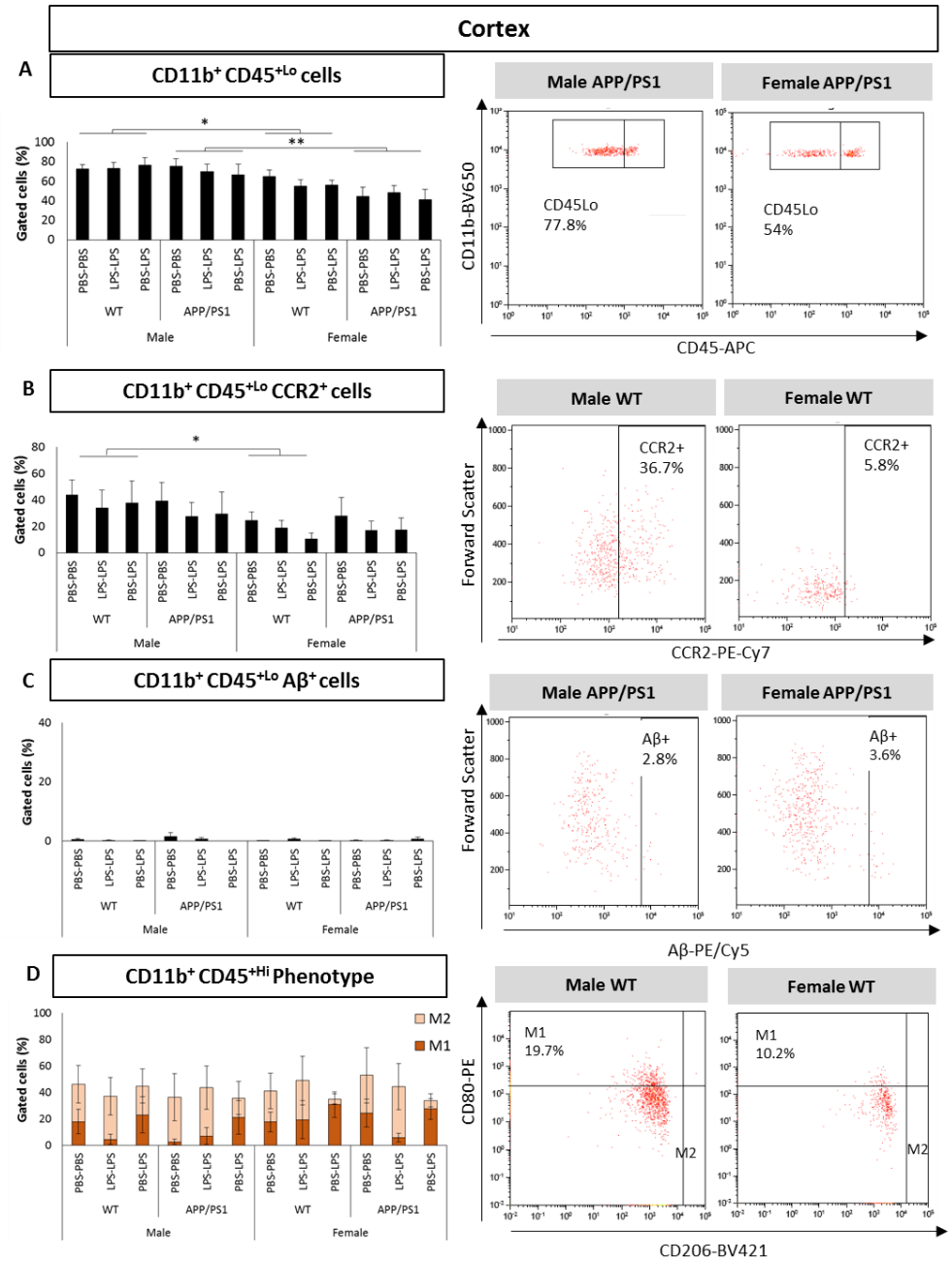

Figure 73. **Microglia analysis with flow cytometry in the cortex.** 4.5 months old males and females mice APPswe/PS1ΔE9 (APP/PS1) and wild-type (WT), (n=3/4 per group), were treated with LPS and vehicle (PBS) and their brain was collected 7 days after the 2nd injection. Flow cytometry analysis of the cellular staining revealed lower percentage of CD11b+ CD45+Lo cells in WT females compared to WT males (p=0.012) and in APP/PS1 females compared to APP/PS1 males (p=0.001) (**A**). Analysis of CCR2+ expression revealed lower percentage of cells having the CCR2 receptor in WT females compared to WT males (p=0.032) (**B**). No significant differences were observed in the analysis of intracellular Aβ (**C**), and the surface phenotypic markers CD80 (M1) and CD206 (M2) (**D**). Data are shown as mean ± S.E.M. [* p< 0.05, **p<0.005].

5.3.6 Characterizing peritoneal macrophages

To characterize the phenotype of peritoneal macrophages, flow cytometry analysis was performed as described in the method chapter (chapter 2). Peritoneal macrophages, identified as $F4/80^{+}$ cells, were characterized by staining for CCR2, to analyse the chemotactic phenotype, for CD80 and CD206, to investigate the inflammatory phenotype, and for Aβ, to show the intracellular presence of the amyloid peptide as an indicator of the cellular phagocytic activity. No significant differences were observed between the experimental groups in the analysis of the CCR2 (Figure 74.A), the M1 (CD80) and M2 (CD206) (Figure 74.C) expression, as well the intracellular Aβ (Figure 74.B).

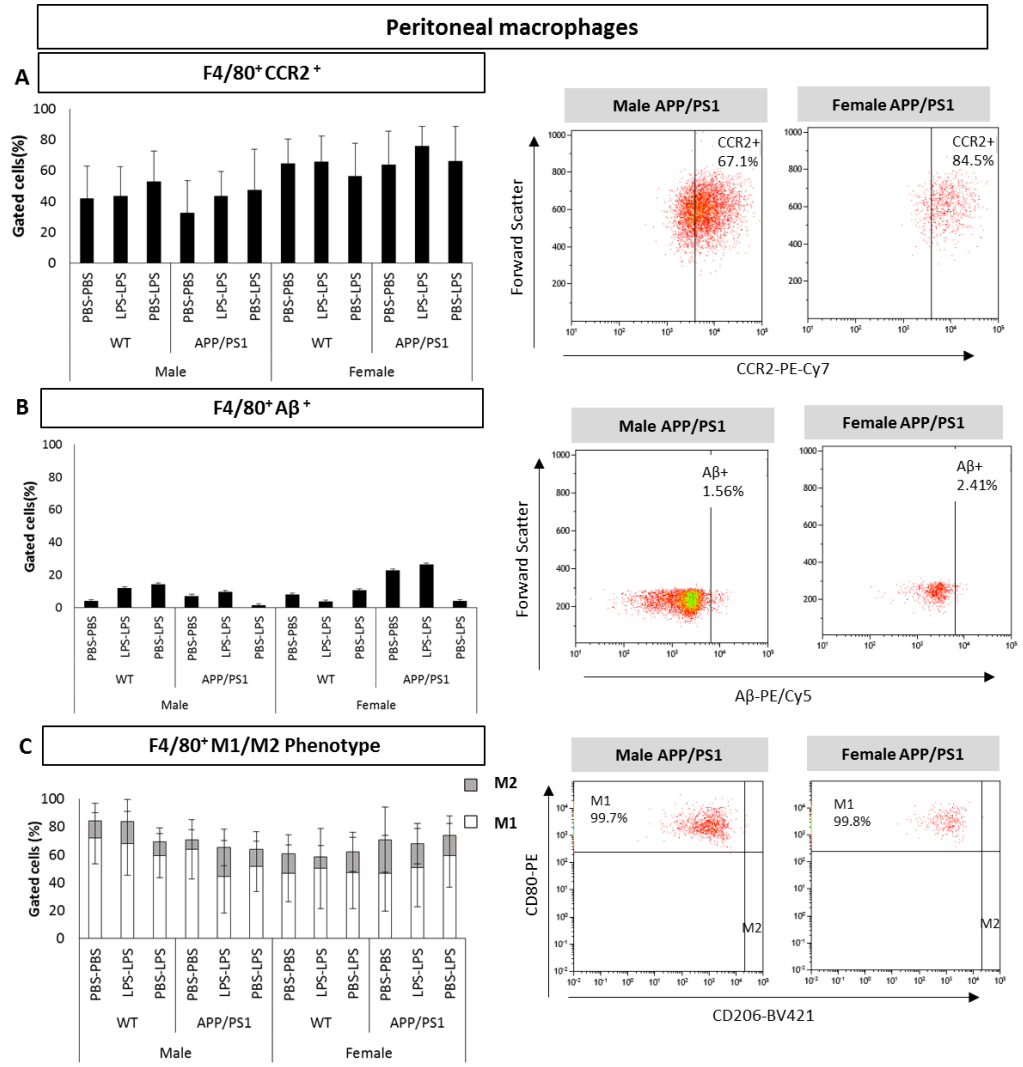

Figure 74. **Peripheral macrophages analysis with flow cytometry.** 4.5 months old males and females mice APPswe/PS1ΔE9 (APP/PS1) and wild-type (WT) (n=3/4 per group) were treated with LPS and vehicle (PBS) and peritoneal macrophages were collected 7 days after the 2nd injection. Flow cytometry analysis revealed no significant differences between experimental groups in the expression of CCR2 (**A**), in the intracellular Aβ staining (**B**) and in the expression of CD80 (M1) and CD206 (M2) (**C**). Data are shown as mean ± S.E.M.

5.4 Summary of the main findings

The present study revealed that both a single and a double systemic LPS challenge, given from 4.5 months of age, increased spatial working memory in wild-type females, with no effects on locomotor and daily living activities (Table 5). Analysis of microglia activation revealed that both single and repeated LPS administration increased the number of microglia cells (Table 6) and reduced the circulating levels of INF-γ (Table 5) Moreover, LPS given once or twice also reduced the size of the smaller plaques in transgenic females, compared to males, with no significant effect on the accumulation of the plaques (Table 6).

No effects of LPS were seen 7 days after a single or a second challenge, on astrocyte density (Table 6), or brain-infiltrated macrophages, resident microglia and peritoneal macrophages (Table 4). Differences between sexes and genotypes have been revealed. Females recovered faster than males, after both treatments. The recovery seen in females was associated with reduced levels of the pro-inflammatory cytokines IL-6, IFN-γ, and the anti-inflammatory cytokine IL-10, compared to the male counterpart. Transgenic females presented higher number of extracellular amyloid plaques and intracellular Aβ staining, as well as higher number of Iba-1 and GFAP clusters, compared to transgenic males. Wild-type females had lower numbers of resident microglia and increased expression of CD80 in microglia, compared to wild-type males (Table 4). Females also showed higher expression of CCR2 in infiltrated macrophages, regardless of genotype. The expression of CCR2 seen higher in females was found associated with a higher intracellular Aβ staining (Table 4). No treatment, genotype or sex effect was observed in the analysis of peritoneal macrophages.

Table 5. Summary of the main findings on behaviour and cytokines levels

	BEHAVIOURAL AND CYTOKINES ANALYSIS		
	TREATMENT	**GENOTYPE**	**SEX**
BODY WEIGHT RECOVERY	–	**LPS-LPS treatment:** APP/PS1 females recover faster than WT females. **PBS-LPS treatment:** WT females recover faster than APP/PS1 females, but APP/PS1 males recover faster than WT males.	**LPS-LPS treatment:** females recover faster than males both after 1 and 2nd injection. **PBS-LPS treatment:** WT females recover faster than WT males, but APP/PS1 males recover faster than APP/PS1 females.
FOOD BURROWING	–	–	Females burrowed more than males post-injection.
SPATIAL WORKING MEMORY	**PBS-LPS-treated** and **LPS-LPS treated** WT females showed an improvement compared to the control group. **LPS-LPS treated** APP/PS1 females and males showed an improved compared to the baseline performance	–	–
LOCOMOTOR ACTIVITY	–	APP/PS1 mice moved more than WT mice in both sexes.	–
CYTOKINES	**LPS-LPS-treated** and **PBS-LPS-treated** APP/PS1 females showed lower IFN-γ levels than the vehicle-treated mice.	–	WT females showed lower **IL-6**, **IFN-γ and IL-10** levels than WT males. APP/PS1 females showed lower **IL-10** levels than APP/PS1 males.

Table 6. Summary of the main immunostaining analysis results.

	IMMUNOSTAINING ANALYSIS		
	TREATMENT	**GENOTYPE**	**SEX**
AMYLOID PLAQUE LOAD	–	N/A	Higher **number of plaques** in females compared to males. **Area of small plaques/mm²** is larger in males compared to females (cortex).
GFAP-IMMUNOREACTIVITY	–	Higher number of **GFAP clusters** in APP/PS1 compared to WT mice (cortex).	Higher number of **GFAP clusters** in APP/PS1 females compared to APP/PS1 males (cortex).
IBA-1-IMMUNOREACTIVITY	**LPS-LPS-treated** APP/PS1 females and **PBS-LPS-treated** mice showed more **iba-1-immunoreactive cells/mm²** than control animals.	Lower **% area stained** in APP/PS1 females compared to WT females (hippocampus). Higher **% area stained** in APP/PS1 males compared to WT males (cortex). Smaller **microglia soma** in APP/PS1 females compared to WT females. Higher number of **Iba-1 clusters** in APP/PS1 compared to WT mice.	Lower **% area stained** in APP/PS1 females compared to APP/PS1 males (hippocampus). Higher number of **iba-1-immunoreactive cells/mm²** in WT females than WT males (hippocampus). Higher number of **Iba-1 clusters** in females compared to males (hippocampus).

Table 7. Summary of the main flow cytometry analysis.

	FLOW CYTOMETRY ANALYSIS		
	TREATMENT	**GENOTYPE**	**SEX**
BRAIN INFILTRATING MACROPHAGES $CD11b^{+}CD45^{+HI}$	–	–	–
MICROGLIA $CD11b^{+}CD45^{+LO}$	–	–	Lower number in females compared to males.
CCR2 EXPRESSION	–	–	Higher in females compared to males in infiltrated macrophages (hippocampus) **F4/80^{+}:** no changes.
INTRACELLULAR Aβ	–	–	Higher in females compared to males in **infiltrated and peritoneal macrophages and resident microglia** (hippocampus). **F4/80^{+}**: no changes
M1/M2 IMMUNE PHENOTYPE	–	–	Higher expression of M1 marker in females compared to males in **infiltrated macrophages and resident microglia** (hippocampus). **F4/80^{+}**: no changes

5.5 Discussion

The present study revealed that two systemic injections of LPS (LPS-LPS-treated group) improved spatial working memory and reduced levels of circulating INF-γ in APPswe/PS1ΔE9 females, also inducing an increase in the number of microglia cells in the brain of these mice. A single systemic LPS (PBS-LPS-treated group), reduced levels of IFN-γ in plasma and increased the number of microglia cells in APPswe/PS1ΔE9 females. Both single and double injection of LPS induced a reduction in the size of small plaques in transgenic females compared to males. LPS did not significantly affect the infiltration of macrophages into the brain, the expression of chemotactic receptor CCR2 or the expression of the pro- and anti-inflammatory markers, CD80 and CD206 respectively.

Analysis of body weight, recorded to monitor the recovery of the animals from the treatment, showed that females recovered faster than males after a single and a double LPS injection. Furthermore, when comparing recovery of the mice at the first and second LPS challenge, all mice lost less body weight after the second injection compared to the first. In particular, females lost less weight than males after the 2nd challenge, suggesting that females are more tolerant than males to a second endotoxin exposure. These findings are in line with a previous study which showed a rapid tolerance development in females compared to males, with females not showing loss in body weight after the second exposure to LPS (100 or 200μg/kg, i.p, within 7 days) (Engeland et al., 2003). Engeland et. al. also analysed locomotor activity in these animals after each injection and observed that females developed behavioural tolerance faster than males, becoming more active after the last LPS injection (Engeland et al., 2003). However, there was no improvement in locomotor activity here, but an improvement in spatial working memory was observed in LPS-

LPS-treated transgenic females and males. Cunningham et al. have tried to elucidate the effect of LPS tolerance on spatial working memory, but revealed that consecutive treatments with LPS did not impair or improve memory (Cunningham and Sanderson, 2008). Thus, improvement in spatial working memory is not associated with LPS tolerance.

PBS-LPS-treated mice didn't show an improvement in spatial working memory, compared to the baseline data. This result can be explained by the data shown by Murray et. al. where an acute systemic LPS challenge (100 μg/kg) induced working memory impairment in a model of prion disease, where microglia are primed (Murray et al., 2012). Here, I did not demonstrate that microglia were primed, by MHC-II immunostaining, but the treatment did not affect microglia soma size, used here as a marker of cell activation, suggesting that the single LPS injection did not activate microglia.

Lower levels of IL-6, IFN-γ and IL-10 were seen in LPS-LPS-treated and PBS-LPS-treated females compared to males, regardless of genotype. In particular, LPS-LPS-treated and PBS-LPS-treated transgenic females showed lower levels of IFN-γ, compared to the vehicle-treated group. Indeed, many investigators showed that repeated LPS administrations induced endotoxin tolerance, reducing the production of pro-inflammatory cytokines and promoting the anti-inflammatory immune response (Biswas and Lopez-Collazo, 2009, Monneret et al., 2008). On the other hand, it was also shown that a repeated high dose of systemic LPS injection (3 mg/kg) could induce an increase in both pro- and anti-inflammatory cytokine in the brain 4 hours after the last LPS injection (Erickson and Banks, 2011). An *in vivo* study using 3-month old APP23 mice, showed that repeated LPS injections (500μg/kg) reduced pro-inflammatory cytokines levels in the serum, while

increasing their levels in the brain, 3 hours after the last injection (Wendeln et al., 2018). Wendeln et al., also showed a marked increase of IL-10 in serum after 2 LPS injections (Wendeln et al., 2018). Levels of the anti-inflammatory cytokine IL-10 have been reported elevated in many studies investigating LPS tolerance after repeated endotoxin injections (Biswas and Lopez-Collazo, 2009, Monneret et al., 2008, Wendeln et al., 2018). Here, a double LPS challenge did not increase in IL-10 plasma levels, but a reduction in IFN-γ plasma levels was observed. IFN-γ has been shown to mediate the hypersensitivity to LPS (Freudenberg et al., 2001), suggesting that low levels of IFN- γ are related to the tolerance response. Indeed, the faster recovery of females from the second challenged is associated with decreased levels of pro-inflammatory cytokines.

Immunostaining analysis showed that PBS-LPS-treated APPswe/PS1ΔE9 females and wild-type animals had greater microglia density in the cortex, compared to controls. It suggests that the single LPS challenge induced a possible activation or proliferation of microglia after 7 days. Indeed, a previous investigation demonstrated that LPS, given at a higher dose (0.33 mg/kg, i.p), increased hippocampal microglial numbers in mice brains, 4 hours after the injection (Chen et al., 2008).

Analysis of amyloid plaque changes in response to LPS, revealed that both the single and double injection of LPS significantly affected amyloid plaque load in the hippocampus and cortex. An increase in plaque accumulation was expected with repeated exposure to LPS, as a previous investigation showed that LPS (500µg/kg of body weight, i.p), given once a week for 12 weeks, induced an increase in the

levels of APP, $A\beta_{40}$ and $A\beta_{42}$, as well as β-secretase activity (Sheng et al., 2003). This report suggested involvement of LPS-induced inflammation in Aβ production. Moreover, repeated injections of LPS (250μg/kg, 3 or 7 times) have been shown to increase the accumulation of $A\beta_{1\text{-}42}$ in the hippocampus and cerebral cortex, through increased β- and γ-secretase activities and generation of Aβ1-42 (Lee et al., 2008). A single systemic administration of LPS (10 mg/kg) was also shown to induce an increase in soluble Aβ in the brain that remained higher than control until 7-9 days post LPS (Wang et al., 2018). Interestingly, a recent study that used 3-month old APP23 mice reported that 6 months after a single LPS injection (500μg/kg) both amyloid plaque load and Aβ levels increased, while decreased after 4 consecutive LPS injections. In the present study, data revealed that a single LPS injection showed a trend to increase the number of amyloid plaques in the cortex of transgenic females, but it did not appear to be significant. Adding more animals to the study might be necessary to show a significant plaque increase.

Females, once again, showed a higher number of plaques compared to males, as seen in the study described in chapter 4. Previous investigations (Wang et al., 2003b, Callahan et al., 2001, Sykova et al., 2005) demonstrated that female mice showed higher age-dependent increase in the number of amyloid plaques compared to age-matched males. In particular, analysis of plaques sizes showed that LPS-LPS-treated and PBS-LPS-treated females had smaller plaques than males in the cortex. Another study reported that smaller plaques exhibited a more prominent rate of growth compared to larger plaques, regardless of age, at the early stage of the pathogenesis (Yan et al., 2009b). However, here, transgenic females did not show a rapid growth of small plaques as no differences were

observed in the size of medium and large plaques post-treatment. Thus, LPS may be limiting the growth of the small plaques.

Interestingly, a recent study elucidated a dual role of IL-10 in APPswe/PS1ΔE9 mice deficient in IL-10, where lack of IL-10 was correlated to an increase in microglial phagocytosis of Aβ (Guillot-Sestier et al., 2015). A significant conclusion on the effect of low levels of IL-10 on the beneficial phagocytic role towards Aβ could have been drawn, in the present study, from the analysis of intracellular Aβ in resident microglia and infiltrated macrophages. However, the presence of intracellular Aβ was also seen in wild-type mice, limiting interpretation of the data. As explained also in the previous chapter (chapter 4), 6E10 anti-Aβ antibody, used here to identified intracellular Aβ, was found unable to distinguish intracellular Aβ from AβPP by another researcher (Aho et al., 2010) and also able to bind proteins that are not derived from APP in wild-type mice (Teich et al., 2013). This non-specific binding was not expected as the 6E10 antibody is widely used to detect human Aβ in APPswe/PS1ΔE9 mice (Ruan et al., 2009, Kuhla et al., 2017)

Analysis of microglia response to LPS revealed that APPswe/PS1ΔE9 females, that received two challenges of LPS, showed higher microglia density in both the hippocampus and cortex compared to vehicle-treated animals. In accordance with this finding, a previous study showed that repeated LPS injections, given at a relative low dose (1 mg/kg, *i.p*) for four consecutive days, induced an increase in the area occupied by microglia and microglia proliferation in the DG region of the hippocampus, 24h after the last injection (Chen et al., 2012). Increased numbers of microglia cells were only seen in transgenic females, here. Interestingly, this group of mice also showed significant smaller plaques compared to males after the single

and double injection, as described above. Considering that microglia play an important role in limiting plaque expansion (Zhao et al., 2017a), LPS injections might have stimulated microglia to proliferate in order to limit the growth of existing small plaques. This hypothesis is supported by decreased levels of IFN-γ found here, in transgenic females. Indeed, a previous study demonstrated the INF-γ-dependent increase of Aβ production, showing that Tg2576 mice knocked out for the IFN-γ receptor had reduced amyloid plaques than the controls animals (Yamamoto et al., 2007). Furthermore, a recent study also showed that repeated injections of LPS induced microglia to migrate towards the site of the injury becoming neuroprotective, and reducing the size of the lesion (Chen et al., 2014).

Analysis of the astrocytes response revealed that a single or double injection of LPS had no effect, regardless of sex and genotype. However, analysis of GFAP clusters in the cortex showed a sex and genotype differences, also seen in chapter 4. A greater density of GFAP clusters was seen in transgenic females, compared to the male counterpart and in transgenic animals compared to wild-type mice. A previous report showed the formation of GFAP cluster in APPswe/PS1dE9 mice at around 6 months of age (Ruan et al., 2009), while in the present study it was demonstrated that astrocytes clusters appeared at around 5 months of age in the cortex of APPswe/PS1dE9 mice.

Flow cytometry analysis revealed that females had a reduced number of resident microglia cells, marked as $CD11b^{+}CD45^{+Lo}$, compared to males, regardless of treatment. However, from the analysis of Iba-1 staining, the opposite was observed, with a higher number of Iba-1 immunoreactive cells in wild-type female mice. This contradictory result might be explained as Iba-1 is known to also stain

macrophages (Bennett et al., 2016), suggesting that the higher number of Iba-1 positive cells observed in wild-type females could include both microglia and macrophages cells. However, analysis of infiltrated macrophages did not show any significant difference between experimental groups.

A lower expression of CCR2 was observed in resident microglia in wild-type females. An *in vitro* study showed downregulation of the chemokine receptors CCR2 on human monocytes exposed to LPS (Biswas and Lopez-Collazo 2009), but here no treatment effect was seen in CCR2 expression levels. Another *in vivo* investigation revealed that CCR2 knockout mice, had macrophages with impaired phagocytic function with a decrease in pro-inflammatory cytokine levels, suggesting that CCR2 knockout mice are more susceptible to infection (Mack et al., 2001). Indeed, wild-type females here also showed a decrease in pro-inflammatory cytokines IL-6 and IFN-γ as a sign of endotoxin tolerance and higher susceptibility to infection. Low levels of CCR2 in resident microglia might be involved in the development of tolerance to LPS. To the best of the current knowledge, no research has been done to clarify the role of CCR2 in the development of endotoxin tolerance, but higher levels of its ligand CCL2 have been found in studies on endotoxin tolerance (Biswas and Lopez-Collazo, 2009, Rajaiah et al., 2013).

Analysis of the immune phenotype of resident microglia revealed higher expression of CD80 (M1 marker) in the hippocampus of transgenic females compared to transgenic males, regardless of treatment. An *in vivo* study showed that repeated injections of LPS (1.0 mg/kg, four times daily, i.p), induced anti-inflammatory phenotype, with no alteration in M1 genes (Chen et al., 2012). However, higher expression of the pro-inflammatory marker in transgenic females can be related to the presence of amyloid plaques, as microglia activation was seen increased with

age, along with amyloid deposition in brain tissue of mouse model of AD (Gordon et al., 2002).

In conclusion, the present study showed that inflammation, due to repeated LPS injections, induced an increase in the number of microglia cells, a reduction of IFN-γ and a reduction in the size of small amyloid plaques in the cortex of APPswe/PS1ΔE9 females. These changes were associated with improvement in spatial working memory seen in these animals. This finding leads to the hypothesis that LPS-induced proliferation of microglia may be limiting the growth of small plaques. Transgenic females also showed higher expression of the M1 marker on resident microglia, which may be linked to the microglia response to amyloid plaques. Further study needs to clarify how the systemic inflammation can modulate activation of microglia and migration of infiltrated macrophages into the brain to induce a beneficial immune response.

CHAPTER 6

General discussion and future direction

The overall aim of the study was to investigate the impact of a systemic inflammation on hippocampal-dependent behaviour, central and peripheral immune response as well as amyloid plaque load, at an early stage of amyloid pathology, focusing on genotype and sex differences.

LPS, administered systemically at a low dose of 100µg/kg, was used to modulate the immune response, and to determine the effect of a single and double immune challenge on behaviour, as well as central and peripheral immune response. 4.5 months old APPswe/PS1ΔE9 and wild-type mice, both males and females, were investigated. Three different time points were considered to examine these effects: 4 hours, 7 days and 3 weeks after the first LPS administration. These studies were planned based on the following hypothesis:

- The 4-hour time point tested the hypothesis that APPswe/PS1ΔE9 mice were more susceptible to the immune challenge than wild-type mice, with more focus on sex-dependent susceptibility (chapter 3).
- The 7-day time point tested the hypothesis that a single systemic LPS challenge would exacerbate glial response and amyloid plaque load in APPswe/PS1ΔE9 mice at 4.5 months (chapter 4) and 5 months (chapter 5) of age.
- The 3-week time point tested the hypothesis that two challenges of LPS would reduce the levels of pro-inflammatory cytokines with further accumulation of amyloid plaques in APPswe/PS1ΔE9 mice.

Summary of the main LPS effects

The main LPS effects found in these studies are summarized in Table 8.

LPS induced an increase in the pro-inflammatory cytokines IL-6 and TNF-α, as well as an increase in the anti-inflammatory cytokine IL-10 after 4 hours, proving that the dose of 100μg/kg does activate the immune system.

LPS increased in TNF-α plasma levels only in females. Within the female mice, wild-types showed higher IL-6 plasma levels compared to the trangenic group. TNF-α and IL-6 are both pro-inflammatory cytokines, suggesting that wild-type females showed higher susceptibility to the immune challenge.

Differences between genotypes were not observed in response to the immune challenge at longer time points. LPS induced an increase in the number of microglial cells associated with a reduction in the levels of IFN-γ in the plasma in APPswe/PS1ΔE9 females challenged at 5 months of age, after 7 days. An improvement in spatial working memory LPS-mediated was also seen in these mice.

A single systemic LPS challenge induced an increase in the number of microglial cells also in APPswe/PS1ΔE9 males and females challenged at 4.5 months of age, after 7 days.

Two challenges of LPS showed reduction in IFN-γ plasma levels in APPswe/PS1ΔE9 females, 7 days after the last injection, associated with increased microglia density in the brain. Increased development of tolerance was suggested in APPswe/PS1ΔE9 female mice.

Unexpectedly, LPS didn't affect the infiltration of peripheral macrophages into the brain and the expression of the phenotypic markers in any of the studies.

Table 8. Summary of the main treatment effects in all the experimental time points.

	TREATMENT EFFECTS			
	SINGLE INJECTION			**TWO INJECTIONS**
AGE AT THE TIME OF LPS INJECTION	**4.5 MONTHS OLD**		**5 MONTHS OLD**	**4.5 MONTH OLD**
TIME-POINT	**4 HOURS**	**7 DAYS**	**7 DAYS**	**3 WEEKS**
BEHAVIOURAL TESTS	–	↑ Food burrowing in APP/PS1 males	–	↑ Spatial working memory in APP/PS1 male and females mice
AMYLOID PLAQUE LOAD	N/A	Tendency to **reduce** the number of plaques in the hippocampus of APP/PS1 females	Tendency to **increase** the number of plaques in the cortex of APP/PS1 females	NS
CYTOKINE LEVELS	↑ IL-6 ↑ IL-10 ↑ TNF-α (females only)	–	↓ IFN-γ in APP/PS1 females	↓ IFN-γ in APP/PS1 females
NUMBER OF IBA-1 IMMUNOREACTIVE CELLS/MM²	–	↑ APP/PS1 males (hippocampus) ↑ APP/PS1 females (hippocampus)	↑ APP/PS1 females (cortex) ↑ WT males (cortex) ↑ WT females (cortex)	↑ APP/PS1 females
RESIDENT MICROGLIA $CD11b^{+}CD45^{+HI}$	N/A	↓ APP/PS1 males (cortex)	–	–

LPS administered systemically does not cross the BBB, and only 0.025% of the dose injected was estimated to reach the brain (Singh and Jiang, 2004, Chakravarty and Herkenham, 2005, Banks and Robinson, 2010). However, in these studies I have demonstrated that LPS increased the number of Iba-1 immunoreactive cells, several days after the treatment, supporting the conclusion from previous findings (Cunningham et al., 2009, Cunningham et al., 2005, Perry et al., 2007, Holmes et al., 2009) reporting that the peripheral immune challenge have an impact on the

central immune system. The immune response in the periphery communicate with the brain through cytokine signalling, in particular IL-1β, IL-6 and TNF-α cytokines are able to cross the BBB inducing the inflammatory response in the CNS (Pan et al., 2011). In this study IL-1β levels in the plasma were not altered by the immune challenge at any time points. IL-6 and TNF-α plasma levels were elevated after 4 hours, but not at longer time points. These cytokines were not seen elevated in plasma but their levels can be higher in the brain. Further analysis is needed to elucidate cytokines response in the brain and evaluate if decreased levels in the periphery correlate to higher levels in the CNS.

Opposite effects of LPS on amyloid plaque load.

LPS did not significantly affect the amyloid plaque load in any of the time point chosen in these studies. However, data showed an opposite trend of LPS-induced amyloid plaque changes 7 days after a single challenge, close to being significant. LPS-treated APPswe/PS1ΔE9 females, challenged at 4.5 months of age (chapter 4) (called *younger* mice from now on), showed a reduction in the total number of plaques in the hippocampus (p=0.067). On the other hand, PBS-LPS-treated APPswe/PS1ΔE9 females, challenged with LPS at 5 months of age (chapter 5) (called *older* mice from now on), showed an increase in the total number of plaques in the cortex (p=0.07).

In this study *younger* and *older* mice underwent the same behavioural test at baseline. However, *older* mice received a PBS injection before being challenged with LPS, contrary to the *younger* animals that received only a singles LPS injection. Moreover, *older* mice had to be weighted every day between the PBS and LPS injections, and also underwent an extra food burrowing test, the night before the

immune challenge. The handling of the animals and the behavioural stress might have influenced the response to LPS seen in *older* animals. Indeed, stress is known to increase susceptibility to infections (Dhabhar, 2009). Growing evidence indicates that physical stressors may activate the hypothalamic-pituitary-adrenal (HPA) axis, accelerating the progression of AD (Dong and Csernansky, 2009). Activity of the HPX axis can be measured by analysis of the plasma cortisol levels (Csernansky et al., 2006). An in-vivo study revealed that chronic stress impacted the LPS-induced activation of microglia: rats exposed to behavioural stress for 9 consecutive days, showed an enhanced microglia activation 24h after LPS injection, compared to non-stressed animals (Espinosa-Oliva et al., 2011). Another in-vivo study on Tg2576 mice, an amyloidogenic mouse model of AD, showed that social stress, induced by isolation of the mice for 6 months, accelerated plaque deposition (Dong and Csernansky 2009). Stressed Tg2576 mice revealed more Aβ plaques in cortex and hippocampus, compared to unstressed mice (Dong and Csernansky, 2009). Influence of stress on plaque deposition was found to be dependent on the levels of Aβ (Dong et al., 2004). These findings support the hypothesis that LPS effects on amyloid plaque load might be influenced by stress. Moreover, an in-vivo study showed that stress, before an LPS challenge, suppressed both mRNA and proteinIFN-γ levels in the serum (Curtin et al., 2009), suggesting dysregulation of cytokine production mediated by stress. Indeed, in this study IFN-γ levels were reduced in the transgenic females.

The effects of the infection is also age-dependent, indicating that inflammation can affect disease progression differently in old and young animals (Shaw et al., 2013). It is well documented that, in aged animals, microglia are primed and their immunomodulatory response is compromised (Norden and Godbout, 2013,

Williams et al., 2015), thus, even moderate doses of LPS could exacerbate the existing pathology in old animals. Association between microglia and amyloid plaques is also reduced by aging, suggesting that an activation of microglia cells at early stage, can be beneficial for Aβ removal in young animals (Wyss-Coray, 2006). In this thesis *younger* and *older* animals had only two weeks difference. However, an in-vivo imaging study reported that new plaques are formed within 2 days, with recruitment of microglia to the site of the plaque (Meyer-Luehmann et al., 2008). This study suggests that the formation of new amyloid plaques and growth of existing plaques might occur in 2 weeks. Indeed, data from this thesis showed that *younger* transgenic females used as a control had 3.14 $\pm$ 0.23 mean number of plaques in the hippocampus and 3.8 $\pm$ 0.71 mean number of plaques in the cortex. *Older* control female mice had 4.16 $\pm$ 0.43 and 5.16 $\pm$ 0.84 mean number of plaques in hippocampus and cortex respectively, confirming the increase number of plaques within the 2 weeks, especially in the cortex. However, herein, microglia cluster density did not differ between young and old animals. Further studies are needed to assess the age-dependent microglia response to amyloid plaques, investigating whether microglia migration towards the plaque is impaired. Further study needs to be done to analyse the morphological activation of microglia around the plaques and clarify the interaction between growing plaques and microglia response. One previous study that analysed the initialization of microglial interaction with small plaques in APP/PS1ΔE9 mice showed that there are different levels of microglia interaction with newborn plaques and one-fifth of the plaques analysed were not even found in association with microglia (Jung et al., 2015). This study suggested that microglia response to the increase in plaque progression may vary.

Analysis of infiltrated macrophages in the brain, investigated to clarify a possible mechanism of Aβ clearance mediated by these cells, did not show any treatment effect in both of the studies. Infiltrated microphages showed the presence of intracellular Aβ, suggesting phagocytic activity mediated by these cells, but the antibody used in this thesis showed significant non-specific staining, thus, a further investigation is needed to clarify the binding properties of this antibody. For example, a western blot technique might be a useful tool to evaluate the binding and compare it with other specific antibodies directed to the C-terminal of the Aβ peptide (i.e., Aβ40, Aβ42, and 12F4), instead of the N-terminal (6E10), as suggested by Aho et al. (Aho et al., 2010).

Effect of LPS on microglia function

LPS did not affect microglia response after 4 hours. However, after 7 days, LPS induced increase of microglia density in *younger* APPswe/PS1ΔE9 males and females, as well as in *older* APPswe/PS1ΔE9 females. Interestingly, LPS seemed affecting amyloid plaque growth in *older* mice only, after 7 days. Analysis of the area of the plaques revealed that LPS significantly reduced the size of small plaques in *older* APPswe/PS1ΔE9 females. This reduction was associated to higher proliferation of microglia cells in LPS-treated *older* APPswe/PS1ΔE9 females, suggesting a role of microglia in limiting the growth of existing small plaques (Zhao et al., 2017a). In-vivo imaging studies that monitored the growth of the amyloid plaques over several weeks revealed that small, or newly formed, plaques grew at a faster rate than large plaques (Burgold et al., 2011, Yan et al., 2009b). Plaque growth was monitored in both APPswe/PS1ΔE9 females and males, but the study didn't distinguish between the sexes (Yan et al., 2009a). Data from these studies also suggested that the reduced size of the small plaques, seen in *older* mice, could

be due to limited growth, but the trend in reduced number of plaques, seen in *younger* mice, might be related to increased clearance.

Effects of LPS on plasma cytokine levels

Interestingly, no effects of LPS were observed in plasma cytokine levels in younger APPswe/PS1ΔE9 females, where a reduction of amyloid plaques was almost significant. On the other hand, LPS induced reduction of circulating IFN-γ levels in older APPswe/PS1ΔE9 females, where an increase of amyloid plaque load was close to be significant. The decrease in pro-inflammatory cytokine IFN-γ, was often associated to higher susceptibility to infection (Cavaillon et al., 2003), suggesting that an enhanced response to LPS might be mediated by low levels of this cytokine. It needs to be considered, however, that cytokines levels in the periphery do not reflect the neuroinflammatory response in the brain (Fu et al., 2014, Qin et al., 2008). Pro-inflammatory cytokine induction in serum is an acute and transient event that subsides by one week (Qin et al., 2008), while cytokines in the brain are regulated in a cascade of event, with feedback loops, that can enhanced their response in the CNS for longer time (Kronfol and Remick, 2000).

The relationship between cytokine signaling and Aβ accumulation is not well understood, but these results seem to suggest that reduced levels of pro-inflammatory cytokines in plasma, IFN-γ in particular, might influence Aβ production. Indeed, an *in vivo* study demonstrated the IFN-γ-dependent increase of Aβ production (Yamamoto et al., 2007a). A further analysis on brain cytokines levels might give a better understanding of the central cytokine response to LPS in APPswe/PS1ΔE9 females after 7 days.

LPS effects on infiltrated macrophages

LPS did not significantly induce infiltration of peripheral macrophages in the brain. However

LPS-treated transgenic males showed reduced number of resident microglia analysed by the flow cytometry technique, but increased number of microglia cells stained by Iba-1. This contradictory finding does suggest that iba-1 stained also infiltrated macrophages in the brain and that LPS did affect the infiltration. However, no significant effect were seen in the

expression of the CCR2 marker, in response to LPS. Thus, further investigation of the CCR2 ligand expression, CCL2, would also be needed to elucidate the function of the infiltrated macrophages. Indeed, CCL2 was seen responsible for the phenotypic shift of the mononuclear cells towards the anti-inflammatory phenotype (Roca et al., 2009) and the Aβ uptake from microglia and macrophages (Kiyota et al., 2009).

Interestingly, a new marker to identify resident microglia in the brain has been found. For many years microglia has been analysed using the Iba-1 antibody, but it is known that Iba-1 also stains infiltrated macrophages in the brain (Bennett et al., 2016), suggesting that this marker is not selective for microglia only. To better understand microglia response to immune challenges, a new antibody has been found to be selective. The transmembrane protein 119 (TMEM119) (Bennett et al., 2016) is a cell-surface protein highly expressed on microglia, but not on recruited macrophages, and it can be used as a specific marker in both mouse and human to better understand microglia function in disease and healthy brains. TMEM119 can be used for immunostaining and flow cytometric analysis to distinguish also the non-activated microglia cells (Zrzavy et al., 2017). TMEM119 can also be usefull to further characterize the phenotype of the microglia surrounding plaques.

Sex differences in LPS-induced amyloid plaque changes.

Data from this thesis showed that sex plays an important role in the pathogenesis of AD.

Transgenic females showed higher number of plaques than males in all the studies investigated herein. In-vivo studies reported that the higher number of plaques revealed in transgenic females are due to the higher Aβ40 and the A42 production in the brain, compared to males (Wang et al., 2003b, Carroll et al., 2010). Interestingly, changes in amyloid plaque load mediated by LPS were seen only in females, and not in males. This may be due to the difference in hormonal levels that might influence the immune response, reported to be also sex-dependent (Simpkins et al., 2009). The response in females is affected by estrogen levels. Low levels of estrogens, instead, are considered a risk factor to Alzheimer's disease, and previous epidemiological studies reported that an estrogen-replacing therapy could potentially reduce the risk to develop AD (Zec and Trivedi 2002). It is important to note that clinical studies have observed a similar prevalence of the disease in males and females at the early stages of AD (Nyarko et al., 2018). A previous study showed that high concentration of estrogens have been effective in reducing Aβ levels in the brain (Xu et al. 2006). Another study have demonstrated the ability of estrogens to promote microglial phagocytosis of Aβ: estrogen-treatment on cultured microglia derived from human cortex was shown to improve uptake of Aβ, through activation of estrogens receptor-α and –β (Li et al., 2000). In another study, 17β-estradiol increased both uptake and degradation of Aβ in cultured murine microglial (Harris-White et al., 2001).

Understanding the mechanism behind sex differences is important in order to investigate whether high levels of estrogen impacted amyloid plaque changes and

microglia response at early stage of amyloid pathology, seen in this study. Possible in-vivo experiments could include androgenized females, or could use a controlled delivery of estradiol in both males and females, to examine whether the response to LPS is mediated by high or low levels of the female hormone.

Genotype susceptibility to the immune challenge.

Finally, LPS did not reveal higher susceptibility to the immune challenge in APPswe/PS1ΔE9 mice compared to wild-type mice. As described in chapter 3, lower numbers of microglial cells could be associated with a lower susceptibility to an immune challenge (Kim et al., 2000), while higher microglia density and pronounced pro-inflammatory response could be

associated to increased susceptibility (Pintado et al., 2011). 4 hours after LPS challenge,

higher levels of the pro-inflammatory cytokine IL-6 were seen in wild-type females compared to transgenic females, suggesting higher susceptibility to the acute systemic LPS in wild-type females. Moreover, a greater increase in anti-inflammatory cytokine IL-10, mediated by LPS, was also revealed in wild-type females 4 hours after the injection. This data also suggested higher susceptibility to the infection in these animals. However, LPS did not affect microglia response after 4 hours. Interestingly, LPS induced an increase in microglia density in younger APP/PS1ΔE9 males and females in the hippocampus, and in older APP/PS1ΔE9 females in the cortex, after 7 days. These results suggest that genotype susceptibility to an acute systemic LPS challenge might be developed after longer-time points.

Concluding remarks

Results showed in this thesis, indicate that inflammation plays a role in modulating microglia activation and amyloid plaque deposition. Macrophages do infiltrate the brain, but a further investigation needs to be undertaken to clarify their role in early stage of amyloid plaque load. Peripheral monocytes recruited into the brain are able to significantly phagocyte aggregated Aβ, contrary to resident microglia (Simard et al., 2006a). Further analysis to examine the selective migration of these cells and the possibility to manipulate their migration towards Aβ plaque deposition makes these cells optimal target for the development of therapeutically compound. Moreover, the present study focused on investigating the role of a systemic challenge of LPS in APPswe/PS1ΔE9 mice, characterized by the overproduction of Aβ. However, NFTs are not present in this animal model. Thus, further studies could be done to investigate the role of a systemic challenge of LPS using a triple transgenic mouse model of AD that is characterized by both amyloid plaque deposition and tau hyperphosphorylation, with focus on sex differences.

CHAPTER 7

Appendix

7.6 Behavioural changes 4 hours post-LPS

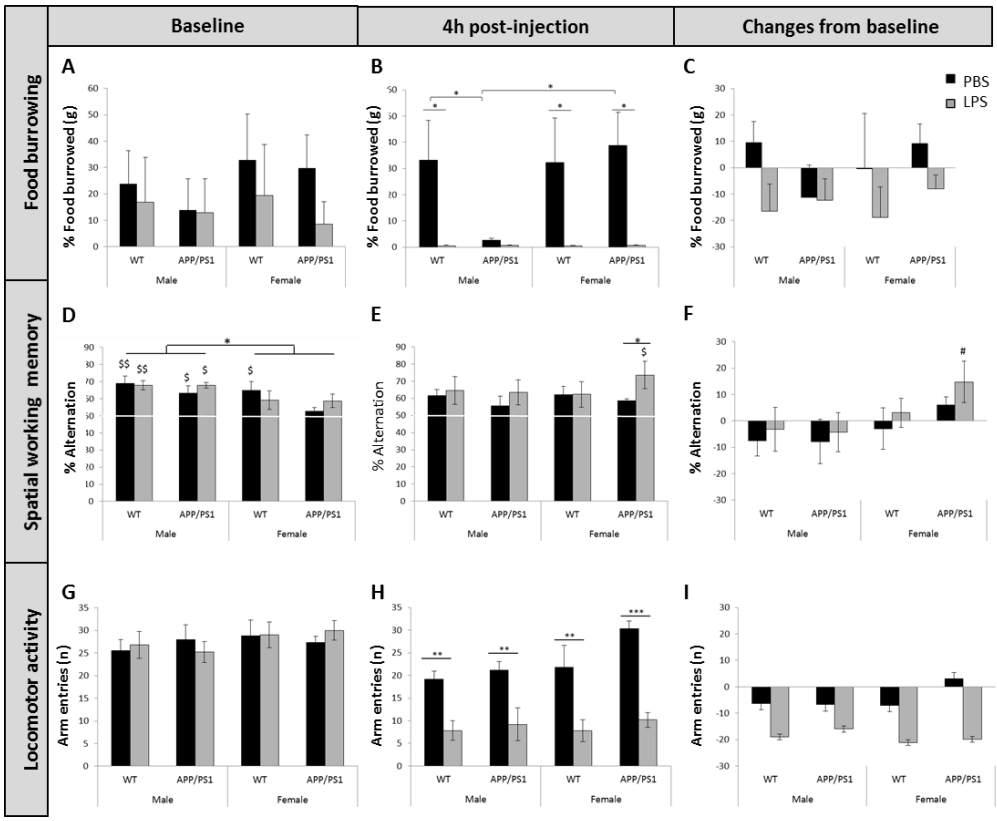

Figure 75. **LPS effects on behaviour at baseline and 4 hours post injection.** 4.5 months old male and female mice APPswe/PS1ΔE9 (APP/PS1) and wild-type (WT) (n=5/6 per group) were treated with LPS or vehicle (PBS). Behaviour was assessed before and 4h post-treatment. Post-injection data showed that 4 hours post injection LPS-treated animals burrowed less food ($p<0.05$) (**B**) and moved less ($p<0.005$) (**H**) than PBS-treated mice. Analysis of the alternation rate revealed that LPS-treated APP/PS1 females performed better than PBS-treated APP/PS1 females ($p=0.0322$) (**E**). Changes in performance were calculated by subtracting the post-injection data from the baseline data. LPS-treated APP/PS1 females showed an improvement in performance ($p=0.0275$) (**F**). Data are shown as mean ± S.E.M. [* $p< 0.05$, ** $p< 0.005$, *** $p<0.0001$]

7.7 Peer-review publications

1) **Novel Methods for Microglia Segmentation, Feature Extraction and Classification** Ding Y. Pardon MC, **Agostini A**, Faas H, Duan J, Ward WO, Easton F, Auer D, Bai L. IEEE/ACM Trans Comput Biol Bioinform, 2016.

2) **Magnetic Resonance Spectroscopy discriminates the response to microglial stimulation of wild-type and Alzheimer's disease models**. Pardon MC, Yanez Lopez M, Yuchun D, Marjańska M, Prior M, Brignell C, Parhizkar S, **Agostini A**, Bai L, Auer DP, Faas HM. Scientific Reports 6, Article number: 19880 (2016).

7.8 Data presented at conferences

1. **Unaltered susceptibility to neuroinflammation in pre-symptomatic APPswe/PS1ΔE9 mice, focus on genotype and sex differences,** was presented as a poster (Figure 76) at the British Association for Phsycopharmacology (BAP) Summer Meeting in Bristol (UK) (26-29 July 2015).

Abstract accepted:

Unaltered susceptibility to neuroinflammation in pre-symptomatic APPswe/PS1ΔE9 mice, focus on genotype and sex differences.

Introduction Alzheimer's disease is a progressive brain disorder characterized by amyloid plaques and neurofibrillary tangles and is more prevalent in women. Neuroinflammation is one of the main events responsible for the cognitive decline and involves the activation of microglia and astrocytes. Lipopolysaccharide (LPS) is used to trigger acute neuroinflammation response through the binding to the microglial exclusive toll-like receptors-4 (TLRs4) and is associated with a transient sickness syndrome. We assessed the susceptibility of Alzheimer's disease (AD)

mouse model to LPS by analysing daily living activity, locomotor activity, spatial working memory and glial cells activation 4 hours post-injection, with a particular focus on sex differences.

Methods 4.5 month-old female (n=12) and male (n=10) APPswe/PS1ΔE9 and wild-type (WT) littermates (n=12 males and 10 females) were used in the study. Sickness syndrome was assessed using the food burrowing test, and the spontaneous alternation test was used to measure locomotor activity and spatial working memory. Baseline behavioural performance was evaluated on on the first two days of the experiment. On Day 3, mice received an injection of LPS (100µg/kg, *i.v.*) or vehicle (PBS) and were assessed behaviourally 4 hours later. Immediately after brain tissue was collected for immunostaining of Iba-1 and GFAP to assess microglia and astrocytes density and activation, respectively. The data were analysed with two-way ANOVA with repeated measures followed Tukey's post hoc analysis where appropriate.

Results LPS suppressed food burrowing ($p=0.0054$) and locomotor activity ($p<0.001$) regardless of genotype or sex, while an improvement in spatial working memory was evident in LPS treated APPswe/PS1ΔE9 female only ($p= 0.0322$). LPS had no effect on microglia and astrocytes, but a higher microglia density in CA2 ($p=0.0253$), CA3 ($p=0.0005$) and DG ($p=0.0233$) and lower microglia activation ($p=0.019$) were observed in APPswe/PS1ΔE9 female compared to wild-type female. In addition, wild-type female showed reduced microglial density in CA3 ($p=0.044$) and DG ($p=0.009$) but higher microglia activation compared to wild-type male ($p=0.0209$)

Conclusion These data show that 100ug/kg LPS did not reveal a higher susceptibility of APPswe/PS1ΔE9 mice compared to wild-type mice, regardless of sex. Indeed, LPS induced suppression of daily living and locomotor activity to a similar extent in both genotypes and sex. But improvement in spatial working memory was observed in APPswe/PS1ΔE9 female, suggesting a beneficial effect of microglia stimulation. Further work needs to be done to clarify the mechanisms underlying this beneficial effect of microglia on behaviour, in response to an immune challenge.

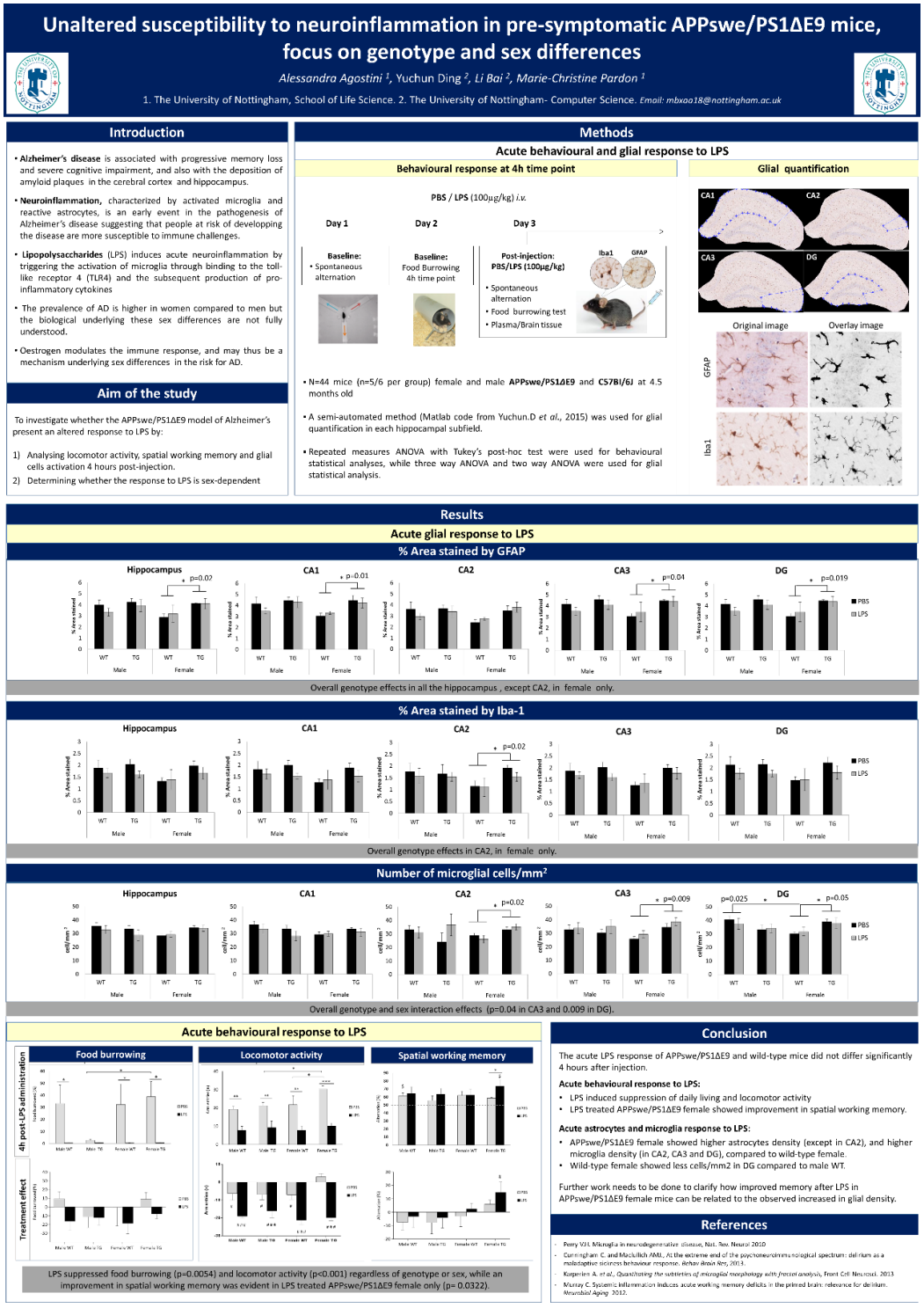

Figure 76. Poster presented at British Association for Phsycopharmacology (BAP) Summer Meeting in Bristol (UK) (2015).

2. **Systemic infection age- and sex-dependently reduces amyloid plaque load in APPswe/PS1ΔE9 mouse model of Alzheimer's disease,** was presented as a poster (Figure 77) at the Keystone Symposia on Neuroinflammation in Keystone in Colorado (USA), 19th-24th June 2017.

Abstract accepted:

Systemic infection age- and sex-dependently reduces amyloid plaque load in APPswe/PS1ΔE9 mouse model of Alzheimer's disease.

Systemic bacterial infection can worsen Alzheimer's disease (AD) progression by compromising the central microglia and astrocyte immune responses implicated in the clearance of amyloid-β (Aβ) plaques, one of the AD hallmarks. Here we investigated whether systemic infection with lipopolysaccharide (LPS) increases Aβ plaque load and glial activation, and whether tolerance occurred following repeated LPS injections.

4.5month-old females and males, APPswe/PS1ΔE9 and wild-type littermates were used (n=4/group). In the first experiment, mice were injected with LPS (100µg/kg, *i.v*) or vehicle (PBS) and brain tissue was collected 7 days later. In the second experiment, mice received a LPS or PBS injection at 4.5months of age, and a second challenge 2 weeks later, yielding the following experimental groups: PBS-PBS, PBS-LPS, LPS-LPS. Quantification of amyloid plaque load, microglia, and astrocytes clusters and density were assessed by immunostaining of Aβ, Iba-1 and GFAP, respectively, in cortex and hippocampus. Data were analysed with two and three-way ANOVA followed by post-hoc analysis.

Number of Aβ plaques and associated glial clusters, that surround plaques, were higher in females than males. A single LPS challenge reduced the numbers of both total and large plaques ($p<0.05$) in the hippocampus of 4.5 months-old females, but not in older female (PBS-LPS group) or males. This was associated with an increased microglial density ($p=0.0064$) and a reduced number of microglial clusters ($p=0.0005$), compared to control mice. Aβ plaque load was unaffected by repeated LPS infection.

These data suggest that the ability of microglia to clear or restrict Aβ plaques growth after acute systemic infection is sex-dependent and diminishes with age. Further work is needed to unravel the underlying mechanisms. Female mice challenged twice did not show significant changes in plaque load, maybe due to the development of immune tolerance.

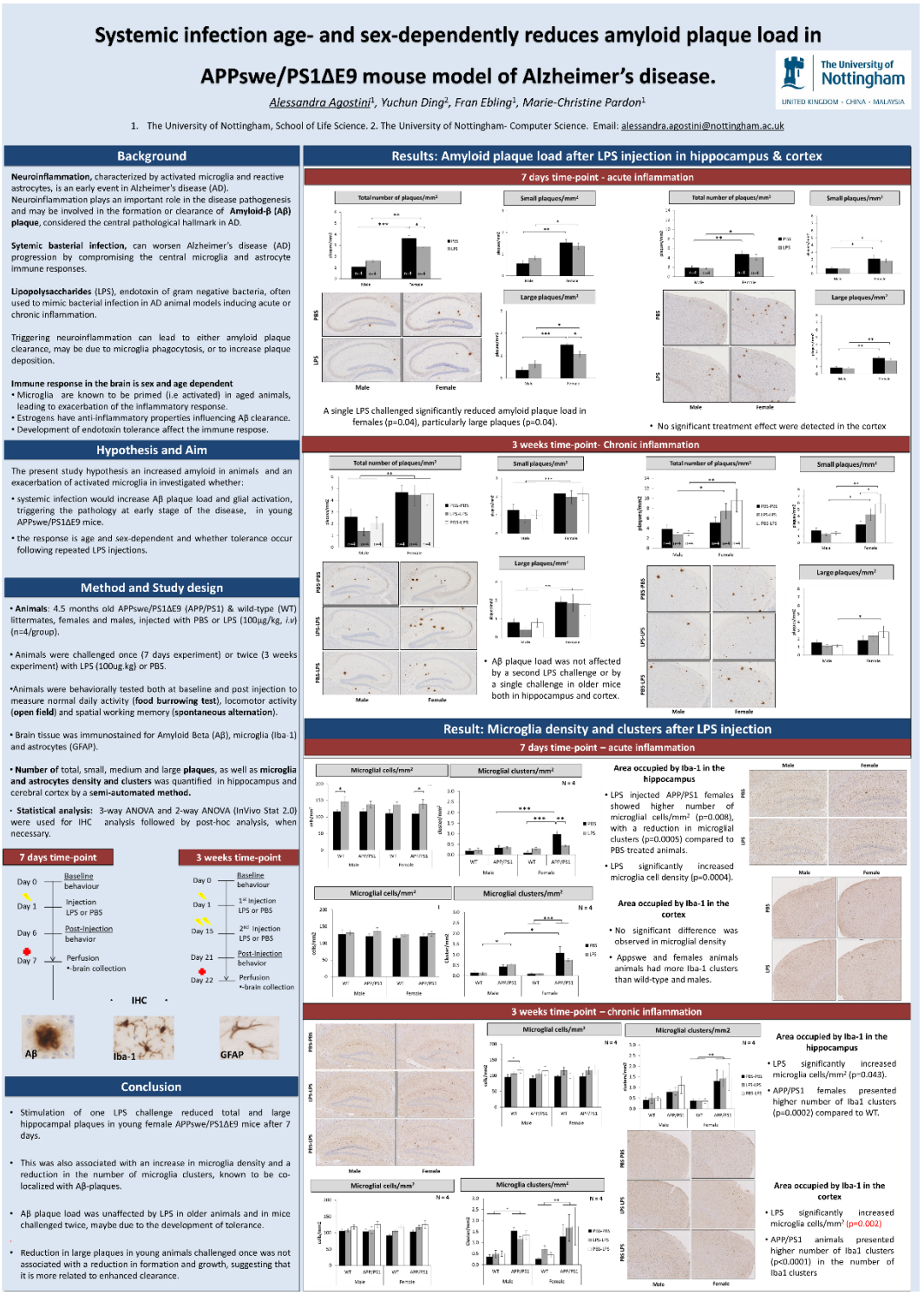

Figure 77. Poster presented at the Keystone Symposia on Neuroinflammation in Colorado (USA) (2017).

CHAPTER 8

Bibliography

AGOSTINHO, P., CUNHA, R. A. & OLIVEIRA, C. 2010. Neuroinflammation, oxidative stress and the pathogenesis of Alzheimer's disease. *Curr Pharm Des,* 16**,** 2766-78.

AHO, L., PIKKARAINEN, M., HILTUNEN, M., LEINONEN, V. & ALAFUZOFF, I. 2010. Immunohistochemical visualization of amyloid-beta protein precursor and amyloid-beta in extra- and intracellular compartments in the human brain. *J Alzheimers Dis,* 20**,** 1015-28.

AKIYAMA, H., ARAI, T., KONDO, H., TANNO, E., HAGA, C. & IKEDA, K. 2000. Cell mediators of inflammation in the Alzheimer disease brain. *Alzheimer Dis Assoc Disord,* 14 Suppl 1**,** S47-53.

ALVAREZ, J. I., KATAYAMA, T. & PRAT, A. 2013. Glial influence on the Blood Brain Barrier. *Glia,* 61**,** 1939-1958.

ANOOP, A., SINGH, P. K., JACOB, R. S. & MAJI, S. K. 2010. CSF Biomarkers for Alzheimer's Disease Diagnosis. *International journal of Alzheimer's disease,* 2010**,** 606802.

ARDEKANI, B. A., CONVIT, A. & BACHMAN, A. H. 2016. Analysis of the MIRIAD Data Shows Sex Differences in Hippocampal Atrophy Progression. *J Alzheimers Dis,* 50**,** 847-57.

ARMSTRONG, R. A. 2014. Factors determining disease duration in Alzheimer's disease: a postmortem study of 103 cases using the Kaplan-Meier estimator and Cox regression. *BioMed research international,* 2014**,** 623487-623487.

AU - RAY, A. & AU - DITTEL, B. N. 2010. Isolation of Mouse Peritoneal Cavity Cells. *JoVE***,** e1488.

AVIGNONE, E., LEPLEUX, M., ANGIBAUD, J. & NÄGERL, U. V. 2015. Altered morphological dynamics of activated microglia after induction of status epilepticus. *Journal of Neuroinflammation,* 12**,** 202.

AZIZI, G., NAVABI, S. S., AL-SHUKAILI, A., SEYEDZADEH, M. H., YAZDANI, R. & MIRSHAFIEY, A. 2015. The Role of Inflammatory Mediators in the Pathogenesis of Alzheimer's Disease. *Sultan Qaboos University Medical Journal,* 15**,** e305-e316.

BACHSTETTER, A. D., XING, B. & VAN ELDIK, L. J. 2014. The p38alpha mitogen-activated protein kinase limits the CNS proinflammatory cytokine response to systemic lipopolysaccharide, potentially through an IL-10 dependent mechanism. *Journal of Neuroinflammation,* 11**,** 175.

BANKS, W. A., GRAY, A. M., ERICKSON, M. A., SALAMEH, T. S., DAMODARASAMY, M., SHEIBANI, N., MEABON, J. S., WING, E. E., MOROFUJI, Y., COOK, D. G. & REED, M. J. 2015. Lipopolysaccharide-induced blood-brain barrier disruption: roles of cyclooxygenase,

oxidative stress, neuroinflammation, and elements of the neurovascular unit. *J Neuroinflammation,* 12**,** 223.

BANKS, W. A. & ROBINSON, S. M. 2010. Minimal penetration of lipopolysaccharide across the murine blood-brain barrier. *Brain Behav Immun,* 24**,** 102-9.

BARDOU, I., KAERCHER, R. M., BROTHERS, H. M., HOPP, S. C., ROYER, S. & WENK, G. L. 2014. Age and duration of inflammatory environment differentially affect the neuroimmune response and catecholaminergic neurons in the midbrain and brainstem. *Neurobiol Aging,* 35**,** 1065-73.

BATEMAN, R. J., MUNSELL, L. Y., MORRIS, J. C., SWARM, R., YARASHESKI, K. E. & HOLTZMAN, D. M. 2006. Human amyloid-beta synthesis and clearance rates as measured in cerebrospinal fluid in vivo. *Nat Med,* 12**,** 856-61.

BAYER A. J., BULLOCK R., JONES R. W., WILKINSON D., PATERSON K. R., JENKINS L. 2005. Evaluation of the safety and immunogenicity of synthetic Abeta42 (AN1792) in patients with AD. *Neurology* 64 94–101.

BEJANIN, A., SCHONHAUT, D. R., LA JOIE, R., KRAMER, J. H., BAKER, S. L., SOSA, N., AYAKTA, N., CANTWELL, A., JANABI, M., LAURIOLA, M., O'NEIL, J. P., GORNO-TEMPINI, M. L., MILLER, Z. A., ROSEN, H. J., MILLER, B. L., JAGUST, W. J. & RABINOVICI, G. D. 2017. Tau pathology and neurodegeneration contribute to cognitive impairment in Alzheimer's disease. *Brain,* 140**,** 3286-3300.

BELKHELFA, M., RAFA, H., MEDJEBER, O., ARROUL-LAMMALI, A., BEHAIRI, N., ABADA-BENDIB, M., MAKRELOUF, M., BELARBI, S., MASMOUDI, A. N., TAZIR, M. & TOUIL-BOUKOFFA, C. 2014. IFN-gamma and TNF-alpha are involved during Alzheimer disease progression and correlate with nitric oxide production: a study in Algerian patients. *J Interferon Cytokine Res,* 34**,** 839-47.

BEN HAIM, L. & ROWITCH, D. H. 2017. Functional diversity of astrocytes in neural circuit regulation. *Nat Rev Neurosci,* 18**,** 31-41.

BENNETT, M. L., BENNETT, F. C., LIDDELOW, S. A., AJAMI, B., ZAMANIAN, J. L., FERNHOFF, N. B., MULINYAWE, S. B., BOHLEN, C. J., ADIL, A., TUCKER, A., WEISSMAN, I. L., CHANG, E. F., LI, G., GRANT, G. A., HAYDEN GEPHART, M. G. & BARRES, B. A. 2016. New tools for studying microglia in the mouse and human CNS. *Proceedings of the National Academy of Sciences of the United States of America,* 113**,** E1738-E1746.

BERNSTEIN SL, WYTTENBACH T, BAUMKETNER A, SHEA JE, BITAN G, TEPLOW DB, BOWERS MT. 2005. Amyloid beta-protein: monomer structure and early aggregation states of Abeta42 and its Pro19 alloform. *Journal of the American Chemical Society*. 127:2075–2084. doi: 10.1021/ja044531p.

BETTENS, K., SLEEGERS, K. & VAN BROECKHOVEN, C. 2013. Genetic insights in Alzheimer's disease. *Lancet Neurol,* 12**,** 92-104.

BIBI, F., YASIR, M., SOHRAB, S. S., AZHAR, E. I., AL-QAHTANI, M. H., ABUZENADAH, A. M., KAMAL, M. A. & NASEER, M. I. 2014. Link between chronic bacterial inflammation and Alzheimer disease. *CNS Neurol Disord Drug Targets,* 13**,** 1140-7.

BIESMANS, S., MEERT, T. F., BOUWKNECHT, J. A., ACTON, P. D., DAVOODI, N., DE HAES, P., KUIJLAARS, J., LANGLOIS, X., MATTHEWS, L. J. R., VER DONCK, L., HELLINGS, N. & NUYDENS, R. 2013. Systemic immune activation leads to neuroinflammation and sickness behavior in mice. *Mediators of inflammation,* 2013**,** 271359.

BISWAS, S. K. & LOPEZ-COLLAZO, E. 2009. Endotoxin tolerance: new mechanisms, molecules and clinical significance. *Trends in Immunology,* 30**,** 475-487.

BLOOM, G. S. 2014. Amyloid-beta and tau: the trigger and bullet in Alzheimer disease pathogenesis. *JAMA Neurol,* 71**,** 505-8.

BOLMONT, T., HAISS, F., EICKE, D., RADDE, R., MATHIS, C. A., KLUNK, W. E., KOHSAKA, S., JUCKER, M. & CALHOUN, M. E. 2008. Dynamics of the microglial/amyloid interaction indicate a role in plaque maintenance. *J Neurosci,* 28**,** 4283-92.

BONARDI, C., DE PULFORD, F., JENNINGS, D. & PARDON, M.-C. 2011. A detailed analysis of the early context extinction deficits seen in APPswe/PS1dE9 female mice and their relevance to preclinical Alzheimer's disease. *Behavioural brain research,* 222**,** 89-97.

BOZA-SERRANO, A., YANG, Y., PAULUS, A. & DEIERBORG, T. 2018. Innate immune alterations are elicited in microglial cells before plaque deposition in the Alzheimer's disease mouse model 5xFAD. *Scientific Reports,* 8**,** 1550.

BRADSHAW, E. M., CHIBNIK, L. B., KEENAN, B. T., OTTOBONI, L., RAJ, T., TANG, A., ROSENKRANTZ, L. L., IMBOYWA, S., LEE, M., VON KORFF, A., ALZHEIMER DISEASE NEUROIMAGING, I., MORRIS, M. C., EVANS, D. A., JOHNSON, K., SPERLING, R. A., SCHNEIDER, J. A., BENNETT, D. A. & DE JAGER, P. L. 2013. CD33 Alzheimer's disease locus: altered monocyte function and amyloid biology. *Nat Neurosci,* 16**,** 848-50.

BRONZUOLI, M. R., IACOMINO, A., STEARDO, L. & SCUDERI, C. 2016a. Targeting neuroinflammation in Alzheimer's disease. *J Inflamm Res,* 9**,** 199-208.

BRONZUOLI, M. R., IACOMINO, A., STEARDO, L. & SCUDERI, C. 2016b. Targeting neuroinflammation in Alzheimer's disease. *Journal of Inflammation Research,* 9**,** 199-208.

BROSSERON, F., KRAUTHAUSEN, M., KUMMER, M. & HENEKA, M. T. 2014a. Body fluid cytokine levels in mild cognitive impairment and Alzheimer's disease: a comparative overview. *Mol Neurobiol,* 50**,** 534-44.

BROSSERON, F., KRAUTHAUSEN, M., KUMMER, M. & HENEKA, M. T. 2014b. Body Fluid Cytokine Levels in Mild Cognitive Impairment and Alzheimer's Disease: a Comparative Overview. *Molecular Neurobiology,* 50**,** 534-544.

BU, X. L., YAO, X. Q., JIAO, S. S., ZENG, F., LIU, Y. H., XIANG, Y., LIANG, C. R., WANG, Q. H., WANG, X., CAO, H. Y., YI, X., DENG, B., LIU, C. H., XU, J., ZHANG, L. L., GAO, C. Y., XU, Z. Q., ZHANG, M., WANG, L., TAN, X. L., XU, X., ZHOU, H. D. & WANG, Y. J. 2015. A study on the association between infectious burden and Alzheimer's disease. *Eur J Neurol,* 22**,** 1519-25.

BUCKLEY, R. F., MORMINO, E. C., AMARIGLIO, R. E., PROPERZI, M. J., RABIN, J. S., LIM, Y. Y., PAPP, K. V., JACOBS, H. I. L., BURNHAM, S., HANSEEUW, B. J., DORÉ, V., DOBSON, A., MASTERS, C. L., WALLER, M., ROWE, C. C., MARUFF, P., DONOHUE, M. C., RENTZ, D. M., KIRN, D., HEDDEN, T., CHHATWAL, J., SCHULTZ, A. P., JOHNSON, K. A., VILLEMAGNE, V. L. & SPERLING, R. A. 2018. Sex, amyloid, and APOE ε4 and risk of cognitive decline in preclinical Alzheimer's disease: Findings from three well-characterized cohorts. *Alzheimer's & Dementia,* 14**,** 1193-1203.

BUDD H. S., O'GORMAN J., CHIAO, P. BUSSIERE, T., ROSENSTIEL, P. TIAN, Y. ZHU, Y. HEHN, C. GHEUENS, S. SKORDOS, L., CHEN T, SANDROCK A. 2017. Clinical development of aducanumab, an anti-Aβ human monoclonal antibody being investigated for the treatment of early Alzheimer's disease. *The Journal of Prevention of Alzheimer's Disease.* 4(4):255–263

BURGOLD, S., BITTNER, T., DOROSTKAR, M. M., KIESER, D., FUHRMANN, M., MITTEREGGER, G., KRETZSCHMAR, H., SCHMIDT, B. & HERMS, J. 2011. In vivo multiphoton imaging reveals gradual growth of newborn amyloid plaques over weeks. *Acta Neuropathologica,* 121**,** 327-335.

CAGNIN, A., BROOKS, D. J., KENNEDY, A. M., GUNN, R. N., MYERS, R., TURKHEIMER, F. E., JONES, T. & BANATI, R. B. 2001. In-vivo measurement of activated microglia in dementia. *The Lancet,* 358**,** 461-467.

CALLAHAN, M. J., LIPINSKI, W. J., BIAN, F., DURHAM, R. A., PACK, A. & WALKER, L. C. 2001. Augmented senile plaque load in aged female beta-amyloid precursor protein-transgenic mice. *Am J Pathol,* 158**,** 1173-7.

CAMERON, B. & LANDRETH, G. E. 2010. Inflammation, Microglia and Alzheimer's Disease. *Neurobiology of disease,* 37**,** 503-509.

CARMONA, S., ZAHS, K., WU, E., DAKIN, K., BRAS, J. & GUERREIRO, R. 2018. The role of TREM2 in Alzheimer's disease and other neurodegenerative disorders. *Lancet Neurol,* 17**,** 721-730.

CARRERA, I., ETCHEVERRIA, I., LI, Y., FERNANDEZ-NOVOA, L., LOMBARDI, V., VIGO, C., PALACIOS, H. H., BENBERIN, V. V., CACABELOS, R. & ALIEV, G. 2013. Immunocytochemical Characterization of Alzheimer's Disease Hallmarks in APP/PS1 Transgenic Mice Treated with a New Anti-Amyloid-beta Vaccine. *Cent Asian J Glob Health,* 2**,** 119.

CATORCE, M. N. & GEVORKIAN, G. 2016. LPS-induced Murine Neuroinflammation Model: Main Features and Suitability for Pre-

clinical Assessment of Nutraceuticals. *Curr Neuropharmacol,* 14**,** 155-64.

CAVAILLON, J. M., ADRIE, C., FITTING, C. & ADIB-CONQUY, M. 2003. Endotoxin tolerance: is there a clinical relevance? *J Endotoxin Res,* 9**,** 101-7.

CLARK, R. A., M. SHOAIB, K. N. HEWITT, S. C. STANFORD, AND S. T. BATE. 2012. A Comparison of InVivoStat with Other Statistical Software Packages for Analysis of Data Generated from Animal Experiments. *Journal of Psychopharmacology* 26(8):1136–42.

CLINE E. N., BICCA M. A., VIOLA K. L., KLEIN W. L. 2018. The Amyloid-β Oligomer Hypothesis: Beginning of the Third Decade. *Journal of Alzheimer's Disease*. 64(1):S567–S610.

CHAN, C. B. & YE, K. 2017. Sex differences in brain-derived neurotrophic factor signaling and functions. *Journal of neuroscience research,* 95**,** 328-335.

CHANG, R., YEE, K.-L. & SUMBRIA, R. K. 2017. Tumor necrosis factor α Inhibition for Alzheimer's Disease. *Journal of Central Nervous System Disease,* 9**,** 1179573517709278.

CHAPUIS, J., HANSMANNEL, F., GISTELINCK, M., MOUNIER, A., VAN CAUWENBERGHE, C., KOLEN, K. V., GELLER, F., SOTTEJEAU, Y., HAROLD, D., DOURLEN, P., GRENIER-BOLEY, B., KAMATANI, Y., DELEPINE, B., DEMIAUTTE, F., ZELENIKA, D., ZOMMER, N., HAMDANE, M., BELLENGUEZ, C., DARTIGUES, J. F., HAUW, J. J., LETRONNE, F., AYRAL, A. M., SLEEGERS, K., SCHELLENS, A., BROECK, L. V., ENGELBORGHS, S., DE DEYN, P. P., VANDENBERGHE, R., O'DONOVAN, M., OWEN, M., EPELBAUM, J., MERCKEN, M., KARRAN, E., BANTSCHEFF, M., DREWES, G., JOBERTY, G., CAMPION, D., OCTAVE, J. N., BERR, C., LATHROP, M., CALLAERTS, P., MANN, D., WILLIAMS, J., BUÉE, L., DEWACHTER, I., VAN BROECKHOVEN, C., AMOUYEL, P., MOECHARS, D., DERMAUT, B. & LAMBERT, J. C. 2013. Increased expression of BIN1 mediates Alzheimer genetic risk by modulating tau pathology. *Molecular Psychiatry,* 18**,** 1225.

CHEN, J., BUCHANAN, J. B., SPARKMAN, N. L., GODBOUT, J. P., FREUND, G. G. & JOHNSON, R. W. 2008. Neuroinflammation and disruption in working memory in aged mice after acute stimulation of the peripheral innate immune system. *Brain, Behavior, and Immunity,* 22**,** 301-311.

CHEN, Z., JALABI, W., HU, W., PARK, H.-J., GALE, J. T., KIDD, G. J., BERNATOWICZ, R., GOSSMAN, Z. C., CHEN, J. T., DUTTA, R. & TRAPP, B. D. 2014. Microglial displacement of inhibitory synapses provides neuroprotection in the adult brain. *Nature Communications,* 5**,** 4486.

CHEN, Z., JALABI, W., SHPARGEL, K. B., FARABAUGH, K. T., DUTTA, R., YIN, X., KIDD, G. J., BERGMANN, C. C., STOHLMAN, S. A. & TRAPP, B. D. 2012. Lipopolysaccharide-Induced Microglial Activation and Neuroprotection against Experimental Brain Injury Is Independent of

Hematogenous TLR4. *The Journal of neuroscience : the official journal of the Society for Neuroscience,* 32**,** 11706-11715.

CHUN, H. & LEE, C. J. 2018. Reactive astrocytes in Alzheimer's disease: A double-edged sword. *Neuroscience Research,* 126**,** 44-52.

CITRON, M., DIEHL, T. S., GORDON, G., BIERE, A. L., SEUBERT, P. & SELKOE, D. J. 1996. Evidence that the 42- and 40-amino acid forms of amyloid beta protein are generated from the beta-amyloid precursor protein by different protease activities. *Proc Natl Acad Sci U S A,* 93**,** 13170-5.

CLARK, R. A., SHOAIB, M., HEWITT, K. N., STANFORD, S. C. & BATE, S. T. 2012. A comparison of InVivoStat with other statistical software packages for analysis of data generated from animal experiments. *Journal of Psychopharmacology,* 26**,** 1136-1142.

COOK, D. G., LEVERENZ, J. B., MCMILLAN, P. J., KULSTAD, J. J., ERICKSEN, S., ROTH, R. A., SCHELLENBERG, G. D., JIN, L. W., KOVACINA, K. S. & CRAFT, S. 2003. Reduced hippocampal insulin-degrading enzyme in late-onset Alzheimer's disease is associated with the apolipoprotein E-epsilon4 allele. *Am J Pathol,* 162**,** 313-9.

COSGROVE, K. P., MAZURE, C. M. & STALEY, J. K. 2007. Evolving Knowledge of Sex Differences in Brain Structure, Function and Chemistry. *Biological psychiatry,* 62**,** 847-855.

COUCH, Y., TROFIMOV, A., MARKOVA, N., NIKOLENKO, V., STEINBUSCH, H. W., CHEKHONIN, V., SCHROETER, C., LESCH, K.-P., ANTHONY, D. C. & STREKALOVA, T. 2016. Low-dose lipopolysaccharide (LPS) inhibits aggressive and augments depressive behaviours in a chronic mild stress model in mice. *Journal of Neuroinflammation,* 13**,** 108.

CROUCH, P. J., HARDING, S. M., WHITE, A. R., CAMAKARIS, J., BUSH, A. I. & MASTERS, C. L. 2008. Mechanisms of A beta mediated neurodegeneration in Alzheimer's disease. *Int J Biochem Cell Biol,* 40**,** 181-98.

CSERNANSKY, J. G., DONG, H., FAGAN, A. M., WANG, L., XIONG, C., HOLTZMAN, D. M. & MORRIS, J. C. 2006. Plasma cortisol and progression of dementia in subjects with Alzheimer-type dementia. *Am J Psychiatry,* 163**,** 2164-9.

CUNNINGHAM, C. 2013. Microglia and neurodegeneration: the role of systemic inflammation. *Glia,* 61**,** 71-90.

CUNNINGHAM, C., CAMPION, S., LUNNON, K., MURRAY, C. L., WOODS, J. F. C., DEACON, R. M. J., RAWLINS, J. N. P. & PERRY, V. H. 2009. Systemic inflammation induces acute behavioral and cognitive changes and accelerates neurodegenerative disease. *Biological psychiatry,* 65**,** 304-12.

CUNNINGHAM, C., CAMPION, S., TEELING, J., FELTON, L. & PERRY, V. H. 2007. The sickness behaviour and CNS inflammatory mediator profile induced by systemic challenge of mice with synthetic double-stranded RNA (poly I:C). *Brain, Behavior, and Immunity,* 21**,** 490-502.

CUNNINGHAM, C. & SANDERSON, D. J. 2008. Malaise in the water maze: untangling the effects of LPS and IL-1beta on learning and memory. *Brain Behav Immun,* 22**,** 1117-27.

CUMMINGS, J.L., COHEN, S., VAN DYCK, C.H., BRODY, M. CURTIS, C. CHO, W. WARD, M., FRIESENHAHN, M., RABE, C.,BRUNSTEIN, F. 2018. A phase 2 randomized trial of crenezumab in mild to moderate Alzheimer disease. *Neurology*, 90, e1889–e1897.

CURTIN, N. M., BOYLE, N. T., MILLS, K. H. G. & CONNOR, T. J. 2009. Psychological stress suppresses innate IFN-γ production via glucocorticoid receptor activation: Reversal by the anxiolytic chlordiazepoxide. *Brain, Behavior, and Immunity,* 23**,** 535-547.

D'ANDREA, M.R., 2005. Add Alzheimer's disease to the list of autoimmune diseases. *Med. Hypotheses,* 64, pp. 458-463

DAWICKI, W. & MARSHALL, J. S. 2007. New and emerging roles for mast cells in host defence. *Current Opinion in Immunology,* 19**,** 31-38.

DE MIRANDA, J., YADDANAPUDI, K., HORNIG, M., VILLAR, G., SERGE, R. & LIPKIN, W. I. 2010. Induction of Toll-like receptor 3-mediated immunity during gestation inhibits cortical neurogenesis and causes behavioral disturbances. *MBio,* 1.

DE SOUZA, D. F., LEITE, M. C., QUINCOZES-SANTOS, A., NARDIN, P., TORTORELLI, L. S., RIGO, M. M., GOTTFRIED, C., LEAL, R. B. & GONCALVES, C. A. 2009. S100B secretion is stimulated by IL-1beta in glial cultures and hippocampal slices of rats: Likely involvement of MAPK pathway. *J Neuroimmunol,* 206**,** 52-7.

DEACON, R. M. J. & RAWLINS, J. N. P. 2006. T-maze alternation in the rodent. *Nature protocols,* 1**,** 7-12.

DEACON R. 2012. Assessing burrowing, nest construction, and hoarding in mice. Journal of visualized experiments : JoVE, (59), e2607.

DEACON, R. 2006 Assessing nest building in mice. *Nat Protoc* 1, 1117–1119.

DEANE, R., BELL, R. D., SAGARE, A. & ZLOKOVIC, B. V. 2009. Clearance of amyloid-beta peptide across the blood-brain barrier: implication for therapies in Alzheimer's disease. *CNS & neurological disorders drug targets,* 8**,** 16-30.

DHABHAR, F. S. 2009. Enhancing versus suppressive effects of stress on immune function: implications for immunoprotection and immunopathology. *Neuroimmunomodulation,* 16**,** 300-17.

DICARLO, G., WILCOCK, D., HENDERSON, D., GORDON, M. & MORGAN, D. 2001. Intrahippocampal LPS injections reduce A?? load in APP+PS1 transgenic mice. *Neurobiology of Aging,* 22**,** 1007-1012.

DINARELLO, C. A. 2000. Proinflammatory cytokines. *Chest,* 118**,** 503-8.

DING, Y., PARDON, M. C., AGOSTINI, A., FAAS, H., DUAN, J., WARD, W. O. C., EASTON, F., AUER, D. & BAI, L. 2017. Novel Methods for Microglia Segmentation, Feature Extraction, and Classification. *IEEE/ACM Transactions on Computational Biology and Bioinformatics,* 14**,** 1366-1377.

DONG, H. & CSERNANSKY, J. G. 2009. Effects of stress and stress hormones on amyloid-beta protein and plaque deposition. *J Alzheimers Dis,* 18**,** 459-69.

DONG Y., LI X., CHENG J., HOU L., 2019. Drug Development for Alzheimer's Disease: Microglia Induced Neuroinflammation as a Target? *International Journal of Molecular Sciences*;20(3):558.

DONG, H., GOICO, B., MARTIN, M., CSERNANSKY, C. A., BERTCHUME, A. & CSERNANSKY, J. G. 2004. Modulation of hippocampal cell proliferation, memory, and amyloid plaque deposition in APPsw (Tg2576) mutant mice by isolation stress. *Neuroscience,* 127**,** 601-9.

DOODY, R. S., THOMAS, R. G., FARLOW, M., IWATSUBO, T., VELLAS, B., JOFFE, S., KIEBURTZ, K., RAMAN, R., SUN, X., AISEN, P. S., SIEMERS, E., LIU-SEIFERT, H. & MOHS, R. 2014. Phase 3 trials of solanezumab for mild-to-moderate Alzheimer's disease. *N Engl J Med,* 370**,** 311-21.

DOODY R. S., AISEN P. S., IWATSUBO T., 2013. Semagacestat for treatment of Alzheimer's disease. N. Engl. J. Med. 369:1661

DROLLE, E., HANE, F., LEE, B. & LEONENKO, Z. 2014. Atomic force microscopy to study molecular mechanisms of amyloid fibril formation and toxicity in Alzheimer's disease. *Drug Metab Rev,* 46**,** 207-23.

DRUMMOND, E. & WISNIEWSKI, T. 2017. Alzheimer's disease: experimental models and reality. *Acta Neuropathol,* 133**,** 155-175.

DUNN, A. J. 2002. Mechanisms by which cytokines signal the brain. *International Review of Neurobiology.* Academic Press.

DZENKO, K. A., ANDJELKOVIC, A. V., KUZIEL, W. A. & PACHTER, J. S. 2001. The chemokine receptor CCR2 mediates the binding and internalization of monocyte chemoattractant protein-1 along brain microvessels. *J Neurosci,* 21**,** 9214-23.

E. HIRBEC, H., NORISTANI, H. N. & PERRIN, F. E. 2017. Microglia Responses in Acute and Chronic Neurological Diseases: What Microglia-Specific Transcriptomic Studies Taught (and did Not Teach) Us. *Frontiers in Aging Neuroscience,* 9**,** 227.

EIKELENBOOM, P., HOOZEMANS, J. J. M., VEERHUIS, R., VAN EXEL, E., ROZEMULLER, A. J. M. & VAN GOOL, W. A. 2012. Whether, when and how chronic inflammation increases the risk of developing late-onset Alzheimer's disease. *Alzheimer's Research & Therapy,* 4**,** 15.

EIKELENBOOM, P., VAN EXEL, E., HOOZEMANS, J. J., VEERHUIS, R., ROZEMULLER, A. J. & VAN GOOL, W. A. 2010. Neuroinflammation - an early event in both the history and pathogenesis of Alzheimer's disease. *Neurodegener Dis,* 7**,** 38-41.

EL KHOURY, J., TOFT, M., HICKMAN, S. E., MEANS, T. K., TERADA, K., GEULA, C. & LUSTER, A. D. 2007a. Ccr2 deficiency impairs microglial accumulation and accelerates progression of Alzheimer-like disease. *Nature Medicine,* 13**,** 432.

EL KHOURY, J., TOFT, M., HICKMAN, S. E., MEANS, T. K., TERADA, K., GEULA, C. & LUSTER, A. D. 2007b. Ccr2 deficiency impairs microglial

accumulation and accelerates progression of Alzheimer-like disease. *Nat Med,* 13**,** 432-8.

ELDER, G. A., GAMA SOSA, M. A. & DE GASPERI, R. 2010. Transgenic Mouse Models of Alzheimer's Disease. *The Mount Sinai journal of medicine, New York,* 77**,** 69-81.

ENGELAND, C. G., KAVALIERS, M. & OSSENKOPP, K.-P. 2003. Sex differences in the effects of muramyl dipeptide and lipopolysaccharide on locomotor activity and the development of behavioral tolerance in rats. *Pharmacology Biochemistry and Behavior,* 74**,** 433-447.

ENGELAND, C. G., NIELSEN, D. V., KAVALIERS, M. & OSSENKOPP, K.-P. 2001. Locomotor activity changes following lipopolysaccharide treatment in mice: a multivariate assessment of behavioral tolerance. *Physiology & Behavior,* 72**,** 481-491.

ENGELHART, M. J., GEERLINGS, M. I., MEIJER, J., KILIAAN, A., RUITENBERG, A., VAN SWIETEN, J. C., STIJNEN, T., HOFMAN, A., WITTEMAN, J. C. & BRETELER, M. M. 2004. Inflammatory proteins in plasma and the risk of dementia: the rotterdam study. *Arch Neurol,* 61**,** 668-72.

ERICKSON, M. A. & BANKS, W. A. 2011. Cytokine and chemokine responses in serum and brain after single and repeated injections of lipopolysaccharide: Multiplex quantification with path analysis. *Brain, Behavior, and Immunity,* 25**,** 1637-1648.

ERTEKIN-TANER, N. 2010. Genetics of Alzheimer disease in the pre- and post-GWAS era. *Alzheimers Res Ther,* 2**,** 3.

ESKANDARI, F., WEBSTER, J. I. & STERNBERG, E. M. 2003. Neural immune pathways and their connection to inflammatory diseases. *Arthritis Res Ther,* 5**,** 251-65.

ESPINOSA-OLIVA, A. M., DE PABLOS, R. M., VILLARÁN, R. F., ARGÜELLES, S., VENERO, J. L., MACHADO, A. & CANO, J. 2011. Stress is critical for LPS-induced activation of microglia and damage in the rat hippocampus. *Neurobiology of Aging,* 32**,** 85-102.

ETMINAN, M., GILL, S. & SAMII, A. 2003. Effect of non-steroidal anti-inflammatory drugs on risk of Alzheimer's disease: systematic review and meta-analysis of observational studies. *BMJ,* 327**,** 128.

EVERHARDT QUEEN, A., MOERDYK-SCHAUWECKER, M., MCKEE, L. M., LEAMY, L. J. & HUET, Y. M. 2016. Differential Expression of Inflammatory Cytokines and Stress Genes in Male and Female Mice in Response to a Lipopolysaccharide Challenge. *PLoS One,* 11**,** e0152289.

FAKHOURY, M. 2018. Microglia and Astrocytes in Alzheimer's Disease: Implications for Therapy. *Curr Neuropharmacol,* 16**,** 508-518.

FARFARA, D., LIFSHITZ, V. & FRENKEL, D. 2008. Neuroprotective and neurotoxic properties of glial cells in the pathogenesis of Alzheimer's disease. *J Cell Mol Med,* 12**,** 762-80.

FARFEL, J. M., YU, L., BOYLE, P.A., LEURGANS, S., SHAH, R.C., SCHNEIDER, J.A., & BENNETT, D.A. (2019). Alzheimer's disease frequency peaks in the

tenth decade and is lower afterwards. Acta neuropathologica communications, 7(1), 104. doi:10.1186/s40478-019-0752-0.

FIEBICH, B. L., BATISTA, C. R. A., SALIBA, S. W., YOUSIF, N. M. & DE OLIVEIRA, A. C. P. 2018. Role of Microglia TLRs in Neurodegeneration. *Front Cell Neurosci,* 12**,** 329.

FIELD, R., CAMPION, S., WARREN, C., MURRAY, C. & CUNNINGHAM, C. 2010. Systemic challenge with the TLR3 agonist poly I:C induces amplified IFNalpha/beta and IL-1beta responses in the diseased brain and exacerbates chronic neurodegeneration. *Brain, behavior, and immunity,* 24**,** 996-1007.

FLODEN, A. M. & COMBS, C. K. 2011. Microglia demonstrate age-dependent interaction with amyloid-beta fibrils. *J Alzheimers Dis,* 25**,** 279-93.

FOLCH, J., PETROV, D., ETTCHETO, M., ABAD, S., SÁNCHEZ-LÓPEZ, E., GARCÍA, M. L., OLLOQUEQUI, J., BEAS-ZARATE, C., AULADELL, C. & CAMINS, A. 2016. Current Research Therapeutic Strategies for Alzheimer's Disease Treatment. *Neural Plasticity,* 2016**,** 8501693.

FONG, T. G., JONES, R. N., SHI, P., MARCANTONIO, E. R., YAP, L., RUDOLPH, J. L., YANG, F. M., KIELY, D. K. & INOUYE, S. K. 2009. Delirium accelerates cognitive decline in Alzheimer disease. *Neurology,* 72**,** 1570-5.

FRENKEL, D., WILKINSON, K., ZHAO, L., HICKMAN, S. E., MEANS, T. K., PUCKETT, L., FARFARA, D., KINGERY, N. D., WEINER, H. L. & EL KHOURY, J. 2013. Scara1 deficiency impairs clearance of soluble amyloid-beta by mononuclear phagocytes and accelerates Alzheimer's-like disease progression. *Nat Commun,* 4**,** 2030.

FREUDENBERG, M. A., MERLIN, T., GUMENSCHEIMER, M., KALIS, C., LANDMANN, R. & GALANOS, C. 2001. Role of lipopolysaccharide susceptibility in the innate immune response to Salmonella typhimurium infection: LPS, a primary target for recognition of Gram-negative bacteria. *Microbes Infect,* 3**,** 1213-22.

FU, H. Q., YANG, T., XIAO, W., FAN, L., WU, Y., TERRANDO, N. & WANG, T. L. 2014. Prolonged neuroinflammation after lipopolysaccharide exposure in aged rats. *PLoS One,* 9**,** e106331.

FUKUSHIMA, S., FURUBE, E., ITOH, M., NAKASHIMA, T. & MIYATA, S. 2015. Robust increase of microglia proliferation in the fornix of hippocampal axonal pathway after a single LPS stimulation. *J Neuroimmunol,* 285**,** 31-40.

GALIC, M. A., RIAZI, K. & PITTMAN, Q. J. 2012. Cytokines and brain excitability. *Frontiers in neuroendocrinology,* 33**,** 116-125.

GALIMBERTI, D. & SCARPINI, E. 2010. Genetics and biology of Alzheimer ' s disease and frontotemporal lobar degeneration. 3**,** 129-143.

GAGE, G. J., KIPKE, D. R., & SHAIN, W., 2012. Whole animal perfusion fixation for rodents. *Journal of visualized experiments* : JoVE, (65), 3564. doi:10.3791/3564

GARCíA-ESTRADA, J. N., LUQUíN, S., FERNÁNDEZ, A. M. & GARCIA-SEGURA, L. M. 1999. Dehydroepiandrosterone, pregnenolone and sexsteroids

down-regulate reactive astroglia in the male ratbrain after a penetrating brain injury. *International Journal of Developmental Neuroscience,* 17**,** 145-151.

GARCÍA-GÓMEZ, E., GONZÁLEZ-PEDRAJO, B. & CAMACHO-ARROYO, I. 2013. Role of Sex Steroid Hormones in Bacterial-Host Interactions. *BioMed Research International,* 2013**,** 928290.

GATE, D., REZAI-ZADEH, K., JODRY, D., RENTSENDORJ, A. & TOWN, T. 2010. Macrophages in Alzheimer's disease: the blood-borne identity. *Journal of Neural Transmission,* 117**,** 961-970.

GATZ, M., REYNOLDS, C. A., FRATIGLIONI, L., JOHANSSON, B., MORTIMER, J. A., BERG, S., FISKE, A. & PEDERSEN, N. L. 2006. Role of genes and environments for explaining Alzheimer disease. *Archives of general psychiatry,* 63**,** 168-74.

GERARD, H. C., DRESES-WERRINGLOER, U., WILDT, K. S., DEKA, S., OSZUST, C., BALIN, B. J., FREY, W. H., 2ND, BORDAYO, E. Z., WHITTUM-HUDSON, J. A. & HUDSON, A. P. 2006. Chlamydophila (Chlamydia) pneumoniae in the Alzheimer's brain. *FEMS Immunol Med Microbiol,* 48**,** 355-66.

GERARD, H. C., WILDT, K. L., WHITTUM-HUDSON, J. A., LAI, Z., AGER, J. & HUDSON, A. P. 2005. The load of Chlamydia pneumoniae in the Alzheimer's brain varies with APOE genotype. *Microb Pathog,* 39**,** 19-26.

GHEZZI, P., SACCO, S., AGNELLO, D., MARULLO, A., CASELLI, G. & BERTINI, R. 2000. LPS INDUCES IL-6 IN THE BRAIN AND IN SERUM LARGELY THROUGH TNF PRODUCTION. *Cytokine,* 12**,** 1205-1210.

GIBBS, E., SILVERMAN, J.M., ZHAO, B. PENG, X., WANG, J., WELLINGTON, C.L., MACKENZIE, I.A., PLOTKIN, S.S., KAPLAN, J.M., CASHMAN, N.R., 2019. A Rationally Designed Humanized Antibody Selective for Amyloid Beta Oligomers in Alzheimer's Disease. *Sci Rep* 9, 9870.

GLASS, C. K., SAIJO, K., WINNER, B., MARCHETTO, M. C. & GAGE, H. 2010. Mechanism Underlying Inflammation in Neurodegeneration. 140**,** 918-934.

GO, M., KOU, J., LIM, J.-E., YANG, J. & FUKUCHI, K.-I. 2016a. Microglial response to LPS increases in wild-type mice during aging but diminishes in an Alzheimer's mouse model: Implication of TLR4 signaling in disease progression. *Biochemical and Biophysical Research Communications,* 479**,** 331-337.

GO, M., KOU, J., LIM, J. E., YANG, J. & FUKUCHI, K. I. 2016b. Microglial response to LPS increases in wild-type mice during aging but diminishes in an Alzheimer's mouse model: Implication of TLR4 signaling in disease progression. *Biochem Biophys Res Commun,* 479**,** 331-337.

GORDON, M. N., HOLCOMB, L. A., JANTZEN, P. T., DICARLO, G., WILCOCK, D., BOYETT, K. W., CONNOR, K., MELACHRINO, J., O'CALLAGHAN, J. P. & MORGAN, D. 2002. Time Course of the Development of Alzheimer-

like Pathology in the Doubly Transgenic PS1+APP Mouse. *Experimental Neurology,* 173**,** 183-195.

GOSSELIN, D. & RIVEST, S. 2011. Estrogen Receptor Transrepresses Brain Inflammation. *Cell,* 145**,** 495-497.

GOTZ, J., CHEN, F., VAN DORPE, J. & NITSCH, R. M. 2001. Formation of neurofibrillary tangles in P301l tau transgenic mice induced by Abeta 42 fibrils. *Science,* 293**,** 1491-5.

GRATHWOHL, S. A., KÄLIN, R. E., BOLMONT, T., PROKOP, S., WINKELMANN, G., KAESER, S. A., ODENTHAL, J., RADDE, R., ELDH, T., GANDY, S., AGUZZI, A., STAUFENBIEL, M., MATHEWS, P. M., WOLBURG, H., HEPPNER, F. L. & JUCKER, M. 2009. Formation and maintenance of Alzheimer's disease β-amyloid plaques in the absence of microglia. *Nature neuroscience,* 12**,** 1361-1363.

GRICIUC, A., SERRANO-POZO, A., PARRADO, A. R., LESINSKI, A. N., ASSELIN, C. N., MULLIN, K., HOOLI, B., CHOI, S. H., HYMAN, B. T. & TANZI, R. E. 2013. Alzheimer's disease risk gene CD33 inhibits microglial uptake of amyloid beta. *Neuron,* 78**,** 631-43.

GU, L. & GUO, Z. 2013. Alzheimer's Abeta42 and Abeta40 peptides form interlaced amyloid fibrils. *J Neurochem,* 126**,** 305-11.

GUERREIRO, R. & HARDY, J. 2013. TREM2 and neurodegenerative disease. *N Engl J Med,* 369**,** 1569-70.

GUERREIRO, R. J., GUSTAFSON, D. R. & HARDY, J. 2012. The genetic architecture of Alzheimer's disease: beyond APP, PSENs and APOE. *Neurobiol Aging,* 33**,** 437-56.

GUILLOT-SESTIER, M.-V., DOTY, K. R., GATE, D., RODRIGUEZ, J., YAN LEUNG, B. P., REZAI-ZADEH, K. & TOWN, T. 2015. Il10 deficiency re-balances innate immunity to mitigate Alzheimer-like pathology. *Neuron,* 85**,** 534-548.

HAASS, C., SELKOE, D., 2007. Soluble protein oligomers in neurodegeneration: lessons from the Alzheimer's amyloid β-peptide. *Nat Rev Mol Cell Biol* 8, 101–112.

HANSEN, D. V., HANSON, J. E. & SHENG, M. 2017. Microglia in Alzheimer's disease. *The Journal of Cell Biology*.

HARDY, J. & SELKOE, D. J. 2002. The amyloid hypothesis of Alzheimer's disease: progress and problems on the road to therapeutics. *Science (New York, N.Y.),* 297**,** 353-6.

HAROLD, D., ABRAHAM, R., HOLLINGWORTH, P., SIMS, R., GERRISH, A., HAMSHERE, M. L., PAHWA, J. S., MOSKVINA, V., DOWZELL, K., WILLIAMS, A., JONES, N., THOMAS, C., STRETTON, A., MORGAN, A. R., LOVESTONE, S., POWELL, J., PROITSI, P., LUPTON, M. K., BRAYNE, C., RUBINSZTEIN, D. C., GILL, M., LAWLOR, B., LYNCH, A., MORGAN, K., BROWN, K. S., PASSMORE, P. A., CRAIG, D., MCGUINNESS, B., TODD, S., HOLMES, C., MANN, D., SMITH, A. D., LOVE, S., KEHOE, P. G., HARDY, J., MEAD, S., FOX, N., ROSSOR, M., COLLINGE, J., MAIER, W., JESSEN, F., SCHÜRMANN, B., HEUN, R., VAN DEN BUSSCHE, H., HEUSER, I., KORNHUBER, J., WILTFANG, J., DICHGANS, M., FRÖLICH,

L., HAMPEL, H., HÜLL, M., RUJESCU, D., GOATE, A. M., KAUWE, J. S. K., CRUCHAGA, C., NOWOTNY, P., MORRIS, J. C., MAYO, K., SLEEGERS, K., BETTENS, K., ENGELBORGHS, S., DE DEYN, P. P., VAN BROECKHOVEN, C., LIVINGSTON, G., BASS, N. J., GURLING, H., MCQUILLIN, A., GWILLIAM, R., DELOUKAS, P., AL-CHALABI, A., SHAW, C. E., TSOLAKI, M., SINGLETON, A. B., GUERREIRO, R., MÜHLEISEN, T. W., NÖTHEN, M. M., MOEBUS, S., JÖCKEL, K.-H., KLOPP, N., WICHMANN, H.-E., CARRASQUILLO, M. M., PANKRATZ, V. S., YOUNKIN, S. G., HOLMANS, P. A., O'DONOVAN, M., OWEN, M. J. & WILLIAMS, J. 2009. Genome-wide association study identifies variants at CLU and PICALM associated with Alzheimer's disease. *Nature genetics,* 41**,** 1088-93.

HASEGAWA-ISHII, S., INABA, M., UMEGAKI, H., UNNO, K., WAKABAYASHI, K. & SHIMADA, A. 2016. Endotoxemia-induced cytokine-mediated responses of hippocampal astrocytes transmitted by cells of the brain–immune interface. *Scientific Reports,* 6**,** 25457.HELLWIG, S., MASUCH, A., NESTEL, S., KATZMARSKI, N., MEYER-LUEHMANN, M. & BIBER, K. 2015. Forebrain microglia from wild-type but not adult 5xFAD mice prevent amyloid-β plaque formation in organotypic hippocampal slice cultures. *Scientific Reports,* 5**,** 14624.

HENNESSY, E., GORMLEY, S., LOPEZ-RODRIGUEZ, A. B., MURRAY, C., MURRAY, C. & CUNNINGHAM, C. 2017. Systemic TNF-α produces acute cognitive dysfunction and exaggerated sickness behavior when superimposed upon progressive neurodegeneration. *Brain, Behavior, and Immunity,* 59**,** 233-244.

HENRY, C. J., HUANG, Y., WYNNE, A. M. & GODBOUT, J. P. 2009. Peripheral lipopolysaccharide (LPS) challenge promotes microglial hyperactivity in aged mice that is associated with exaggerated induction of both pro-inflammatory IL-1beta and anti-inflammatory IL-10 cytokines. *Brain Behav Immun,* 23**,** 309-17.

HEPPNER, F. L., RANSOHOFF, R. M. & BECHER, B. 2015. Immune attack: the role of inflammation in Alzheimer disease. *Nature Reviews Neuroscience,* 16**,** 358.

HERBER, D. L., MALONEY, J. L., ROTH, L. M., FREEMAN, M. J., MORGAN, D. & GORDON, M. N. 2006. Diverse microglial responses after intrahippocampal administration of lipopolysaccharide. *Glia,* 53**,** 382-91.

HERBER, D. L., ROTH, L. M., WILSON, D., WILSON, N., MASON, J. E., MORGAN, D. & GORDON, M. N. 2004. Time-dependent reduction in Abeta levels after intracranial LPS administration in APP transgenic mice. *Exp Neurol,* 190**,** 245-53.

HERSI, M., IRVINE, B., GUPTA, P., GOMES, J., BIRKETT, N. & KREWSKI, D. 2017. Risk factors associated with the onset and progression of Alzheimer's disease: A systematic review of the evidence. *NeuroToxicology,* 61**,** 143-187.

HICKMAN, S. E. & EL KHOURY, J. 2010. Mechanisms of Mononuclear Phagocyte Recruitment in Alzheimer's Disease. *CNS & neurological disorders drug targets,* 9**,** 168-173.

HOEIJMAKERS, L., HEINEN, Y., VAN DAM, A. M., LUCASSEN, P. J. & KOROSI, A. 2016. Microglial Priming and Alzheimer's Disease: A Possible Role for (Early) Immune Challenges and Epigenetics? *Front Hum Neurosci,* 10**,** 398.

HOHSFIELD, L. A. & HUMPEL, C. 2015. Migration of blood cells to β-amyloid plaques in Alzheimer's disease. *Experimental gerontology,* 65**,** 8-15.

HOLMES, C., CUNNINGHAM, C., ZOTOVA, E., WOOLFORD, J., DEAN, C., KERR, S., CULLIFORD, D. & PERRY, V. H. 2009. Systemic inflammation and disease progression in Alzheimer disease. *Neurology,* 73**,** 768-74.

HONG, Y., XU, J., HU, Y., LI, L., DONG, Z., ZHU, T.-K. & WEI, Y.-Q. 2018. Neuroinflammation and Neuroimmunomodulation in Alzheimer's Disease. *Current Pharmacology Reports,* 4**,** 408-413.

HONJO, K., VAN REEKUM, R. & VERHOEFF, N. P. L. G. 2009. Alzheimer's disease and infection: Do infectious agents contribute to progression of Alzheimer's disease? *Alzheimer's & Dementia,* 5**,** 348-360.

HOOGLAND, I. C. M., HOUBOLT, C., VAN WESTERLOO, D. J., VAN GOOL, W. A. & VAN DE BEEK, D. 2015. Systemic inflammation and microglial activation: systematic review of animal experiments. *Journal of Neuroinflammation,* 12**,** 114.

HURTADO, D. E., MOLINA-PORCEL, L., IBA, M., ABOAGYE, A. K., PAUL, S. M., TROJANOWSKI, J. Q. & LEE, V. M. 2010. A{beta} accelerates the spatiotemporal progression of tau pathology and augments tau amyloidosis in an Alzheimer mouse model. *Am J Pathol,* 177**,** 1977-88.

IMBIMBO, B. P., SOLFRIZZI, V. & PANZA, F. 2010. Are NSAIDs useful to treat Alzheimer's disease or mild cognitive impairment? *Frontiers in aging neuroscience,* 2**,** 19.

ISING, C. & HENEKA, M. T. 2018. Functional and structural damage of neurons by innate immune mechanisms during neurodegeneration. *Cell Death Dis,* 9**,** 120.

ITZHAKI, R. F. 2014. Herpes simplex virus type 1 and Alzheimer's disease: increasing evidence for a major role of the virus. *Front Aging Neurosci,* 6**,** 202.

IWATA, N., TSUBUKI, S., TAKAKI, Y., SHIROTANI, K., LU, B., GERARD, N. P., GERARD, C., HAMA, E., LEE, H. J. & SAIDO, T. C. 2001. Metabolic regulation of brain Abeta by neprilysin. *Science,* 292**,** 1550-2.

JABLONSKI, K. A., AMICI, S. A., WEBB, L. M., RUIZ-ROSADO, J. D. D., POPOVICH, P. G., PARTIDA-SANCHEZ, S. & GUERAU-DE-ARELLANO, M. 2015. Novel Markers to Delineate Murine M1 and M2 Macrophages. *PLOS ONE,* 10**,** e0145342.

JACK, C. R., JR., ALBERT, M. S., KNOPMAN, D. S., MCKHANN, G. M., SPERLING, R. A., CARRILLO, M. C., THIES, B. & PHELPS, C. H. 2011. Introduction to the recommendations from the National Institute on Aging-

Alzheimer's Association workgroups on diagnostic guidelines for Alzheimer's disease. *Alzheimers Dement,* 7**,** 257-62.

JAMIESON, G. A., MAITLAND, N. J., WILCOCK, G. K., YATES, C. M. & ITZHAKI, R. F. 1992. Herpes simplex virus type 1 DNA is present in specific regions of brain from aged people with and without senile dementia of the Alzheimer type. *J Pathol,* 167**,** 365-8.

JANKOWSKY, J. L., FADALE, D. J., ANDERSON, J., XU, G. M., GONZALES, V., JENKINS, N. A., COPELAND, N. G., LEE, M. K., YOUNKIN, L. H., WAGNER, S. L., YOUNKIN, S. G. & BORCHELT, D. R. 2004. Mutant presenilins specifically elevate the levels of the 42 residue beta-amyloid peptide in vivo: evidence for augmentation of a 42-specific gamma secretase. *Human molecular genetics,* 13**,** 159-70.

JAROSZ-GRIFFITHS, H. H., NOBLE, E., RUSHWORTH, J. V. & HOOPER, N. M. 2016. Amyloid-β Receptors: The Good, the Bad, and the Prion Protein. *The Journal of Biological Chemistry,* 291**,** 3174-3183.

JAWHAR, S., TRAWICKA, A., JENNECKENS, C., BAYER, T. A. & WIRTHS, O. 2012. Motor deficits, neuron loss, and reduced anxiety coinciding with axonal degeneration and intraneuronal Aβ aggregation in the 5XFAD mouse model of Alzheimer's disease. *Neurobiology of Aging,* 33**,** 196.e29-196.e40.

JIANG, W., ST-PIERRE, S., ROY, P., MORLEY, B. J., HAO, J. & SIMARD, A. R. 2016. Infiltration of CCR2+Ly6Chigh Proinflammatory Monocytes and Neutrophils into the Central Nervous System Is Modulated by Nicotinic Acetylcholine Receptors in a Model of Multiple Sclerosis. *J Immunol,* 196**,** 2095-108.

JOHN, G. R., LEE, S. C., SONG, X., RIVIECCIO, M. & BROSNAN, C. F. 2005. IL-1-regulated responses in astrocytes: relevance to injury and recovery. *Glia,* 49**,** 161-76.

JOHNSON, G. V. W. & STOOTHOFF, W. H. 2004. Tau phosphorylation in neuronal cell function and dysfunction. *Journal of Cell Science,* 117**,** 5721.

JONSSON, T., ATWAL, J. K., STEINBERG, S., SNAEDAL, J., JONSSON, P. V., BJORNSSON, S., STEFANSSON, H., SULEM, P., GUDBJARTSSON, D., MALONEY, J., HOYTE, K., GUSTAFSON, A., LIU, Y., LU, Y., BHANGALE, T., GRAHAM, R. R., HUTTENLOCHER, J., BJORNSDOTTIR, G., ANDREASSEN, O. A., JONSSON, E. G., PALOTIE, A., BEHRENS, T. W., MAGNUSSON, O. T., KONG, A., THORSTEINSDOTTIR, U., WATTS, R. J. & STEFANSSON, K. 2012. A mutation in APP protects against Alzheimer's disease and age-related cognitive decline. *Nature,* 488**,** 96-9.

JONSSON, T., STEFANSSON, H., STEINBERG, S., JONSDOTTIR, I., JONSSON, P. V., SNAEDAL, J., BJORNSSON, S., HUTTENLOCHER, J., LEVEY, A. I., LAH, J. J., RUJESCU, D., HAMPEL, H., GIEGLING, I., ANDREASSEN, O. A., ENGEDAL, K., ULSTEIN, I., DJUROVIC, S., IBRAHIM-VERBAAS, C., HOFMAN, A., IKRAM, M. A., VAN DUIJN, C. M., THORSTEINSDOTTIR,

U., KONG, A. & STEFANSSON, K. 2013. Variant of TREM2 associated with the risk of Alzheimer's disease. *N Engl J Med,* 368**,** 107-16.

JUNG, C. K., KEPPLER, K., STEINBACH, S., BLAZQUEZ-LLORCA, L. & HERMS, J. 2015. Fibrillar amyloid plaque formation precedes microglial activation. *PLoS One,* 10**,** e0119768.

KAMPHUIS, W., MIDDELDORP, J., KOOIJMAN, L., SLUIJS, J. A., KOOI, E. J., MOETON, M., FRERIKS, M., MIZEE, M. R. & HOL, E. M. 2014. Glial fibrillary acidic protein isoform expression in plaque related astrogliosis in Alzheimer's disease. *Neurobiol Aging,* 35**,** 492-510.

KAMPHUIS, W., ORRE, M., KOOIJMAN, L., DAHMEN, M. & HOL, E. M. 2012. Differential cell proliferation in the cortex of the APPswePS1dE9 Alzheimer's disease mouse model. *Glia,* 60**,** 615-29.

KARCH, C. M. & GOATE, A. M. 2015. Alzheimer's Disease Risk Genes and Mechanisms of Disease Pathogenesis. *Biological Psychiatry,* 77**,** 43-51.

KARPERIEN, A., AHAMMER, H. & JELINEK, H. F. 2013. Quantitating the subtleties of microglial morphology with fractal analysis. *Front Cell Neurosci,* 7**,** 3.

KASTIN, A. J., AKERSTROM, V. & PAN, W. 2003. Interleukin-10 as a CNS therapeutic: the obstacle of the blood-brain/blood-spinal cord barrier. *Brain Res Mol Brain Res,* 114**,** 168-71.

KATAFUCHI, T., KONDO, T., YASAKA, T., KUBO, K., TAKE, S. & YOSHIMURA, M. 2003. Prolonged effects of polyriboinosinic:polyribocytidylic acid on spontaneous running wheel activity and brain interferon-α mRNA in rats: a model for immunologically induced fatigue. *Neuroscience,* 120**,** 837-845.

KELBEL, I. & WEISS, M. 2001. Anaesthetics and immune function. *Curr Opin Anaesthesiol,* 14**,** 685-91.

KIERDORF, K. & PRINZ, M. 2013. Factors regulating microglia activation. *Frontiers in cellular neuroscience,* 7**,** 44.

KIM, S., KIM, M. J., KIM, S., KANG, H. S., LIM, S. W., MYUNG, W., LEE, Y., HONG, C. H., CHOI, S. H., NA, D. L., SEO, S. W., KU, B. D., KIM, S. Y., KIM, S. Y., JEONG, J. H., PARK, S. A., CARROLL, B. J. & KIM, D. K. 2015. Gender differences in risk factors for transition from mild cognitive impairment to Alzheimer's disease: A CREDOS study. *Compr Psychiatry,* 62**,** 114-22.

KIM, W. G., MOHNEY, R. P., WILSON, B., JEOHN, G. H., LIU, B. & HONG, J. S. 2000. Regional difference in susceptibility to lipopolysaccharide-induced neurotoxicity in the rat brain: role of microglia. *J Neurosci,* 20**,** 6309-16.

KITAZAWA, M., ODDO, S., YAMASAKI, T. R., GREEN, K. N. & LAFERLA, F. M. 2005. Lipopolysaccharide-induced inflammation exacerbates tau pathology by a cyclin-dependent kinase 5-mediated pathway in a transgenic model of Alzheimer's disease. *J Neurosci,* 25**,** 8843-53.

KIYOTA, T., YAMAMOTO, M., XIONG, H., LAMBERT, M. P., KLEIN, W. L., GENDELMAN, H. E., RANSOHOFF, R. M. & IKEZU, T. 2009. CCL2

accelerates microglia-mediated Abeta oligomer formation and progression of neurocognitive dysfunction. *PLoS One,* 4**,** e6197.

KOK, E. H., ALANNE-KINNUNEN, M., ISOTALO, K., LUOTO, T., HAIKONEN, S., GOEBELER, S., PEROLA, M., HURME, M. A., HAAPASALO, H. & KARHUNEN, P. J. 2011. CRP gene variation affects early development of Alzheimer's disease-related plaques. *Journal of Neuroinflammation,* 8**,** 96.

KOTILINEK, L. A., WESTERMAN, M. A., WANG, Q., PANIZZON, K., LIM, G. P., SIMONYI, A., LESNE, S., FALINSKA, A., YOUNKIN, L. H., YOUNKIN, S. G., ROWAN, M., CLEARY, J., WALLIS, R. A., SUN, G. Y., COLE, G., FRAUTSCHY, S., ANWYL, R. & ASHE, K. H. 2008. Cyclooxygenase-2 inhibition improves amyloid-beta-mediated suppression of memory and synaptic plasticity. *Brain,* 131**,** 651-64.

KOZLOWSKI, C., WEIMER R.M., 2012. "An Automated Method to Quantify Microglia Morphology and Application to Monitor Activation State Longitudinally in Vivo." PloS one 7(2):e31814.

KRABBE, G., HALLE, A., MATYASH, V., RINNENTHAL, J. L., EOM, G. D., BERNHARDT, U., MILLER, K. R., PROKOP, S., KETTENMANN, H. & HEPPNER, F. L. 2013. Functional impairment of microglia coincides with Beta-amyloid deposition in mice with Alzheimer-like pathology. *PLoS One,* 8**,** e60921.

KRONFOL, Z. & REMICK, D. G. 2000. Cytokines and the brain: implications for clinical psychiatry. *Am J Psychiatry,* 157**,** 683-94.

KRSTIC, D. & KNUESEL, I. 2013. Deciphering the mechanism underlying late-onset Alzheimer disease. *Nat Rev Neurol,* 9**,** 25-34.

KRSTIC, D., MADHUSUDAN, A., DOEHNER, J., VOGEL, P., NOTTER, T., IMHOF, C., MANALASTAS, A., HILFIKER, M., PFISTER, S., SCHWERDEL, C., RIETHER, C., MEYER, U. & KNUESEL, I. 2012. Systemic immune challenges trigger and drive Alzheimer-like neuropathology in mice. *J Neuroinflammation,* 9**,** 151.

KUHLA, A., RÜHLMANN, C., LINDNER, T., POLEI, S., HADLICH, S., KRAUSE, B. J., VOLLMAR, B. & TEIPEL, S. J. 2017. APPswe/PS1dE9 mice with cortical amyloid pathology show a reduced NAA/Cr ratio without apparent brain atrophy: A MRS and MRI study. *NeuroImage: Clinical,* 15**,** 581-586.

KUO, S. M. 2016. Gender Difference in Bacteria Endotoxin-Induced Inflammatory and Anorexic Responses. *PLoS One,* 11**,** e0162971.

LAFERLA, F. M. & GREEN, K. N. 2012. Animal Models of Alzheimer Disease. *Cold Spring Harbor Perspectives in Medicine,* 2**,** a006320.

LAI, A. Y. & MCLAURIN, J. 2012. Clearance of amyloid-β peptides by microglia and macrophages: the issue of what, when and where. *Future neurology,* 7**,** 165-176.

LALONDE, R. 2002. The neurobiological basis of spontaneous alternation. *Neuroscience and biobehavioral reviews,* 26**,** 91-104.

LAMBERT, J.-C., HEATH, S., EVEN, G., CAMPION, D., SLEEGERS, K., HILTUNEN, M., COMBARROS, O., ZELENIKA, D., BULLIDO, M. J., TAVERNIER, B.,

LETENNEUR, L., BETTENS, K., BERR, C., PASQUIER, F., FIÉVET, N., BARBERGER-GATEAU, P., ENGELBORGHS, S., DE DEYN, P., MATEO, I., FRANCK, A., HELISALMI, S., PORCELLINI, E., HANON, O., DE PANCORBO, M. M., LENDON, C., DUFOUIL, C., JAILLARD, C., LEVEILLARD, T., ALVAREZ, V., BOSCO, P., MANCUSO, M., PANZA, F., NACMIAS, B., BOSSÙ, P., PICCARDI, P., ANNONI, G., SERIPA, D., GALIMBERTI, D., HANNEQUIN, D., LICASTRO, F., SOININEN, H., RITCHIE, K., BLANCHÉ, H., DARTIGUES, J.-F., TZOURIO, C., GUT, I., VAN BROECKHOVEN, C., ALPÉROVITCH, A., LATHROP, M. & AMOUYEL, P. 2009. Genome-wide association study identifies variants at CLU and CR1 associated with Alzheimer's disease. *Nature genetics,* 41**,** 1094-9.

LAMBERT, J. C., IBRAHIM-VERBAAS, C. A., HAROLD, D., NAJ, A. C., SIMS, R., BELLENGUEZ, C., DESTAFANO, A. L., BIS, J. C., BEECHAM, G. W., GRENIER-BOLEY, B., RUSSO, G., THORTON-WELLS, T. A., JONES, N., SMITH, A. V., CHOURAKI, V., THOMAS, C., IKRAM, M. A., ZELENIKA, D., VARDARAJAN, B. N., KAMATANI, Y., LIN, C. F., GERRISH, A., SCHMIDT, H., KUNKLE, B., DUNSTAN, M. L., RUIZ, A., BIHOREAU, M. T., CHOI, S. H., REITZ, C., PASQUIER, F., CRUCHAGA, C., CRAIG, D., AMIN, N., BERR, C., LOPEZ, O. L., DE JAGER, P. L., DERAMECOURT, V., JOHNSTON, J. A., EVANS, D., LOVESTONE, S., LETENNEUR, L., MORON, F. J., RUBINSZTEIN, D. C., EIRIKSDOTTIR, G., SLEEGERS, K., GOATE, A. M., FIEVET, N., HUENTELMAN, M. W., GILL, M., BROWN, K., KAMBOH, M. I., KELLER, L., BARBERGER-GATEAU, P., MCGUINESS, B., LARSON, E. B., GREEN, R., MYERS, A. J., DUFOUIL, C., TODD, S., WALLON, D., LOVE, S., ROGAEVA, E., GALLACHER, J., ST GEORGE-HYSLOP, P., CLARIMON, J., LLEO, A., BAYER, A., TSUANG, D. W., YU, L., TSOLAKI, M., BOSSU, P., SPALLETTA, G., PROITSI, P., COLLINGE, J., SORBI, S., SANCHEZ-GARCIA, F., FOX, N. C., HARDY, J., DENIZ NARANJO, M. C., BOSCO, P., CLARKE, R., BRAYNE, C., GALIMBERTI, D., MANCUSO, M., MATTHEWS, F., EUROPEAN ALZHEIMER'S DISEASE, I., GENETIC, ENVIRONMENTAL RISK IN ALZHEIMER'S, D., ALZHEIMER'S DISEASE GENETIC, C., COHORTS FOR, H., AGING RESEARCH IN GENOMIC, E., MOEBUS, S., MECOCCI, P., DEL ZOMPO, M., MAIER, W., HAMPEL, H., PILOTTO, A., BULLIDO, M., PANZA, F., CAFFARRA, P., et al. 2013. Meta-analysis of 74,046 individuals identifies 11 new susceptibility loci for Alzheimer's disease. *Nat Genet,* 45**,** 1452-8.

LAND, W. G. 2015. The Role of Damage-Associated Molecular Patterns (DAMPs) in Human Diseases: Part II: DAMPs as diagnostics, prognostics and therapeutics in clinical medicine. *Sultan Qaboos Univ Med J,* 15**,** e157-70.

LAU, A. A., CRAWLEY, A. C., HOPWOOD, J. J. & HEMSLEY, K. M. 2008. Open field locomotor activity and anxiety-related behaviors in mucopolysaccharidosis type IIIA mice. *Behav Brain Res,* 191**,** 130-6.

LAUW, F. N., PAJKRT, D., HACK, C. E., KURIMOTO, M., VAN DEVENTER, S. J. & VAN DER POLL, T. 2000. Proinflammatory effects of IL-10 during human endotoxemia. *J Immunol,* 165**,** 2783-9.

LEE, J.-E. & HAN, P.-L. 2013. An Update of Animal Models of Alzheimer Disease with a Reevaluation of Plaque Depositions. *Experimental Neurobiology,* 22**,** 84-95.

LEE, J. W., LEE, Y. K., YUK, D. Y., CHOI, D. Y., BAN, S. B., OH, K. W. & HONG, J. T. 2008. Neuro-inflammation induced by lipopolysaccharide causes cognitive impairment through enhancement of beta-amyloid generation. *J Neuroinflammation,* 5**,** 37.

LEE, J. Y. & SULLIVAN, K. E. 2001. Gamma interferon and lipopolysaccharide interact at the level of transcription to induce tumor necrosis factor alpha expression. *Infect Immun,* 69**,** 2847-52.

LEE, W.-J., LIAO, Y.-C., WANG, Y.-F., LIN, I. F., WANG, S.-J. & FUH, J.-L. 2018. Plasma MCP-1 and Cognitive Decline in Patients with Alzheimer's Disease and Mild Cognitive Impairment: A Two-year Follow-up Study. *Scientific Reports,* 8**,** 1280.

LEHNARDT, S., MASSILLON, L., FOLLETT, P., JENSEN, F. E., RATAN, R., ROSENBERG, P. A., VOLPE, J. J. & VARTANIAN, T. 2003. Activation of innate immunity in the CNS triggers neurodegeneration through a Toll-like receptor 4-dependent pathway. *Proceedings of the National Academy of Sciences of the United States of America,* 100**,** 8514-8519.

LENZ, K. M., NUGENT, B. M., HALIYUR, R. & MCCARTHY, M. M. 2013. Microglia are essential to masculinization of brain and behavior. *The Journal of neuroscience : the official journal of the Society for Neuroscience,* 33**,** 2761-2772.

LEWIS, D. K., JOHNSON, A. B., STOHLGREN, S., HARMS, A. & SOHRABJI, F. 2008. Effects of estrogen receptor agonists on regulation of the inflammatory response in astrocytes from young adult and middle-aged female rats. *Journal of Neuroimmunology,* 195**,** 47-59.

LEWIS, J., DICKSON, D. W., LIN, W. L., CHISHOLM, L., CORRAL, A., JONES, G., YEN, S. H., SAHARA, N., SKIPPER, L., YAGER, D., ECKMAN, C., HARDY, J., HUTTON, M. & MCGOWAN, E. 2001. Enhanced neurofibrillary degeneration in transgenic mice expressing mutant tau and APP. *Science,* 293**,** 1487-91.

LI, J. W., ZONG, Y., CAO, X. P., TAN, L. & TAN, L. 2018. Microglial priming in Alzheimer's disease. *Ann Transl Med,* 6**,** 176.

LICASTRO, F., CARBONE, I., RASCHI, E. & PORCELLINI, E. 2014. The 21st century epidemic: infections as inductors of neuro-degeneration associated with Alzheimer's Disease. *Immunity & Ageing : I & A,* 11**,** 22.

LICHTENSTEIN, M. P., CARRIBA, P., MASGRAU, R., PUJOL, A. & GALEA, E. 2010. Staging anti-inflammatory therapy in Alzheimer's disease. *Front Aging Neurosci,* 2**,** 142.

LIDDELOW, S. A. & BARRES, B. A. 2017. Reactive Astrocytes: Production, Function, and Therapeutic Potential. *Immunity,* 46**,** 957-967.

LIDDELOW S.A., GUTTENPLAN K.A., CLARKE L.E., BENNETT F.C., BOHLEN C.J., SCHIRMER L., BARRES B.A. 2017 Neurotoxic reactive astrocytes are induced by activated microglia. *Nature*, 541, pp. 481-487.

LIM, S. L., RODRIGUEZ-ORTIZ, C. J. & KITAZAWA, M. 2015. Infection, systemic inflammation, and Alzheimer's disease. *Microbes and Infection,* 17**,** 549-556.

LISTA, S., O'BRYANT, S. E., BLENNOW, K., DUBOIS, B., HUGON, J., ZETTERBERG, H. & HAMPEL, H. 2015. Biomarkers in Sporadic and Familial Alzheimer's Disease. *J Alzheimers Dis,* 47**,** 291-317.

LIU, C., CUI, G., ZHU, M., KANG, X. & GUO, H. 2014. Neuroinflammation in Alzheimer's disease: chemokines produced by astrocytes and chemokine receptors. *International journal of clinical and experimental pathology,* 7**,** 8342-8355.

LIU, J., WANG, D., LI, S. Q., YU, Y. & YE, R. D. 2016. Suppression of LPS-induced tau hyperphosphorylation by serum amyloid A. *J Neuroinflammation,* 13**,** 28.

LIU, X., WU, Z., HAYASHI, Y. & NAKANISHI, H. 2012. Age-dependent neuroinflammatory responses and deficits in long-term potentiation in the hippocampus during systemic inflammation. *Neuroscience,* 216**,** 133-42.

LOBO-SILVA, D., CARRICHE, G. M., CASTRO, A. G., ROQUE, S. & SARAIVA, M. 2016. Balancing the immune response in the brain: IL-10 and its regulation. *J Neuroinflammation,* 13**,** 297.

LORAM, L. C., SHOLAR, P. W., TAYLOR, F. R., WIESELER, J., BABB, J. A., STRAND, K. A., BERKELHAMMER, D., DAY, H. E. W., MAIER, S. F. & WATKINS, L. R. 2012a. Sex and estradiol influence glial pro-inflammatory responses to lipopolysaccharide in rats. *Psychoneuroendocrinology,* 37**,** 1688-1699.

LORAM, L. C., SHOLAR, P. W., TAYLOR, F. R., WIESLER, J. L., BABB, J. A., STRAND, K. A., BERKELHAMMER, D., DAY, H. E., MAIER, S. F. & WATKINS, L. R. 2012b. Sex and estradiol influence glial pro-inflammatory responses to lipopolysaccharide in rats. *Psychoneuroendocrinology,* 37**,** 1688-99.

LOTT, I. T. & HEAD, E. 2001. Down syndrome and Alzheimer's disease: a link between development and aging. *Ment Retard Dev Disabil Res Rev,* 7**,** 172-8.

LU, M., VARLEY, A. W., OHTA, S., HARDWICK, J. & MUNFORD, R. S. 2008. Host inactivation of bacterial lipopolysaccharide prevents prolonged microbial tolerance following Gram-negative bacterial infection. *Cell host & microbe,* 4**,** 293-302.

LU, Y.-P., ZENG, M., HU, X.-Y., XU, H., SWAAB, D. F., RAVID, R. & ZHOU, J.-N. 2003. Estrogen receptor α-immunoreactive astrocytes are increased in the hippocampus in Alzheimer's disease. *Experimental Neurology,* 183**,** 482-488.

LUCAS, S. M., ROTHWELL, N. J. & GIBSON, R. M. 2006. The role of inflammation in CNS injury and disease. *Br J Pharmacol,* 147 Suppl 1**,** S232-40.

MACK, M., CIHAK, J., SIMONIS, C., LUCKOW, B., PROUDFOOT, A. E., PLACHY, J., BRUHL, H., FRINK, M., ANDERS, H. J., VIELHAUER, V., PFIRSTINGER, J., STANGASSINGER, M. & SCHLONDORFF, D. 2001. Expression and characterization of the chemokine receptors CCR2 and CCR5 in mice. *J Immunol,* 166**,** 4697-704.

MALLARD, C. 2012. Innate immune regulation by toll-like receptors in the brain. *ISRN Neurol,* 2012**,** 701950.

MALM, T., KOISTINAHO, J. & KANNINEN, K. 2011. Utilization of APPswe/PS1dE9 Transgenic Mice in Research of Alzheimer's Disease: Focus on Gene Therapy and Cell-Based Therapy Applications. *International Journal of Alzheimer's Disease,* 2011**,** 517160.

MALM, T., KOISTINAHO, M., MUONA, A., MAGGA, J. & KOISTINAHO, J. 2010. The role and therapeutic potential of monocytic cells in Alzheimer's disease. *Glia,* 58**,** 889-900.

MALM, T. M., KOISTINAHO, M., PAREPALO, M., VATANEN, T., OOKA, A., KARLSSON, S. & KOISTINAHO, J. 2005. Bone-marrow-derived cells contribute to the recruitment of microglial cells in response to beta-amyloid deposition in APP/PS1 double transgenic Alzheimer mice. *Neurobiol Dis,* 18**,** 134-42.

MANDREKAR-COLUCCI, S. & LANDRETH, G. E. 2010. Microglia and inflammation in Alzheimer's disease. *CNS & neurological disorders drug targets,* 9**,** 156-67.

MANITZ, M. P., PLÜMPER, J., DEMIR, S., AHRENS, M., EßLINGER, M., WACHHOLZ, S., EISENACHER, M., JUCKEL, G. & FRIEBE, A. 2016. Flow cytometric characterization of microglia in the offspring of PolyI:C treated mice. *Brain Research,* 1636**,** 172-182.

MARIC, M., DE HAAN, E., HOGENDOORN, S. M., WOLTERS, L. H. & HUIZENGA, H. M. 2015. Evaluating statistical and clinical significance of intervention effects in single-case experimental designs: an SPSS method to analyze univariate data. *Behav Ther,* 46**,** 230-41.

MARLATT, M. W., BAUER, J., ARONICA, E., VAN HAASTERT, E. S., HOOZEMANS, J. J., JOELS, M. & LUCASSEN, P. J. 2014. Proliferation in the Alzheimer hippocampus is due to microglia, not astroglia, and occurs at sites of amyloid deposition. *Neural Plast,* 2014**,** 693851.

MARTIN, E., EL-BEHI, M., FONTAINE, B. & DELARASSE, C. 2017. Analysis of Microglia and Monocyte-derived Macrophages from the Central Nervous System by Flow Cytometry. *J Vis Exp*.

MARTINEZ, F. O. & GORDON, S. 2014. The M1 and M2 paradigm of macrophage activation: time for reassessment. *F1000Prime Reports,* 6**,** 13.

MARTINS, R. N. 2006. 09-01 Role of apolipoprotein E in Alzheimer's disease. *Acta Neuropsychiatr,* 18**,** 333.

MASTERS, C. L., BATEMAN, R., BLENNOW, K., ROWE, C. C., SPERLING, R. A. & CUMMINGS, J. L. 2015. Alzheimer's disease. *Nature Reviews Disease Primers,* 1**,** 15056.

MATSUMOTO, M. & SEYA, T. 2008. TLR3: interferon induction by double-stranded RNA including poly(I:C). *Adv Drug Deliv Rev,* 60**,** 805-12.

MAWUENYEGA, K. G., SIGURDSON, W., OVOD, V., MUNSELL, L., KASTEN, T., MORRIS, J. C., YARASHESKI, K. E. & BATEMAN, R. J. 2010. Decreased clearance of CNS beta-amyloid in Alzheimer's disease. *Science,* 330**,** 1774.

MAZURE, C. M. & SWENDSEN, J. 2016a. Sex differences in Alzheimer's disease and other dementias. *The Lancet. Neurology,* 15**,** 451-452.

MAZURE, C. M. & SWENDSEN, J. 2016b. Sex differences in Alzheimer’s disease and other dementias. *The Lancet. Neurology,* 15**,** 451-452.

MCCARTHY, M. M., & NUGENT, B. M. 2015. At the frontier of epigenetics of brain sex differences. *Frontiers in behavioral neuroscience*, 9, 221. https://doi.org/10.3389/fnbeh.2015.00221

MCNAUGHTON, D., KNIGHT, W., GUERREIRO, R., RYAN, N., LOWE, J., POULTER, M., NICHOLL, D. J., HARDY, J., REVESZ, T., LOWE, J., ROSSOR, M., COLLINGE, J. & MEAD, S. 2012. Duplication of amyloid precursor protein (APP), but not prion protein (PRNP) gene is a significant cause of early onset dementia in a large UK series. *Neurobiol Aging,* 33**,** 426 e13-21.

MEDEIROS, R. & LAFERLA, F. M. 2013. Astrocytes: conductors of the Alzheimer disease neuroinflammatory symphony. *Experimental neurology,* 239**,** 133-8.

MEDVEDEV, A. E., KOPYDLOWSKI, K. M. & VOGEL, S. N. 2000. Inhibition of lipopolysaccharide-induced signal transduction in endotoxin-tolerized mouse macrophages: dysregulation of cytokine, chemokine, and toll-like receptor 2 and 4 gene expression. *J Immunol,* 164**,** 5564-74.

MEDVEDEV, A. E., SABROE, I., HASDAY, J. D. & VOGEL, S. N. 2006. Tolerance to microbial TLR ligands: molecular mechanisms and relevance to disease. *J Endotoxin Res,* 12**,** 133-50.

MEYER-LUEHMANN, M., SPIRES-JONES, T. L., PRADA, C., GARCIA-ALLOZA, M., DE CALIGNON, A., ROZKALNE, A., KOENIGSKNECHT-TALBOO, J., HOLTZMAN, D. M., BACSKAI, B. J. & HYMAN, B. T. 2008. Rapid appearance and local toxicity of amyloid-beta plaques in a mouse model of Alzheimer's disease. *Nature,* 451**,** 720-4.

MIELKE, M. M., VEMURI, P. & ROCCA, W. A. 2014a. Clinical epidemiology of Alzheimer's disease: assessing sex and gender differences. *Clinical epidemiology,* 6**,** 37-48.

MIELKE, M. M., VEMURI, P. & ROCCA, W. A. 2014b. Clinical epidemiology of Alzheimer’s disease: assessing sex and gender differences. *Clinical Epidemiology,* 6**,** 37-48.

MILDNER, A., SCHLEVOGT, B., KIERDORF, K., BOTTCHER, C., ERNY, D., KUMMER, M. P., QUINN, M., BRUCK, W., BECHMANN, I., HENEKA, M.

T., PRILLER, J. & PRINZ, M. 2011. Distinct and non-redundant roles of microglia and myeloid subsets in mouse models of Alzheimer's disease. *J Neurosci,* 31**,** 11159-71.

MILLER, M. C. & MAYO, K. H. 2017. Chemokines from a Structural Perspective. *International journal of molecular sciences,* 18**,** 2088.

MILLER S. J., 2018. Astrocyte Heterogeneity in the Adult Central Nervous System. *Frontiers in cellular neuroscience*, 12, 401. doi:10.3389/fncel.2018.00401

MIYAGAWA, T., EBINUMA, I., MOROHASHI, Y., HORI, Y., YOUNG CHANG, M., HATTORI, H., MAEHARA, T., YOKOSHIMA, S., FUKUYAMA, T., TSUJI, S., IWATSUBO, T., PRENDERGAST, G. C. & TOMITA, T. 2016. BIN1 regulates BACE1 intracellular trafficking and amyloid-beta production. *Hum Mol Genet,* 25**,** 2948-2958.

MONASTERO, R., CARUSO, C. & VASTO, S. 2014. Alzheimer's disease and infections, where we stand and where we go. *Immunity & Ageing : I & A,* 11**,** 26.

MONASTERO, R., MANGIALASCHE, F., CAMARDA, C., ERCOLANI, S. & CAMARDA, R. 2009. A systematic review of neuropsychiatric symptoms in mild cognitive impairment. *J Alzheimers Dis,* 18**,** 11-30.

MONNERET, G., VENET, F., PACHOT, A. & LEPAPE, A. 2008. Monitoring Immune Dysfunctions in the Septic Patient: A New Skin for the Old Ceremony. *Molecular Medicine,* 14**,** 64-78.

MORIMOTO, K., HORIO, J., SATOH, H., SUE, L., BEACH, T., ARITA, S., TOOYAMA, I. & KONISHI, Y. 2011. Expression profiles of cytokines in the brains of Alzheimer's disease (AD) patients, compared to the brains of non-demented patients with and without increasing AD pathology. *Journal of Alzheimer's disease : JAD,* 25**,** 59-76.

MORRIS, G. P., CLARK, I. A. & VISSEL, B. 2014. Inconsistencies and Controversies Surrounding the Amyloid Hypothesis of Alzheimer's Disease. *Acta Neuropathologica Communications,* 2**,** 135.

MOTT, R. T. & HULETTE, C. M. 2005. Neuropathology of Alzheimer's disease. *Neuroimaging Clin N Am,* 15**,** 755-65, ix.

MRAK, R. E. 2009. Neuropathology and the neuroinflammation idea. *J Alzheimers Dis,* 18**,** 473-81.

MURRAY, C., SANDERSON, D. J., BARKUS, C., DEACON, R. M., RAWLINS, J. N., BANNERMAN, D. M. & CUNNINGHAM, C. 2012. Systemic inflammation induces acute working memory deficits in the primed brain: relevance for delirium. *Neurobiol Aging,* 33**,** 603-616 e3.

MUYLLAERT, D., TERWEL, D., BORGHGRAEF, P., DEVIJVER, H., DEWACHTER, I. & VAN LEUVEN, F. 2006. Transgenic mouse models for Alzheimer's disease: the role of GSK-3B in combined amyloid and tau-pathology. *Rev Neurol (Paris),* 162**,** 903-7.

NAERT, G. & RIVEST, S. 2013. A deficiency in CCR2+ monocytes: the hidden side of Alzheimer's disease. *J Mol Cell Biol,* 5**,** 284-93.

NAZEM, A., SANKOWSKI, R., BACHER, M. & AL-ABED, Y. 2015. Rodent models of neuroinflammation for Alzheimer's disease. *Journal of neuroinflammation,* 12**,** 74-74.

NEUMANN, H. & TAKAHASHI, K. 2007. Essential role of the microglial triggering receptor expressed on myeloid cells-2 (TREM2) for central nervous tissue immune homeostasis. *Journal of neuroimmunology,* 184**,** 92-9.

NOMURA, F., AKASHI, S., SAKAO, Y., SATO, S., KAWAI, T., MATSUMOTO, M., NAKANISHI, K., KIMOTO, M., MIYAKE, K., TAKEDA, K. & AKIRA, S. 2000. Cutting Edge: Endotoxin Tolerance in Mouse Peritoneal Macrophages Correlates with Down-Regulation of Surface Toll-Like Receptor 4 Expression. *The Journal of Immunology,* 164**,** 3476.

NORDEN, D. M. & GODBOUT, J. P. 2013. Review: microglia of the aged brain: primed to be activated and resistant to regulation. *Neuropathology and applied neurobiology,* 39**,** 19-34.

NORDEN, D. M., MUCCIGROSSO, M. M. & GODBOUT, J. P. 2015a. Microglial priming and enhanced reactivity to secondary insult in aging, and traumatic CNS injury, and neurodegenerative disease. *Neuropharmacology,* 96**,** 29-41.

NORDEN, D. M., MUCCIGROSSO, M. M. & GODBOUT, J. P. 2015b. Microglial priming and enhanced reactivity to secondary insult in aging, and traumatic CNS injury, and neurodegenerative disease. *Neuropharmacology,* 96**,** 29-41.

NYARKO, J. N. K., QUARTEY, M. O., PENNINGTON, P. R., HEISTAD, R. M., DEA, D., POIRIER, J., BAKER, G. B. & MOUSSEAU, D. D. 2018. Profiles of β-Amyloid Peptides and Key Secretases in Brain Autopsy Samples Differ with Sex and APOE ε4 Status: Impact for Risk and Progression of Alzheimer Disease. *Neuroscience,* 373**,** 20-36.

O'CARROLL, C., FAGAN, A., SHANAHAN, F. & CARMODY, R. J. 2014. Identification of a unique hybrid macrophage-polarization state following recovery from lipopolysaccharide tolerance. *J Immunol,* 192**,** 427-36.

O'BRIEN, R. J. & WONG, P. C. 2011. Amyloid Precursor Protein Processing and Alzheimer's Disease. *Annual review of neuroscience,* 34**,** 185-204.

ODDO, S., CACCAMO, A., KITAZAWA, M., TSENG, B. P. & LAFERLA, F. M. 2003. Amyloid deposition precedes tangle formation in a triple transgenic model of Alzheimer's disease. *Neurobiol Aging,* 24**,** 1063-70.

OKELLO, A., EDISON, P., ARCHER, H. A., TURKHEIMER, F. E., KENNEDY, J., BULLOCK, R., WALKER, Z., KENNEDY, A., FOX, N., ROSSOR, M. & BROOKS, D. J. 2009. Microglial activation and amyloid deposition in mild cognitive impairment: a PET study. *Neurology,* 72**,** 56-62.

OLSSON, B., LAUTNER, R., ANDREASSON, U., ÖHRFELT, A., PORTELIUS, E., BJERKE, M., HÖLTTÄ, M., ROSÉN, C., OLSSON, C., STROBEL, G., WU, E., DAKIN, K., PETZOLD, M., BLENNOW, K. & ZETTERBERG, H. 2016. CSF and blood biomarkers for the diagnosis of Alzheimer's disease: a

systematic review and meta-analysis. *The Lancet Neurology,* 15**,** 673-684.

OPAL, S. M. & DEPALO, V. A. 2000. Anti-Inflammatory Cytokines. *Chest,* 117**,** 1162-1172.

OSTROWITZKI, S. LASSER, R.A. DORFLINGER, E. SCHELTENS, P. BARKHOF, F. NIKOLCHEVA, T. ASHFORD, E. RETOUT, S. HOFMANN, C. DELMAR, P. 2017. A phase III randomized trial of gantenerumab in prodromal Alzheimer's disease. *Alzheimer's Res. Ther.*, 9, 95.

PANPALLI ATES, M., KARAMAN, Y., GUNTEKIN, S. & ERGUN, M. A. 2016. Analysis of genetics and risk factors of Alzheimer's Disease. *Neuroscience,* 325**,** 124-131.

PANZA F., LOZUPONE M., SOLFRIZZI V., SARDONE R., PICCININNI C., DIBELLO V. 2018. BACE inhibitors in clinical development for the treatment of Alzheimer's disease. *Expert Rev. Neurother.* 18 847–857.

PARADOWSKI, B., JAREMKO, M., DOBOSZ, T., LESZEK, J. & NOGA, L. 2007. Evaluation of CSF-Chlamydia pneumoniae, CSF-tau, and CSF-Abeta42 in Alzheimer's disease and vascular dementia. *J Neurol,* 254**,** 154-9.

PARAMESWARAN, N. & PATIAL, S. 2010. Tumor Necrosis Factor-α Signaling in Macrophages. *Critical reviews in eukaryotic gene expression,* 20**,** 87-103.

PARDON, M.-C., YANEZ LOPEZ, M., YUCHUN, D., MARJAŃSKA, M., PRIOR, M., BRIGNELL, C., PARHIZKAR, S., AGOSTINI, A., BAI, L., AUER, D. P. & FAAS, H. M. 2016. Magnetic Resonance Spectroscopy discriminates the response to microglial stimulation of wild type and Alzheimer's disease models. *Scientific Reports,* 6**,** 19880.

PARDON, M. C. 2015. Lipopolysaccharide hyporesponsiveness: protective or damaging response to the brain? *Rom J Morphol Embryol,* 56**,** 903-13.

PARK, S. Y. & FERREIRA, A. 2005. The generation of a 17 kDa neurotoxic fragment: an alternative mechanism by which tau mediates beta-amyloid-induced neurodegeneration. *J Neurosci,* 25**,** 5365-75.

PARSONS, C. G., DANYSZ, W., DEKUNDY, A. & PULTE, I. 2013. Memantine and cholinesterase inhibitors: complementary mechanisms in the treatment of Alzheimer's disease. *Neurotoxicity research,* 24**,** 358-369.

PATEL, N. S., PARIS, D., MATHURA, V., QUADROS, A. N., CRAWFORD, F. C. & MULLAN, M. J. 2005. Inflammatory cytokine levels correlate with amyloid load in transgenic mouse models of Alzheimer's disease. *J Neuroinflammation,* 2**,** 9.

PEARSON, H. A. & PEERS, C. 2006. Physiological roles for amyloid beta peptides. *The Journal of physiology,* 575**,** 5-10.

PEFEROEN, L. A., VOGEL, D. Y., UMMENTHUM, K., BREUR, M., HEIJNEN, P. D., GERRITSEN, W. H., PEFEROEN-BAERT, R. M., VAN DER VALK, P., DIJKSTRA, C. D. & AMOR, S. 2015. Activation status of human microglia is dependent on lesion formation stage and remyelination in multiple sclerosis. *J Neuropathol Exp Neurol,* 74**,** 48-63.

PERRY, V. H., CUNNINGHAM, C. & HOLMES, C. 2007. Systemic infections and inflammation affect chronic neurodegeneration. *Nature reviews. Immunology,* 7**,** 161-7.

PERRY, V. H. & HOLMES, C. 2014. Microglial priming in neurodegenerative disease. *Nature reviews. Neurology,* 10**,** 217-24.

PERRY, V. H., NICOLL, J. A. R. & HOLMES, C. 2010. Microglia in neurodegenerative disease. *Nature reviews. Neurology,* 6**,** 193-201.

PIACERI, I., NACMIAS, B. & SORBI, S. 2013. Genetics of familial and sporadic Alzheimer's disease. *Front Biosci (Elite Ed),* 5**,** 167-77.

PIKE, C. J. 2017. Sex and the development of Alzheimer's disease. *J Neurosci Res,* 95**,** 671-680.

PINTADO, C., REVILLA, E., VIZUETE, M. L., JIMENEZ, S., GARCIA-CUERVO, L., VITORICA, J., RUANO, D. & CASTANO, A. 2011. Regional difference in inflammatory response to LPS-injection in the brain: role of microglia cell density. *J Neuroimmunol,* 238**,** 44-51.

PORCELLINI, E., CARBONE, I., IANNI, M. & LICASTRO, F. 2010. Alzheimer's disease gene signature says: beware of brain viral infections. *Immunity & Ageing,* 7**,** 16.

POZZI, S., BENEDUSI, V., MAGGI, A. & VEGETO, E. 2006. Estrogen action in neuroprotection and brain inflammation. *Ann N Y Acad Sci,* 1089**,** 302-23.

PRASANSUKLAB, A. & TENCOMNAO, T. 2013. Amyloidosis in Alzheimer's Disease: The Toxicity of Amyloid Beta (A beta), Mechanisms of Its Accumulation and Implications of Medicinal Plants for Therapy. *Evid Based Complement Alternat Med,* 2013**,** 413808.

PRINZ, M. & PRILLER, J. 2010. Tickets to the brain: Role of CCR2 and CX3CR1 in myeloid cell entry in the CNS. *Journal of Neuroimmunology,* 224**,** 80-84.

PROKOP, S., MILLER, K. R. & HEPPNER, F. L. 2013. Microglia actions in Alzheimer's disease. *Acta Neuropathologica,* 126**,** 461-477.

PROPES, M. J. & JOHNSON, R. W. 1997. Role of corticosterone in the behavioral effects of central interleukin-1 beta. *Physiol Behav,* 61**,** 7-13.

PUNTENER, U., BOOTH, S. G., PERRY, V. H. & TEELING, J. L. 2012. Long-term impact of systemic bacterial infection on the cerebral vasculature and microglia. *J Neuroinflammation,* 9**,** 146.

QIAN, X. S. & GE, S. 2018. [The state of the art research findings on the relationship between chronic periodontitis and Alzheimer's disease: a review]. *Zhonghua Kou Qiang Yi Xue Za Zhi,* 53**,** 275-279.

QIN, L., HE, J., HANES, R. N., PLUZAREV, O., HONG, J.-S. & CREWS, F. T. 2008. Increased systemic and brain cytokine production and neuroinflammation by endotoxin following ethanol treatment. *Journal of Neuroinflammation,* 5**,** 10-10.

QIU, W. Q. & FOLSTEIN, M. F. 2006. Insulin, insulin-degrading enzyme and amyloid-beta peptide in Alzheimer's disease: review and hypothesis. *Neurobiol Aging,* 27**,** 190-8.

QIU, C., KIVIPELTO, M., & VON STRAUSS, E. (2009). Epidemiology of Alzheimer's disease: occurrence, determinants, and strategies toward intervention. *Dialogues in clinical neuroscience,* 11(2), 111–128.

QUINTANILLA, R. A., ORELLANA, J. A. & VON BERNHARDI, R. 2012. Understanding risk factors for Alzheimer's disease: interplay of neuroinflammation, connexin-based communication and oxidative stress. *Archives of medical research,* 43**,** 632-44.

RAHKONEN, T., LUUKKAINEN-MARKKU, R., PAANILA, S., SIVENIUS, J. & SULKAVA, R. 2000. Delirium episode as a sign of undetected dementia among community dwelling elderly subjects: a 2 year follow up study. *Journal of Neurology, Neurosurgery, and Psychiatry,* 69**,** 519-521.

RAJAIAH, R., PERKINS, D. J., POLUMURI, S. K., ZHAO, A., KEEGAN, A. D. & VOGEL, S. N. 2013. Dissociation of endotoxin tolerance and differentiation of alternatively activated macrophages. *J Immunol,* 190**,** 4763-72.

RAK, M., DEL BIGIO, M. R., MAI, S., WESTAWAY, D. & GOUGH, K. 2007. Dense-core and diffuse Abeta plaques in TgCRND8 mice studied with synchrotron FTIR microspectroscopy. *Biopolymers,* 87**,** 207-17.

RANSOHOFF, R. M. 2016. A polarizing question: do M1 and M2 microglia exist? *Nat Neurosci,* 19**,** 987-91.

RAO, J. S., KELLOM, M., KIM, H. W., RAPOPORT, S. I. & REESE, E. A. 2012. Neuroinflammation and synaptic loss. *Neurochem Res,* 37**,** 903-10.

REITZ, C., HONIG, L., VONSATTEL, J. P., TANG, M. X. & MAYEUX, R. 2009. Memory performance is related to amyloid and tau pathology in the hippocampus. *J Neurol Neurosurg Psychiatry,* 80**,** 715-21.

REZAI-ZADEH, K., GATE, D. & TOWN, T. 2009. CNS infiltration of peripheral immune cells: D-Day for neurodegenerative disease? *J Neuroimmune Pharmacol,* 4**,** 462-75.

RIVEST, S. 2003. Molecular insights on the cerebral innate immune system. *Brain Behav Immun,* 17**,** 13-9.

ROCA, H., VARSOS, Z. S., SUD, S., CRAIG, M. J., YING, C. & PIENTA, K. J. 2009. CCL2 and interleukin-6 promote survival of human CD11b+ peripheral blood mononuclear cells and induce M2-type macrophage polarization. *J Biol Chem,* 284**,** 34342-54.

RODRIGUEZ, J. J., WITTON, J., OLABARRIA, M., NORISTANI, H. N. & VERKHRATSKY, A. 2010. Increase in the density of resting microglia precedes neuritic plaque formation and microglial activation in a transgenic model of Alzheimer's disease. *Cell Death Dis,* 1**,** e1.

ROSEN, C., HANSSON, O., BLENNOW, K. & ZETTERBERG, H. 2013. Fluid biomarkers in Alzheimer's disease - current concepts. *Mol Neurodegener,* 8**,** 20.

ROUBAUD BAUDRON, C., VARON, C., MEGRAUD, F. & SALLES, N. 2016. [Alzheimer's disease and Helicobacter pylori infection: a possible link?]. *Geriatr Psychol Neuropsychiatr Vieil,* 14**,** 86-94.

ROVED, J., WESTERDAHL, H. & HASSELQUIST, D. 2017. Sex differences in immune responses: Hormonal effects, antagonistic selection, and evolutionary consequences. *Hormones and Behavior,* 88**,** 95-105.

ROVELET-LECRUX, A., HANNEQUIN, D., RAUX, G., LE MEUR, N., LAQUERRIÈRE, A., VITAL, A., DUMANCHIN, C., FEUILLETTE, S., BRICE, A., VERCELLETTO, M., DUBAS, F., FREBOURG, T. & CAMPION, D. 2006. APP locus duplication causes autosomal dominant early-onset Alzheimer disease with cerebral amyloid angiopathy. *Nature genetics,* 38**,** 24-6.

RUAN, L., KANG, Z., PEI, G. & LE, Y. 2009. Amyloid deposition and inflammation in APPswe/PS1dE9 mouse model of Alzheimer's disease. *Curr Alzheimer Res,* 6**,** 531-40.

SAIJO, K. & GLASS, C. K. 2011. Microglial cell origin and phenotypes in health and disease. *Nature Reviews Immunology,* 11**,** 775-787.

SALLOWAY, S., SPERLING, R., FOX, N. C., BLENNOW, K., KLUNK, W., RASKIND, M., SABBAGH, M., HONIG, L. S., PORSTEINSSON, A. P., FERRIS, S., REICHERT, M., KETTER, N., NEJADNIK, B., GUENZLER, V., MILOSLAVSKY, M., WANG, D., LU, Y., LULL, J., TUDOR, I. C., LIU, E., GRUNDMAN, M., YUEN, E., BLACK, R., BRASHEAR, H. R., BAPINEUZUMAB & CLINICAL TRIAL, I. 2014. Two phase 3 trials of bapineuzumab in mild-to-moderate Alzheimer's disease. *The New England journal of medicine,* 370**,** 322-333.

SARAIVA, M. & O'GARRA, A. 2010. The regulation of IL-10 production by immune cells. *Nat Rev Immunol,* 10**,** 170-81.

SARDI F., FASSINA L., VENTURINI L., INGUSCIO M., GUERRIERO F., ROLFO E., ET AL. . (2011). Autoimmunity reviews Alzheimer's disease, autoimmunity and inflammation. The good, the bad and the ugly. *Autoimmun. Rev.* 11, 149–153. 10.1016/j.autrev.2011.09.005

SAUNDERS, A. M., STRITTMATTER, W. J., SCHMECHEL, D., GEORGE-HYSLOP, P. H., PERICAK-VANCE, M. A., JOO, S. H., ROSI, B. L., GUSELLA, J. F., CRAPPER-MACLACHLAN, D. R., ALBERTS, M. J. & ET AL. 1993. Association of apolipoprotein E allele epsilon 4 with late-onset familial and sporadic Alzheimer's disease. *Neurology,* 43**,** 1467-72.

SCHEFFLER, K., STENZEL, J., KROHN, M., LANGE, C., HOFRICHTER, J., SCHUMACHER, T., BRUNING, T., PLATH, A. S., WALKER, L. & PAHNKE, J. 2011. Determination of spatial and temporal distribution of microglia by 230nm-high-resolution, high-throughput automated analysis reveals different amyloid plaque populations in an APP/PS1 mouse model of Alzheimer's disease. *Curr Alzheimer Res,* 8**,** 781-8.

SCHWARZ, J. M., SHOLAR, P. W. & BILBO, S. D. 2012. Sex differences in microglial colonization of the developing rat brain. *J Neurochem,* 120**,** 948-63.

SELKOE, D. J. 1991. Alzheimer's disease. In the beginning. *Nature,* 354**,** 432-3.

SELKOE, D. J. & HARDY, J. 2016. The amyloid hypothesis of Alzheimer's disease at 25 years. *EMBO Molecular Medicine,* 8**,** 595-608.

SERRANO-POZO, A., FROSCH, M. P., MASLIAH, E. & HYMAN, B. T. 2011. Neuropathological alterations in Alzheimer disease. *Cold Spring Harbor perspectives in medicine,* 1**,** a006189-a006189.

SERRANO-POZO, A., GÓMEZ-ISLA, T., GROWDON, J. H., FROSCH, M. P. & HYMAN, B. T. 2013. A Phenotypic Change But Not Proliferation Underlies Glial Responses in Alzheimer Disease. *The American Journal of Pathology,* 182**,** 2332-2344.

SHAFTEL, S. S., KYRKANIDES, S., OLSCHOWKA, J. A., MILLER, J. N., JOHNSON, R. E. & O'BANION, M. K. 2007. Sustained hippocampal IL-1 beta overexpression mediates chronic neuroinflammation and ameliorates Alzheimer plaque pathology. *J Clin Invest,* 117**,** 1595-604.

SHAW, A. C., GOLDSTEIN, D. R. & MONTGOMERY, R. R. 2013. Age-dependent dysregulation of innate immunity. *Nature reviews. Immunology,* 13**,** 875-887.

SHENG, J. G., BORA, S. H., XU, G., BORCHELT, D. R., PRICE, D. L. & KOLIATSOS, V. E. 2003. Lipopolysaccharide-induced-neuroinflammation increases intracellular accumulation of amyloid precursor protein and amyloid beta peptide in APPswe transgenic mice. *Neurobiol Dis,* 14**,** 133-45.

SHIBATA, M., YAMADA, S., KUMAR, S. R., CALERO, M., BADING, J., FRANGIONE, B., HOLTZMAN, D. M., MILLER, C. A., STRICKLAND, D. K., GHISO, J. & ZLOKOVIC, B. V. 2000. Clearance of Alzheimer's amyloid-ss(1-40) peptide from brain by LDL receptor-related protein-1 at the blood-brain barrier. *J Clin Invest,* 106**,** 1489-99.

SIMARD, A. R. & RIVEST, S. 2004. Bone marrow stem cells have the ability to populate the entire central nervous system into fully differentiated parenchymal microglia. *FASEB J,* 18**,** 998-1000.

SIMARD, A. R., SOULET, D., GOWING, G., JULIEN, J.-P. & RIVEST, S. 2006a. Bone marrow-derived microglia play a critical role in restricting senile plaque formation in Alzheimer's disease. *Neuron,* 49**,** 489-502.

SIMARD, A. R., SOULET, D., GOWING, G., JULIEN, J. P. & RIVEST, S. 2006b. Bone marrow-derived microglia play a critical role in restricting senile plaque formation in Alzheimer's disease. *Neuron,* 49**,** 489-502.

SKELLY, D. T., HENNESSY, E., DANSEREAU, M. A. & CUNNINGHAM, C. 2013. A systematic analysis of the peripheral and CNS effects of systemic LPS, IL-1beta, [corrected] TNF-alpha and IL-6 challenges in C57BL/6 mice. *PLoS One,* 8**,** e69123.

SLATTERY, C. F., BECK, J. A., HARPER, L., ADAMSON, G., ABDI, Z., UPHILL, J., CAMPBELL, T., DRUYEH, R., MAHONEY, C. J., ROHRER, J. D., KENNY, J., LOWE, J., LEUNG, K. K., BARNES, J., CLEGG, S. L., BLAIR, M., NICHOLAS, J. M., GUERREIRO, R. J., ROWE, J. B., PONTO, C., ZERR, I., KRETZSCHMAR, H., GAMBETTI, P., CRUTCH, S. J., WARREN, J. D., ROSSOR, M. N., FOX, N. C., COLLINGE, J., SCHOTT, J. M. & MEAD, S. 2014. R47H TREM2 variant increases risk of typical early-onset

Alzheimer's disease but not of prion or frontotemporal dementia. *Alzheimers Dement,* 10**,** 602-608 e4.

SLY, L. M., KRZESICKI, R. F., BRASHLER, J. R., BUHL, A. E., MCKINLEY, D. D., CARTER, D. B. & CHIN, J. E. 2001. Endogenous brain cytokine mRNA and inflammatory responses to lipopolysaccharide are elevated in the Tg2576 transgenic mouse model of Alzheimer's disease. *Brain Res Bull,* 56**,** 581-8.

SOLITO, E. & SASTRE, M. 2012. Microglia function in Alzheimer's disease. *Frontiers in pharmacology,* 3**,** 14-14.

SONG, M., JIN, J., LIM, J. E., KOU, J., PATTANAYAK, A., REHMAN, J. A., KIM, H. D., TAHARA, K., LALONDE, R. & FUKUCHI, K. 2011. TLR4 mutation reduces microglial activation, increases Abeta deposits and exacerbates cognitive deficits in a mouse model of Alzheimer's disease. *J Neuroinflammation,* 8**,** 92.

SOUCY, G., BOIVIN, G., LABRIE, F. & RIVEST, S. 2005. Estradiol Is Required for a Proper Immune Response to Bacterial and Viral Pathogens in the Female Brain. *The Journal of Immunology,* 174**,** 6391-6398.

SPANGENBERG, E. E., LEE, R. J., NAJAFI, A. R., RICE, R. A., ELMORE, M. R. P., BLURTON-JONES, M., WEST, B. L. & GREEN, K. N. 2016. Eliminating microglia in Alzheimer's mice prevents neuronal loss without modulating amyloid-β pathology. *Brain : a journal of neurology,* 139**,** 1265-1281.

SPINNEY, L. 2014. Alzheimer's disease: The forgetting gene. *Nature,* 510**,** 26-8.

STALDER, M., PHINNEY, A., PROBST, A., SOMMER, B., STAUFENBIEL, M. & JUCKER, M. 1999. Association of microglia with amyloid plaques in brains of APP23 transgenic mice. *Am J Pathol,* 154**,** 1673-84.

STORCK, S. E., MEISTER, S., NAHRATH, J., MEISSNER, J. N., SCHUBERT, N., DI SPIEZIO, A., BACHES, S., VANDENBROUCKE, R. E., BOUTER, Y., PRIKULIS, I., KORTH, C., WEGGEN, S., HEIMANN, A., SCHWANINGER, M., BAYER, T. A. & PIETRZIK, C. U. 2016. Endothelial LRP1 transports amyloid-beta(1-42) across the blood-brain barrier. *J Clin Invest,* 126**,** 123-36.

STRAUB, R. H. 2007. The Complex Role of Estrogens in Inflammation. *Endocrine Reviews,* 28**,** 521-574.

SUBRAMANIAM, S. R. & FEDEROFF, H. J. 2017. Targeting Microglial Activation States as a Therapeutic Avenue in Parkinson's Disease. *Frontiers in Aging Neuroscience,* 9**,** 176.

SUNG, S., YANG, H., URYU, K., LEE, E. B., ZHAO, L., SHINEMAN, D., TROJANOWSKI, J. Q., LEE, V. M. & PRATICO, D. 2004. Modulation of nuclear factor-kappa B activity by indomethacin influences A beta levels but not A beta precursor protein metabolism in a model of Alzheimer's disease. *Am J Pathol,* 165**,** 2197-206.

SYKOVA, E., VORISEK, I., ANTONOVA, T., MAZEL, T., MEYER-LUEHMANN, M., JUCKER, M., HAJEK, M., ORT, M. & BURES, J. 2005. Changes in

extracellular space size and geometry in APP23 transgenic mice: a model of Alzheimer's disease. *Proc Natl Acad Sci U S A,* 102**,** 479-84.

SZEKELY, C. A., BREITNER, J. C., FITZPATRICK, A. L., REA, T. D., PSATY, B. M., KULLER, L. H. & ZANDI, P. P. 2008. NSAID use and dementia risk in the Cardiovascular Health Study: role of APOE and NSAID type. *Neurology,* 70**,** 17-24.

TAGLIALATELA, G., HOGAN, D., ZHANG, W.-R. & DINELEY, K. T. 2009. Intermediate- and Long-Term Recognition Memory Deficits in Tg2576 Mice Are Reversed with Acute Calcineurin Inhibition. *Behavioural brain research,* 200**,** 95-99.

TAKAHASHI, K., ROCHFORD, C. D. P. & NEUMANN, H. 2005. Clearance of apoptotic neurons without inflammation by microglial triggering receptor expressed on myeloid cells-2. *The Journal of experimental medicine,* 201**,** 647-57.

TANG, Y. & LE, W. 2016. Differential Roles of M1 and M2 Microglia in Neurodegenerative Diseases. *Mol Neurobiol,* 53**,** 1181-94.

TANZI, R. E. 2012. The genetics of Alzheimer disease. *Cold Spring Harbor perspectives in medicine,* 2.

TEICH, A. F., PATEL, M. & ARANCIO, O. 2013. A reliable way to detect endogenous murine beta-amyloid. *PLoS One,* 8**,** e55647.

TERWEL, D., MUYLLAERT, D., DEWACHTER, I., BORGHGRAEF, P., CROES, S., DEVIJVER, H. & VAN LEUVEN, F. 2008. Amyloid activates GSK-3beta to aggravate neuronal tauopathy in bigenic mice. *Am J Pathol,* 172**,** 786-98.

TOLAR, M., ABUSHAKRA, S., SABBAGH, M., 2019. The path forward in Alzheimer's disease therapeutics: Reevaluating the amyloid cascade hypothesis, *Alzheimer's & Dementia*, ISSN 1552-5260,

TORRES-PLATAS, S. G., COMEAU, S., RACHALSKI, A., BO, G. D., CRUCEANU, C., TURECKI, G., GIROS, B. & MECHAWAR, N. 2014. Morphometric characterization of microglial phenotypes in human cerebral cortex. *J Neuroinflammation,* 11**,** 12.

TOWN, T., LAOUAR, Y., PITTENGER, C., MORI, T., SZEKELY, C. A., TAN, J., DUMAN, R. S. & FLAVELL, R. A. 2008. Blocking TGF-β–Smad2/3 innate immune signaling mitigates Alzheimer-like pathology. *Nature Medicine,* 14**,** 681.

TRONEL, C., LARGEAU, B., SANTIAGO RIBEIRO, M. J., GUILLOTEAU, D., DUPONT, A.-C. & ARLICOT, N. 2017. Molecular Targets for PET Imaging of Activated Microglia: The Current Situation and Future Expectations. *International journal of molecular sciences,* 18**,** 802.

TSAI-TENG, T., CHIN-CHU, C., LI-YA, L., WAN-PING, C., CHUNG-KUANG, L., CHIEN-CHANG, S., CHI-YING, H. F., CHIEN-CHIH, C. & SHIAO, Y. J. 2016. Erinacine A-enriched Hericium erinaceus mycelium ameliorates Alzheimer's disease-related pathologies in APPswe/PS1dE9 transgenic mice. *J Biomed Sci,* 23**,** 49.

UDEOCHU, J., SAYED, F. A. & GAN, L. 2018. TREM2 and Amyloid Beta: A Love-Hate Relationship. *Neuron,* 97**,** 991-993.

UNGAR, L., ALTMANN, A. & GREICIUS, M. D. 2014. Apolipoprotein E, Gender, and Alzheimer's Disease: An Overlooked, but Potent and Promising Interaction. *Brain imaging and behavior,* 8**,** 262-273.

VALERO, J., MASTRELLA, G., NEIVA, I., SÁNCHEZ, S. & MALVA, J. O. 2014. Long-term effects of an acute and systemic administration of LPS on adult neurogenesis and spatial memory. *Frontiers in Neuroscience,* 8.

VAN DE HAAR, H. J., BURGMANS, S., JANSEN, J. F., VAN OSCH, M. J., VAN BUCHEM, M. A., MULLER, M., HOFMAN, P. A., VERHEY, F. R. & BACKES, W. H. 2016. Blood-Brain Barrier Leakage in Patients with Early Alzheimer Disease. *Radiology,* 281**,** 527-535.

VANLEUVEN, F. 2011. GSK3 and Alzheimer's Disease: Facts and Fiction…. *Frontiers in Molecular Neuroscience,* 4.

VARATHARAJ, A. & GALEA, I. 2017. The blood-brain barrier in systemic inflammation. *Brain Behav Immun,* 60**,** 1-12.

VEGETO, E., BENEDUSI, V. & MAGGI, A. 2008. Estrogen anti-inflammatory activity in brain: a therapeutic opportunity for menopause and neurodegenerative diseases. *Front Neuroendocrinol,* 29**,** 507-19.

VEGETO, E., BONINCONTRO, C., POLLIO, G., SALA, A., VIAPPIANI, S., NARDI, F., BRUSADELLI, A., VIVIANI, B., CIANA, P. & MAGGI, A. 2001. Estrogen prevents the lipopolysaccharide-induced inflammatory response in microglia. *J Neurosci,* 21**,** 1809-18.

VENTURA, G., MOINARD, C., SEGAUD, F., LE PLENIER, S., CYNOBER, L. & DE BANDT, J. P. 2010. Adaptative response of nitrogen metabolism in early endotoxemia: role of ornithine aminotransferase. *Amino Acids,* 39**,** 1417-1426.

VERGHESE, P. B., CASTELLANO, J. M., GARAI, K., WANG, Y., JIANG, H., SHAH, A., BU, G., FRIEDEN, C. & HOLTZMAN, D. M. 2013. ApoE influences amyloid-beta (Abeta) clearance despite minimal apoE/Abeta association in physiological conditions. *Proc Natl Acad Sci U S A,* 110**,** E1807-16.

VILLA, A., GELOSA, P., CASTIGLIONI, L., CIMINO, M., RIZZI, N., PEPE, G., LOLLI, F., MARCELLO, E., SIRONI, L., VEGETO, E. & MAGGI, A. 2018. Sex-Specific Features of Microglia from Adult Mice. *Cell Reports,* 23**,** 3501-3511.

WALKER, D. G. & LUE, L. F. 2015. Immune phenotypes of microglia in human neurodegenerative disease: challenges to detecting microglial polarization in human brains. *Alzheimers Res Ther,* 7**,** 56.

WALTER, S., LETIEMBRE, M., LIU, Y., HEINE, H., PENKE, B., HAO, W., BODE, B., MANIETTA, N., WALTER, J., SCHULZ-SCHUFFER, W. & FASSBENDER, K. 2007. Role of the toll-like receptor 4 in neuroinflammation in Alzheimer's disease. *Cell Physiol Biochem,* 20**,** 947-56.

WAN, Y., WANG, G. & CHEN, S. D. 2008. Genetic predisposition to inflammation: a new risk factor of Alzheimer's disease. *Neurosci Bull,* 24**,** 314-22.

WANG, J., TANILA, H., PUOLIVÄLI, J., KADISH, I. & GROEN, T. V. 2003a. Gender differences in the amount and deposition of amyloidβ in APPswe and PS1 double transgenic mice. *Neurobiology of Disease,* 14**,** 318-327.

WANG, J., TANILA, H., PUOLIVALI, J., KADISH, I. & VAN GROEN, T. 2003b. Gender differences in the amount and deposition of amyloidbeta in APPswe and PS1 double transgenic mice. *Neurobiol Dis,* 14**,** 318-27.

WANG, L.-M., WU, Q., KIRK, R. A., HORN, K. P., EBADA SALEM, A. H., HOFFMAN, J. M., YAP, J. T., SONNEN, J. A., TOWNER, R. A., BOZZA, F. A., RODRIGUES, R. S. & MORTON, K. A. 2018. Lipopolysaccharide endotoxemia induces amyloid-β and p-tau formation in the rat brain. *American Journal of Nuclear Medicine and Molecular Imaging,* 8**,** 86-99.

WANG, S., WANG, R., CHEN, L., BENNETT, D. A., DICKSON, D. W. & WANG, D.-S. 2010. Expression and functional profiling of neprilysin, insulin-degrading enzyme, and endothelin-converting enzyme in prospectively studied elderly and Alzheimer's brain. *Journal of neurochemistry,* 115**,** 47-57.

WANG, W.-Y., TAN, M.-S., YU, J.-T. & TAN, L. 2015. Role of pro-inflammatory cytokines released from microglia in Alzheimer's disease. *Annals of translational medicine,* 3**,** 136-136.

WANG, Y., ULLAND, T. K., ULRICH, J. D., SONG, W., TZAFERIS, J. A., HOLE, J. T., YUAN, P., MAHAN, T. E., SHI, Y., GILFILLAN, S., CELLA, M., GRUTZENDLER, J., DEMATTOS, R. B., CIRRITO, J. R., HOLTZMAN, D. M. & COLONNA, M. 2016. TREM2-mediated early microglial response limits diffusion and toxicity of amyloid plaques. *J Exp Med,* 213**,** 667-75.

WEGGEN, S., ERIKSEN, J. L., DAS, P., SAGI, S. A., WANG, R., PIETRZIK, C. U., FINDLAY, K. A., SMITH, T. E., MURPHY, M. P., BULTER, T., KANG, D. E., MARQUEZ-STERLING, N., GOLDE, T. E. & KOO, E. H. 2001. A subset of NSAIDs lower amyloidogenic Abeta42 independently of cyclooxygenase activity. *Nature,* 414**,** 212-6.

WEGNER, A., ELSENBRUCH, S., REBERNIK, L., RODERIGO, T., ENGELBRECHT, E., JAGER, M., ENGLER, H., SCHEDLOWSKI, M. & BENSON, S. 2015. Inflammation-induced pain sensitization in men and women: does sex matter in experimental endotoxemia? *Pain,* 156**,** 1954-64.

WELLER, J. & BUDSON, A. 2018. Current understanding of Alzheimer's disease diagnosis and treatment. *F1000Research,* 7**,** F1000 Faculty Rev-1161.

WELLER, R. O., MASSEY, A., KUO, Y. M. & ROHER, A. E. 2000. Cerebral amyloid angiopathy: accumulation of A beta in interstitial fluid drainage pathways in Alzheimer's disease. *Ann N Y Acad Sci,* 903**,** 110-7.

WELLER, R. O., SUBASH, M., PRESTON, S. D., MAZANTI, I. & CARARE, R. O. 2008. Perivascular drainage of amyloid-beta peptides from the brain

and its failure in cerebral amyloid angiopathy and Alzheimer's disease. *Brain Pathol,* 18**,** 253-66.

WENDELN, A. C., DEGENHARDT, K., KAURANI, L., GERTIG, M., ULAS, T., JAIN, G., WAGNER, J., HASLER, L. M., WILD, K., SKODRAS, A., BLANK, T., STASZEWSKI, O., DATTA, M., CENTENO, T. P., CAPECE, V., ISLAM, M. R., KERIMOGLU, C., STAUFENBIEL, M., SCHULTZE, J. L., BEYER, M., PRINZ, M., JUCKER, M., FISCHER, A. & NEHER, J. J. 2018. Innate immune memory in the brain shapes neurological disease hallmarks. *Nature,* 556**,** 332-338.

WESTIN, K., BUCHHAVE, P., NIELSEN, H., MINTHON, L., JANCIAUSKIENE, S. & HANSSON, O. 2012. CCL2 is associated with a faster rate of cognitive decline during early stages of Alzheimer's disease. *PLoS One,* 7**,** e30525.

WILLIAMS, A. E., JOSE, R. J., BROWN, J. S. & CHAMBERS, R. C. 2015. Enhanced inflammation in aged mice following infection with Streptococcus pneumoniae is associated with decreased IL-10 and augmented chemokine production. *Am J Physiol Lung Cell Mol Physiol,* 308**,** L539-49.

WIRZ, K. T. S., BOSSERS, K., STARGARDT, A., KAMPHUIS, W., SWAAB, D. F., HOL, E. M. & VERHAAGEN, J. 2013. Cortical beta amyloid protein triggers an immune response, but no synaptic changes in the APPswe/PS1dE9 Alzheimer's disease mouse model. *Neurobiology of Aging,* 34**,** 1328-1342.

WOZNIAK, M. A., ITZHAKI, R. F., SHIPLEY, S. J. & DOBSON, C. B. 2007. Herpes simplex virus infection causes cellular β-amyloid accumulation and secretase upregulation. *Neuroscience Letters,* 429**,** 95-100.

WU, D., ZHANG, X., ZHAO, M. & ZHOU, A. L. 2015. The role of the TLR4/NF-kappaB signaling pathway in Abeta accumulation in primary hippocampal neurons. *Sheng Li Xue Bao,* 67**,** 319-28.

WU J, LI L. 2016. Autoantibodies in Alzheimer's disease: potential biomarkers, pathogenic roles, and therapeutic implications. *J Biomed Res.* 30(5):361–372. doi:10.7555/JBR.30.20150131.

WU, S.-Y., CHEN, Y.-W., TSAI, S.-F., WU, S.-N., SHIH, Y.-H., JIANG-SHIEH, Y.-F., YANG, T.-T. & KUO, Y.-M. 2016. Estrogen ameliorates microglial activation by inhibiting the Kir2.1 inward-rectifier K(+) channel. *Scientific Reports,* 6**,** 22864.

WYNNE, A. M., HENRY, C. J., HUANG, Y., CLELAND, A. & GODBOUT, J. P. 2010. Protracted downregulation of CX3CR1 on microglia of aged mice after lipopolysaccharide challenge. *Brain, Behavior, and Immunity,* 24**,** 1190-1201.

WYSS-CORAY, T. 2006. Inflammation in Alzheimer disease: driving force, bystander or beneficial response? *Nature medicine,* 12**,** 1005-15.

XIANG, Y., BU, X. L., LIU, Y. H., ZHU, C., SHEN, L. L., JIAO, S. S., ZHU, X. Y., GIUNTA, B., TAN, J., SONG, W. H., ZHOU, H. D., ZHOU, X. F. & WANG, Y. J. 2015. Physiological amyloid-beta clearance in the periphery and

its therapeutic potential for Alzheimer's disease. *Acta Neuropathol,* 130**,** 487-99.

YAMAMOTO, M., KIYOTA, T., HORIBA, M., BUESCHER, J. L., WALSH, S. M., GENDELMAN, H. E. & IKEZU, T. 2007. Interferon-γ and Tumor Necrosis Factor-α Regulate Amyloid-β Plaque Deposition and β-Secretase Expression in Swedish Mutant APP Transgenic Mice. *The American Journal of Pathology,* 170**,** 680-692.

YAN, P., BERO, A. W., CIRRITO, J. R., XIAO, Q., HU, X., WANG, Y., GONZALES, E., HOLTZMAN, D. M. & LEE, J.-M. 2009a. Characterizing the appearance and growth of amyloid plaques in APP/PS1 mice. *The Journal of neuroscience : the official journal of the Society for Neuroscience,* 29**,** 10706-10714.

YAN, P., BERO, A. W., CIRRITO, J. R., XIAO, Q., HU, X., WANG, Y., GONZALES, E., HOLTZMAN, D. M. & LEE, J. M. 2009b. Characterizing the appearance and growth of amyloid plaques in APP/PS1 mice. *J Neurosci,* 29**,** 10706-14.

YANG, J., ZHANG, L., YU, C., YANG, X.-F. & WANG, H. 2014. Monocyte and macrophage differentiation: circulation inflammatory monocyte as biomarker for inflammatory diseases. *Biomarker Research,* 2**,** 1-1.

YASOJIMA, K., SCHWAB, C., MCGEER, E. G. & MCGEER, P. L. 2000. Human neurons generate C-reactive protein and amyloid P: upregulation in Alzheimer's disease. *Brain Res,* 887**,** 80-9.

YRLID, U., JENKINS, C. D. & MACPHERSON, G. G. 2006. Relationships between distinct blood monocyte subsets and migrating intestinal lymph dendritic cells in vivo under steady-state conditions. *J Immunol,* 176**,** 4155-62.

YUAN, P., CONDELLO, C., KEENE, C. D., WANG, Y., BIRD, T. D., PAUL, S. M., LUO, W., COLONNA, M., BADDELEY, D. & GRUTZENDLER, J. 2016. TREM2 Haplodeficiency in Mice and Humans Impairs the Microglia Barrier Function Leading to Decreased Amyloid Compaction and Severe Axonal Dystrophy. *Neuron,* 90**,** 724-39.

ZAGHI, J., GOLDENSON, B., INAYATHULLAH, M., LOSSINSKY, A. S., MASOUMI, A., AVAGYAN, H., MAHANIAN, M., BERNAS, M., WEINAND, M., ROSENTHAL, M. J., ESPINOSA-JEFFREY, A., DE VELLIS, J., TEPLOW, D. B., & FIALA, M.2009. Alzheimer disease macrophages shuttle amyloid-beta from neurons to vessels, contributing to amyloid angiopathy. *Acta Neuropathol* 117, 111–124.

ZHAN, X., STAMOVA, B. & SHARP, F. R. 2018. Lipopolysaccharide Associates with Amyloid Plaques, Neurons and Oligodendrocytes in Alzheimer's Disease Brain: A Review. *Front Aging Neurosci,* 10**,** 42.

ZHANG, F. & JIANG, L. 2015. Neuroinflammation in Alzheimer's disease. *Neuropsychiatr Dis Treat,* 11**,** 243-56.

ZHANG, X., GONCALVES, R. & MOSSER, D. M. 2008. The Isolation and Characterization of Murine Macrophages. *Current protocols in immunology / edited by John E. Coligan ... [et al.],* CHAPTER**,** Unit-14.1.

ZHAO, R., HU, W., TSAI, J., LI, W. & GAN, W.-B. 2017a. Microglia limit the expansion of β-amyloid plaques in a mouse model of Alzheimer's disease. *Molecular Neurodegeneration,* 12**,** 47.

ZHAO, R., HU, W., TSAI, J., LI, W. & GAN, W.-B. 2017b. Microglia limit the expansion of β-amyloid plaques in a mouse model of Alzheimer's disease. *Molecular Neurodegeneration,* 12**,** 47.

ZHAO, Z., SAGARE, A. P., MA, Q., HALLIDAY, M. R., KONG, P., KISLER, K., WINKLER, E. A., RAMANATHAN, A., KANEKIYO, T., BU, G., OWENS, N. C., REGE, S. V., SI, G., AHUJA, A., ZHU, D., MILLER, C. A., SCHNEIDER, J. A., MAEDA, M., MAEDA, T., SUGAWARA, T., ICHIDA, J. K. & ZLOKOVIC, B. V. 2015. Central role for PICALM in amyloid-beta blood-brain barrier transcytosis and clearance. *Nat Neurosci,* 18**,** 978-87.

ZHENG, C., ZHOU, X. W. & WANG, J. Z. 2016. The dual roles of cytokines in Alzheimer's disease: update on interleukins, TNF-alpha, TGF-beta and IFN-gamma. *Transl Neurodegener,* 5**,** 7.

ZHU, B., WANG, Z. G., DING, J., LIU, N., WANG, D. M., DING, L. C. & YANG, C. 2014. Chronic lipopolysaccharide exposure induces cognitive dysfunction without affecting BDNF expression in the rat hippocampus. *Exp Ther Med,* 7**,** 750-754.

ZOTOVA, E., NICOLL, J. A. R., KALARIA, R., HOLMES, C. & BOCHE, D. 2010. Inflammation in Alzheimer's disease: relevance to pathogenesis and therapy. *Alzheimer's Research & Therapy,* 2**,** 1-1.

ZRZAVY, T., HAMETNER, S., WIMMER, I., BUTOVSKY, O., WEINER, H. L. & LASSMANN, H. 2017. Loss of 'homeostatic' microglia and patterns of their activation in active multiple sclerosis. *Brain,* 140**,** 1900-1913.

ZUROFF, L., DALEY, D., BLACK, K. L. & KORONYO-HAMAOUI, M. 2017. Clearance of cerebral Aβ in Alzheimer's disease: reassessing the role of microglia and monocytes. *Cellular and Molecular Life Sciences,* 74**,** 2167-2201.